Delft Cluster

Title:	**Numerical modelling of vanes and screens**

Development of vanes and screens in Delft3D-MOR

Author:	Ir. C. Flokstra	Institute:	WL | Delft Hydraulics
Author:	Dr. Ir. H.R.A. Jagers	Institute:	WL | Delft Hydraulics
Author:	Ir. F.E. Wiersma	Company:	Royal Haskoning
Author:	Dr. Ir. E. Mosselman	Institute:	Technical University Delft – Faculty of Civil Engineering and Geo Sciences
Author:	Ir. T.H.G. Jongeling	Institute:	WL | Delft Hydraulics

June 2003

Number of pages	:	187	
Keywords (3-5)	:	Bed vanes, screens, river morphology, river flow, river engineering, river management, numerical modelling	
DC-Publication-number	:	DC1-331-3	
Institute Publication-number (optional)	:	Q2849	WL | Delft Hydraulics
Report Type	:	☐	Intermediary report or study
	:	☒	Final projectreport
DUP-publication Type	:	☒	DUP Standard
		☐	DUP-Science

Abstract

The morphological modelling system Delft3D-MOR has been updated and extended with respect to the effect of vanes on the flow and the bed level. Two types of vanes have been distinguished, type 1 being a vane not affecting the near field area of the vane and type 2 affecting the nearby area of the vane. The type 1 vane model, already introduced in the past according to a concept of Odgaard, has been updated and applied to suspended sediment transport, in addition to bed load transport. The type 2 vane model has been developed within the present study. The flow past this vane type is based on the same approach as used for levees and weirs in a depth-averaged flow model, but instead of a discharge relation based on a broad-crested weir concept, a discharg relation derived from a sharp-crested weir is used.

Morphological simulations have been carried out for type 1 vanes in a curved flume, in which case a reasonable agreement with the measured bed level was obtained. Furthermore, a model has been composed of the Ganges/Gorai bifurcation (Bangladesh) to demonstrate the effect of the vanes on the sediment transport to the Gorai. The vanes show a significant effect, but in this case no measured data are available to check the outcomes.
Finally a number of tests have been carried out to judge the model of type 2 vanes. Physical experiments will be required to judge and validate this model in detail.

The project was executed by WL | Delft Hydraulics , TU Delft (Delft Cluster Partners) and Royal Haskoning in the period 2000-2003.

PROJECT NAME:	**Vanes and Screens**	PROJECT CODE:	**03.03.01**
BASEPROJECT NAME:	**Rivers**	BASEPROJECT CODE:	**03.03**
THEME NAME:	**Coast and River**	THEME CODE:	**03**

Executive Summary

Vanes are constructions to be placed in a river flow to affect the flow, the sediment transport and the alluvial bed level. These vanes may be an alternative for other river engineering constructions or constitute a supplementary measure to prevent or reduce dredging, to generate or stabilise channels, etc. The determination of the effect of vanes on the bed level in a design stage requires the use of a physical model or of a morphological modelling system to simulate the prototype conditions. The present report concerns the extension of the numerical modelling system Delft3D-MOR with the effects of vanes and the application of this system to a number of cases.

Two types of vanes are distinguished which requires a different computational model:

- Type 1 vanes are submerged vanes with a small length and a large number of these vanes has to be used to obtain the required effect on the bed level.
- Type 2 vanes are submerged or surface vanes with a large length and one or a few vanes have to be used to obtain the required effect.

The type 1 vanes are described by a vortex line generated at the end of the vane and running downstream. The vortex strength just downstream of the vane is related to flow conditions around the vane and the vane dimensions. Along the vortex line the vortex strength damps out. The vane itself is a subgrid effect and only the induced flow resistance is accounted for. The vortex line affects the sediment transport direction and thereby the bed level. This vane model has been developed primarily by Odgaard et al.

The definition of the type 2 vanes and the modelling of these vanes have been carried out in the present study. The effect of the vane on the near field is not a subgrid effect, because of the vane length. The chosen flow model is a depth-averaged model, which is used in the case of type 1 vanes too. The alternative is a multi-layer flow model, where a sigma transformation creates variable layer levels that do not fit quit well to the fixed upper side of the vane(s). Furthermore the computational effort increases significantly with the number of layers. The use of the depth-averaged flow model allows modelling the vanes similar to the model of levees and weirs, already used since long time. In the case of overflow weirs a discharge relation of broad-crested weirs is used. In the case of a vane this relation is replaced by the sharp-crested discharge relation. The vane induced vortex line as used for type 1 vanes is neglected. The effect of the vane type 2 on the sediment transport direction is obtained via the effected depth-averaged flow field.

These two vane models have been implemented in the modelling system Delft3D-MOR, a system developed at WL | Delft Hydraulics. It is suitable to include these vane models in this system as the model of type 1 vanes was included in an earlier version of this system.

The implementation of the vane model type 1 has been carried out and concerns an update, as in the past this model has been implemented in a previous version of Delft3D-MOR. Furthermore the vane model type 1 has been extended to the suspended mode of the system in addition to the bed load mode. The vane type 2 has been implemented for both the submerged and the surface vane option and includes modifications of the FLOW, TRANSP and BOTTOM modules in Delft3D-MOR. Test cases have been carried out and the vane models have been improved.

PROJECT NAAM:	**Vanes and Screens**	PROJECT CODE:	**03.03.01**
BASISPROJECT NAAM:	**Rivers**	BASEPROJECT CODE:	**03.03**
THEMA NAAM:	**Coast and River**	THEME CODE:	**03**

Executive Summary (continuation)

Different test cases were designed for vanes of type 1 and 2. For vanes of type 1 some of tests carried out previously with the outdated code were repeated. The presently computed bed levels show no differences with respect to the earlier results. These tests concern the flow in the curved flume of WL | Delft Hydraulics in which physical tests were carried out with a movable bed, a constant discharge and with 4x19 vanes. The simulation reproduced reasonably the measured bed level and this confirms the capability of the model to predict the effect of vanes on the bed level.

The 'Gorai River Restoration Project' carried out by Royal Haskoning contains a study to determine whether submerged vanes can reduce sufficiently the sediment transport from the Ganges to the Gorai river. A simulation model has been built of the bifurcation Ganges/Gorai in which additional to other training works 212 vanes of type 1 are used. The model has been calibrated for the case without vanes using the available site data. Three significant inflow directions are used to simulate the large-scale inflow variations within the period 1973-2000, in the case of a fixed vane field. The efficiency of the vanes is reduced in this case, as the suspended sediment transport is dominant to the bed load. In the present inflow direction the sediment transport to the Gorai reduces 10 to 20%. The outcomes of the model could not be checked as measured data are lacking.

With respect to vanes of type 2 only submerged vanes have been tested. All tests carried out primarily were aimed to check the model implementation. Most tests were carried out in a straight channel and the vane consists of a few grid cells. Finally some tests were carried out of one vane placed near a bifurcation. The use of different computational grids for the same configuration generates different results, which indicate the need for a fine grid.

The following conclusions are drawn:

- The present computations confirm the suitability of the type I vane model implemented in a morphological modelling system to compute in a reasonable way the effect of vanes on an alluvial bed;
- The simulations with the type 2 vanes show the expected effects on flow, sediment transport and bed level, but these results could not be checked by experimental data.

The following recommendations are given:

- The dedicated Delft3D-MOR version extended with type I vanes should be added within short term to the centrally maintained Delft3D model line;
- The applicability of the model of type I vanes should be extended to large angles of flow attack;
- The theoretical base of the type I vane model should be reconsidered;
- The modelling of the type 2 vanes has to be continued: some shortcomings, observed now, have to be removed, measurements have to be executed together with detailed 3D-computations to check the validity of the model and if necessary to extend it. The neglect of the vortex line should be checked, together with the vane end effects and the used discharge relations.

PROJECT NAAM:	**Vanes and Screens**	PROJECT CODE:	**03.03.01**
BASISPROJECT NAAM:	**Rivers**	BASEPROJECT CODE:	**03.03**
THEMA NAAM:	**Coast and River**	THEME CODE:	**03**

Applicability for the sector

The new numerical tools developed in the present project enhance the existing practical knowledge, thus providing a solid basis for cost-effective design and extension to innovative applications with respect to fairway improvement, protection against bank erosion, sediment control at intakes, maintenance of alluvial channels and control of the morphological development of bifurcated river channels.

PROJECT NAME:	**Vanes and Screens**	PROJECT CODE:	**03.03.01**
BASEPROJECT NAME:	**Rivers**	BASEPROJECT CODE:	**03.03**
THEME NAME:	**Coast and River**	THEME CODE:	**03**

Table of contents

List of Figures

List of Tables

1 Introduction and summary

1.1 Justification of the study

River management in the Netherlands in the long term will gradually pay more attention to restoring and recovering the natural river dynamics processes.
This means that river research, more than in the past, should be directed towards a better understanding, description and control of the secondary natural river dynamics processes (channel formation, freely-eroding banks, bank protection, impact of secondary flows, etc.)

The present study concerns fundamental research on the secondary hydraulic and morphological processes due to screens (surface screens and bottom screens) and bottom vanes (with minor influence on the main flow).

The interest in this research subject of the civil engineering sector may be summarised as follows:

- In the Netherlands gradually more interest is attached to restoring/recovering the natural river dynamics processes and management measures that make use of secondary processes in the river (vanes, screens, side-channel development, vegetation, etc.);
- In the Netherlands a river engineering project has been prepared to improve the navigation of two river bends in the Waal River (near Hulhuizen and Haalderen) by using submerged vanes. The design study has been carried out by HASKONING and WL | Delft Hydraulics;
- Recent morphological simulations with vanes has been carried out for the river IJssel.
- In the FAP 21/22-project in Bangladesh WL | Delft Hydraulics (in co-operation with Rhein Ruhr) has successfully carried out field experiments with large-scale surface screens to control the movement of water and sediment;
- In Bangladesh, India and Pakistan much experience has been gained by 'bandalling' (screens) to control the secondary movement of sediment and water. This practical experience is important for further research on the theoretical description of the hydraulic and morphological processes due to screens;
- The problems related to the sedimentation of the Gorai River offtake of the Ganges River most probably have been caused by secondary hydraulic and morphological river dynamics processes during and after the Ganges peak and high monsoon flows;
- The General Consultant (HASKONING/DHV) for the Gorai River Restoration Project (GRRP) will investigate the feasibility of the application of vanes and screens to restore the dry season flows in the Gorai River. In the short term the design process of GRRP will benefit from the 'state-of-the-art' knowledge and experience as available within Delft Cluster;
- WL | Delft Hydraulics has carried out substantial research (literature studies, scale model tests) on river dynamical processes induced by bottom vanes. This research has resulted in a first model description of the processes involved.

1.2 Objectives of study

Short term objectives:

1. report and publication of the 'state-of-the-art' knowledge concerning the hydraulic and morphological processes induced by bottom vanes (type 1 bottom vanes with small angle to the main flow direction);
2. implementation of present bottom vane description (type 1) in Delft3D-Mor;
3. CFX computation (full 3D flow simulation) to support the development of type 2 surface screens and bottom screens with large angle to the main flow direction;
4. development and implementation of type 2 screen description (surface screens and bottom screens) in Delft3D-MOR;
5. application of Delft3D-MOR with type 1 vane description to curved-flume tests with type

1 bottom vanes;
6. application of Delft3D-MOR with type 2 screen description to bifurcation problem;
7. application of Delft3D-MOR with type 1 vane description and / or type 2 screen; description to Gorai River Restoration Project (Bangladesh);
8. analysis and evaluation of the obtained results for type 1 vanes and type 2 screens.

Long term objectives:

1. improvement of the description of hydraulic and morphological processes induced by vanes and screens;
2. supporting CFX computation of the 3D flow near type 2 screens;
3. implementation of the improved descriptions in Delft3D-Mor;
4. application of the improved descriptions on (i) flume tests, (ii) bifurcation (bottom screens), (iii) bifurcation (surface screens), (iv) Gorai River Restoration Project (Bangladesh);
5. analysis and evaluation of the obtained results for the improved type 1 vanes and type 2 screens and search for further developments;
6. evaluation of potential applications for controlling the hydraulic and morphological processes related to the development of side-channels, groin sections and bifurcations.

The project was executed in the period 2000-2003 by WL | Delft Hydraulics, TU Delft (Delft Cluster Partner) and Royal Haskoning.

1.3 Modifications with respect to the original project plan

The activities envisaged at the outset of the study were :

1. 'State-of-the-art' publication in a 'peer-reviewed' international journal (November 2000):
   - flume tests in HRI Egypt and in WL | Delft Hydraulics;
   - bottom vane description in RIVCOM;
   - application on the Hulhuizen Waal river bend improvement project;
   - Wiersma's MSc thesis;
   - flume tests WL | Delft Hydraulics 1998-1999;
   - shortcomings present bottom vane description;
2. Implementation of present bottom vane description (type 1) in Delft3D-Mor; development and implementation of screen description (type 2) in Delft3D-Mor (September 2000);
3. Application in Gorai River Restoration Project (December 2000);
4. Application in flume tests and bifurcation problem (January 2001);
5. Evaluation and reporting of experiences (March 2001);
6. Improvement of type 1 and type 2 descriptions and implementation in Delft3D-Mor (June 2001);
7. Application of the improved type 1 and type 2 descriptions in Delft3D-Mor on (a) the flume tests, (b) bifurcation, (c) Gorai River Restoration Project (April 2002);
8. Evaluation and reporting of experiences with improved type 1 and type 2 descriptions (June 2002)
9. Publication on the 3D-descriptions of vanes and screens and their potential benefit to river management (channel development, bifurcations, etc.) and conclusions and recommendations for further research (June 2002).

Besides of a time delay of about 8 months all activities have been carried out. However the first part of the project took significant more time than was planned. Therefore the model corrections foreseen to be determined after the first project part and to be implemented in the second part are restricted to a small number of modifications. Furthermore the update of the model of the type 2 vane requires physical experiments which were not planned within the present project.

1.4 Approach

The project 'Vanes & Screens' is directed on the research of hydraulic and morphological processes involved in the case of installation of vanes on an alluvial bed.

Two types of vanes are distinguished:

Type 1: relatively small, submerged vanes placed at small angles with the main flow and intend to affect downstream the spiral motion and the bed level;

Type 2: relatively large submerged or surface vanes affecting the nearby area of the vane by blocking and redirecting the flow and/or the sediment transport.

In the past attention has been focussed on type 1 vanes only, with respect to physically testing of both hydraulics and morphology and to the development of a morphological modelling system including vane effects. An update of the code and an extension the test case set are the main items within the present project. Furthermore an article of the state-of-the-art of this type of vanes is given based on previous work carried out at WL | Delft Hydraulics.

The type 2 vane is a new concept, which is introduced, in the present study. Attention will be paid to the modelling of this vane type and to the basic tests to judge the results obtained by this concept.

In the present study there was no room for the execution of physical tests. Therefore the results of the test cases obtained by numerical simulation could not be verified.

In Chapter 2 the vane models are introduced roughly and the choice of the morphological modelling system used to implement the vane options is explained. In Chapter 3 attention is paid to the vane of type 1 with respect to implementation and applications to the 'curved flume' tests and the 'Gorai' model. In Chapter 4 the choice of the model of type 2 vanes is clarified and the implementation and the test results are discussed. In Chapter 5 conclusions and recommendations are given. In the appendices several details of the models will be given.

1.5 Results

Within the project the following main results have been obtained.

The morphological system Delft3D-MOR has been updated with respect to the type 1 vane option. Its application range has been extended to suspended sediment transport. A repetition of a set of test cases concerning the 'curved flume' model with the updated code shows no significant changes of the simulated bed level.

The updated code has been applied to a prototype test case being the Ganges/Gorai bifurcation. The monsoon simulation shows the effect of vanes placed additional to other works on the sediment transport to the Gorai. As the vanes are placed space-fixed at the bifurcation morphological simulations were carried out to show the effect of the large-scale upstream variation of the flow direction within a period of thirty year.

A computational model of type 2 vanes has been developed, based on the levees and weirs approach in a depth-averaged flow. The model has been implemented in the Delft3D-MOR code. A number of test cases has been carried out to check the type 2 vane model.

A report has been prepared to discuss measurements carried out previously in the sand flume on a vane in relation to the vane model of Odgaard.

A publication has been prepared to present the morphological simulation model and the measurements on vanes carried out at WL | Delft Hydraulics. Furthermore a publication has been prepared to

comment the application range of vanes within river engineering and river management.

1.6 Conclusions and recommendations

The morphological modelling system extended with the type 1 vane option can be applied to support decisions on the use of vanes. In the case of a flow in a curved flume, where measured model results are available, the vane affected bed level could be computed quantitatively in a reasonable way. In the case of the prototype model Ganges/Gorai in which not a vane-affected bed level has been measured, the qualitative results correspond to the expectations.

The type 1 vane model can be refined, especially with respect to the near-field description. However from a detailed comparison of the model results and the measured data, the model appears to be suitable for practical application. Knowledge of the model restrictions is recommended when the model is used.

The type 2 vane model presented here is a first step to a vane with a main effect on flow and sediment transport direction and on the near-field bed level. The neglect of the effect of the wake in the case of this vane is questionable. The application of this model with respect to advisory work is still too premature.

With respect to further research the next recommendations can be given:

- Extend the number validation tests so that the computed bed level can be checked for both types of vanes;
- Extend the type 1 vane model to large flow angles. A revision of the near field description is advised;
- The model of type 2 vanes has to be tested in more detail, both with respect to the flow distribution around the vane and with respect to the morphology. Physical experiments are required to judge and adapt this model.

Furthermore it is recommended to extend in the short term the central maintained modelling system Delft3D-MOR with the type 1 vane option.

1.7 Prospects

Vanes and screens can be used for fairway improvement, protection against bank erosion, sediment control at intakes, maintenance of alluvial channels and control of the morphological development of bifurcated river channels. Application in the form of “bandalling” has a long tradition in South-Asia. In the former Soviet Union, the possibilities of both standing and floating screens have been studied extensively, constructing and testing them in several rivers. The applicability of Type 2 screens is limited to rivers with clear vertical gradients in the concentration of suspended sediments, where the screens can effectively divide relatively clear water from sediment-laden water and bedload. Type 1 screens do not have this limitation. The new numerical tools developed in the present project enhance the existing practical knowledge, thus providing a solid basis for cost-effective design and extension to innovative applications. This section explores the prospects for using Type 1 bottom screens as fairway improvement measures and Type 2 floating screens as temporary measures for river training and the maintenance of secondary channels.

Figure 1 Improved high-water bandals under construction in the Brahmaputra-Jamuna river, Bangladesh

Figure 2 Improved high-water bandals during flood in the Brahmaputra-Jamuna river, Bangladesh.

In the Netherlands, Rijkswaterstaat Directie Oost-Nederland (DON) has started preparations for the construction of Type 1 bottom vanes to improve the navigability of the sharp Hulhuizen bend in the river Waal near Doornenburg. The underlying idea is as follows. River bends give rise to a natural spiral flow which creates outer-bend pools and inner-bend point bars. The water depth is usually sufficient in the pools, but the width of the zone of sufficient depth may be too small in such an asymmetric cross-section. Fairway improvement in river bends therefore aims at making cross-sections more symmetrical. This decreases the largest depths, but makes the depth required for navigation available over a larger width. Bottom vanes make cross-sections in river bends more symmetrical because they generate a concentrated spiral water motion that counteracts the effect of the natural spiral flow. The current preparation works by Rijkswaterstaat DON have been preceded by extensive

physical and mathematical model tests. Bottom vanes are found to be more effective, less expensive and less harmful to river ecology than alternative measures of fairway improvement. As the concentrated spiral water motion of a single vane remains confined within a narrow zone, batteries of parallel vanes need to be installed.

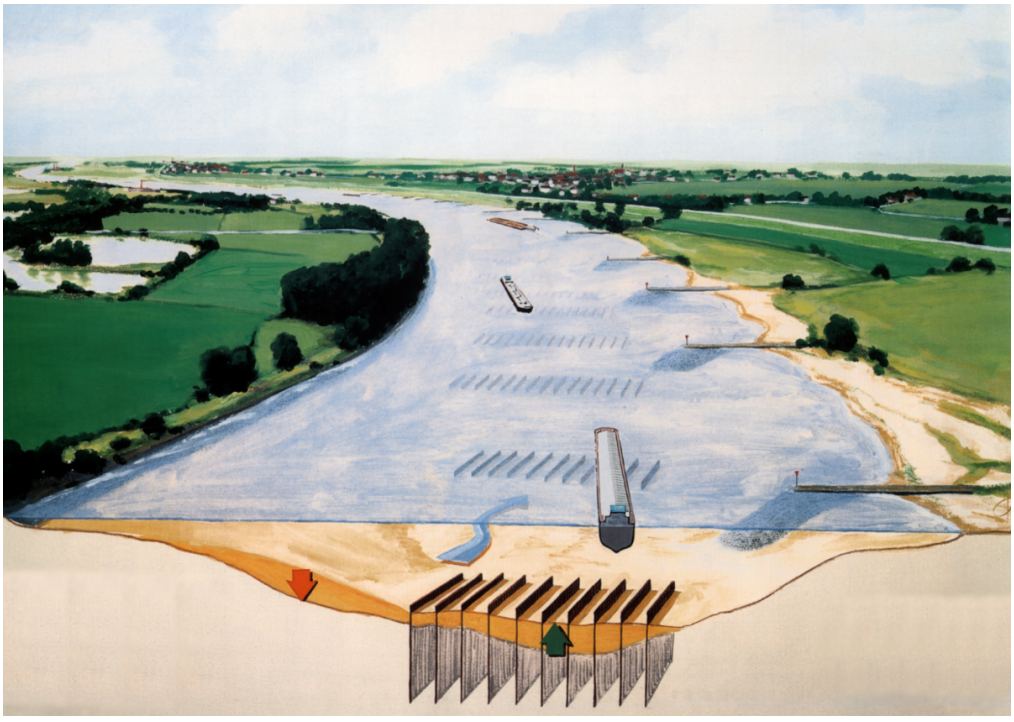

Figure 3 Batteries of bottom vanes to improve the navigability of river bends (artist impression Kees Nuijten).

The present practice in the river Waal and other Dutch branches of the river Rhine is that river bends are kept navigable by dredging. As the natural processes in the rivers gradually restore the original bed topography, dredging needs to be repeated regularly. In the future, this will be necessary more often, if, in accordance with present expectations, low discharges will occur more frequently and shipping will impose higher demands on navigability. As dredging involves costs and by itself hinders navigation, more structural measures are becoming mandatory. This is the rationale for the current preparations to construct Type 1 bottom vanes in the sharp Hulhuizen bend. It is likely that more bends will follow.

Rijkswaterstaat Dienst Weg- en Waterbouwkunde (DWW) is considering the use of Type 2 floating screens as temporary measures. Screens composed of geotextiles mounted on a frame might be a cost-effective solution for this, as long as they are designed with care and as long as the various possible loads are not underestimated. Rijkswaterstaat DWW has summarized field experiences and has drafted a design method for floating screens. In the nineties, the German-Dutch-French-Bangladeshi consortium “Jamuna Test Works Consultants” has tested the performance of floating screens in the Brahmaputra-Jamuna river. The vision behind these tests is that channels responsible for aggressive bank erosion may be closed and hence rendered harmless by overloading them with sediment. For the large braided and anabranched Brahmaputra-Jamuna river, this is called “Active Floodplain Management”.

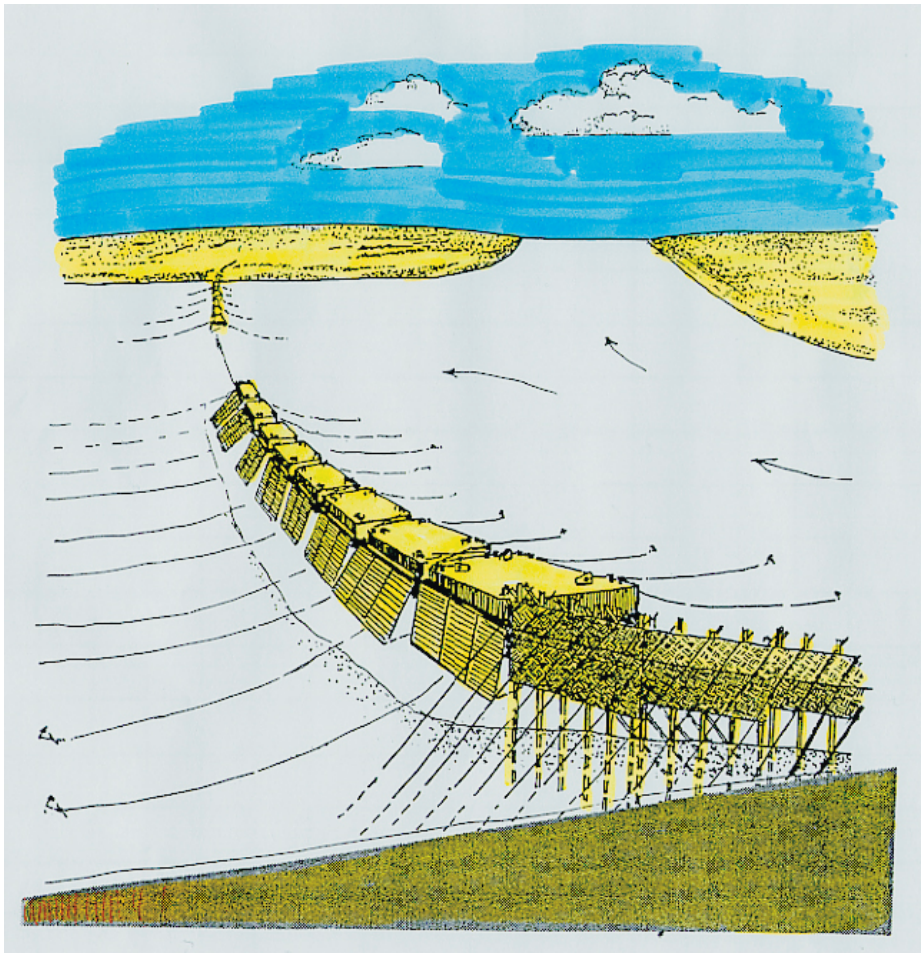

Figure 4 Vision of floating screens for Active Floodplain Management in the Brahmaputra-Jamuna river, Bangladesh (artist impression Maarten van der Wal).

Figure 5 Floating-screen test by Jamuna Test Works Consultants using vertical screens mounted between country boats

A particular possibility to apply floating screens in the Netherlands arises from the expectation that the design flood levels of rivers in the Netherlands will continue to rise. A policy of continually raising the dikes is in the long run not sustainable. That insight has led to the new policy of Room for Rivers, to a large extent based on lowering and relandscaping of floodplains. Secondary channels play an important role in the corresponding plans, but predicting their morphological development is notoriously difficult. Too much erosion produced shoals in the fairway. Too much sedimentation reduces the lifetime of the secondary channels and hence their contribution to a sustainable solution. This poor predictability is the reason why secondary channels are designed with sills or weirs to keep the morphological development under control. The original objective of secondary channels was, however, to allow more freedom for Nature to take its course. That is why sills and weirs are actually

undesirable. Preferably, Rijkswaterstaat would let secondary channels develop freely as long as possible, interfering only every now and then, if necessary. A suitable tool of interference might be the application of floating screens (Mosselman, 2003). By positioning them appropriately in the channels during minor floods, erosion and sedimentation may be induced according to some pre-defined scheme. Nature will do the actual work. As floating screens can be transported easily from one place to another, they constitute a flexible and cost-effective tool.

2 Description of vanes and screens

2.1 Introduction into physical aspects of vanes and screens

A vane or screen is a construction placed in a water flow to affect the flow and consequently to affect the bed level in the case of an alluvial bed. The vanes considered in the present study are considered including their effect on the bed level. Primarily these vanes are applied to affect the bed level. For example vanes can be applied in a river bend: The natural bed level shows a transverse slope generated by the spiral motion of the flow. Vanes can reduce this bed slope and therefore increase the navigability width. In this way vanes can be used as an alternative of a local fixed bed or of local dredging. The low increase of the flow resistance by the presence of vanes may be a reason for the choice of this alternative. Different applications of vanes can be considered.

A vane is a vertical plate blocking the incoming flow and allowing the flow to pass partially around the plate. The flow is passing partially, because the flow can not pass below the plate in the case of a bottom vane or flow over the plate in the case of a surface vane. Generally the angle of flow attack between a vane and the undisturbed incoming flow will be small. Behind and downstream of a vane a rotating wake is generated by the passing flow. The rotating flow has an axis approximately parallel to the main flow direction. The near bed transverse flow velocity component of this rotation normal to the mean flow direction essentially affects the transverse bed slope. This component may increase or decrease the corresponding flow component of the spiral motion and therefore changes the sediment transport direction and the transverse bed slope. In the case of a sufficient number of vanes a significant bed slope modification can be obtained. Apart of the wake related change of the sediment transport direction, outside of the wake an area will be present where the flow field is significantly affected by the vane and consequently the sediment transport direction. In the case of a large vane this latter area may be the dominant reason of the vane impact on the bed level.

The magnitude of the effect of a vane on the bed level depends on the angle of flow attack on the vane and on the vane dimensions. Generally a field of vanes may be applied. The interaction between the vanes will affect their effectiveness.

Near the vane scour will be generated by the flow and when placing a vane this effect has to be accounted for. Besides of this local scour large scale bed level variation will be generated and only this effect will be considered in this study.

Vanes are applied in prototype. Sometimes bamboo screens have been applied to arrive at the same effect on the bed level as described above. In this study vanes are assumed to be impermeable, whereas screens may be permeable by fabrication imperfection. In the sequence the notion ‘screen’ will be dropped, as the notion ‘vane’ will cover sufficiently the intended construction concept of a screen.

2.2 Mathematical description of effects of vanes on flow and morphology

The vanes to be considered in the present study are divided in two types.

Type 1:

Vertical submerged vanes mounted on the riverbed making a small angle with respect to the main flow direction. The aim of these vanes is to affect the downstream bed slope transverse to the main flow direction, without affecting the main flow too much. Each vane generates one vortex line. The vane-induced vortex lines cause the change of the sediment transport direction and therefore of the bed slope. Local effects of these vanes can be neglected.

Type 2:

2a Vertical submerged vanes making not necessarily a small angle with the main flow. These vanes will change the original sediment transport direction (especially bed load) at their locations, parallel to their direction. No significant change of the main flow direction occurs as the flow is passing mostly over the vanes.

2b Vertical vanes piercing through the water surface and making not necessarily small angles with the main flow. These vanes are free from the bed. These vanes will modify mostly the flow direction, while the direction of the sediment transport will not be changed essentially.

2.3 Numerical description of vanes and screens

The mathematical model of a vane to be used in a morphological simulation depends on the vane type and on the chosen flow, transport and bed level models used in the simulation system. At WL | Delft Hydraulics a vane model has been developed in the past for type 1 vanes only.

In the used model a type 1 vane is described as a subgrid element, as the local blocking of the flow and the sediment transport by this vane is neglected. The only local effect accounted for is the flow resistance induced by the vane. The model assumes the generation of a vortex line by the vane at the downstream end of the vane. The vortex line runs downstream and coincides with a streamline running through the vane end. Locally this vortex line creates normal to its direction a near bed velocity which affects the present velocity component of the main flow and of the natural spiral motion. Depending on the rotation direction of the local vortex the induced transverse velocity will reduce or increase the present velocity component and affect the sediment transport direction and therefore the bed level slope. The rotation direction of the vortex depends on the angle of flow attack at the vane. The vortex strength along the vortex line damps out because of the flow turbulence. The vortex strength at the beginning of the vortex line is related to the local flow conditions and the dimensions of the vane. The used relation is an algebraic function, just as the description of the vortex strength damping function. The upper edge of the vane is fixed in space. The vane height used in the algebraic function depends on the current bed level and therefore changes during a morphological simulation.

The described vane model allows the use of a depth-averaged flow model. In this flow model the additional vane resistance to the flow has to be added to the bed friction. The transport model of the sediment transport has to be adapted with respect to the transport direction because of the vortex line effect. Furthermore the transport model will be extended with the vortex line computations. The bed level model needs no modifications.

The present model is based on the model description presented by Odgaard, 1991. In [Flokstra, 2002] the morphological simulation model is presented and comment is given with respect to the weak points of the model, based on experiments carried out at WL | Delft Hydraulics. Although the use of the potential theory to describe the flow and to derive the algebraic relations in the near field of the vane is questionable, the presented model still allows acceptable results. A mathematical model that will not use such algebraic functions requires a 3-D description of the flow past the vane. Although existing models allow such 3-D computations, the effect on the required computational time is rather large, especially in the case of morphological computations. In the present model the vane dimensions have to be small with respect to the grid increments, while in the 3-D approach the grid increment has to be small with respect to the vane dimensions, whereas the third dimension has to be added. Clearly the number of required grid points in a 3-D computation increases significantly with respect to the present model.

Contrary to vanes of type 1, vanes of type 2 essentially operate locally and therefore a subgrid approach will not be suitable. The possible vortex lines in the far-field are neglected. Again a 3-D model would be possible and simplify the modelling but again a time-consuming morphological model will originate. Therefore a mathematical model has been designed based on the depth-averaged flow model, joining the experience of modelling levees and weirs in such a model. In the present model the used expression concern sharp-crested weirs. The effect of the vane on the sediment transport is by blocking and redirecting the bed load transport and by reducing the suspended sediment transport in the direction perpendicular to the vane.

In the morphological model a back coupling occurs of the bed level variation on the flow field and on the vane dimension.

The presented vane types have a primary effect on the bed load transport and a secondary effect on suspended sediment transport.

Details of these models are given in the Chapters 3 and 4 and in the Appendix A.

2.4 Selection of model system

The development of a morphological modelling system concerns a rather large effort, certainly compared to the effort to implement the vane options in it. Therefore an existing model system will be used.

Since some decades morphological modelling systems has been developed at WL | Delft Hydraulics. Because of the knowledge of the own systems and the possibility to extend and to support these systems, an in-house modelling system is to be preferred and will be chosen to extend for the vane options.

The next morphological modelling systems has been developed in historical sequence:

SEDIBO	First research model.
RIVCOM	Integrated model based on flow model ULYSSE. This model contains the type 1 vane option. This model is no longer maintained.
Delft3D-MOR	Modular system, present WL standard.
Delft3D-OnlineSED	Integral system based on Delft3D-FLOW.

Delft3D-MOR is one of the Delft3D models maintained, supported and extended by the service and support group of WL | Delft Hydraulics. From these centrally supported models a number of dedicated versions have been derived, which are not maintained by this group and therefore tends to age fast. Besides of the model RIVCOM, one of the dedicated versions derived from Delft3D-MOR concerns type 1 vanes too, and belongs to the set of Delft2D-rivers programs and needs urgently to be upgraded to match to the new Delft3D-MOR and to allow the new FLOW input format.

At the start of the present project the Delft3D-OnlineSED version was still in an experimental stage, but will be maintained in future by the central service/support group too. Therefore basically one of these two modelling systems had to be chosen: Delft3D-MOR or Delft3D-OnlineSED. However, because of the experimental stage of the Delft3D-OnlineSED system, there was no really free choice. The system Delft3D-MOR has been chosen for the vane model extensions.

If both systems were available at the start of this project, still the system Delft3D-MOR would be

preferred. In [Flokstra, Jagers, Wiersma, Jongeling, 2002] a detailed discussion has been given to found the choice. The type 1 vane option has already been fitted to Delft3D-MOR and requires a restricted effort to update. The chosen model of a type 2 vane fits in the same system, as in both cases the depth-averaged flow description is used. Furthermore the Delft3D-MOR system allows a much general choice in the definition of the morphological process than Delft3D-OnlineSED.

If a 3-D description of the flow past a vane would be required, the Delft3D-OnlineSED system would be a more serious candidate. However even in this case it is questionable as the hydrostatic pressure approach used in the flow model would not be sufficient accurate to describe the flow past a vane. Furthermore the used vertical grid distribution (sigma transformations) generates in time changing grid lines that do not fit to the different and fixed top edges of the vanes.

3 Development of type 1 bed vanes

3.1 Introduction

Since 1987 submerged vanes of type 1 have been studied at WL | Delft Hydraulics both with respect to mathematically modelling and physical experiments, as listed below:

- morphological testing of vanes in a physical model;
- testing of single vane effects on a flow and of vane interaction;
- development of a computational morphological model system accounting for the effect of vanes;
- application of the computational to model and prototype situations.

In the next sections the computational model will be considered and morphological simulations will be presented for two configurations. At WL | Delft Hydraulics simulations has been executed for the 'curved flume' case. For this case physical experiments with vanes have been carried out to determine the effect of a set of vanes on the sand bed of the flume. These data have been used to calibrate the vane model. Furthermore simulations with the computational model have been carried out by Royal Haskoning on the Ganges / Gorai bifurcation as a part of the 'Gorai River Restoration Project'. The aim of these simulations is to study the use of vanes to reduce the sediment transport from the Ganges to the Gorai and to reduce the sediment load on the Gorai.

3.2 Description of type 1 vanes

The application of submerged vanes in a morphological modelling system has been applied first at WL | Delft Hydraulics in the RIVCOM system. The used vane model concerns type 1. In section 2 a rough description of the model has been given. Details of the model are described in Appendix A. Below some remarks are given on the weak points of the vane model

The mathematical model of type 1 vanes has been proposed by Odgaard et al. A vane is supposed to be a wing to which the usual wing theory applies. Therefore the proposed relations between the initial vortex strength and the incoming flow and the vane dimensions are derived from potential theory, which is used to describe the flow. Experimental tests with a physical model show the insufficiency of these assumptions. The potential theory including the Kutta-Youkovsky condition suggests a vortex line originating at the end of the vane, while the measurements show a lee side wake of the vane which is continued downstream of the vane and is the real 'vortex line'. In fact the used relation between the vortex strength just downstream of the vane, the vane dimensions and the incoming flow field has to be replaced by a wake-based formula. However it is shown that the presently used formula still leads to acceptable results.

The interaction between the vanes may seriously reduce their effectiveness. Two types of interaction can be distinguished:

- The interaction between vanes in a downstream oriented row, (longitudinal interaction);
- The interaction between vane in a transverse to the flow directed row, (sidewise interaction).

The model accounts for the first kind of interaction as the vane-generated vortex lines affect the local incoming flow conditions of a downstream located vane and therefore the angle of flow attack on the vane. The second type of interaction has to be corrected by a calibration factor. In the model this reduced effectiveness of the vanes by sidewise interaction is realised by the underestimation of the initial vortex strength. In [Flokstra and Wiersma, 1997] these interactions as present in the

mathematical model have been compared to experimental flow results and without a correction of the sidewise interaction correct transverse vane-induced velocities were obtained. The interaction between vanes placed in some grid configuration generally reduces their effectiveness

The adaptation of the morphological model in the case of type 1 vanes concern:

- the use of the vane-induced flow resistance additional to the bed resistance in the flow module;
- the correction of the spiral motion strength in the sediment transport direction in the transport module;
- the use of the corrected spiral motion strength in the suspended sediment transport computation;
- the computation of the initial vortex strength and vortex damping, of the vortex lines and of the vortex influence area .

The differences between the vane approach in RIVCOM and in Delft3D-MOR do not concern essential points. All options of RIVCOM are available in Delft3D-MOR. Some options are extended and some restrictions of RIVCOM have been removed:

- The location of a vane is not restricted to a grid point;
- The location of a vortex line is not restricted to grid line but follows a stream-line;
- The distribution of the vane induced transverse velocity allows different choices;
- The decrease of the vortex strength along the vortex line can be computed with space steps smaller than the grid step;
- Several vane options can be specified by the user;
- Vanes can be combined with suspended sediment transport.

The modifications of the dedicated vane version derived from Delft2D-rivers and the present version concern:

- The use of the most recent MAIN, TRANSP and BOTTOM modules;
- Modification of the data input routines;
- Adaptation of suspended sediment transport.

The test cases described in the next section have been carried out with the most recent code.

3.3 Test cases

3.3.1 Introduction

To validate the current implementation of the type 1 vane option a model simulating the physical experiments carried out in the curved flume in 1987 at WL | Delft Hydraulics is used. These experimental results have been used to test the RIVCOM and proved to be successfully. These tests of the Delft3D-MOR code are described in section 3.3.2. Furthermore type 1 vanes are applied to a model of the bifurcation of the Ganges and the Gorai in Bangladesh. A description of the model and the results are given in section 3.3.3.

3.3.2 Curved bend tests

3.3.2.1 Description of the computational model and tests

In the investigation Q98 carried out at WL | Delft Hydraulics, the effect of submerged vanes on an alluvial bed has been determined in the case of a curved flume. This model consisted of a straight inflow channel followed by a 140° bend and a straight outflow channel. All channel parts have the

same width. Table 1 shows the dimensions of the bend and Table 2 the steady flow conditions.

Quantity	Dimension
Width of the flume	2,0 m
Length of straight inflow flume part	5,.25 m
Length of straight outflow part	15,0 m
Bend part	141°
Radius of curvature of flume axis	11,75 m

Table 1 Description of the flume dimensions

Quantity	Dimension
Discharge	0,09 m³/s
Water depth	0,106 m
Average flow velocity	0,425 m/s
Chézy coefficient	27,66 $m^{0.5}$/s
Grain size D_{50}	0,78 mm

Table 2 Overview of reference values used in all morphological simulations for the curved flume

Two vane configurations have been applied: 10x4 vanes and 19x4 vanes. The dimensions of all vanes are identical, as indicated in Table 3 and the height of the vanes with respect to the initial bed level is the same. The initial bed level is horizontal in each transverse section and the bed slope along the channel axis equals the equilibrium slope. Morphological simulations have been carried out starting from this initial bed.

Vane characteristics	Value
Vane length	0,16 m
Level of upper vane edge *	0,0 m
Angle between vane and flume axis	15°

Table 3 Overview of reference values of the submerged vanes used in the morphological simulations.(with respect to the equilibrium bed level along the flume axis)*

In the present computations the fine grid has been applied being equal to the RIVCOM grid. The present computations only concern the 19x4 vane configuration, as their purpose is to determine whether the code update does not affect the known results. Table 4 shows the vane configuration and Table 5 the computational grid.

Vane configuration (experiment T7,Q98)	Value
Number of vanes in a transverse section	4
Number of vanes in a longitudinal section	19
Longitudinal distance between vanes	0.75 m
Transverse distance between vanes	0.2 m
Distance of vane to bank	0.2 m

Table 4 Overview of used grid configuration in curved bend.

Grid characteristics	Value
Number of points in a transverse section	13
Number of points along a longitudinal section	198
Grid increment in a transverse section	0.25 m
Grid increment in longitudinal direction	0.2 m

Table 5 Overview of computational grid characteristics of the curved bend

3.3.2.2 Computational results

Several morphological simulations have been executed for the configuration described in section 3.3.2.1. These tests coincide with the tests carried out in past with the RIVCOM and the Delft2D-Rivers system. These tests are intended to determine whether the updated code will produce the same results, as the mathematical model is not modified. The next tests have been repeated:

bb0: curved flume without submerged vanes and a fine computational grid;

bb2: curved flume with 4x19 submerged vanes, fine computational grid and vortex lines coinciding with the grid lines;

bb4: curved flume with 4x19 submerged vanes, fine computational grid and vortex lines coinciding with the stream lines;

The computational grid is shown in Figure C-1. The computed equilibrium bed level is shown in the Figures C-2 and C-3. The computed bed levels are given along two longitudinal sections, 0.3 m of the inner bend and 0.3 m of the outer bend. The equivalent results of the previous computations are presented in the figures too, but coincide with the newly computed bed level. This means that no model modifications have been introduced in the new code of the modules FLOW and TRANSP, as far as the vane model is concerned.

To show the effect of the vanes on the bed level the figures contain the equilibrium bed level originating in the case without vanes. In Figures C-4 the 2-D bed level distribution is shown for the case without vanes both the absolute values as the values relative to the initial bed level of the

simulation. In Figure C-5 the vane-affected bed level is shown relative to the initial simulation bed level and to the equilibrium bed level without vanes. This figure shows a clear decrease of the bed level in the outer bend and an increase of the bed level at the inner bend.

In the present computations the same tuning constants have been used as in the earlier computations, where a calibration was executed with respect to experimental data (WL | Delft Hydraulics, Q98, 1987).

3.3.3 Gorai River

3.3.3.1 Description of the computational model and tests

The 'Gorai River Restoration Project' carried out by a consortium with Royal Haskoning as lead firm contains among others a study to determine whether submerged vanes can reduce sufficiently the sediment transport from the Ganges to the Gorai river. The application of vanes is intended to be an additional measure to other training works. Appendix D contains the full report on the vane simulations with Delft3D-MOR. The present section contains the most important results of this study.

The 2D-model used in the study concerns the bifurcation area of the Ganges and the Gorai. The model area covers the Ganges from 4 km upstream to 4 km downstream of the bifurcation and 5.3 km of the Gorai. Upstream of the bifurcation a constant discharge has been imposed, 38950 m^3/s, being 95% of the Ganges discharge. Downstream fixed water levels are imposed both in the Ganges and the Gorai. The bed level measured in October 2000 is used as initial bed level for the Ganges, while the bed level measured in June 2000, containing a dredged bed channel is used in the Gorai. This data set is used, as in October a large siltation of the channel takes place. A constant overall roughness value of the bed has been used: Chézy = 90 $m^{0.5}/s$. The sediment transport has been described by the van Rijn formula, as an important part of the sediment transport consists of suspended sediment transport. As characteristic grain size has been chosen: in the Ganges 190 μm and in the Gorai river160 μm, where in the transition area near the bifurcation an interpolation between these values has been applied.

Contrary to previous considerations (Lesleighter, febr. 2000) to apply type 2 vanes, the present study has been carried out with type 1 vanes. These vanes have been located near the bifurcation on a field of 1500 m x 200 m, 220 vanes of equal length 16 m. The computational grid comprises 55x165 points, having as minimal cell dimensions 30 m x 30 m. Clearly the applied vanes have subgrid dimensions.

The effect of the vanes on the bed level depends on the angle of flow attack on the vane. Therefore the test cases have been selected to account for the large-scale variation of the flow direction within the last 30 years to investigate the angle sensitivity. The vane directions are assumed to be fixed in this period, while the incoming flow direction will change. Usually the used computational model of the type 1 vane is applied to small angles of flow attack. In the present test case large angles may occur. Assuming the vane to be less effective in the case of flow separation the effect of the vane is dropped when the angle of attack exceeds 22°. The computational model concerns three flow cases with respect to the flow distribution at the upstream Ganges boundary:

Case A	the main channel runs from the east side along the right bank to Talbaria (1997-2000);
Case B	the main channel runs from the northeast side to Talbaria (1985-1987);
Case C	the main channel runs from the north-northeast side to Talbaria (1985-1987).

In the case A the initial bed level is obtained from measurements. In the cases B and C the initial bed in the upstream part of the Ganges is adapted with respect to case A to account for the changed flow direction.

For each of the three cases A to C the following variants have been tested:

- Case without works;
- Case with training works only: offtake guide and offtake divider;
- Case with training works and bottom vanes.

In model A the direction angles of all vanes are chosen to make an angle of flow attack of 13° with respect to the initial local flow direction. In the cases B and C the absolute direction angles of the vanes is taken from case A.

The calibration has been executed in such a way that the model can serve as conceptual model to determine the effect of the measures on the bed level and sediment transport. First the flow model has been calibrated and finally the morphology, using available experimental data. Concerning the submerged vanes no calibration has been executed as no data are available with respect to the Gorai and the tuning data of the 'curved flume' are applicable for this case too.

After the calibration of the model the initial bed level of the several morphology simulations is composed in the following way:

The bed level used during the calibration runs is used as initial bed level of a morphological simulation, which is continued, till an equilibrium bed level occurs. The initial bed level of the next runs is composed of the simulated equilibrium bed level of the Ganges combined with the June 2000 bed level of the Gorai. This procedure has been applied to prevent model deviations of the Ganges to be dominant for the Gorai area.

3.3.3.2 Computational results

The computational results concern the simulation of the monsoon period of 4 months. In the appendix E the bed levels occurring after 1, 2 and 4 months are shown.

The change of the sediment transport ratio and the discharge ratio of the Ganges and the Gorai during the simulation for each of the cases A to C are shown in the figures 5.2 to 5.4 of Appendix E.

Clearly the effect of the vanes on these ratios depends on the case (A to C). In case A the effect of the vanes is about 10 to 20%, while in case C the effect is negligible. The change of the discharge ratio in the cases A and C is opposite: in case A the discharge ratio decreases during the simulation, in the case C it increases. In case B an average tendency can be observed. This behaviour can be explained by the used vane model: In case A the angle of flow attack on a vane is about 13°, in the case C the angle of attack exceeds the imposed limit angle which stops the vane activity. In case B the effective angle of attack increases by 7° to 10° and therefore the vane activity increases with respect to case A.

Generally the effectiveness of the vanes depends on the occurring angle of flow attack, but it depends on the type of sediment transport too. Primarily a vane is effective for bed load transport. In the present case mainly suspended sediment transport occurs, while in the case of suspended sediment transport its rate and the vertical distribution of the sediment concentration will have a significant effect on the vane effectiveness. The more uniform a vertical concentration distribution becomes, the less effect the vane-induced vortices have on the transport direction.

At a number of locations the computational model shows a not expected behaviour, such as a flow circulation in the Gorai near the bifurcation. A reason for this effect may be the simple roughness description, being a constant Chézy value for the whole area. Furthermore this area shows a stronger sedimentation than observed in reality. Besides of the locally deviating flow the used transport relation may be a reason for this effect. The morphological model can be improved for these deviations, however these improvements will not directly affect the vane effectiveness.

The introduction of vanes in the cases A to C shows a reduction of the relative sediment transport, as could be expected. Data to judge the rate to which this effect occurs fail.

3.4 Evaluation of the type 1 vane results

The update of the type 1 vane option in Delft3D-MOR has been carried out. The morphological computations previously carried out for the curved flume could be successfully reproduced without an adaptation of the tuning constants. This means the vane model reasonably reproduce the measured bed level. The required tuning constants range within physically realistic bounds.

The model has been applied to a prototype location: the Ganges/Gorai bifurcation. The available experimental data have been used for the calibration of the morphological model. In this case no vanes were present in the prototype. With respect to the vanes the 'curved flume' calibrated parameters have been used. The morphological simulations in the case of vanes show effects on the bed level and the sediment transport as may be expected qualitatively. Because of the lack of experimental data in the case of vanes no quantitative conclusion could be drawn.

The computations carried out in this study show the mathematical model describing vanes of type 1 to be suitable for a morphological simulation model. As no additional experimental data were available no further qualitative validation could be carried out. The restrictions of the vane model as known from physical experiments could not been considered closer in these simulations.

3.5 Possible improvements

The simulations carried out with the Gorai model show the next points to be improved:

- Improvement of the computer code in case of flooding and drying with respect to the robustness of the vortex-line and influence area computation;
- A large angle of flow attack on a vane at least generates flow resistance, which has to be included in the model. Furthermore [Marelius, 1998] concluded from experiments a maximum effect on the bed level at an angle of 40° with respect to the vane-induced momentum and a maximum vane-induced transverse bed slope at an angle of 45°. Clearly, dropping the effect of a vane on the bed level if the angle exceeds 22° is an insufficient description and has to be improved.

Further recommendations are:

- Improvement of the relation between the 'vortex strength' generated by a vane, the vane properties and the incoming flow field;
- Extending validation of the vane model for cases with known experimental determined vane-effected bed levels.

4 Development of type 2 vanes

4.1 Introduction

Vanes of type 2 have not been considered in research of WL | Delft Hydraulics and literature till now. In a note of Lesleighter (February 2000) a type of vanes has been considered in the Gorai study, deviating from vanes of type 1. In the present study that type of vanes are indicated as type 2 vanes. At the start of the present project this note was the most recent note on the choice of vanes in the Gorai project.

In the sections 2.2.2 and 2.2.3 a short description of type 2 vanes has been given. In the next sections 4.2 to 4.4 this type will be discussed in more detail. Within the present project there was no room for physical experiments, therefore the model has been based on theoretical considerations. The model chosen in section 4.3 has been implemented in the morphological modelling system. Simulations have been carried out to judge the correctness of the model. In section 4.5 tests are described for a vane in a straight channel and at the bifurcation of two channels.

4.2 Starting points of model choice

4.2.1 Introduction

In the next sections a computational model of a type 2 vane is chosen. To a large extent the definition of this vane type depends on the considerations carried out by Royal Haskoning in the 'Gorai River Restoration Project. The type specification is believed to be sufficient general and different from a type 1 vane to justify a new type.

At one of the Ganges bifurcation's the river Gorai originates. At the inflow side of the Gorai River sedimentation occurs with a tendency of the closure of this river, while even in the low water case a channel in the Gorai has to stay open for sufficient water supply. Recently attention has been paid to solve this sedimentation problem by the use of vanes. Two different suggestions have been indicated:

- The sediment transported by the Ganges and entering the Gorai has to be transported to the right bank of the Gorai to keep open the channel near the left bank of the Gorai;
- The sediment tending to enter the Gorai River has to be transported to the Ganges. The discharge entering the Gorai has to be guided as much as possible to the channel at the left side of the Gorai.

To reach these aims two possibilities with vanes have been considered: Using about 500 vanes of type 1 or using a very restricted number of type 2 vanes. This latter possibility has been proposed in february 2000.

The siltation occurring in the Gorai has to be reduced by 6 vanes, each with a length of about 500 m. This vane length is large compared to the type 1 vane length of 16 m. The proposed vane height is rather large. At a discharge of 12000 m^3/s the upper edge of the vanes equals the water level, where the yearly average discharge amounts to about 11000 m^3/s. During a part of the year these vanes will pierce through the water surface. Therefore the vanes will affect both the flow and sediment transport direction.

Aware of the principles of type 1 vanes Lesleighter suggests applying a vane without the use of the generated vortex line. The proposed angle of attack amounts about 20°.

Several vane constructions were mentioned:

- Closed vane plates
- Row of piles (permeable)
- Rubble mount dams

The upper side of the vane may show a non-zero slope.

It has to be determined whether the action ascribed to this vane type (2) as described in the note is correct. Furthermore alternatives to solve the sedimentation problem may involve vanes of type 1 too. It is not clear whether the sediment, which is deposited now near the right-hand bank of the Gorai, will pass the Gorai offtake by the action of type 2 vanes. Possibly the vortex action of vanes of type 1 will be required to reach this goal.

Besides of the sedimentation problem in the Gorai River, the left bank of the Ganges upstream of the bifurcation (located at the right-hand bank of the Ganges) has to be protected against erosion. One of the possible solutions is the use of a large set of type 1 vanes.

The sediment transport in the Ganges and the Gorai consists to a large degree of suspended sediment. Till now the development of the computational model of the vanes (type 1) is directed to bed load or total transport. In the case of suspended sediment a vane is less effective than in the case of bed load:

- A part of the sediment will be transported over the vane in the case of vanes of type 2 and therefore the splitting between the flow direction and the sediment transport direction will be reduced;
- In a vertical a vortex generated by a vane of type 1 will transport suspended sediment in two opposite horizontal directions normal to the vortex axis. Therefore the net depth-averaged sediment transport is reduced compared to bed load transport. This reduction depends on the vertical distribution of the sediment concentration.

4.2.2 Modelling aspects

4.2.2.1 Introduction

Below a number of computational models will be discussed which can be used to describe a vane of type 2. A model of this vane type concerns a model of the flow past the vane and a model of the morphology. In the morphology a number of problems occur that are closely related to the flow model and will be mentioned there.

4.2.2.2 Flow model

Below three flow models will be discussed.

A. A depth-averaged flow model

   A vane will be described as a weir. The wake behind the vane can not be represented correctly with respect to the velocity distribution. The energy loss caused by the wake is simulated by the use of a discharge relation concerning the flow over the vane. A surface vane can be described in the same way using an adapted discharge relation. The vane will concern several grid cells. Per grid cell the discharge relation will be applied to the local conditions. The discharge relations are described in the appendices A.3 (submerged vanes) and A.4 (surface vanes).

   The type 1 vanes use the depth-averaged flow model too. The required adaptations of the FLOW module with respect to type 2 vanes do not conflict to type 1 vanes.

Required adaptations of the FLOW module

- The weir formulas present in Delft3D-FLOW concern broad-crested weirs; vanes behave like sharp-crested weirs. Therefore in the case of type 2 vanes adapted discharge relations have to be used and implemented;
- The available discharge relations for sharp-crested vanes concern an equal bed level in front and behind the vane. These relations have to adapted as usually different levels will occur;
- The discharge relation is applied piecewise to the vane, by splitting up the vane in vane elements. Near both ends of a vane the relations have to be corrected for 3D effects;
- To determine the spiral motion intensity in a depth-averaged flow model a separate advection-diffusion equation has to be solved. In the case of vanes of type 2 internal bounds occur and therefore the scheme to solve this equation has to be modified.

Modifications of the TRANSP module

- Direction of the sediment transport near a vane;
- Determination of sediment transport magnitude near vane because of bed level discontinuity.

Modifications of the BOTTOM module

- To allow a two-valued bed level. The vane runs through bed level grid points. At such points the bed level has different values in front of and behind a vane.

Restrictions

- An arbitrary directed vane will be approximated by a staircase line because of the computational grid
- A vane consists of a series of connected vane parts, each part coinciding with a grid cell edge, oriented normally to concerning velocity component. The discharge relations apply to a flow normal to the vane. In the case of a small angle between the flow and the vane direction this approach is probably less correct.
- The discharge relations correspond to a 2DV-flow configuration. At the ends of the vanes 3D flow effects occur;
- The vortex line created by this vane type is neglected;
- The wake behind the vane has no effect on the sediment transport direction.

B. A multi-layered FLOW model

In the multi-layered flow model the vane has to be approximated by the closure of vertical grid cell planes. The vane thickness can be simulated by the use of two parallel planes at a distance of one or more grid cells. However in this case there is a flow inside of the vane that is connected to the outer flow. The friction of the vane affects the local bed friction. The number of layers has to be small to arrive at acceptable simulation times. The vane resistance produced by the flow will be incorrect because of the restricted number of layers and because of the hydrostatic pressure assumption.

The number of layers to be used in a simulation is fixed, together with the relative distribution of layer levels over the water depth (sigma transformation of the vertical co-ordinate). If the water depth or the bed level change the layer levels will change too. The upper edge of the bottom vanes and the lower edge of surface vanes are located fixed in space and can be approximated only roughly by a time-dependent location of a layer. Initially a best guess can be made of a layer level to fit a vane edge and to each vane edge a separate layer level can be allocated. The vertical layer distribution composed in this way will create an irregular vertical grid distribution. If during

a morphological simulation the bed level rises by sedimentation and the vane tends to disappear below the bed level, the relation between a vane edge and the corresponding layer level will be very poor. After each morphological time step the layer distribution has to be revised or the closed vane planes have to be redefined. In the case of a low number of layers this procedure leads to a rough approximation of the vane height. In the case of a large vane length the vane edge generally will not coincide with the layer level and a staircase line will occur.

In principle a 3D-flow model reproduces the occurring spiral motion as an inherent part of the flow field. If a low number of layers are defined the computed spiral motion may be too inaccurate to be used directly. Possibly near the vane the near bed velocity can be used, but far from the vane a depth-averaged advection-diffusion equation may still be required to describe the spiral motion intensity.

Required modification of FLOW

- Derivation and implementation of spiral motion equation valid for a two or more layers model;
- Introduction of a correction method with respect to the sigma transformation. (At the end of the present project a FLOW version exists in which fixed horizontal layers are defined and in which a hydrodynamic pressure description is applied. This approach overcomes a number of the indicated difficulties);
- Implementation of the vane roughness computation, similar to the weir approach.

Required modification with respect to the morphology:

- Derivation of depth-averaged velocity in the transport model;
- Solution of the two-valued bed level problem in the case of an thin vane.

Restrictions:

- A weak reproduction of the upper edge of a vane;
- The number of vanes to be preferred, being one;
- The simultaneous use of type 1 and 2 vanes requires additional modifications;
- Vanes are approximated horizontally by staircase lines and the upper edge too;
- The hydrostatic pressure distribution may be insufficient to reproduce the vane resistance;
- The variation of the layer level independent of an associated vane edge introduces invalid vane results;
- The disappearance of the vane below the bed level does not fit in the layer concept.

C. A fully 3D FLOW model

Such a model is not attractive at the moment because of the required computation time in the case of morphological simulations. Near the vane a hydrodynamic approach with respect to the pressure distribution will be required, which urge to solve the complete flow equations. The required number of the grid points in a vertical has to be large to describe the wake correctly. The computation time increases at least linearly with the number of points in the vertical direction.

A stand-alone use of a 3-D model may be suitable to study the flow distribution around and downstream of a vane to judge or adapt simplified flow models. Preliminary tests are described later on, where the CFX code is applied.

4.2.2.3 Morphology model

When the sediment transport is described by a formula for bed load or total sediment transport, its direction is computed as if it concerns bed load only. This means the use of the near bed flow to determine the transport direction. In the case of total sediment transport a part of the sediment concerns suspended sediment. A vane will block the bed load or transport it parallel to the vane, but at least a part of the suspended sediment will be transported over it. The extent to which the sediment is transported over the vane depends on the vertical distribution of sediment concentration. A formula to estimate the rate of sediment passing over the vane is derived in appendix A.3.2.2

The direction of the bed load transport near a vane depends on the vane direction and the bed slope. The direction of the sediment transport over the vane equals the flow direction.

A part of the sediment transported over the vane will enter the wake behind the vane by turbulent diffusion. This part will be transported in a direction related to the wake orientation. It is not clear whether this wake generates only a local scour. Such an effect is outside the scope of a Delft3D-MOR model. For the time being the effect of the wake downstream of the vane on the sediment transport is neglected.

4.3 Model choice

Below the final choice of the computational model of a vane of type 2 to be used in a morphological modelling system is given:

Flow model

A depth-averaged model is chosen to describe the flow past a type 2 vane because:

- The similarity of vanes and weirs, where the description of weirs within a depth-averaged flow model appeared to be successful since a large number of years;
- The breathing layers in the case of the 3D FLOW model as a consequence of the sigma transformation of the vertical co-ordinate do not fit well to the fixed location of the vanes upper or lower bound;
- The use of this flow model is expected to be as accurate as the use of a restricted number of layers in the case of the 3D FLOW model;
- The use of a fine layer distribution and a fine grid leads to a too large computational effort
- In the case of a 3D FLOW model and a restricted number of layers, the spiral motion intensity equation has to be used and adapted;
- A depth-averaging of the 3D-velocity will not be necessary for the TRANSP module;
- The type 1 vanes are implemented for a depth-averaged flow model, allowing the use of both vane types within one morphological simulation model.

Above the required adaptations of the FLOW module have been indicated.

Sediment transport

Both the total sediment transport module and the suspended module have to be adapted:

Total sediment transport module:

- The above-mentioned adaptations;
- Partial transport over a vane according to a given fraction or estimated by a formula.

Suspended sediment transport module:

- Introduction of the effect of the vane generated spiral motion on the depth-averaged suspended sediment transport;
- Adaptation of the concentration equation near a vane;
- Other adaptations as in the case of the total sediment transport module.

Bed level model

- The above-mentioned adaptations;
- Blocking of bed load transport by a vane, but partial sediment transport over vane allowed.

4.4 Final modifications of Delft3D-MOR

The considerations of the previous sections resulted in the next extensions of Delft3D-MOR

Extensions of the FLOW module of Delft3D-MOR

- The weirs in Delft3D-FLOW are defined at a grid point as a u- or v-weirs depending on the weir direction. A vane is defined as a series of weirs that are connected to each other. Although the vane itself is in principle a straight plane, within the grid it may be represented as a staircase line. Concerning the energy loss the real vane direction will be used;
- The 3D end effect correction of the vanes will be neglected;
- As the vane runs through the bed level points of the computational grid, different bed levels occur at the same point. In the FLOW module the averaged bed level is used;
- Extension of the input data and the reading routines;
- No spiral motion activity over the vane;
- Introduction of the vane formulas describing the energy loss by a vane element;
- Allowing special cases: the drying of the bed with a vane element, the piercing of the vane through the free water surface, the decrease of the water level below the lower bound of a surface vane.

Extensions of the TRANSP module of Delft3D-MOR

- Introduction of a sediment transport relation concerning the sediment transport over a vane;
- Modification of the sediment transport computation near a vane;
- Modifications with respect to the multi-valued bed level and velocity near the vanes;
- Extension of the communication file with respect to the sediment transport.

Extensions of the BOTTOM module of Delft3D-MOR

- Extension to the use of a multi-valued bed level;
- Adaptation of the bed level scheme to allow for splitting up of a grid cell by a vane and sediment transport over the vane;
- The account of sediment transport over a vane.

4.5 Test cases

4.5.1 Introduction

Contrary to the situation with type 1 submerged vanes, no experimental data are available to validate the model of type 2 vanes. To check the implementation of the type 2 model in Delft3D-MOR a number of elementary tests have been carried out. These are described in section 4.5.2. Furthermore tests are executed for a bifurcation point including one vane of type 2. Two different computational

grids have been used in this case to judge the grid dependency of the computed bed level and the vane discretisation. These results are described in section 4.5.3.

4.5.2 Basic tests

The flow model of type 2 vanes implemented in Delft3D-FLOW has been tested for a channel with a width of one cell and a length of 9 cells. The cell area is 20x20 m^2. The channel bed is fixed and horizontal, downstream a fixed water level of 7 meter above bed is used and upstream a discharge is imposed of 100 m^3/s, initially increasing from 0 to this level. Eleven tests are described in Table 6 (the indicated fall over the vane is an estimate as it is the total fall over the channel minus 1 cm, being the fall if no vane is present). The channel runs in x-direction if U is indicated and in y-direction if V is indicated.

case	U/V	angle with x-axis (in °)	Height of vane(m)	Description of result	figure
s1u	U	90	8,0	fall 2.8 m, small oscillation	D-1
s2u	U	90	-1,0	Vane below bed, no effect	D-2
s2v	V	0	-1,0	Vane below bed, no effect	D-3
s3u	U	90	0,001	1 mm gives fall 3 cm	D-4
s4u	U	90	3,0	reference case, fall 13 cm	D-5
s4v	V	0	3,0	fall 13 cm	D-6
s5u	U	60	3,0	fall 11 cm	D-7
s6u	U	30	3,0	fall 7 cm	D-8
s7u	U	15	3,0	fall 3 cm	D-9
s8u	U	0	3,0	vane parallel to flow	D-10
s8v	V	90	3,0	vane parallel to flow	D-11

Table 6 List of elementary flow tests in case of type 2 vanes in one-cell channel

The figure number mentioned in Table 6 refers to a figure present in Appendix D. The upper part of each figure shows the time-dependent water level variation near the inflow bound, and just upstream and downstream of the vane. These locations are marked by x in the plot left below, where the velocity vectors are shown too. The bold line indicates the vane location and the fine line the vane direction. The plot located right below shows the final spatial distribution of the water level and the vertical lines refer to the x-locations. Later on tests are described for channels with a width of several grid cells. In the corresponding figures the water level will be shown along the middle and the two outer grid lines.

In the first test (s1u) modular flow occurs. The water level shows small oscillations that are observed too in the case of the levees and weirs option in FLOW. In that case the problem has been solved by the use of under-relaxation. This numerical approach is not yet implemented for the present case as mostly the flow over the vane concerns fully submerged conditions. The under-relaxation method can easily be implemented.

When in the same channel of one-cell width the vane element is turned over 90°, it is parallel to the flow. In principle the vane should be placed at a v-grid point instead of a u-point, but this is not

possible in this case. An unstable situation arises: When the water level exceeds the vane height the flow resistance vanishes because the flow is parallel to the vane and in the model the resistance is coupled to the discharge component normal to the vane. The vane resistance parallel to the vane is neglected. Clearly a flow results without the effect of the vane. When the water level falls below the vane height the present vane implementation assumes a complete blocking of the flow. In principle the control cell to solve the u-momentum should be split up in two parts, introducing different u-velocities for each part. This cell splitting introduces a bi-valued velocity field and a serious complication of the solution procedure of FLOW.

The tests s2u and s2v concern a vane below the bed level. In a morphological simulation such a situation arises when the bed level rises above the upper vane edge. The computed velocities do not show an effect of the vanes. However if the vane rises a small distance above the bed (test s3u) a fall over the vane occurs which is a multiple of the active vane height. This inaccurate result has to be ascribed to the used discharge relation and has to be corrected.

The tests s4u and s4v show a realistic situation of a vane with a height of 3 m in a water depth of 7 m. For both U and V directed channels the same fall is obtained, indicating no dependency on grid orientation. The observed fall deviates somewhat from the theoretical fall, probably because of the local bed friction. The same differences have been observed in the case of the levees and weirs option in Delft3D-FLOW and Waqua. Compared to the other uncertainties of the flow modelling of the type 2 vanes, this effect may probably be neglected.

The tests s4u to s8u show the effect of the vane angle on the flow. A decrease of the angle of flow attack on the vane reduces the effect on the water level. The effect on the flow is nil when the flow is parallel to the vane (tests s8u and s8v). As the upper vane edge is far below the water level the above-mentioned flow-instabilities do not occur.

In the previous tests the width of the channel is one grid cell, allowing the computation of one velocity component only. Therefore seven simulations have been carried out with an increased channel width, and vanes running over the complete width or over a part of it.

case	Number of cells in channel width	U/V	angle (º)	height (m)	Description of result	figure
s1m	3	V	0	3.0	fall 9 cm	D-12
s3m	3	V	162	3.0	fall 8.5 cm	D-13
s1c	3	V	0	3.0	fall 2.3 cm	D-14
s2c	3	V	45	3.0	fall 2.0 cm	D-15
s3c	3	V	45	6.5	fall 9 cm	D-16
s4c	3	V	45	6.5	fall 9.5 cm	D-17
s5c	9	V	45	6.5	fall 10.5 cm	D-18

Table 7 List of elementary tests on type 2 vanes in a multi-cell wide channel.

The cases s1m and s3m concern a channel width of 3 cells. One vane runs over the whole width and has the same staircase shape in both cases (see Fig D-12 and D-13). In case s1m it is an approximation of a vane normal to the channel walls and in case s3m of vane making an angle of 72°. The difference in fall between the two cases is less than 5 mm. The vane part at the right channel side is located one cell upstream compared to the vane parts at the left side. Therefore the vane resistance creates an

upstream redistribution of discharge (increase left and a decrease right) and a small increase of the water level at the right side and decrease at the right side. At the downstream side of the vane the opposite effect can be observed. The flow tends to cross the vane perpendicular as can be observed from the figures D-12 and D-13. In these cases the turning of the flow direction depends more on the locations of the vane elements (u and v grid points) than on the vane angle specified in the model input. The modification of numerical scheme of the u-momentum near the u-grid point of the u-vane element is dominant to the added vane resistance in these cases.

The tests s1c to s4c concern flow configurations with only one vane element in the central grid cell which partially blocks the flow and has different vane orientations. The water level in the middle of the channel shows an increase in front of the vane because of flow deceleration. Along the grid lines passing at both ends of the vane the water level distribution is identical, when the vane orientation is normal to the wall. If the vane make an angle of ±45° with the channel wall, the absolute values of the water level changes somewhat, but the symmetry along the passing grid lines is maintained. The reason is the modelling of the vane by a resistance that is included only in the momentum equation concerning the velocity component at which the vane element is located. In fact a resistance component should be added to the momentum equation of the other velocity component. This approach is not present in the levees and weirs algorithm. By the introduction of an additional vane element as done in test s4c the asymmetry will be introduced. Although the effect on the flow distribution is significant the effect on the fall is small. In test s5c the vane configuration of s4c is repeated but by the use of a refined grid (6.7x6.7 m^2 instead of 20x20 m^2). The computed water levels are similar to those of test s4c but within increased smoothness of the curves. The fall is increased somewhat. All these results are shown in the figures D-14 to D-18.

Subsequently six tests have been carried out with a surface vane. The tests concern a channel with a width of one grid cell. The cells are 20x20 m^2. The tests are listed in Table 8.

case	U/V	angle with x-as (°)	level underside of vane (m)	description of result	figure
s1o	V	0	9,0	vane above water level, no effect	D-19
s2o	V	0	-1,0	water blocked completely	D-20
s3o	V	0	7,0	vane just enters water, fall negligible	D-21
s4o	V	0	4,0	fall 6 cm	D-22
s5o	V	60	4,0	fall 1 cm	D-23
s6o	V	90	4,0	vane parallel to flow	D-24

Table 8 List of elementary tests on surface vanes in a one-cell channel.

Test s1o concerns a surface vane located above the water level and shows no effect on the flow. If the vane underside is located below bed level, test s2o shows a complete blockage of the flow. A surface vane just entering the water level affects negligibly the channel flow. Contrary to the submerged vane model no revision of the surface vane model is required with respect to a small active vane height.

When the surface vane enters the flow about 3 m and the vane is situated normal to the channel wall the fall is about 6 cm (test s4o). When the vane angle to the wall is 60° the fall reduces to only 1 cm (test s5o). The reason is the model of the vane resistance that relates the resistance to the discharge component normal to the vane and equals the effective vane element length to the length of cell edge

projected on the vane direction. If the vane direction is parallel to the channel wall no effect on the water flow is observed (test s6o). The flow instability introduced by water level rising or decrease as observed in case of submerged vanes can not occur in case of surface vanes.

The above-discussed tests concern a flow over a fixed channel bed. Two tests have been carried out including morphology. The first test concerned a submerged vane with its top edge located below the bed level. As could be expected no vane effect on the bed level was observed. The second test again concerns the one-cell wide channel. The water depth is about 7 m, the vane height 10 cm and the grid cells 10x10 cm^2. The vane blocks all sediment transport as long as the vane exceeds the upstream bed level. Figure D-25 shows the bed level in the upper plot on a number of times and in the lower plot as function of time at a number of locations. Finally an equilibrium bed level is obtained.

To arrive at the equilibrium bed level the following choices have been made.

1. The magnitude of the sediment transport has to be bed slope dependent. The stability option NSTAB = 1 has been chosen to simulate this effect. This option is a numerical correction, which includes a bed slope. In fact the required correction has a physical meaning and the ALFABD option should be used. However as both corrections are expressed in a similar way the NSTAB=1 option can be used for the present case too.
2. The grid step and the time step have to be chosen small enough to satisfy the cell Reynolds number and Courant number conditions.
3. The depth-averaged flow model together with the vane model do not represent the recalculating flow area just behind the vane and therefore can not reproduce the sediment transport downstream of the vane within the wake area in which it is directed to the vane.

4.5.3 Tests on bifurcation point

The elementary tests described in the previous section on submerged and surface vanes in a straight channel have shown that the implementation of the vane models in the code is probably correct and stable. The morphological modelling system uses a rectangular, curvilinear, computational grid. In general the vanes are flat plates and will not coincide with a grid line. In the present flow code the type 2 vane can be described only as a set of connected grid cell edges. Therefore the vanes have to be approximated by staircase lines. The real vane direction will only be used to determine the resistance of each vane element. A number of schematisation errors will be introduced by:

1. a shift normal or parallel of the vane to the nearest gridline;
2. difference in vane length because of cell dimensions;
3. angle rotation because of difference in vane orientation and cell edge orientation;
4. Deformation of vane by the projection on the grid cell edges.

These differences between the real vane and the approximated vane may have no significant effect on the model results when a sufficient fine grid has been chosen.

To test the effect of a staircase line approximation of vane and bounds on the model outcomes simulations have been carried out for a model concerning a bifurcation point: a river is split up into two branches making a mutual angle of 60°. Two different grids have been created: the first grid is a transformation of a I-shaped area. The second grid is a transformation of a T shaped area. In these cases different staircase lines occur. In Figure D-26 both grids are shown. Figure D-27 shows the schematisation of the vanes. First the case with a submerged vane will be considered and next the case with a surface vane.

To show the effect of the schematisation of the vanes on the results first the effect of the grid in the cases without vanes has to be determined. Starting from a flat bed level the equilibrium bed level has

been determined for both grids, using an inflow velocity of 1 m/s and a downstream water depth of 7 m. The bed levels are shown in Figure D-28 and the general patterns correspond reasonably well. The bed levels of the left river side and the left branch compares the best, as the grids used here correspond to the same transformed area. With respect to the right riverside and the right branch the grids correspond to different transformed areas. Furthermore staircase bounds occur in case of grid 2. These differences have a significant effect on the bed levels at the right side. The effect of the grids on the flow distribution and the sediment transport distribution is likewise as can be seen in the figures D-29 and D-30. The discharge distribution over both branches is about the same for both grids (discharge via right branch 35-40% of river discharge).

Next a type 2 submerged vane with a height of approximately 4 m (average water depth about 7 m) has been placed at the indicated location (Figure D-27). In fact this vane is not a real vane, as the flow has to pass around the vane too. In the present case the vane is fixed at one side to the wall. However for a first testing of the vane flow model the present vane configuration is suitable, as these conditions fits well to the model equations. Using the final bed level of the simulation without vane the velocity distribution has been computed in case of the model with vane. Figure D-31 shows the depth-averaged flow distribution and Figure D-32 the details near the vane. The streamline that enters the right branch and is nearest to the dividing streamline is indicated as a bold line. The discharge distribution slightly changes over the two branches with a tendency of decrease of the right branch discharge. The effect of the vane on the flow direction increases close to the end of the vane, because the flow is free to pass around this end. The effect of the vane on the upstream flow distribution is nearly equal for both grids (See also Figure D-33 both plots, each showing the same case but different grids). Downstream of the vane the flow field of grid 1 shows a faster decrease of the vane effect than the flow field of grid 2.

Next the morphological simulations are continued over a period of 7.5 month. The simulation is based on the assumption the bed load to be 50% of the total sediment transport. From the suspended sediment transport a part will pass over the vane (based on the rouse profile). The final bed level is shown in Figure D-34. To show the effect of the vane on the bed level the difference of the initial bed level and the final bed level is shown in Figure D-35 (being bed level Figure D-34 minus bed level Figure D-28). In Figure D-36 details around the vane are shown. In spite of the differences between the absolute bed levels, the erosion and sedimentation pattern induced by the vanes are nearly equal for the two grids. Sedimentation occurs just upstream of the vane (the sedimentation just downstream of the vane does not occur, as it is a post-processing effect) and some erosion occurs near the right branch bank. In the case of grid 2 a part of this eroded sediment is deposited within short distance, which does not occur in the case of grid 1. Beside the vane end strong erosion occurs which is of interest with respect to vane foundation, however to determine the real occurring scour holes near the vane a 3D flow model including turbulence will be required. Downstream of this erosion area a sedimentation area occurs that is located somewhat differently dependent on the grid. Finally the magnitude of the sediment transport is considered (Figures D-37 and D-38). As can be expected on base of the implemented concept the vane blocks the sediment transport. Around the vane significant sediment transport occurs and downstream in the right branch the sediment transport is nearly nil. The change of the transport magnitude is shown in Figure D-39. The efficiency of the vane is clearly demonstrated by the increase of the sediment transport in the left branch and a decrease in the right branch.

Tests with surface vanes have been carried out in the case of the bifurcation model, where at the same location the surface vane replaces the submerged vane. The underside of the vane is located approximately 4 m above the bed level, blocking about 3 m of the water column. The figures D-40 and D-41 show the effect of a surface vane on the flow distribution and the bed level. Figure D-40 shows the effect of the surface vane on the flow to be less than of the submerged vane (blocking 4 m). The flow direction significantly changes near the vane end.

Beside of the vane erosion occurs because of the local, increased flow velocity (See Figure D-41). The

model results below the vane differ considerably with respect to the erosion and sedimentation pattern. The sedimentation near the vane does not correspond to expectations. In the transport model the velocity beside of the vane has been used instead of below. Therefore a too low sediment transport is computed, which is the probably the reason for this sedimentation.

4.5.4 Tests with CFX flow model

CFX is a 3D simulation program developed by AEA Technology, Harwell, UK for hydrodynamic problems related to industrial applications. Compared to the Delft3D program, which was developed for large-scale open channel hydrodynamics (environmental studies), its strength lies in the non-hydrostatic simulation of flow in complex 3D geometries; its weakness is the handling of free surfaces. These differences can be explained easily based on the differences in development background. Simulating the detailed flow around structures (such as vanes) in open channels is application that requires features of both models. Therefore, we have also set up a CFX model to study the detailed flow over and along vanes of type 2. In a previous study, some CFX simulations were carried out for a vane of type 1 (see Fig. 6).

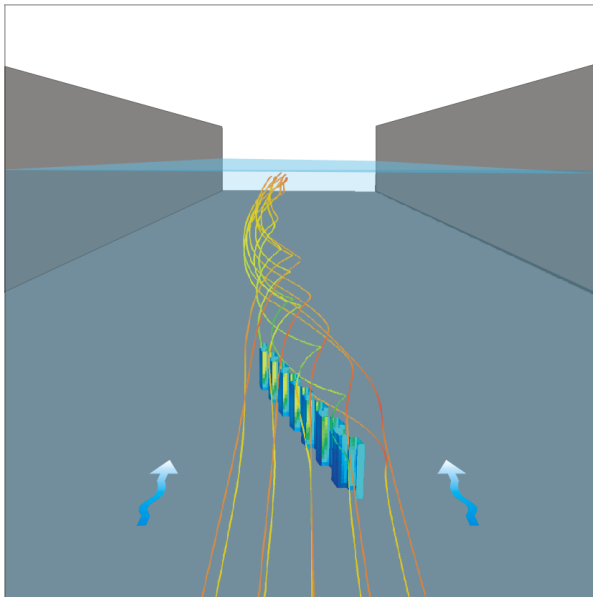

Figure 6 Secondary flow induced by a flow along a vane

The basic flow pattern around the larger vanes of type 2 was studied for a straight flume channel (1 m wide, 11 m long). The water surface was modelled using a free slip (frictionless) wall at 28 cm above the rough bed (roughness height of 1.2 mm). Both side walls were also modelled as free slip walls. Halfway the flume (5.5 m from the inlet) the flow was partially blocked by a vane of type 2 (or weir, or thin dam). Simulations have been carried for conditions in which the whole flume or only one half of the flume blocked over 1/3 or 2/3 or 100% of the height. It should be noted that these simulations were carried out to determine the qualitative effect of the vane geometry; the size of the vane is relatively large compared to the overall channel width.

Figure 7 shows the results of three simulations in which the right half of the flume was partially or completely blocked. Flow is away from the reader. The colors indicate the magnitude of the local flow velocity varying from blue (low velocity, almost stagnant) to red (high velocity). Furthermore, streamlines are drawn originating from a plane just downstream of the vanes (i.e. blockage). One of the streamlines is marked using white spheres; this line starts in the center of the flume at 2/3 of the

height (top left corner of the vane in 2b).

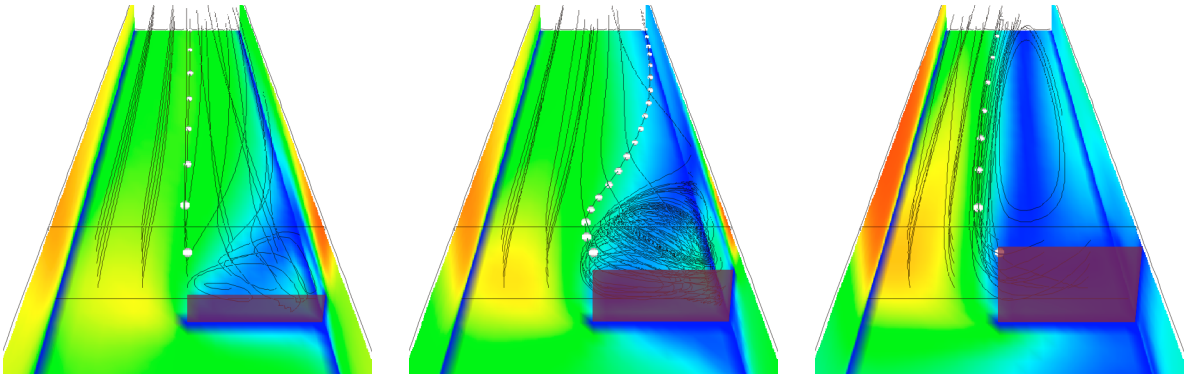

Figure 7 Flow blocked by vane (left 1/3 of water depth; middle 2/3 ; right fully blocked)

The first simulation shows that the flow in the left part of the flume is influenced only slightly by the presence of the vane (mainly a slight increase in the local flow velocity). The flow near the bed behind the vane is directed towards the right, whereas the flow near the surface is directed towards the left: a low intensity secondary flow is excited by the vane. The error introduced by keeping the free surface fixed (rigid lid) will be small. Locally behind the vane, the flow is more three-dimensional. In the second simulation, the local three-dimensional flow is much more pronounced. The influence of the rigid lid assumption for the free surface has a much larger influence on the local flow conditions. In the third case, the effect of the vane blocking the full height (sometimes referred to as a thin dam) is quite different. The recirculation zone extends much further downstream (the downstream boundary may play a role), and the flow pattern is mainly two-dimensional. The increase in blockage area causes increasingly higher velocities in the left part of the channel, which will result in constriction scour in a morphological model.

The CFX simulations indicate that the local flow in the neighborhood of the vane can be quite complex. It depends in general on the height of the (bottom)vane, the river geometry, water levels, and bed topography; only a very simple case has been examined here. It is not the intention to simulate the local flow patterns using Delft3D. The redistribution of the flow further downstream of the vane (at a distance larger than several times the vane length) is the main focus of the Delft3D simulations.

4.6 Evaluation of results of type 2 vanes

The computational model of type 2 vanes has been composed on the base of models of similar flow cases (levees and weirs). By lack of experimental data the physical quality of the model can not be determined. As far as it concerns the flow model, it is derived from the flow model of the levees and weirs present in Delft3D-FLOW. The wake of the vane is included as a local energy loss only, and the further effect as modelled in the case of type 1 vanes is not included. The wake of the vane leads to local scour but this effect is not included as only depth-averaged velocities are computed. These velocities are suitable to determine large-scale morphological changes of the bed level.

The chosen computational model is implemented in the morphological modelling system Delft3D-MOR and concerns modifications of the flow module FLOW, the transport module TRSTOT/TRSSUS and the bed level variation module BOTTOM. The chosen implementation allows the application of type 1 and type 2 vanes in the same model.

The tests carried out are aimed to determine the presence of the required functionality, the absence of code errors, the desired effect on the flow and the grid independence of the solution. Mostly the test

outcomes correspond to the expectations and if not it can be explained. Schematisation effects play an important role. Some details of the model have to be adapted.

The tests on the bifurcation point indicate that with this type of vanes the sediment transport distribution to the two river branches can be effected as is expected.

4.7 Improvements and recommendations

With respect to the computational model of a type 2 vane a number of improvements can be implemented in the program code. Furthermore a number of recommendations are given to validate the model:

- As long as the upper edge of a submerged type 2 vane rises above the bed level a significant effect on the flow occurs even if the active vane height is negligible small. This problem arises from the used discharge relation. The relation have to be adapted to avoid the discontinuity in energy loss when the active vane height becomes positive;
- The effect of type 2 surface vanes to the morphology is restricted to the consequences of a modified flow field. The consequences of the flow area reduction below the vane was not included in the first code version of the model and therefore too low sediment transports occur. This flow area reduction in transport computation has been included later on;
- The effect of the bed level slope on the magnitude of the sediment transport has to be extended. A few options are added in the recent program version;
- Model experiments have to be carried out to judge the results of the computational model. It has to be determined whether the effect of the wake is restricted to the local scour. If an significant effect on the large scale morphology can be observed like in the case of type 1 vanes the type 2 model has to be adapted, with a direct effect of the wake on the sediment transport direction;
- The computation of the 3D flow field with CFX to determine whether the depth-averaged field derived from this field corresponds the averaged flow field computed with the vane model in Delft3D-FLOW;
- The computation of the 3D flow field with CFX to analyse the near vane flow field and to determine to which extent the wake is active downstream of the vane;
- The execution of a morphological simulation for a vane in a flume, for which case bed level measurements have been carried out. Even if the vane has the dimensions of a type 1 vane, it can be a reasonable reference for testing the computational model of the type 2 vane;
- To implement the vane-induced vortex in the computational model.

5 Conclusions and recommendations

Within the framework of the Delft Cluster project ‘ Vanes and Screens’ a number of activities has been carried out. In the present report these activities are presented and the results have been discussed.

In this project two types of vanes are distinguished. The mathematical modelling of these types has been carried out partially within the present project:

- A type 1 vane is described according to the theory of Odgaard. At WL | Delft Hydraulics this model has been applied since a number of years. This concept is maintained within the present project, but the code has been updated. In the past this model was applied to bed load or total sediment transport only. The model is extended now to suspended sediment transport;
- A type 2 vane has been introduced within the present project as a new concept. A mathematical model has been defined based on the discharge relations known from weirs. This model has been implemented in the code for both the total sediment transport module and the suspended sediment transport module. This model could not be validated because of the lack of experimental data;

Both vane types have been implemented in the morphological modelling system Delft3D-MOR, in such a way that both types can be used within the same simulation model. Therefore the choice of the same flow model for both vane types is essential. The depth-averaged flow model already used in the case of type 1 vanes is suitable for the type 2 vanes too and is therefore selected as the common flow model.

Several morphological simulations have been carried out with the updated and extended version of Delft3D-MOR:

- In the past morphological simulations have been carried out for the test case ‘curved flume’. For this case measured bed levels are available including the effect of vanes. The previous computational results show a reasonable reproduction of the bed level. The present computations reproduce the previous computations identically;
- In the simulation model of the Ganges/Gorai bifurcation the effect of type 1 vanes on the sediment transport distribution and the bed level has been computed. In this case the suspended sediment transport is dominant. The computed tendencies correspond to expert expectation. However the results could not be verified because of the lack of measured data in the case of vanes;
- A number of elementary simulation runs has been carried out for type 2 vanes in a straight channel to test the code implementation by inspection of the computed velocity distribution; Furthermore morphological simulations were carried out for the same channel. The results correspond to expectations;
- Morphological simulations with a type 2 submerged vane located near an artificial bifurcation have been carried out. The results of this model could not be verified by lack of measured data. Different computational grids were used. The computed bed levels appeared to be grid dependent.

Till now the following shortcomings or uncertainties of the model concerning type 1 vanes could be determined:

- The values of the lift and drag force on the vane, computed according to the Odgaard model appear to deviate substantially from the experimentally determined values. Also the measured flow distribution near the vane deviates from the distribution as assumed in the theoretical model. The interaction between the vanes is represented partially by the model. The length dimension of

the vane appears to have a weak effect on the results;

- Till now the vanes of type 1 have been tested for small angles of flow attack. An extension of the model with respect to large angles is advisable;
- In the case of drying areas the code is not robust with respect to the influence area computation of the vortex lines;
- The application of the vane model with respect to suspended sediment transport is not yet validated;
- The extension of the number test cases that can be verified by use of measured data is desirable.

The following shortcomings or uncertainties of the type 2 vanes could be determined:

- The mathematical description of this vane type has not yet been checked by physical experiments. In the present model the vane wake is modelled as a flow resistance only. It is unknown how far the end effects of the vane will extend along the vane and whether the standard discharge relations will be applicable. The effect of the wake on the total sediment transport and on the suspended sediment transport is neglected. It is not sure whether this wake affects the local scour only, as is assumed.
- A decrease of the vane height shows a discontinuity in the vane resistance at the moment of vane disappearance below the bed level.
- Results of physical experiments for both flow and morphology are lacking for calibration and verification of the computational model.

Recommendations

The Delft3D-MOR version including vanes developed and used in the present project is based on the most recent officially maintained Delft3D-MOR version (date :2000) without vanes, available at the start of the project. The resulting code is still a dedicated version and therefore it is strongly recommended to implement the type 1 vane option in the official code:

- A dedicated code tends to get outdated fast.
- The model of type 1 vanes was already active in the official RIVCOM code.
- The vane contributions to the code are concentrated at a few locations; therefore the maintenance effort of the general code will not significantly increase by its presence. The update of the vane option can be generally carried as a separate action, as low code interaction is present between the vane option and the main part of the code;
- The increase of the computational effort in the case of no vanes can be neglected;
- The option is used for advisory work;

In the case of vanes of type 2 the arguments are less clear because the modelling of this type of vanes is still in an initial phase, the model may seriously be modified with equal consequences for the code. Furthermore the modifications of the code are less concentrated than in the case of type 1 vanes. Therefore the status of ‘dedicated version’ may be the most acceptable status.

Further recommendations are:

- The extension of the type 1 vane model with respect to large angles of flow attack;
- The extension of the vane type 2 model with a vortex line model;
- The execution of additional morphological simulations for cases with available data sets of

measurement;

- test case of Marelius
- test case of Odgaard

- The simulation of the Ganges/Gorai model, using type 2 vanes.

References

Flokstra, C.,
Modelling of submerged vanes,
J. of Hydr Res.,IAHR, to be published

Flokstra, C., Jagers, H.R.A., Wiersma, F.E., Jongeling, T.H.G.,
Coast and River, Vanes & Screens, Development of vanes and screens in Delft3D-MOR
Report Q2849, WL | Delft Hydraulics, 03.03.01, Delft Cluster, April 2002

Flokstra, C. and Wiersma, F.E.,
Waalbocht Hulhuizen, Flankerend Onderzoek Bodemschermen,
Report Q2322, WL | Delft Hydraulics, 1997

Jongeling, T.H.G. and C. Flokstra,
Bodemschermen, Stromingskrachten en Snelheidsveld bij variatie van schermhoogte,
Report Q2677/Q2849, WL | Delft Hydraulics, 2001

Lesleighter, E.J.,
Development of schemes for Ganges/Gorai River works, some proposals,
Note Gorai River restoration project, 1 February, 2000a

Lesleighter, E.J.,
Vanes in the zones A2 and A3 - the entrance to the Gorai,
Note Gorai River restoration project, 10 February, 2000b.

Lesleighter, E.J.,
Gorai River restoration project, project preparation and detailed design, Annex C Details on innovative approach,
Report, 2000c

Marelius, F.,
Flow training structures as erosion protection.
Thesis Royal Inst. of Techn. Stockholm, 1998

Mosselman, E,
Bodemschermen kunnen rivier diep houden,
Land+Water, Vol.43, No.6, pp.44-45.

Miller, D.S.,
Discharge Characteristics,
Part 8 of Hydraulic structures design manual. IAHR publication, 1994

Odgaard, A.J. and Wang, Y.,
Sediment management with submerged vanes. I: Theory,
J. of Hydr Engineering, ASCE, Vol. 117 no. 3., 1990

Potapov, M.V.,
Sochineniya v trekh tomakh,
Gos. Izd. Si'skokhozyaistvennoi Lit. Moscov(in Russian), 1950.

WL | Delft Hydraulics,
Werking grondkribben ten behoeve van waterwegverbreding in rivierbochten.,
Report Q98, 1987.

Appendix A Technical reference manual vanes and screens in Delft3D-MOR

A.1 Introduction

The present manual describes the use of a Delft3D-MOR version in which the effect of bottom vanes on the bed level development is an option. In this manual only the modifications of Delft3D-MOR with respect to this option are described. Two types of bottom vanes are included in the program:

The first type of bottom vane is relatively small (subgrid scale) and placed in a direction slightly deviating from the flow direction. The goal of this type of bottom vane is to counteract the spiral motion present in curved flow and thereby to reduce, for example, the transverse bed level slope in a river bend. The bottom vane generates a vortex line at the topside of the vane running downstream. This vortex line generates at the bed a transverse velocity, which interacts with the spiral motion and affects the sediment transport direction. Odgaard and co-workers have derived the original theory for this type of vane. The Delft3D-MOR code contains some extensions of this theory. Furthermore an empirical approach of the bottom vanes based on model measurements of vane induced flows is included.

The second type of bottom vane is relative large (multiple grid cells in length) and it is intended to be placed at a not necessarily small angle to the main flow. The goal of this type of bottom vane, which blocks the lower part of the water column, is to impose a flow direction near the bed and, thereby, to steer the main direction of sediment transport. The relatively clear water near the surface should continue over the bottom vane. An alternative to this second type of bottom vane is the surface vane. The surface vane, which blocks the upper part of the water column, intends to change the flow direction near the water surface. The sediment transport near the bed should continue under the surface vane.

A.2 Description of type 1 bottom vanes

This section describes the type 1 bottom vanes which serve the purpose to counteract the spiral motion present in a curved flow and thereby to reduce, for example, the transverse bed level slope in a river bend. The bottom vane generates a vortex line at the topside of the vane running downstream. This vortex line generates at the bed a transverse velocity, which interacts with the spiral motion and affects the sediment transport direction.

A.2.1 Description of a bottom vane

A.2.1.1 The shape of a bottom vane

A bottom vane is a rigid rectangular plate that is attached to the riverbed. The plate is placed vertically upward and has a horizontally directed upper edge below the water surface. Generally the thickness of the plate is small. The longitudinal cross section of the vane may be flat, wing-like or having the profile of a sheet pile. The active height of the vane, h_v, being the part of the vane above the riverbed, depends by definition on the morphological activities at the bed level:

$$h_v = z_{vanet} - z_b \qquad \text{(A.1)}$$

where:

h_v	active vane height, [m]
z_{vanet}	vertical z- co-ordinate of the crest of the bottom vane, [m]
z_b	local bed level, [m]

Usually the horizontal length, L_v, of the bottom vane exceeds the height.

The horizontal orientation of the vane, α_{vane}, is fixed with respect to the riverbed. This orientation is chosen in such a way that the flow will make a small angle of attack with the vane.

Usually a field of bottom vanes is present when such a device is applied to affect the bed level.

A.2.1.2 The physics of a bottom vane

Bottom vanes are devices applied to affect the bed level of a river or a channel, with the goal to increase or decrease bed slopes.

A bottom vane affects the flow distribution in a river, mostly downstream of the vane over an area restricted in width and over a length of many times the water depth. The vane affects the flow velocity in main direction but its effect on the transverse velocity is essential for the required effect of the vanes on the bed level. The induced transverse velocity near the bed affects the direction of sediment transport and therefore the development of the bed level. The direction of the vane-induced transverse flow component depends on the orientation of the vane with respect to the incoming flow. The orientation chosen leads to a transverse bed slope increase or decrease. An example of the application of the vanes is its use in a river bend to decrease the transverse bed slope in order to increase the navigability width. In this case the vane-induced transverse velocity counteracts the spiral motion.

To obtain a sufficient effect on the bed level development mostly a field of vanes is applied. The effect of the vanes on the bed primarily depends on the dimensions of the vanes and the angle of flow attack. The interaction between the bottom vanes seriously reduces the efficiency of the device.

A.2.1.3 The mathematical model of a bottom vane

The physics of the bottom vane is too complicated to be incorporated straightforwardly in Delft3D because a 3D description is essential for the vortex-generation by the vane. It requires a very small grid step and therefore a large computational effort. Far-reaching simplifications are applied. Two approaches are implemented, which can be selected by the user of the simulation system. Approach A concerns a model based on vortex generation and lifting line theory. Approach B is based on an empirical relation derived from velocity measurements past bottom vanes.

The model requires the following items:

1. Determination of the vortex lines downstream of each bottom vane;
2. Determination of the incoming flow for each bottom vane;
3. Determination of the vortex strength just behind the vane;
4. Determination of the vortex strength along the vortex line;
5. Determination of the vortex induced transverse shear stress;
6. Determination of the bottom vane resistance.

In the model description a rectangular co-ordinate system (x, y) and an orthogonal curvilinear co-ordinate system (ξ,η) are used.

With respect to the description of the mathematical model it is convenient to distinguish between the

near field and the far field of the bottom vane.

A.2.2 Near field description of a bottom vane

A.2.2.1 Introduction

The near field of a bottom vane concerns a strictly 3-D flow characterised by:

1. the presence of the closed surface of the vane on which a zero normal velocity condition holds;
2. the generation of boundary layers;
3. the flow past sharp edges;
4. The generation of vorticity sheets.

The near field description is simplified in the following way:

1. No direct effect of the vane on the sediment transport direction is accounted for. The sediment transport passes over the vane. Therefore the scour around the vane will not be calculated;
2. The horse shoe vortex is neglected;
3. The relation between the incoming flow and the generated transverse velocity/ vortex strength just past the vane will be described by an algebraic relation;
4. The longitudinal velocity will not be affected by the vane;
5. The resistance of a vane will be located in the near field only.

The mathematical models A and B use a different relation between the incoming flow and the transverse velocity generated downstream of the bottom vane. The incoming flow consists of different contributions and has to be evaluated over the height of the vane.

A.2.2.2 The incoming flow

The incoming flow of a bottom vane consists of the depth-averaged flow, the spiral motion and the flow induced by the upstream bottom vanes. The velocity of interest is the incoming velocity averaged over the vane height. This velocity is denoted by (u_{vane}, v_{vane}).

The velocity components parallel to the local co-ordinate directions in the orthogonal curvilinear co-ordinate system (ξ,η) are ($u_{vane\xi}$, $v_{vane\eta}$). The different velocity components are described below.

The depth-averaged velocities are (u_ξ , v_η) (the indices do not indicate derivatives). Assuming a power law profile to be the vertical distribution belonging to the depth-averaged main velocities, the velocity components averaged over the vane height can be derived according to:

$$u^a_{vane\xi} = \frac{m+1}{\sqrt{m(m+2)}}\left(\frac{h_v}{h}\right)^{1/m} u_\xi \qquad \text{(A.2)}$$

$$v^a_{vane\eta} = \frac{m+1}{\sqrt{m(m+2)}}\left(\frac{h_v}{h}\right)^{1/m} v_\eta \qquad \text{(A.3)}$$

$$m = \frac{\kappa C}{\sqrt{g}} \qquad \text{(A.4)}$$

where:

C	Chézy coefficient, [$m^{0.5}$/s]
κ	von Karman constant, (=0.41), [-]
g	acceleration of gravity, [m/s^2]
h	water depth, [m]
h_v	active vane height, [m]

The spiral motion introduces a velocity transverse to main flow, denoted by u_{nspir}. I_{spir} denotes the spiral motion intensity is denoted by. Near the bed the corresponding transverse velocity reads:

$$u_{nspir} = -\frac{3m-6}{2m\kappa^2} I_{spir} \qquad (A.5)$$

The upstream-located bottom vanes introduce an additional flow field. Each passing vortex line creates a velocity normal to the vortex line. Decomposing this velocity into components parallel to the local co-ordinate directions (ξ,η), the resulting expressions are:

$$u_{vane\xi i} = \sum_{\text{j vane upstream}} u_{vane\xi ij} \qquad (A.6)$$

$$v_{vane\eta i} = \sum_{\text{j vane upstream}} v_{vane\eta ij} \qquad (A.7)$$

where:

($u_{vane\xi i}$, $v_{vane\eta i}$)	the resulting incoming velocity at vane i induced by the upstream vanes, [m/s]
($u_{vane\xi ij}$, $v_{vane\eta ij}$)	the incoming velocity components at vane i induced by the upstream vane j, [m/s]

The calculation of the components ($u_{vane\xi ij}$, $v_{vane\eta ij}$) requires the determination of the vortex line. The magnitude of the velocity contribution depends on the local vortex strength and the distance to the passing vortex line. As the contribution of these velocities is important for the reproduction of the downstream interaction between the vanes and as the really occurring transverse velocity distribution induced by a vortex deviates from the theoretical vortex distribution, some options are implemented to compensate for the lack of a precise model description.

If the distance to a passing vortex line exceeds some critical distance d_{cr} this passing vortex line will not affect the incoming flow field of the vane passed. The critical distance reads

$$d_{cr} = 0.5\,(d_{cra} h + d_{crb} h_v) \qquad (A.8)$$

where:

d_{cra}, d_{crb}	coefficients to affect critical distance, [-]

In model A the recommended values are $d_{cra} = 1.0$ and $d_{crb} = 0.0$. In model B the recommended values are $d_{rca} = 0.0$ and $d_{crb} = 1.6$.

The velocities ($u_{vane\xi ij}$, $v_{vane\eta ij}$) are derived in three steps from a quantity j_b, being the integrated vortex

induced transverse velocity. The quantity j_b is computed along the whole vortex line and the j_b value at the point of the vortex line closest to the point to determine ($u_{vane\xi ij}$, $v_{vane\eta ij}$) has to be used. In the first step some specific velocities are derived from j_b being the averaged velocity v_{ave} and the peak velocity v_{max}. The formulas to be used depend on the method selected. In the second step, according to a selected option, the near bed velocity is computed from the velocities v_{max} and v_{ave} or from the assumed transverse velocity distribution. The third step concerns the derivation of the incoming velocity contribution averaged over the vane height from the near bed velocity.

The first step:

$$\text{Method A: } v_{max} = \frac{j_b}{\alpha_{jbA} h}$$

$$\text{Method B: } v_{max} = \frac{j_b}{2.42 * 0.8\, \alpha_{jbB}\, h_v}$$

where:

α_{jbA}, α_{jbB} tuning coefficients

The coefficient α_{jbA} of method A is a tuning coefficient to be tuned by morphological computations. In method B the recommended value of the tuning coefficient is $\alpha_{jbB} = 1.0$.

The average velocity v_{ave} reads:

$$\text{Method A: } v_{ave} = \alpha_{jbA} v_{max}$$

$$\text{Method B: } v_{ave} = \frac{1}{2} v_{max}$$

The second step:

The magnitude of the near bed velocity v_{winc} at the incoming flow location reads

option 1: $v_{winc} = \alpha_{wma}(\omega_{w\,max} v_{max} + (1 - \omega_{w\,max}) v_{ave})$

This option includes the neglect of the vortex-induced contribution to the incoming flow ($\alpha_{wma} = 0$). Furthermore a weighted average between the average velocity and the maximum velocity is possible.

option 2: $v_{winc} = v_{max} \varphi_{Dv}(d_{vl})$

where:

d_{vl} horizontal distance between incoming flow location and the vortex line, [-]

φ_{Dv} transverse distribution of vortex induced velocity, [-]:

Method A:

$$\varphi_{Dv}(d_{vl}) = \cos\left(\frac{2\pi d_{vl}}{h}\right) \qquad \text{if} \quad d_{vl} \le \frac{h}{2}$$

$$= 0.0 \qquad \text{if} \quad d_{vl} > \frac{h}{2}$$

Method B: $$\varphi_{Dv}(d_{vl}) = \frac{1}{1+\left|\frac{d_{vl}}{0.8\,\alpha_{jbB}h_v}\right|^3}$$

The near bed incoming flow velocity components ($u_{vane\xi ij}$, $v_{vane\eta ij}$) generated by vortex-line j at vane I are expressed as:

$$\begin{aligned} u_{vane\xi ij} &= -v_{winc}\sin(\alpha_{vlx}-\alpha_{ux}) \\ v_{vane\eta ij} &= -v_{winc}\cos(\alpha_{vlx}-\alpha_{ux}) \end{aligned} \qquad \text{(A.9)}$$

where:

α_{vlx} angle between the tangent of the vortex line at the point closest to the incoming flow location and the x co-ordinate, [rad].

α_{ux} angle of the u_ξ at the incoming flow location, [rad]

The third step:

The incoming velocity contributions averaged over the vane height and concerning the spiral motion and the flow induced by the upstream vanes are derived from the near bed velocities by multiplication with the same reduction factor c_{have}. The reduction factor is based on a linear distribution of the transverse velocity with respect to depth, with a correction of the profile near the bed. The profile is acceptable for the spiral motion, but for the vortex contribution it is less correct. The expressions read:

$$\begin{aligned} u_{nspira} &= u_{nspir}\, c_{have} \\ u_{vane\xi ia} &= u_{vane\xi i} c_{have} \\ v_{vane\eta ia} &= v_{vane\eta i} c_{have} \end{aligned} \qquad \text{(A.10)}$$

where:

u_{nspira} transverse velocity derived from spiral motion averaged over the vane height, [m/s]

$u_{vane\xi ia}$ velocity component parallel to u_ξ, derived from the upstream generated vortex lines and averaged over the vane height, [m/s].

$u_{vane\eta ia}$ velocity component normal to u_ξ, derived from the upstream generated vortex lines and averaged over the vane height, [m/s].

c_{have} coefficient to reduce the velocity magnitude at the bed to a vane height averaged velocity magnitude, [-].

The reduction coefficient c_{have} reads:

$$\begin{aligned} c_{have} &= \frac{m}{m+1}\left(1-2z^+\right)\left(\frac{h_v}{hz^+}\right)^{1/m} \qquad \text{if} \quad h_v/h < z^+ \\ &= \frac{m}{m+1}\left(1-2z^+\right)\left(\frac{z^+h}{h_v}\right)+\left(1-\frac{z^+h}{h_v}\right)\left(1-z^+-\frac{h_v}{h}\right) \\ &\qquad \text{if} \quad h_v/h \geq z^+ \end{aligned} \qquad \text{(A.11)}$$

where:

$$z_+ = \frac{1.6 + 0.2m}{m(m+3)} \tag{A.12}$$

Above the three contributions to the incoming flow of a vane have been specified. Now the resulting incoming flow components can be written as:

$$\begin{aligned} u_{vane\xi} &= u^a_{vane\xi} - u_{spira}\sin(\alpha_{uhave}) + u_{vane\xi ia} \\ v_{vane\eta} &= v^a_{vane\eta} + u_{spira}\cos(\alpha_{uhave}) + v_{vane\eta ia} \end{aligned} \tag{A.13}$$

where:

α_{uhave} angle between depth-averaged main velocity and the $+u_\xi$ direction.

The angle of incidence of the flow on the vane is expressed as

$$\alpha_{uvanei} = \alpha_{vanei} - \alpha_{ui} \tag{A.14}$$

where:

α_{uvanei} angle between vane i and the incoming flow, [rad]
α_{vanei} angle between vane i and the +x direction, [rad]
α_{ui} angle between the incoming flow direction at vane i and the +x direction, [rad]

A.2.2.3 Initial vortex strength according to model A

Model A is based on potential theory and wing theory. By the incoming flow a bottom vane generates downstream of the vane a vortex line with a vortex strength distribution. The incoming flow consists of the depth-averaged flow, the spiral motion and the flow induced by the upstream bottom vanes. The velocity of interest is the incoming velocity averaged over the vane height. This velocity is denoted by ($u_{vane\xi}$, $v_{vane\eta}$). The vorticity strength just behind the vane is computed according to the formulas described below.

The initial vorticity strength Γ generated by the bottom vane can be derived from the occurring lift force on the bottom vane:

$$\Gamma = -\frac{F_L}{\rho_w h_v \sqrt{u^2_{vane\xi} + v^2_{vane\eta}}} \tag{A.15}$$

where:

F_L the lift force on the bottom vane, [N]

The lift force is described by

$$F_L = \frac{1}{2}\rho_w c_L h_v L_v \left(u^2_{vane\xi} + v^2_{vane\eta}\right) \tag{A.16}$$

The lift coefficient c_L is computed as

$$c_L = \frac{2\pi\alpha_{vu} c_{La}}{1+\delta_s \frac{L_v}{h_v}} \qquad (A.17)$$

where:

α_{vu} angle of flow attack on the vane, [rad]
c_{La} user-specified lift coefficient correction (default = 1.0), [-]
δ_s correction coefficient of vortex effect to account for the reflections in the free surface and the bed, [-]

The correction coefficient δ_s to account for the reflection of the vortex in the free surface and the bed is expressed by:

$$\delta_s = 1 - \sum_{i=1}^{\infty} \frac{2}{\left(\frac{2ih}{\alpha_{hv} h_v}\right)^2 - 1} \qquad (A.18)$$

where:

α_{hv} correction coefficient for the point of separation of the vortex line. The location of this point above the bed is $\alpha_{hv}\, h_v$, [-].

From the vortex strength the velocity near the bed will be derived.

A.2.2.4 Initial j_b according to model B

The empirical model B describes the integrated transverse velocity j_b that is defined by:

$$j_b = \int_{y_0 - b_v/2}^{y_0 + b_v/2} v_{vane}(y)\,dy \qquad (A.19)$$

where:

y_0 the transverse location of the vortex line, [m]
y transverse co-ordinate, [m]
v_{vane} vane-induced transverse velocity of a single vane near the bed, [m/s]
b_v width over which the vane-induced velocity has significant non-zero values, [m]

The relation between the incoming flow and the value of j_b just downstream of the vane, being j_{bb}, obtained by data fitting reads:

$$j_{bb} = 1.58\, c_{intt}\, U \tan(\alpha) \frac{h_v^{0.8} L_v^{0.3}}{h^{0.1}} \qquad (A.20)$$

where:

U the magnitude of the incoming depth-averaged flow velocity, [m/s]
c_{intt} interaction coefficient to account for interaction between vanes in row normal to the flow direction, (recommended value 0.5), [-]
L_v length of the vane, [m]

α angle of flow attack, [rad]

The relation (A.20) has a restricted validity range, defined by the experimental conditions used. The validity range reads:

$$\begin{aligned} & h_v / h \le 0.4 \\ & 4 \le L_v / h_v \le 8 \\ & \alpha \le 0.35 \text{ rad} \\ & C \approx 45 \text{ m}^{0.5} / \text{s} \\ & Fr \approx 0.13 \end{aligned} \qquad \text{(A.21)}$$

where:

C the Chézy coefficient, [$m^{0.5}$/s]
Fr the Froude number, [-]

The used measurements have been carried out in straight flumes. Therefore the spiral motion as generated in a curved flow was not accounted for in the empirical formulas. To include this effect in method B the velocity U of formula (A.20) is re-defined. The actual incoming velocity, which generates the vorticity line behind the vane, is the total averaged incoming flow defined in Section A.3.2 (The incoming flow). This averaged velocity u_{svane} contains contributions of the main flow, the spiral motion and the vanes upstream. The averaged velocity u_{svane} is recomputed to a depth-averaged U as if this velocity was generated by the main flow only. The relation is based on a power law velocity profile. The relation reads:

$$\frac{u_{svane}}{U} = \frac{m+1}{\sqrt{m(m+2)}} \left(\frac{h_v}{h} \right)^{1/m} \qquad \text{(A.22)}$$

where:

u_{svane} the incoming velocity averaged over the vane height, [m/s]
U the corresponding depth-averaged velocity, [m/s]

A.2.2.5 Vane induced local bed friction

The bottom vanes affect the depth-averaged flow distribution, primarily by the effect on the bed level but secondly by the induced flow resistance. Especially the effect of the resistance of bottom vanes on the water level is of interest for prototype applications. Therefore the resistance of the vanes will be included in the flow model. The resistance will be restricted to the location of the vane and will be distributed over the corresponding grid cell, resulting in additional stress components in the momentum equation. Below the corresponding formulas are described.

The resistance F_D of a bottom vane with respect to the flow reads:

$$F_D = c_D \left| \frac{F_L}{c_L} \right| \qquad \text{(A.23)}$$

where:

F_L the lift force on the bottom vane, [N]
c_L the lift coefficient, [-]

c_D the drag coefficient, [-]

The drag coefficient is related to the lift coefficient by

$$c_D = \frac{L_v c_L^2}{2\pi h_v} \tag{A.24}$$

The resulting momentum equations read

$$\begin{aligned} &\frac{\partial u}{\partial t} + \frac{u}{\sqrt{G_{\xi\xi}}}\frac{\partial u}{\partial \xi} + \cdots + F_{v\xi} = 0 \\ &\frac{\partial v}{\partial t} + \frac{u}{\sqrt{G_{\xi\xi}}}\frac{\partial v}{\partial \xi} + \cdots + F_{v\eta} = 0 \end{aligned} \tag{A.25}$$

where:

t	time, [s]
(ξ,η)	orthogonal curvilinear co-ordinates, [-]
$G_{\xi\xi}$, $G_{\eta\eta}$	transformation coefficient of co-ordinate system, [m^2]
$F_{v\xi}$, $F_{v\eta}$	depth-averaged force density, [N/kg]

Suppose the flow velocity of attack on the bottom vane in the (ξ,η) plane is denoted by $(u_{vane,\xi}, v_{vane\eta})$ then the depth-averaged forces denote:

$$F_{v\xi} = \frac{u_{vane\xi}}{\sqrt{u_{vane\xi}^2 + v_{vane\eta}^2}} \frac{F_D}{\rho_w h A_v} \tag{A.26}$$

$$F_{v\eta} = \frac{v_{vane\eta}}{\sqrt{u_{vane\xi}^2 + v_{vane\eta}^2}} \frac{F_D}{\rho_w h A_v} \tag{A.27}$$

where:

ρ_w	density of water, [kg/m^3]
A_v	grid cell area, [m^2]

The quantities are evaluated at the water level point in the staggered grid point of Delft3D-FLOW. As the momentum equations are solved at u- and v-points the quantity F_D/A_v has to be split into:

$$\left.\frac{F_D}{A_v}\right|_{(m,n)} = \frac{F_D|_{(n,m)}}{2}\left(\frac{1}{A_{vu}|_{(n,m-1)}} + \frac{1}{A_{vu}|_{(n,m)}}\right) \tag{A.28}$$

where:

A_{vu}	cell area related to u-velocity point, [m^2]
n,m	grid point numbers, [-]

A similar expression holds for the v-momentum equation.

Each bottom vane contributes in this way to the momentum equations.

The contribution of the lift forces and the vane-induced shear stresses at the bed to the momentum

equations is neglected.

A.2.3 Far-field description

A.2.3.1 Introduction

The far field description of the flow past a vane consists of the undisturbed main flow field and a vortex line leaving the vane at the downstream end. The vortex line introduces a velocity normal to the vortex line. The vortex line runs downstream. The vortex strength along the vortex line damps out because of the flow turbulence. Apart from the contribution of the vortex line to the flow, a second vortex contribution concerns the vortex connected to the vane itself. Depending on the method this contribution will be accounted for separately. The concerning vortex generates a transverse velocity too.

Approximately the vortex line follows a streamline leaving the vane at the separation point. The location of the separation point is located below the topside of the vane.

The vortex line is a concept that belongs to the potential theory and within this theory the transverse velocity will be inversely proportional to the distance between the vortex line and the velocity point considered. This relation introduces a variation of the transverse velocity in transverse direction that deviates from the really observed distribution. Therefore, instead of using the individual transverse velocity distribution, the integrated transverse velocity will be used. Furthermore the transverse width over which the vortex will be active is restricted to a finite width proportional to the water depth and/or the vane height.

In the case of a field of bottom vanes each vane generates a vortex line. The resulting local transverse velocity will be obtained by linear superposition of all upstream-located vane contributions. If vortex lines generated by different vanes run along the same line, these vortex lines are dealt with separately. At the starting point of each vortex line the vortex strength depends on the local flow conditions. The damping function for each vortex line is identical and is a function of the distance to the starting point of the concerning vortex line.

The interaction between the vanes occurs with respect to vanes placed in the same transverse row and with respect to vanes placed in a streamwise row. These interaction effects primarily affect the initial vortex strength, but can affect the damping too.

A.2.3.2 Model of a vortex line

A vortex line starts at the separation point on the vane and runs downstream. The curve followed by the vortex line is determined according to one of the following user specified options.

Option 1:

> The vortex line coincides with the downstream part of the grid line running through the location of the vane centre. Which of the two co-ordinate directions is chosen and whether the vortex line runs in + or - direction depends on the flow field. The same choice will be made for all vortex lines. If the averaged u-velocity of the flow exceeds the averaged v-velocity the ξ-grid lines are chosen, else the η-grid lines are chosen. The + or - direction depends on the sign of the average velocity. Of course the magnitudes of the average u and v components has to differ significantly in order to be a correct criterion for this option choice. A warning has to be generated when the absolute difference between the average u- and v- components is below 70% of the magnitude of the average velocity. The direction of the vortex lines does not change during the whole

morphological simulation. The option is suitable when the main flow direction coincides with one of the co-ordinate lines.

Option 2:

The vortex line is constructed by computing the streamline starting at the separation point on the vane. The used velocity field pertains to the plane through the separation point on the vane and running parallel to the free surface. The velocity at that plane will be composed of the following contributions: the depth-averaged velocity and its vertical distribution, the spiral motion intensity and the vertical distribution of the spiral motion. The vortex lines affect each other, but this effect is neglected.

The streamline is described by the equation:

$$\frac{\partial x_s}{\partial t} = u_{vanes} \tag{A.29}$$

$$\frac{\partial y_s}{\partial t} = v_{vanes} \tag{A.30}$$

where:

t	time, [s]
(x_s , y_s)	co-ordinates of the stream-line/vortex line, [m]
(u_{vanes} , v_{vanes})	flow velocity components at the level of the vortex line, [m/s]

The expressions of the velocities (u_{vanes} , v_{vanes}) read:

$$u_{vanes} = u\, f_l(\frac{z_v}{h}) - \frac{v}{q} I\, f_d(\frac{z_v}{h}) \tag{A.31}$$

$$v_{vanes} = v\, f_l(\frac{z_v}{h}) + \frac{u}{q} I\, f_d(\frac{z_v}{h}) \tag{A.32}$$

where:

(u,v)	depth-averaged flow velocity, [m/s]
h	water depth, [m]
z_v	vertical location of the vortex line with respect to bed level, [m]
I	spiral motion intensity, [m/s]
f_l	vertical distribution of the main velocity, [-]
f_d	vertical distribution of the spiral motion, [-]

A number of options are implemented to describe the vertical distributions:

option 1: $f_l = 1.0$ $f_d = 0.0$

option 2: z_v / h constant along the stream-line and equal to its value at the separation point on the vane.

option 3: z_v / h equal to the local value.

The expressions for the vertical distributions read:

$$f_l\left(\frac{z_v}{h}\right) = \frac{m+1}{m}\left(\frac{z_v}{h}\right)^{1/m} \qquad \text{(A.33)}$$

$$\begin{aligned} f_d\left(\frac{z_v}{h}\right) &= \alpha_{fd}\left(\frac{1}{2} - \frac{z_v}{h}\right) \quad \text{if} \quad \frac{z_v}{h} \geq z^+ \\ &= \alpha_{fd}\left(\frac{z_v}{hz^+}\right)^{1/m} \quad \text{if} \quad \frac{z_v}{h} < z^+ \end{aligned} \qquad \text{(A.34)}$$

where:

$$m = \frac{\kappa C}{\sqrt{g}}$$

$$z^+ = \frac{1.6 + 0.2\,m}{m(m+3)}$$

$$\alpha_{fd} = -\frac{3m-6}{m\kappa^2}$$

κ von Karman constant (= 0.4), [-]
g gravity acceleration, [m]
C bed friction coefficient, Chézy coefficient, [$m^{0.5}$/s]

The function f_d is a simplification of the real profile of the transverse velocity. Near the bed the profile is equal to the distribution of the longitudinal velocity and above the critical level z^+ the profile equals the frequently used linear approximation. However the linear approximation is incorrect near the bed. The integral of f_d over the depth should be zero, but the defect by changing the lower level profile has not been corrected. The reason for the modification near the bed is to prevent the angle of flow attack on the vane to approach 90° because of the wrong description of the transverse velocity. In case of a small active vane height this deviation would occur.

Both methods to determine the vortex line seriously differ with respect to the required computational effort. RIVCOM uses the first method only, with a fixed flow direction. First option has been implemented for comparison with the results obtained from RIVCOM. The second option has been implemented to prevent additional restrictions to be imposed on the grid generation because of the location of the vortex-line.

A.2.3.3 The damping along the vortex line

A.2.3.3.1 Damping of vortex strength according to method A

To get the vortex strength at some location s of the vortex line, the initial vortex strength (at s=0) is multiplied with a damping function $\varphi_D(s)$, where s is the distance measured along the vortex line between the concerning point and the origin of the vortex line. Several expressions are available to describe the damping function. The options available in RIVCOM are implemented in Delft3D-MOR too:

Option 1: $\phi_D(s) = e^{-\frac{s}{\lambda_d}}$, $\lambda_d = \beta mh / \kappa$ (A.35)

Option 2: $\phi_D(s) = e^{-\frac{s}{\lambda_d}}$, $\lambda_d = \frac{mh}{2\kappa^2}\left(1-\frac{2}{m}\right)$ (A.36)

Option 3: $\phi_D(s) = e^{-\frac{s}{\lambda_d}}$, $\lambda_d = \frac{(m+1)h}{2\kappa^2}$ (A.37)

Option 4: $\phi_D(s) = 1-e^{-\frac{\lambda_d}{s}}$, $\lambda_d = \frac{3mh_v^2}{2\kappa^2 h}$ if $s < s_{max\,d}$ (A.38)

$= 0.0$ if $s \geq s_{max\,d}$

$\phi_{D1}(s) = 1-e^{-\frac{\lambda_{d1}}{s}}$, $\lambda_{d1} = \frac{3mh_v^2}{2\kappa^2 h}$

Option 5: $\phi_{D2}(s) = e^{-\frac{s}{\lambda_{d2}}}$, $\lambda_{d2} = \frac{\beta mh}{\kappa}$ (A.39)

$\phi_D(s) = \max(\phi_{D1}, \phi_{D2})$

Option 6: $\phi_D(s) = 1-e^{-\frac{\lambda_d}{s}}$, $\lambda_d = \frac{3mh_v^2}{2\kappa^2 h}$ (A.40)

where:

β	constant to be specified by the user (advised: 0.66667), [-]
s_{maxd}	distance to be specified by the user, [m]
h	water depth, [m]
h_v	active bottom vane height, [m]
κ	von Karman constant, [-]

Option 5 is frequently used in RIVCOM applications.

A.2.3.3.2 Damping of j_b according to method B

The damping function of method B partly stems from data fitting. The function reads:

$$\phi_D(s) = 1-e^{-\left(\frac{\lambda_d}{s}\right)^{1.1}}, \quad \lambda_d = 6.8\frac{\beta h_v^{0.9} h^{0.1}}{(\tan\alpha)^{0.7}} \tag{A.41}$$

where:

α	the angle of flow attack on the vane.
β	a user-specified coefficient (= 1, corresponds to original fit)

The present fit has been based on damping of the integrated transverse velocity. The present fit has a restricted validity range.

A.2.3.4 Computation of shear stress induced by vortex line

A.2.3.4.1 Computation of j_b along vortex line

The quantity j_b is used to describe the integrated transverse velocity generated locally by a vortex line. The determination of this quantity differs for methods A and B, because in method A the contribution of the vane and the vortex line are accounted for separately whereas in method B both effects are included in the empirical relations. From this quantity the additional shear stress induced by the bottom vanes at the bed is derived. This stress is used to correct the direction of sediment transport, being the ultimate goal of the bottom vanes. As the effect of the vortex line in transverse direction concerns a restricted width that may be small with respect to grid cell dimensions reduction factors have to be introduced to obtain grid cell averaged values of the induced stresses.

According to method A, the quantity j_b is determined according to:

$$j_b = \alpha_{int\,v}\alpha_{jbA} hv_{max} \qquad \text{(A.42)}$$

where:

v_{max} maximum transverse velocity induced by the vortices at the bed below the vortex line, [m/s]

α_{intv} vane interaction coefficient concerning interaction of vane located in a row normal to flow direction (default =1), [-].

The maximum velocity v_{max} is obtained as:

$$v_{max} = \left(\frac{\Gamma \delta_s}{\pi h_v \alpha_{hv}} \right)_{s=0} \varphi_D(s) + \frac{\Gamma \alpha_{gamh}}{2\pi(0.5L_v + s)} \qquad \text{(A.43)}$$

where:

s distance along the vortex line to the point of separation on the vane, [m]

α_{gamh} user-specified coefficient to take into account the vane bounded vortex, default =1, [-]

The other quantities of formula (A.43) are defined in the previous sections. The damping formula φ_D has to be chosen according to Section A.2.3.3.1.

The quantity j_b at s according to method B is determined according to the relation:

$$j_b = \alpha_{int\,v}\, j_b\big|_{s=0} \varphi_D(s) \qquad \text{(A.44)}$$

where:

α_{intv} vane interaction coefficient for interaction of vane located in a row normal to flow direction (default = 0.5), [-]

The damping formula φ_D has to be chosen according to section A.3.4.

For each vane separately this quantity j_b has to be determined along the vortex line considered.

2.3.4.2 Determination of the shear stress for a field of vanes

The determination of j_b along a vortex line has been described above. In the numerical approach the line-oriented quantity j_b is transformed to area-oriented shear stresses. Therefore j_b will be transformed to an averaged velocity over an area around the vortex line with a restricted transverse width. This area

may overlap grid cells completely, but mostly a partial overlap will occur. As the cell-oriented shear stresses apply to the whole cell area a correction has to be applied to the partially filled cells.

The variation of j_b along the vortex line may be strong by the occurring damping in such a way that the length of the grid cell requires an integration step Δs_{int} along the vortex line, which is small with respect to this cell length.

The width B_{vor} of the active area along a vortex line depends on the method used. In case of method A the width is h and in case of method B the width equals 1.6 h_v.

The quantity to be made cell-oriented will be the averaged velocity consisting of two components parallel to the +ξ direction and the +η direction respectively of the grid cell. Therefore the averaged transverse velocity j_b/B_{vor} directed normal to the vortex line would be decomposed into:

$$u_{vor\xi i} = \frac{\iint_{\text{active cell part}} \left(\frac{j_b}{B_{vor}} \right)_\xi dxdy}{A_{cel}} \qquad \text{(A.45)}$$

$$v_{vor\eta i} = \frac{\iint_{\text{active cell part}} \left(\frac{j_b}{B_{vor}} \right)_\eta dxdy}{A_{cel}} \qquad \text{(A.46)}$$

where:

$(f)_\xi,(f)_\eta$	the components in ξ and η direction
A_{cel}	area of the cell considered, [m^2]
$u_{vor\xi i}$	velocity component in ξ-direction used to derive the shear stress, originating from an upstream bottom vane i, [m/s]
$v_{vor\eta i}$	velocity component in η-direction used to derive the shear stress, originating from an upstream bottom vane i, [m/s]

All velocity contributions of upstream vanes to a computational grid cell are added:

$$u_{vor\xi} = \sum_{\text{from all upstream vanes i}} u_{vor\xi i} \qquad \text{(A.47)}$$

$$v_{vor\eta} = \sum_{\text{from all upstream vanes i}} v_{vor\eta i} \qquad \text{(A.48)}$$

where:

$u_{vor\xi}$	velocity component in ξ-direction at a computational grid cell used to derive the shear stress, originating from all upstream bottom vanes, [m/s]
$v_{vor\eta}$	velocity component in η-direction at a computational grid used to derive the shear stress, originating from an upstream bottom vanes, [m/s]

The relation between the velocity ($u_{vor\xi}$,$v_{vor\eta}$) and the induced shear stress at the bed is assumed to be equal to the relation used for the spiral motion. The corresponding relation for the spiral motion reads:

$$\tau_{spir} = \alpha_I I_{spir} \frac{\tau_b}{\sqrt{u^2 + v^2}} \tag{A.49}$$

$$\alpha_I = \frac{2E_s(m-1)}{m\kappa^2} \tag{A.50}$$

where:

(u,v) depth-averaged velocity, [m/s]
τ_b bed shear stress belonging to the depth-averaged main velocity, being directed normal to the main shear stress, [Pa]
E_s tuning constant (default =1), [-]

The relation between the velocity near the bed and the spiral motion intensity reads:

$$I_{spir} = \alpha_{spir} u_{spir} \tag{A.51}$$

$$\alpha_{spir} = -\frac{2m\kappa^2}{3(m-2)} \tag{A.52}$$

where:

u_{spir} near bed velocity of the spiral motion, [m/s]

For convenience the velocity ($u_{vor\xi}$,$v_{vor\eta}$) will be transformed to artificial spiral motion components ($I_{vor\xi}$,$I_{vor\eta}$):

$$I_{vor\xi} = \alpha_{spir} u_{vor\xi} \tag{A.53}$$

$$I_{vor\eta} = \alpha_{spir} v_{vor\eta} \tag{A.54}$$

The spiral motion components ($I_{vor\xi}$,$I_{vor\eta}$) are computed for each grid point. However generally these quantities will be equal to zero for a large number of grid points.

The direction of sediment transport α_I in the case of bottom vanes is composed from the shear stresses belonging to the main flow, the spiral motion and the bottom vanes. The corresponding formula reads:

$$\tan(\alpha_\tau) = \frac{v - \alpha_I\left(\frac{u}{\sqrt{u^2+v^2}} I_{spir} + I_{vor\eta}\right)}{u + \alpha_I\left(\frac{v}{\sqrt{u^2+v^2}} I_{spir} + I_{vor\xi}\right)} \tag{A.55}$$

The angle α_I is used to determine the direction of sediment transport. The angle α_I is the only quantity adapted in the sediment transport computations that accounts explicitly for the bottom vanes.

A.3 Description of type 2 bottom vanes

A.3.1 Hydrodynamic effects

Bottom vanes can be regarded as sharp-crested overflow structures, provided that the height p of the vanes is not too small. The next notation is applied (all water depths are related to the crest level of the vanes):

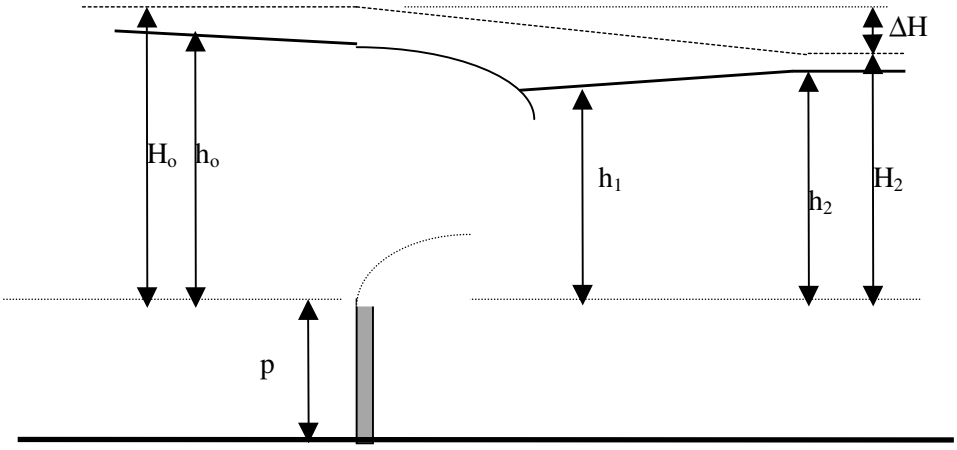

A.3.1.1 Perpendicular approach flow

A.3.1.1.1 Simple formula

The next simple formula relates the overflow discharge per unit length of the bottom vane to the upstream water depth:

$$q = \mu . \frac{2}{3} . h_o . \sqrt{2gh_o} \qquad \text{(A.56)}$$

where: q = discharge per unit width (m^3/sm)

μ = discharge coefficient (-)

g = acceleration caused by gravity (m/s^2)

valid for: $h_o > h_2$

The discharge coefficient has to be supplied by the user. This coefficient includes all geometrical and hydraulic effects such as influence of downstream water level, influence of vane height to water depth ratio, transition from submerged flow to modular flow.

A.3.1.1.2 Advanced formula

The general discharge relationship reads:

$$q = C_s . q_o \qquad \text{(A.57)}$$

where: q = actual overflow discharge (m^3/sm)

C_s = reduction coefficient in the case of submerged flow (-)

q_o = overflow discharge in the case of modular flow (m^3/sm)

The flow is said to be modular when the downstream water has no influence on the overflow discharge. The modular overflow discharge per unit length of the bottom vane is equal to (Rehbock):

$$q = C_d . \frac{2}{3} . h_o . \sqrt{2 g h_o} \qquad \text{(A.58)}$$

where: C_d = discharge coefficient

The discharge coefficient can be estimated by (Kindsvater and Carter, page 76 in Miller [Miller, 1994]):

$$C_d = 0.602 + 0.075 . \frac{h_o}{p} \qquad \text{(A.59)}$$

where: p = height of vane above upstream bottom (m)

In fact p has to be corrected for the influence of water surface tension; the correction is of the order of 1 mm and can be neglected in the present application.

The Rehbock formula is valid for relatively small h_o/p values (up to about 1.0 maximum), which is a disadvantage, because in most practical cases h_o/p is greater.

The discharge formula proposed by Schönfeld is valid for all vane heights, but is based on the upstream energy height H_o instead of the upstream water depth h_o. Application of this formula thus requires the computation of $H_o = h_o + v_o^2/2g$.

The modular overflow discharge per unit vane length reads:

$$q = C_d . \frac{2}{3} . H_o . \sqrt{2 g H_0} \qquad \text{(A.60)}$$

where:

$$C_d = \mu . \sqrt{\frac{1}{3}} \qquad \text{(A.61)}$$

and:

$$\mu = 1 + \frac{1.5}{\frac{H_o}{p} + 1.3 + \frac{30}{\frac{H_o}{p} + 1.3}} \qquad \text{(A.62)}$$

The value of μ equals 1 for p = 0, which implies that the critical-flow discharge over a flat bottom is similar to the modular-flow discharge of a broad-crested weir.

The submerged-flow reduction coefficient C_s can be estimated by:

$$C_s = (1 - S^{1.5})^{0.385} \qquad \text{for } h_2 > 0 \qquad \text{(A.63)}$$

$$C_s = 1 \qquad \text{for } h_2 < 0$$

where: S = submergence ratio = h_2/h_o

The formula for C_s was first presented by Villemonte (page 78 in Miller [Miller, 1994]).

A.3.1.2 Obliquely approach flow

In almost all applications of bottom vanes the approach flow is not perpendicular to the screen. The effect of the flow angle on the discharge relationship can be taken into account as follows.

The energy height H_o as applied in equation (A.60) is based on the approach flow velocity v_o. When the approach flow makes an angle ϕ with the line normal to the bottom vane, the velocity component $v_{o,n}$ perpendicular to the bottom vane has to be taken for the computation of the energy height $H_{o,n}$ (Schönfeld):

$$H_{o,n} = h_o + \frac{v_{o,n}^{\ 2}}{2g} \qquad \text{(A.64)}$$

where: $v_{o,n} = v_o . \cos\varphi$

and the modular overflow discharge per unit length of bottom vane reads:

$$q = C_d . \frac{2}{3} . H_{o,n} . \sqrt{2 g H_{o,n}} \qquad \text{(A.65)}$$

The discharge coefficient C_d is similar as presented in the equations (A.61) and (A.62).
The flow direction just downstream of the vane is assumed perpendicular to the vane.

A.3.1.3 Energy loss and conversion to local roughness coefficient

When the discharge q has been computed the depth-averaged flow velocities v_o (upstream side) and v_2 (downstream side) can be derived as well as the energy levels H_o and H_2. In the case of an obliquely approach flow the energy loss is assumed to be related to the normal velocity components $v_{o,n}$ an $v_{2,n}$. The energy loss thus equals: $\Delta H_n = H_{o,n} - H_{2,n}$.

In Delft3D computations the energy loss caused by weirs etc. is converted to a local, additional bottom roughness value. This procedure is also applied to the energy loss caused by a bottom vane.

A.3.2 Morphological effects

A.3.2.1 Introduction

The bottom vane of type 2 influence both the flow and the sediment transport. A part of the flow and sediment transport will go over the vane and a part of the sediment will be transported along the vane.

Two extreme cases have been formulated:

- In case of only bed load transport, the sediment will be blocked for any height of the vane;
- In case of only suspended transport, which moves along the flow streamlines, the sediment transport normally to the vane will continue over the vane. The sediment transport is not influenced directly by the presence of the vane, but indirectly via the effect of the vane on the motion of the water.

However, in practise these extreme cases will seldom occur. Bed load will not be transported over the bed and suspended load will not follow streamlines due to turbulence near the vane, the fall velocity of the sediment and the curvature of the streamlines near the vane. The cases are not that clearly defined as suggested by the above-mentioned extremes.

Based on this consideration, the following preliminary implementation has been selected for the module TRSTOT, concerning bed load or total sediment transport and for the module TRSSUS, concerning bed load and suspended sediment transport.

A.3.2.2 TRSTOT module

In this module no distinction is made between bed load and suspended sediment transport. Both sediment transport methods are combined into a total transport load. It is assumed that the sediment transport is in local equilibrium that is the concentration distribution over the vertical is assumed to be instantaneous with respect to the local flow conditions.

Some of the sediment transport formulae do not distinguish the two transport components (bed load and suspended), like Engelund-Hansen, whereas others do (for instance, van Rijn). In the latter case the two transport components are immediately after computation combined into a total transport rate: S_{tot}.

The sediment transport rate over the vane S_{over} is determined by:

$$S_{over} = \alpha_{red} * \alpha_{sus} * S_{totn} \qquad \text{(A.66)}$$

where:

S_{totn}	transport component normal to the vane
α_{sus}	fraction of the total transport rate acting as suspended transport
α_{red}	reduction coefficient indicating the fraction of the suspended sediment transported over the vane

The reduction coefficient is approximated using:

$$\alpha_{red} = \frac{\int_{\alpha_h h}^{H} e^{-\lambda_c \frac{z}{H}} \ln \frac{z}{z_0} dz}{\int_{0}^{H} e^{\lambda_c \frac{z}{H}} \ln \frac{z}{z_0} dz} \qquad \text{(A.67)}$$

where:

z_0 local roughness height
H water depth at the upstream side of the vane
h vane height
α_h effective vane height coefficient (<1)
λ_c gradient in the concentration distribution (=0 if sediment is uniformly distributed over the water column)

The user has to specify the coefficients α_{sus} , α_h and λ_c.

A.3.2.3 TRSSUS module

In this module bed load and suspended transport rates are dealt with separately. The suspended sediment transport rate is not necessarily in local equilibrium with the flow conditions.

For this module it is assumed that the vane blocks the bed load transport whereas all suspended sediment is transported over the vane.

A.4 Description of (type 2) surface vanes

A.4.1 Introduction

The next notation is applied in the discharge relationships for surface screens:

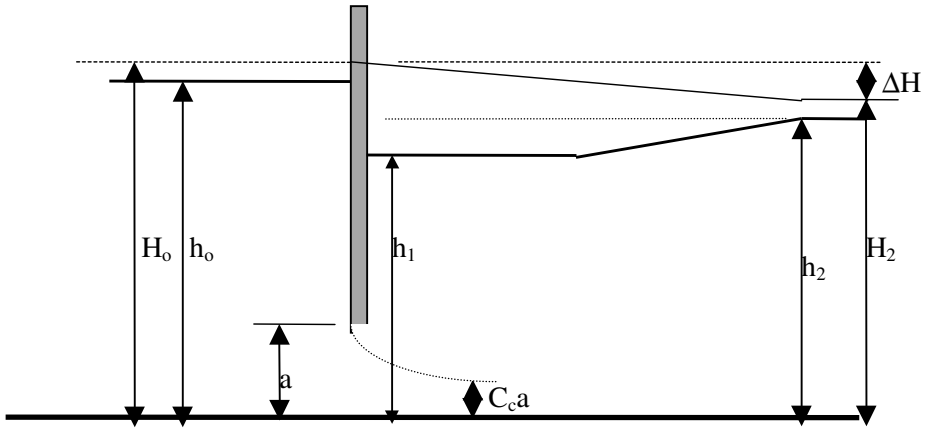

A.4.2 Perpendicular approach flow

A.4.2.1 Simple formula

The next simple formula relates the underflow discharge to the water-level difference:

$$q = \mu.a.\sqrt{2g(h_o - h_2)} \qquad \text{(A.68)}$$

where: q = discharge per unit width (m^3/sm)
μ = discharge coefficient (-)
g = acceleration caused by gravity (m/s^2)

valid for: $h_o > h_2$
$h_o > a$

The discharge coefficient has to be supplied by the user. This coefficient includes all geometrical and hydraulic effects such as influence of downstream water level, influence of flow opening to water depth ratio, transition from submerged flow to modular flow.

A.4.2.2 Advanced formula

Discharge relationship:

$$q = C_d . a . \sqrt{2 g h_o} \qquad \text{(A.69)}$$

where: q = discharge per unit width (m^3/sm)
C_d = discharge coefficient (-)
g = acceleration caused by gravity (m/s^2)

In the case of submerged flow the discharge coefficient equals:

$$C_d = \frac{C_{c,subm} \cdot \sqrt{1 - \frac{h_1}{h_o}}}{\sqrt{1 - (\frac{C_{c,subm} \cdot a}{h_o})^2}} \qquad \text{(A.70)}$$

where: $C_{c,\,subm}$ = submerged-flow contraction coefficient

The contraction coefficient $C_{c,subm}$ can be read as a function of a/h_o from Figure 3.44 in Miller [Miller, 1994), data from Nago, and is referred to as $(C_c)_o$.

The water depth h_1 just downstream of the screen can be deduced from the next momentum equation:

$$\frac{1}{2}\rho g h_1^{\,2} + \rho \frac{q^2}{C_{c,subm} . a} = \frac{1}{2}\rho g h_2^{\,2} + \rho \frac{q^2}{h_2} \qquad \text{(A.71)}$$

The water depth h_1 is a function of $C_{c,subm}$.a, q and h_2 and computation of h_1 and q for given h_2 and $C_{c,subm}$.a requires iteration.

In the case of modular flow the downstream water level has no influence on the discharge and the discharge coefficient C_d can be deduced from:

$$C_d = \frac{C_{c,\mathrm{mod}}}{\sqrt{1 + C_{c,\mathrm{mod}} \cdot \frac{a}{h_o}}} \qquad \text{(A.72)}$$

where: $C_{c,mod}$ = modular-flow contraction coefficient.

The contraction coefficient $C_{c,mod}$ can be read as a function of a/h_o from Figures 3.44 and 3.43 in Miller [Miller, 1994], data from Nago, and is the sum of $(C_c)_o$ and ΔC_c (correction for modular flow).

The flow condition, submerged flow or modular flow, depends on discharge and downstream water level. The transition from submerged flow to modular flow can be read from Figure 3.40 as a function of h_2/h_o and h_o/a in Miller [Miller, 1994].

Instead of the above discharge formula based on h_o and Nago data the next discharge formula based on the energy head H_o can be applied (discharge per unit length):

$$q = C_c.a.\sqrt{2g(H_o - h_1)} \qquad \text{(A.73)}$$

where: C_c = contraction coefficient

This formula is valid for submerged flow. The contraction coefficient C_c can be read from Figure 3.39 in Miller [Miller, 1994], data from McNown. The data for $\alpha = 90^o$ closely correspond to the data of Nago for a flat gate. Again the downstream water depth h_1 just downstream of the screen has to be determined in an iterative way, as indicated before, using C_c instead of $C_{c,subm}$. In the case of free flow the discharge formula (A.73) is not valid and the next formula can be applied:

$$q = C_c.a.\sqrt{2g(H_o - C_c.a)} \qquad \text{(A.74)}$$

The contraction coefficient C_c in Figure 3.39 is still valid provided that the Froude number Fr fulfils:

$$Fr = \frac{v_c}{\sqrt{gC_c a}} > 6 \qquad \text{(A.75)}$$

where: v_c = flow velocity in contracted jet.

If not, the C_c coefficient being a function of a/h_o and Fr, can be estimated from Figure 3.36 in Miller [Miller, 1994].

It may also be convenient to transfer formula (A.74), modular flow, into:

$$q = C_{dH}.a.\sqrt{2gH_o} \qquad \text{(A.76)}$$

where: C_{dH} = discharge coefficient based on upstream energy height H_o

The coefficient C_{dH} can be read in Figure 3.37 in Miller [Miller, 1994] as a function of H_o/a ($H_o/a > 2$).

The transition from submerged flow to free flow is presented in Figure 3.40 as a function of h_2/h_o and h_o/a in Miller [Miller, 1994]; for a flat, vertical gate transition to modular flow occurs when:

$$\frac{h_2}{h_0} \le \left(\frac{h_0}{a}\right)^{\delta} \qquad \text{(A.77)}$$

The coefficient δ can be selected -0,32 for h_o/a values in the range $2 < h_o/a < 10$ and -0.37 for h_o/a in the range $10 < h_o/a < 50$. The discharge formula based on H_o provides the possibility to take into account the effect of an obliquely approach flow.

A.4.3 Oblique flow

In almost all applications of surface screens the approach flow is not perpendicular to the screen. The effect of the flow angle ϕ (= angle with the line normal to the surface screen) on the discharge relationship can be assessed by utilising the upstream energy height $H_{o,n}$ related to the upstream velocity component $v_{o,n}$ perpendicular to the surface screen:

$$H_{o,n} = h_o + \frac{v_{o,n}^{\ 2}}{2g} \qquad \text{(A.78)}$$

where: $v_{o,n} = v_o.\cos\varphi$

The discharge per unit length of bottom vane reads:

$$q = C_c.a.\sqrt{2g(H_{o,n} - h_1)} \qquad \text{(A.79)}$$

The contraction coefficient C_c is similar to C_c in the equations (A.73) and (A.74).

The flow direction just downstream of the surface screen can be assumed perpendicular to the surface

screen.

A.4.4 Energy loss and conversion to local roughness coefficient

When the discharge q has been computed the depth-averaged flow velocities v_o (upstream side) and v_2 (downstream side) can be derived as well as the energy levels H_o and H_2. The energy loss ΔH caused by the screen equals: $\Delta H = H_o - H_2$. In the case of an obliquely approach flow the energy loss is assumed to be related to the velocity components $v_{o,n}$ and $v_{2,n}$ perpendicular to the surface screen, thus $\Delta H_n = H_{o,n} - H_{2,n}$.

In Delft3D computations the energy loss caused by weirs is converted to a local, additional bottom roughness value. This procedure is also applied to the energy loss caused by a surface screen.

Appendix B User manual vanes and screens in Delft3D-MOR

B User manual vanes and screens

B.1 Introduction

Two types of vanes and screens are available in this version Delft3D-MOR. This includes bottom vanes of type 1 and bottom and surface screens of type 2.

Vanes and screens influence the flow in two ways. First, the vanes influence the flow field locally by blocking a part of the water column and by changing the flow direction. Flow blocked by the surface of the vane will be redirected such that the flow direction matches the vane angle. Flow over a bottom vane, or under a surface vane, will be change direction such that it flows more perpendicular to the vane. These two changes in flow direction induce a secondary flow effect that may be noticeable downstream of the vane (in the far field).

The bottom vane included in the model is expected to be relatively small (subgrid scale) and oriented such that its direction deviates only slightly from the main flow direction. Under these conditions, local effects are limited to some additional bed resistance. The far field effect is schematised using a vortex line.

Generally the bottom screens and surface screens of type 2 are placed at a larger angle to the flow, than vanes of type 1. Local effects redirecting flow and sediment transport are assumed to be dominant and therefore no far field effect is included.

This section describes the extra input required for including these vanes and screens in the model.

B.2 Input for the FLOW module

There is no adaptation of the FLOW input file necessary for the use of the type 1 bottom vanes. The type 2 bottom and surface vanes require the following input Bottom vanes have to be specified in the flow module using the keyword Filvnb. Surface vanes have to be specified using the keyword Filvno. Both keywords are followed by a filename according to Delft3D-FLOW conventions, for example

Filvno = #ovane2.fil #

The specified file should satisfy the format described in the following section.

B.2.1 Vane specification

File contents: Location, dimensions and energy losses of (bottom or surface) vanes. A vane consists of one or more vane parts and a vane part consist of elementary vane parts. An elementary vane part is part of the vane running between two neighbouring bed level grid points which are located at both sides of a velocity grid point. Per vane all vane parts have to be specified. The specified vane is an approximation of the real vane following grid lines.

File format: Free formatted.

File name: User defined.

Generated by: Manually off-line.

Record description:

Record set 1	{S1}
Record 1.1: IVAN ANGVN NDVN	[I,R,I]

IVAN	Number of vane
ANGVN	Angle of the real vane in degrees with respect to x direction
NDVN	Number of vane parts of the approximated vane described in record set 1.2

Record set 1.2	{S2}
Record 1.2.1: UTYPE MB NB ME NE FRIC ZT DUM	[A1,4I,3R]

{S1}	Number of vanes to be specified
{S2}	Number of vane parts (NDVN) to be specified of vane IVAN
UTYPE	Character (A*1) indicating the location of the vane parts: U vane parts at the u-velocity grid point normal to the u direction, V vane parts at the v-velocity grid point normal to the v direction
MB,NB	Beginning co-ordinates of the vane parts in {M,N} co-ordinates (2 integers).
ME,NE	End co-ordinates of the vane parts in {M,N} co-ordinates (2 integers).
FRIC	A friction calibration coefficient normally equal to 1.0 (1 real).
ZT	The top level of the bottom vane or the bottom level of the surface vane in meters, positive direction down (1 real).
DUM	A real number; not yet used (1 real).

Restrictions:

- The vane direction (U or V) must be given in record position one.
- Vanes may not be defined along the model boundaries (which by default lie along the lines M = 1, N = 1, M = Mmax or N = Nmax). Therefore, the co-ordinates of these points must lie between M = 2 and Mmax-1 and N = 2 and Nmax-1, respectively.
- The friction calibration coefficient must have a positive value.
- Input items in a record must be separated by one or more blanks.

After records 1 and 2 they may be repeated to specify more vanes.

Example:

A vane at an angle of 162 degrees with the x-direction is defined at locations M = 2, N = 6 to M = 4, N = 5. The calibration coefficient is 1.0 and the characteristic level is 3.0 meters above the reference level.

```
1  162.0 3
V  2 6  3 6 1   -3.0 1
U  3 6  3 6 1   -3.0 1
V  4 5  4 5 1   -3.0 1
```

B.3 Input for the TRANSPORT module

Both types of bottom vane require a small change in the transport module supplemented by a number of extra parameters in an extra input file. The surface vanes do not require additional input for the transport module.

B.3.1 Typographic conventions

The records in the input files with an asterisk at the first position are regarded as comment.

In the description of the input records the following conventions are used:

[ ]	indicates the format of the specified data: R real, nR n sequential reals, I integer, A character etc.
{C}	the record has to be added if the condition described below has been satisfied.
{S}	the record will be repeated as much as indicated by S.

B.3.2 Modification of the TRANSPORT input file (md-tran)

The md-tran file has to be adapted in the following way to activate the vane option. The standard application is described in the manual. To activate the vane option the first record has to be modified and a new record (record 12) has to be added.

Record 1 has to be modified to:

Record 1: MODSDA NUMOPT (1), ...,NUMOPT(NOPT) [2I]

MODSDA	(see manual)
NUMOPT	option choice (multiple selection possible):
	type 1 bottom vane option: 1
	type 2 bottom vane option: 2
NOPT	number of options to be specified

After record 11, record 12 is added:

Record 12.i: NAMVAN(i) {C}[A]

{C} NUMOPT in record 1 has been specified to activate option i

NAMVAN(i) specifies the name of the input file containing the vane data. The name can be chosen freely. If multiple options are activated in record 1, an equal number of files should be specified here, following the option specification sequence of record 1.

B.3.3 Description bottom vane type 1 input file

In a separate ASCII file of which the name is specified in the md-tran.<case> file, data are specified to run the vane option in Delft2D-Rivers. The record conventions are equal to the conventions of the md-tran file. A record starting with an asterisk on the first position is a comment record.

Record 1: NVANES [I]

NVANES specifies the number of bottom vanes

Record 2: NVANNM [I]

NVANNM specifies the way in which the locations of the vanes are specified

NVANNM	= 1	The location of the vane centre is at water level grid point indicated by the (n,m) grid numbers.
	= 2	The locations of the vanes are specified by the (x,y) co-ordinates. The co-ordinates do not need to coincide with grid locations.

Record 3 : iv, N(iv), M(iv), ZTVANE(iv), HKVANE(iv) {C}{S}[3I,2R]

{C} NVANNM = 1

{S} NVANES The sequence of the vanes has to be specified in such a way that a vane affected by an upstream vane must have a larger vane number than the upstream vane.

Iv	the vane number
N(iv)	the n grid number of the vane centre
M(iv)	the m grid number of the vane centre
ZTVANE(iv)	the level of the upper side of the vane with respect to the vertical reference level (positive upward)
HKVANE(iv)	the horizontal direction angle of the vane with respect to the positive x co-ordinate axis (positive counter-clockwise) [-,-,-,m,-]

Record 4 : iv Xv(iv) Yv(iv) ZTVANE(iv) HKVANE(iv) {C}{S}[I,4R]

{C} NVANNM = 2

{S} NVANES The sequence of the vanes has to be specified in such way that a vane affected by an upstream vane must have a larger vane number than the upstream vane

iv	the vane number
Xv(iv)	the x co-ordinate of the vane centre
Yv(iv)	the y co-ordinate of the vane centre
ZTVANE(iv)	the level of the upper side of the vane with respect to the vertical reference level (positive upward)
HKVANE(iv)	the horizontal direction angle of the vane with respect to the positive x-co-ordinate axis (positive counter-clockwise) [-,m,m,m,-]

Record 5: RLVANE [R]

RLVANE specifies the length of vane, [m].

Record 6: NRIVFT [I]

NRIVFT specifies the used mathematical model for the vanes
NRIVFT = 1 empirical description
= 2 Odgaard vane model

Record 7: DELTAD DELTAL [2R]

Specification of the effect of the vane resistance on the flow

DELTAD = 1.0 the vane resistance is included in the flow computation [-]
= 0.0 the vane resistance is not included
DELTAL = 1.0 the vane lift force is included in the flow computation [-]
= 0.0 the vane lift force is not included

Record 8: NVLTYP [I]

NVLTYP specifies the way in which the vortex lines generated by the vanes are determined.
NVLTYP = 1 the vortex lines run parallel to the grid lines
= 2 the vortex lines follow the streamlines

Record 9: CHORV [R]

CHORV specifies whether the body-fixed vortex is included in the model, [-].
CHORV = 0.0 the body fixed vortex is neglected
= 1.0 the body fixed vortex is included

Record 10: ALFHV [R]

ALFHV specifies the distance of the vortex line from the bed as a fraction of the active vane height, [-].

Record 11: CLU [R]

CLU specifies a correction coefficient for the lift coefficient of a vane (multiplies the theoretical lift coefficient), [-].

Record 12: NDMPVS [I]

NDMPVS specifies an option of the available damping formula used to damp out the initial vortex strength downstream along the vortex line (five options are available).

Record 13: DAMPCR BETAVS SMAXVS [3R]

Specification of coefficients used in the damping formulas (record 12) [-,-,m]

Record 14: INCFLO ALFBVV [I,R]

INCFLO specifies the way in which the incoming flow velocity induced by the vanes located upstream is computed.
INCFLO = 1 the induced velocity magnitude is independent of the distance to the corresponding vortex line
= 2 the induced velocity magnitude depends on the distance to the corresponding vortex line
The effect of the option chosen depends on the method chosen at record 6.

ALFBVV specifies a reduction of the lateral distance over which a vortex line will affect the incoming velocity of a vane, [-].

Record 15: ALFWMA XOMWMX [2R]

Specification of coefficients which are used to compute the induced incoming flow of a vane if INCFLO = 1.

ALFWMA multiplying coefficient to reduce the standard vane-induced incoming velocity. [-]
XOMWMX weighting coefficient of the peak velocity and the average transverse velocity used to determine the standard vane-induced velocity, [-].

Record 16: NJBINT [I]

NJBINT specifies the integration way of the vortex strength along the vortex line.

Record 17: DWINTC [R]

DWINTC specifies a tuning coefficient for the initial vortex strength used in case of mathematical model NRIVFT=1, [-].

Record 18: ALFJBA ALFJBB [2R]

Specification of coefficients concerns the transverse vane-induced velocity distribution.

ALFJBA coefficient of vane-induced transverse velocity integral used in NRIVFT = 2, [-].
ALFJBB coefficient in transverse velocity distribution used in NRIVFT = 1, [-].

Record 19: DCRH DCRHV [2R]

Specification of coefficients to determine the width over which the vortex line will be active with

respect to the effect of the incoming velocity of a downstream vane.

DCRH coefficient of the water depth, [-].
DRCHV coefficient of the vane height, [-].

Record 20: UPFLDS [R]

UPFLDS specifies the upstream location of a vane at which the incoming velocity will be determined. The velocity point will be situated at UPFLDS times the vane length upstream of the vane centre, [-].

Record 21: DSMAX [R]

DSMAX specifies the maximum length of an increment along a vortex line. If DSMAX exceeds the local grid cell length, the increment used will be kept equal the cell length. The vortex intensity variation along the vortex line will be computed with this length step [m].

Record 22: NEWSQM [I]

NEWSQM specifies the maximum number of times the sequence of the vane numbering may be adapted by the program. The numbering sequence should be chosen according to the rule given in record 4. If the specified sequence does not obey this rule, the program will adapt the sequence at most NEWSQM times. This option is not implemented yet, a dummy value 1 has to be specified.[-]
Only a warning will be given if the vane sequence is out of order.

Record 23: ITVANA ITVANB IDTVAN [3I]

Specification of the time interval of vane output.

ITVANA starting time expressed in TSCALE
ITVANB stopping time expressed in TSCALE
IDTVAN time increment expressed in TCSALE

Record 24: NUVVAN [I]

NUVVAN specifies an option to define the flow field to be used to compute a stream line and vortex line. Four options are available:

1. depth-averaged flow field
2. velocity field at vane height, derived from the depth-averaged flow field, using a vertical power law distribution
3. As 2 but including the spiral motion
4. As 3 but also including the upstream vane-induced flow

Record 25: RDXEPS MODCOM NTESTU NTESTT IVANTS [R,3I,R]

TTESTV

Specification of test parameters

RDXEPS	relative accuracy, too high or too low accuracy may abort the run. The absolute grid co-ordinates may be so large that difference between two neighbouring co-ordinates is rather inaccurate because of data loss.
MODCOM	= 0 if during the vortex line computation an error occurs, the computation proceeds with the next vortex line = 1 if during the vortex line computation an error occurs, the computation stops after generation of some additional output
NTESTU	= 0 no test output = 1 output of computed data after at each time step
NTESTT	= 0 No test output = 1 test output (should not be used in applications)
IVANTS	number of the vane for which details of the vortex line computation will be printed on tra-diag.<case> file
TTESTV	the vortex details of vane IVANTS are stored if the simulation time exceeds TTESTV (in TSCALE).

If in the computations an error occurs during the vortex line computation, the program stops and generates a large number of test data. A change of the accuracy RDXEPS or a grid origin closer too the model area may solve the problem. If not, please contact WL | Delft Hydraulics.

B.3.4 Description bottom vane type 2 input file

This input file contains just one record containing the values of three parameters

Record 1: ALFSUS ALFV XLAB [3R]

Specification of type 2 bottom vane parameters with respect morphology.

ALFSUS	sediment fraction representing suspended transport (in case of total load formula)
ALFV	effective vane height coefficient (<1.0)
XLAB	gradient of the concentration distribution in front of the vane. Equals 0 if the suspended sediment concentration is uniformly distributed over the water column.

Appendix C Results of type 1 vanes

Curved flume tests

C-1: Computational grid and locations of bottom vanes.
C-2: Comparison of results for new and old Delft3D version, case bb2.
C-3: Comparison of results for new and old Delft3D version, case bb4.
C-4: Absolute bed level and bed level relative to initial bed level with uniform bed slope in the case without bottom vanes.
C-5: Bed level in the case with bottom vanes relative to initial bed level with uniform slope and relative to bed level in case of no vanes.

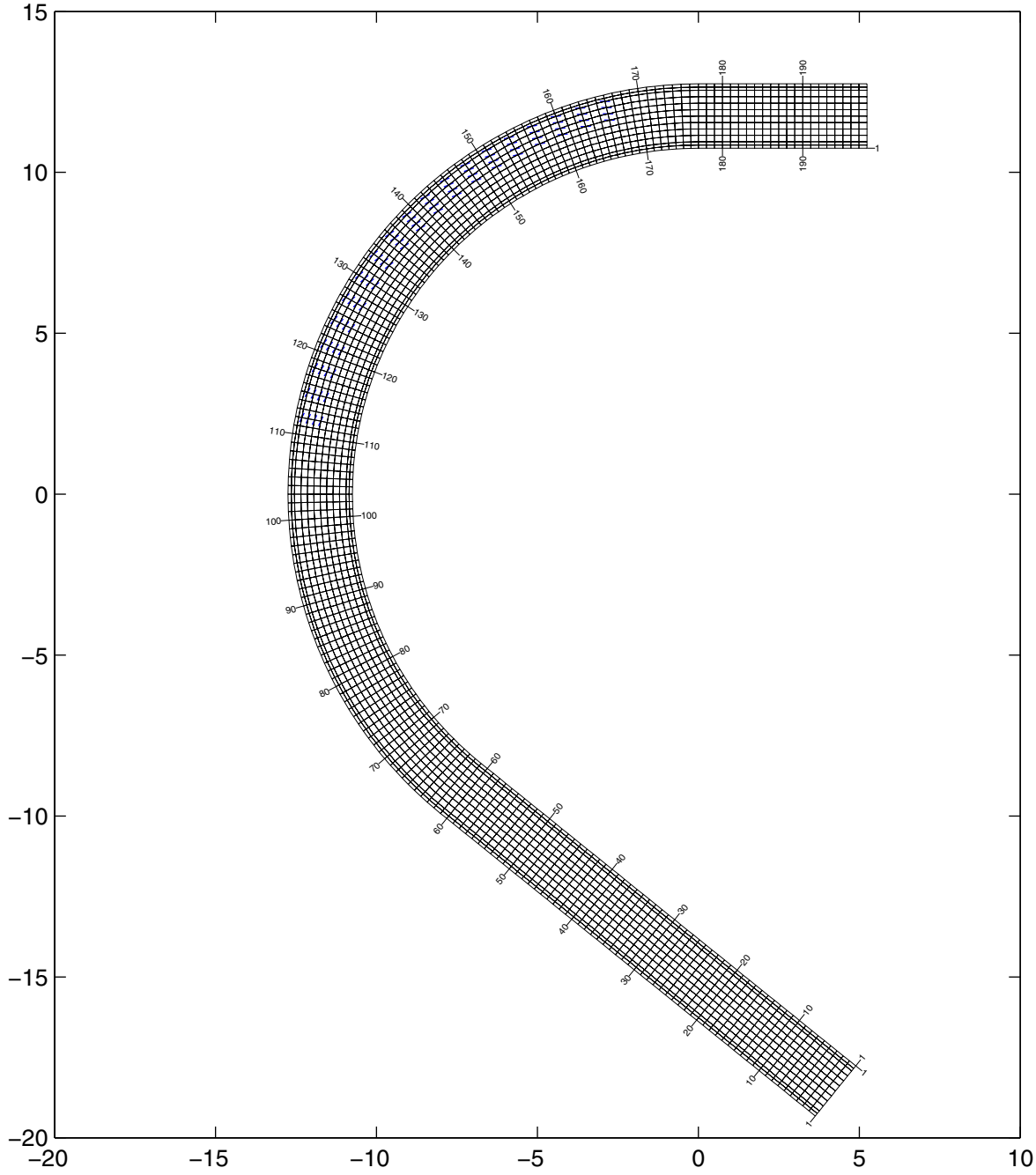

Computational grid and location of submerged vanes		
	Curved flume case	
WL | DELFT HYDRAULICS		C−1

Comparison of updated Delft3D version (points) and old Delft3D version (lijn) Reference situation without vanes indicated in red.	bb2	
	curved flume case	
WL | DELFT HYDRAULICS	Q2681	C–2

WL | DELFT HYDRAULICS

Comparison of new Delft3D version (points)
and old Delft3D version (line)
Reference situation without vanes indicated in red.

Q2681

bb4

C–3

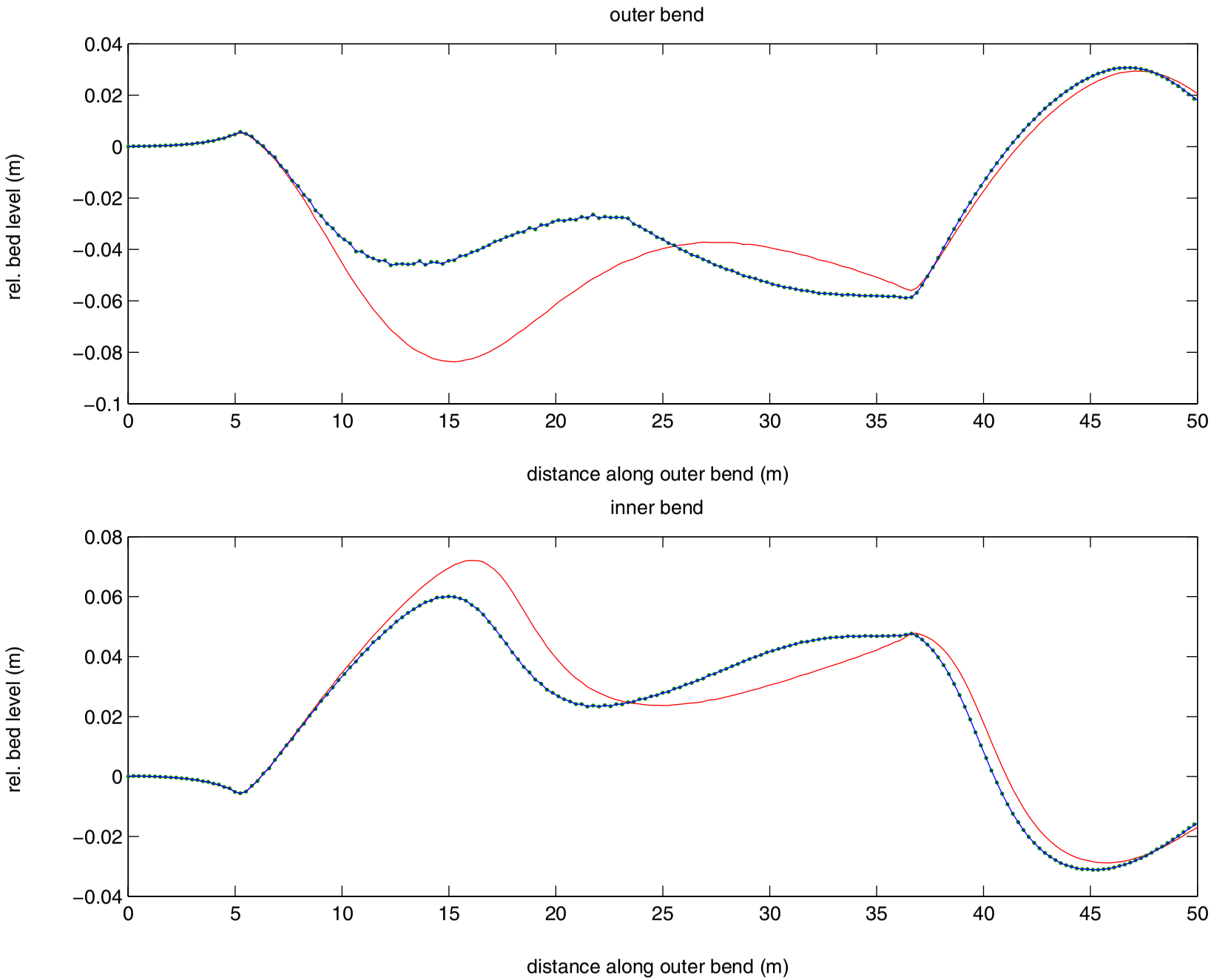

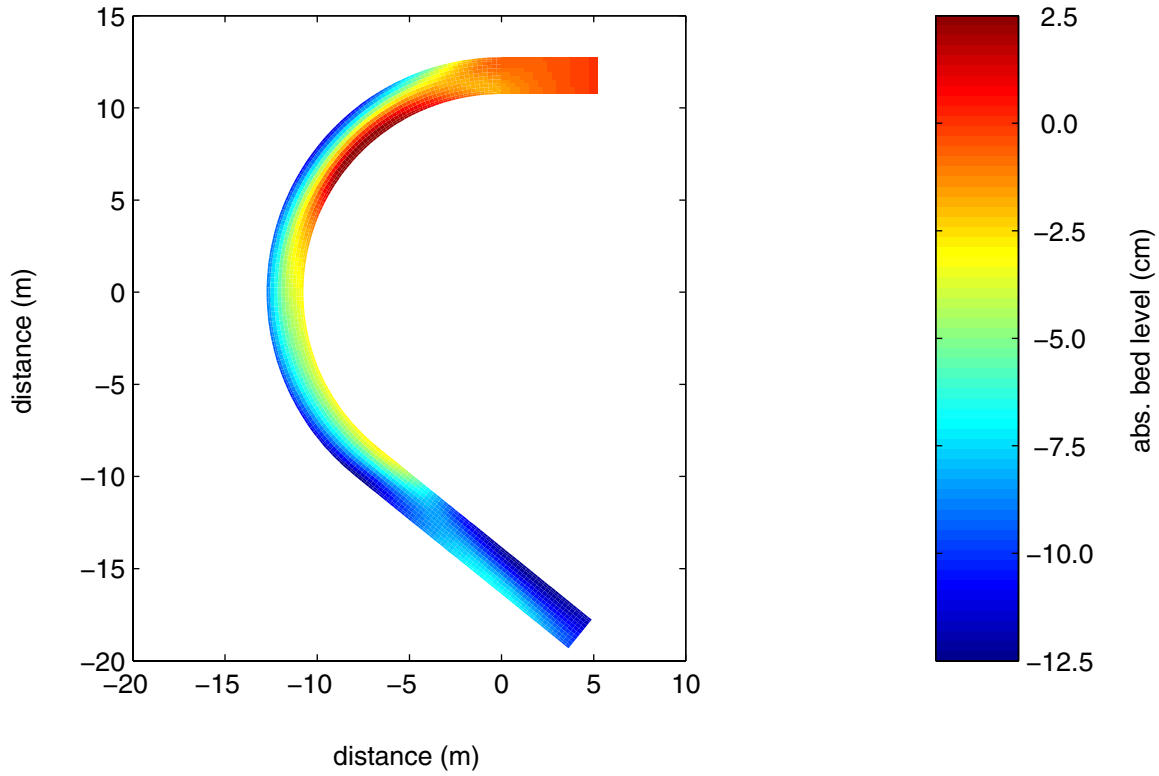

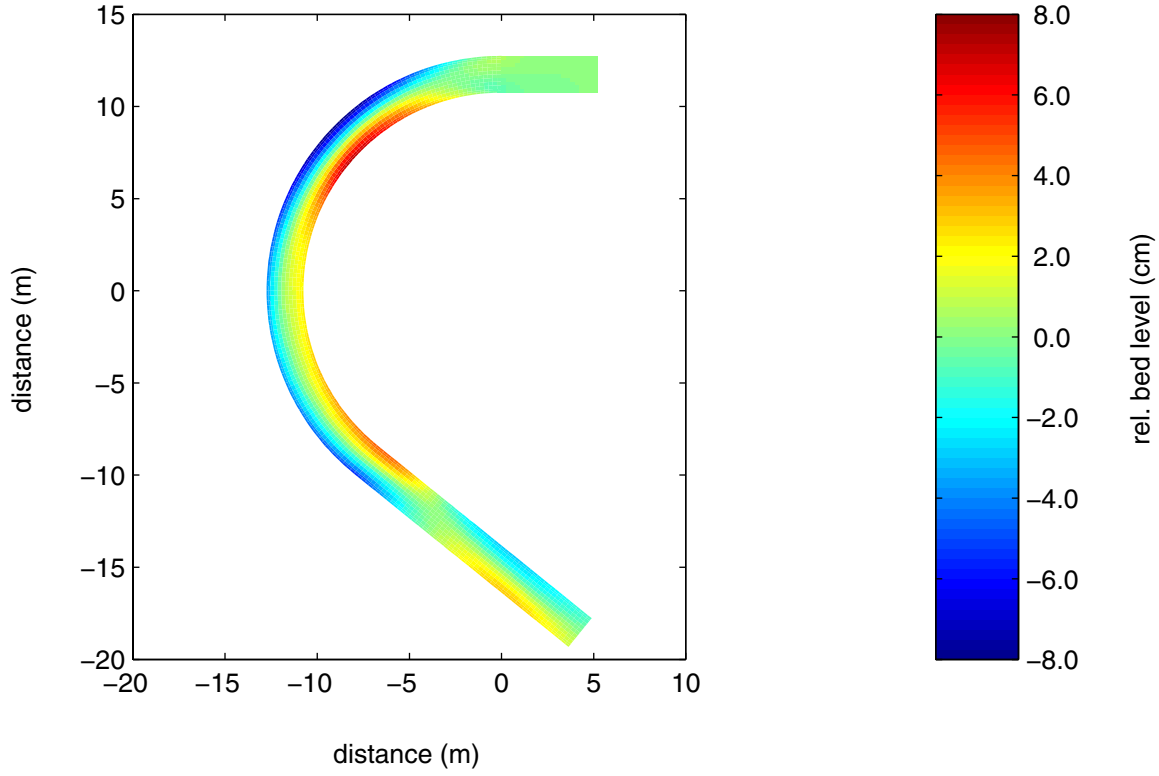

Absolute bed level and bed level relative to the initial bed level with uniform bed slope in case of situation without submerged vanes	bb0	
	Curved flume case	
WL | DELFT HYDRAULICS	Q2681	C–4

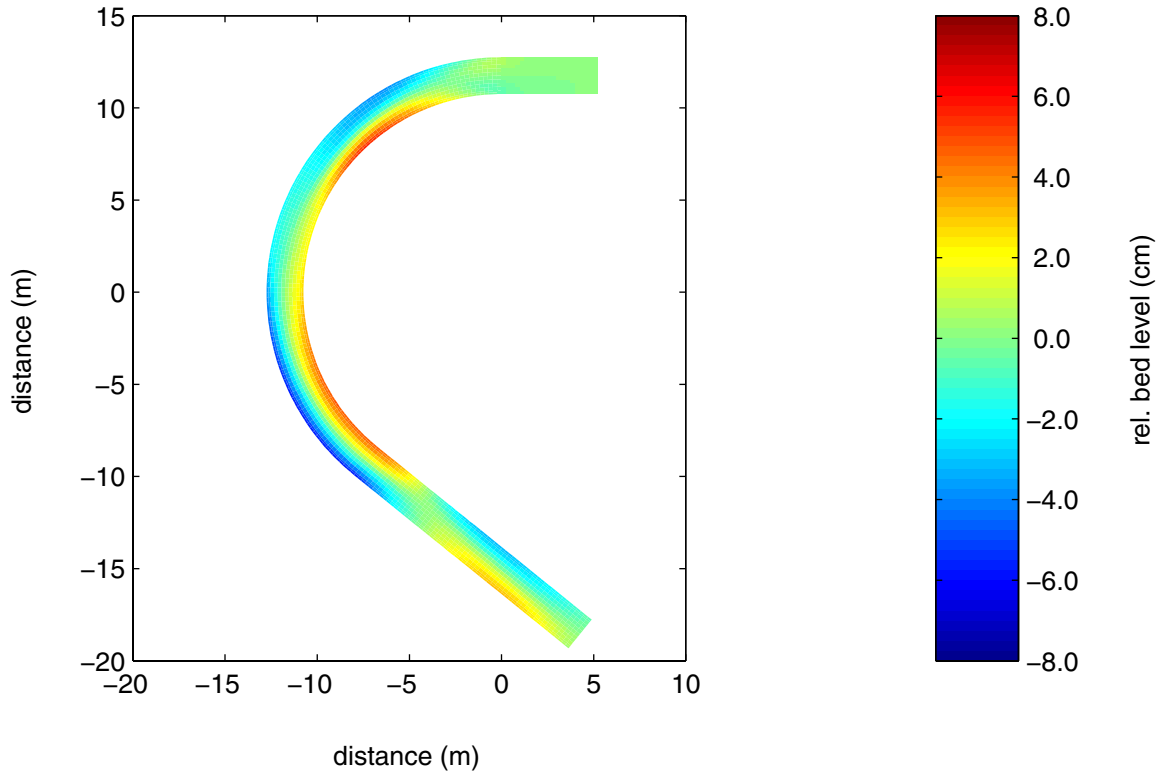

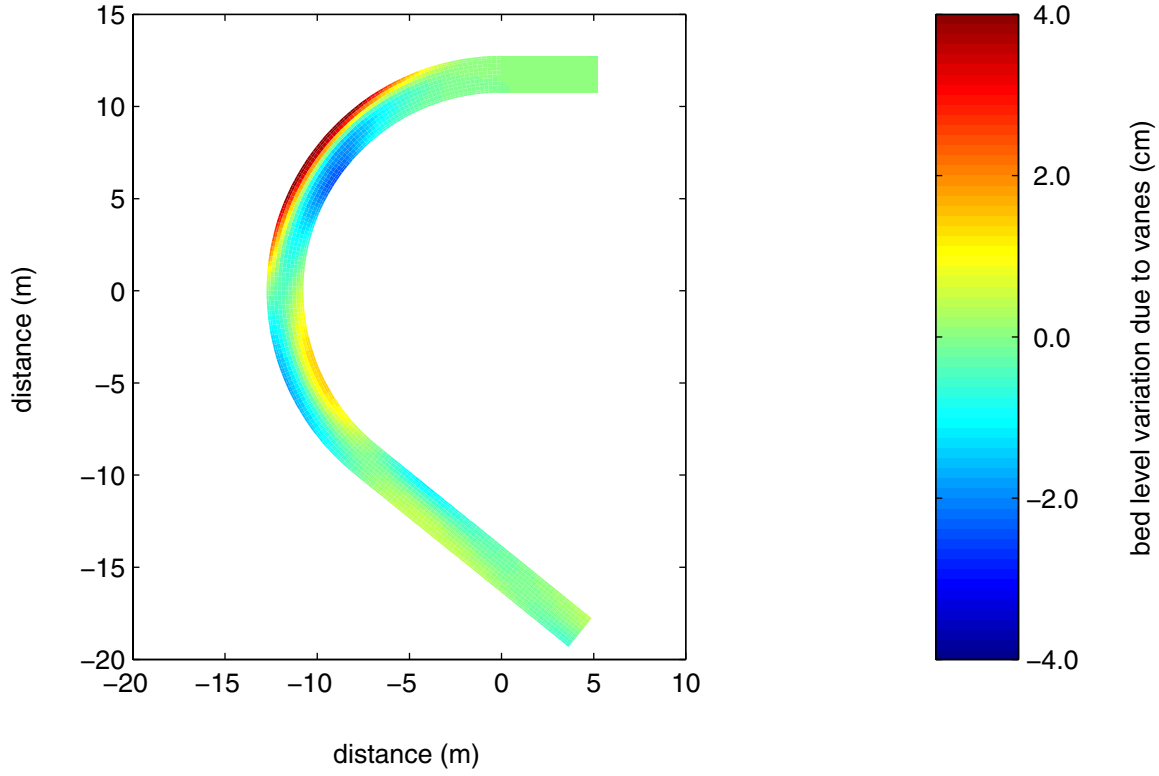

Bed level in case of situation with submerged vanes, relative to initial bed level with uniform slope and relative to bed level in case of no vanes.	bb2	
	Curved flume case	
WL | DELFT HYDRAULICS	Q2681	C–5

Appendix D Results of type 2 vanes

Basic tests:

D-1: Simulation of a vane height of 8.0 m and vane angle of 90 degrees relative to the positive x-axis.
D-2: Simulation of a vane height of -1.0 m and vane angle of 90 degrees relative to the positive x-axis.
D-3: Simulation of a vane height of –1.0 m and vane angle of 0 degrees relative to the positive x-axis.
D-4: Simulation of a vane height of 1 mm and vane angle of 90 degrees relative to the positive x-axis.
D-5: Simulation of a vane height of 3.0 m and vane angle of 90 degrees relative to the positive x-axis.
D-6: Simulation of a vane height of 3.0 m and vane angle of 0 degrees relative to the positive x-axis.
D-7: Simulation of a vane height of 3.0 m and vane angle of 60 degrees relative to the positive x-axis.
D-8: Simulation of a vane height of 3.0 m and vane angle of 30 degrees relative to the positive x-axis.
D-9: Simulation of a vane height of 3.0 m and vane angle of 15 degrees relative to the positive x-axis.
D-10: Simulation of a vane height of 3.0 m and vane angle of 0 degrees relative to the positive x-axis.
D-11: Simulation of a vane height of 3.0 m and vane angle of 90 degrees relative to the positive x-axis.
D-12: Simulation of a vane height of 3.0 m and vane angle of 0 degrees relative to the positive x-axis.
D-13: Simulation of a vane height of 3.0 m and vane angle of 162 degrees relative to the positive x-axis.
D-14: Simulation of a vane height of 3.0 m and vane angle of 0 degrees relative to the positive x-axis.
D-15: Simulation of a vane height of 3.0 m and vane angle of 45 degrees relative to the positive x-axis.
D-16: Simulation of a vane height of 6.5 m and vane angle of 45 degrees relative to the positive x-axis.
D-17: Simulation of a vane height of 6.5 m and vane angle of 45 degrees relative to the positive x-axis.
D-18: Simulation of a vane height of 6.5 m and vane angle of 45 degrees relative to the positive x-axis.
D-19: Simulation for a surface vane above water (lower level at +9.0 m and a vane angle of 0 degrees relative to the positive x-axis.
D-20: Simulation for a surface vane blocking the flow (lower level at -1.0 m and a vane angle of 0 degrees relative to the positive x-axis.
D-21: Simulation for a surface vane with its lower level at 7.0 m and a vane angle of 0 degrees relative to the positive x-axis.
D-22: Simulation for a surface vane with its lower level at 4.0 m and a vane angle of 0 degrees relative to the positive x-axis.
D-23: Simulation for a surface vane with its lower level at 4.0 m and a vane angle of 60 degrees relative to the positive x-axis.
D-24: Simulation for a surface vane with its lower level at 4.0 m and a vane angle of 90 degrees relative to the positive x-axis.
D-25: Upper plot: evolution of bed levels (50 computational steps between lines); Lower plot: bed

level development at the location of the vane and in two points just upstream and downstream of the vane.

Simple bifurcation point

D-26: Two different computational grids for the same bifurcation; flow from left to right; distances in m.
D-27 Representation of the type 2 vane on the two variants of the grid; flow from left to right; distances in m.
D-28 Equilibrium bed levels without vanes, determined for the 2 schematization variants.
D-29 Flow pattern for the equilibrium bed levels without vanes, determined for the 2 schematization variants.
D-30 Sediment transport rates associated with the equilibrium conditions; determined for the 2 schematization variants.
D-31 Depth-averaged flow pattern before (gray) and after (blue) the construction of the bottom vane; determined for the 2 schematization variants.
D-32 Depth-averaged flow pattern before (gray) and after (blue) the construction of the bottom vane; determined for the 2 schematization variants.
D-33 Depth-averaged flow pattern before (top) and after (bottom) the construction of the bottom vane; determined for the 2 schematization variants (gray and blue).
D-34 Bed levels 7.5 months after the construction of the bottom vane; determined for the 2 schematization variants.
D35 Bed level changes during the first 7.5 months after the construction of the bottom vane; determined for the 2 schematization variants.
D36 Bed level changes during the first 7.5 months after the construction of the bottom vane; differences determined for 2 schematization variants.
D37 Sediment transport rate after 7.5 months; determined for 2 schematization variants.
D38 Sediment transport rate after 7.5 months; determined for 2 schematization variants.
D39 Changes in sediment transport rate after 7.5 months; differences determined for 2 schematization variants.
D40 Depth-averaged flow pattern before (gray) and after (blue) the construction of the surface vane; determined for 2 schematization variants.
D41 Bed level changes during the first 7.5 months after the construction of the bottom vane; determined for 2 schematization variants.

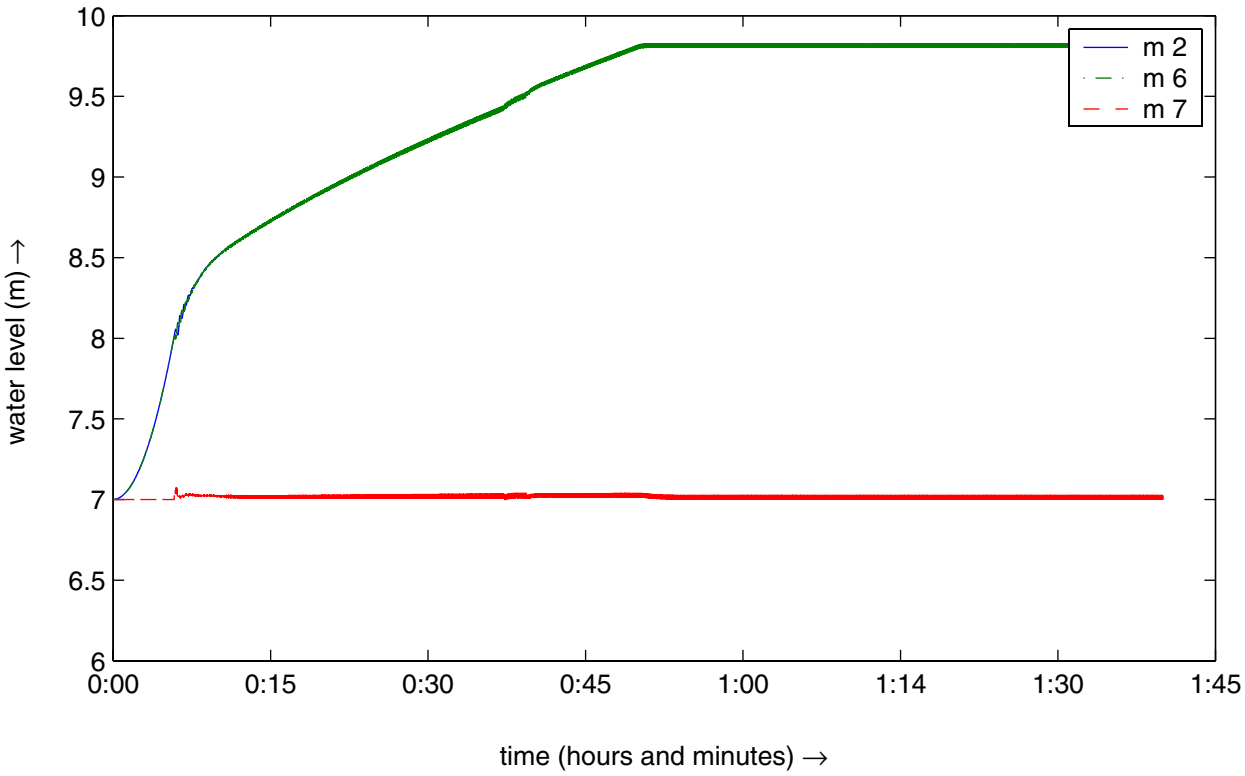

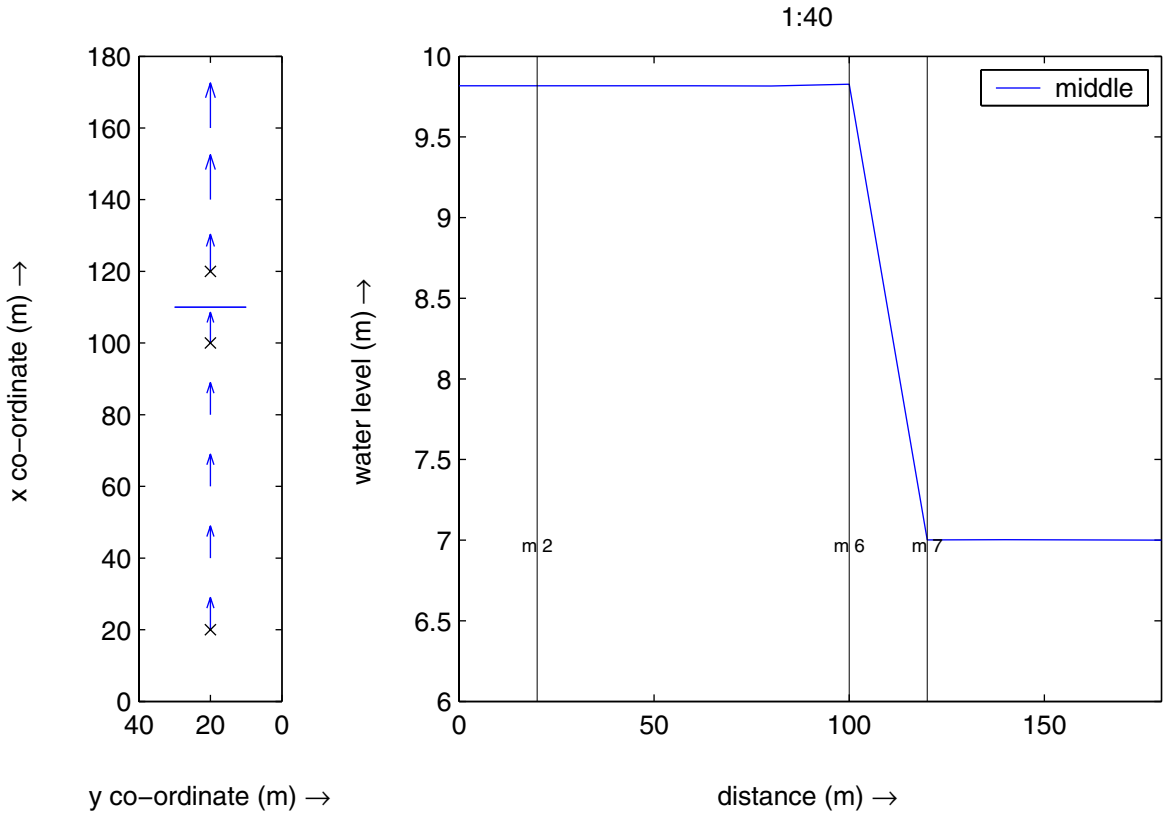

Simulation for a vane height of 8.0 m and a vane angle of 90 degrees relative to the pos. x−axis.	s1u	
WL | DELFT HYDRAULICS	Q2681	D−1

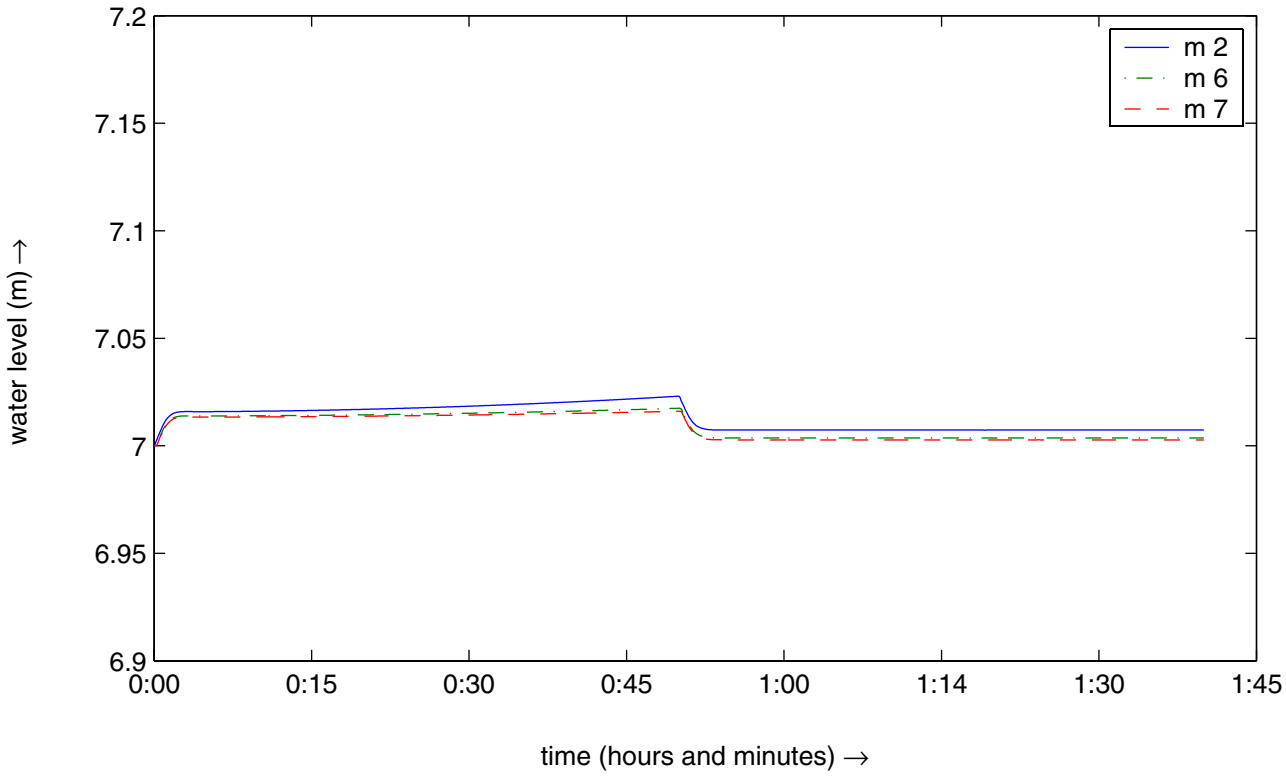

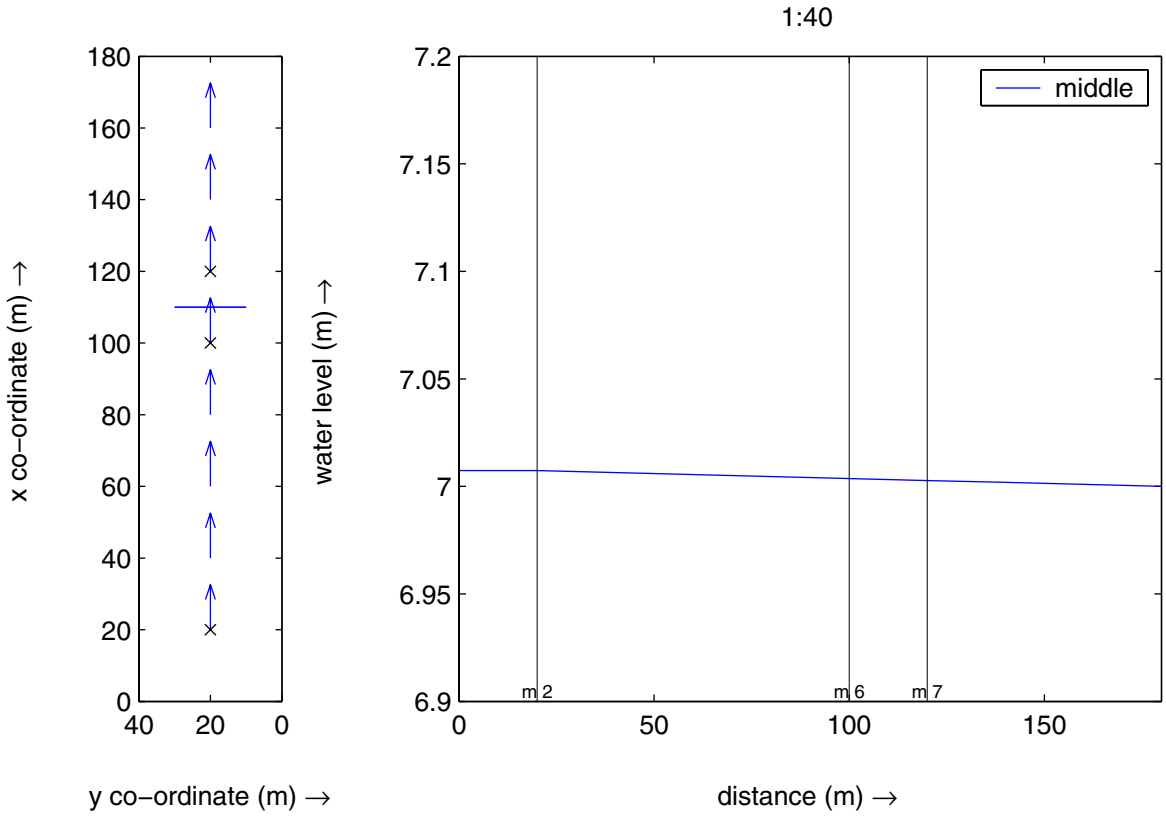

Simulation for a vane height of −1.0 m and a vane angle of 90 degrees relative to the pos. x−axis.	s2u	
WL | DELFT HYDRAULICS	Q2681	D−2

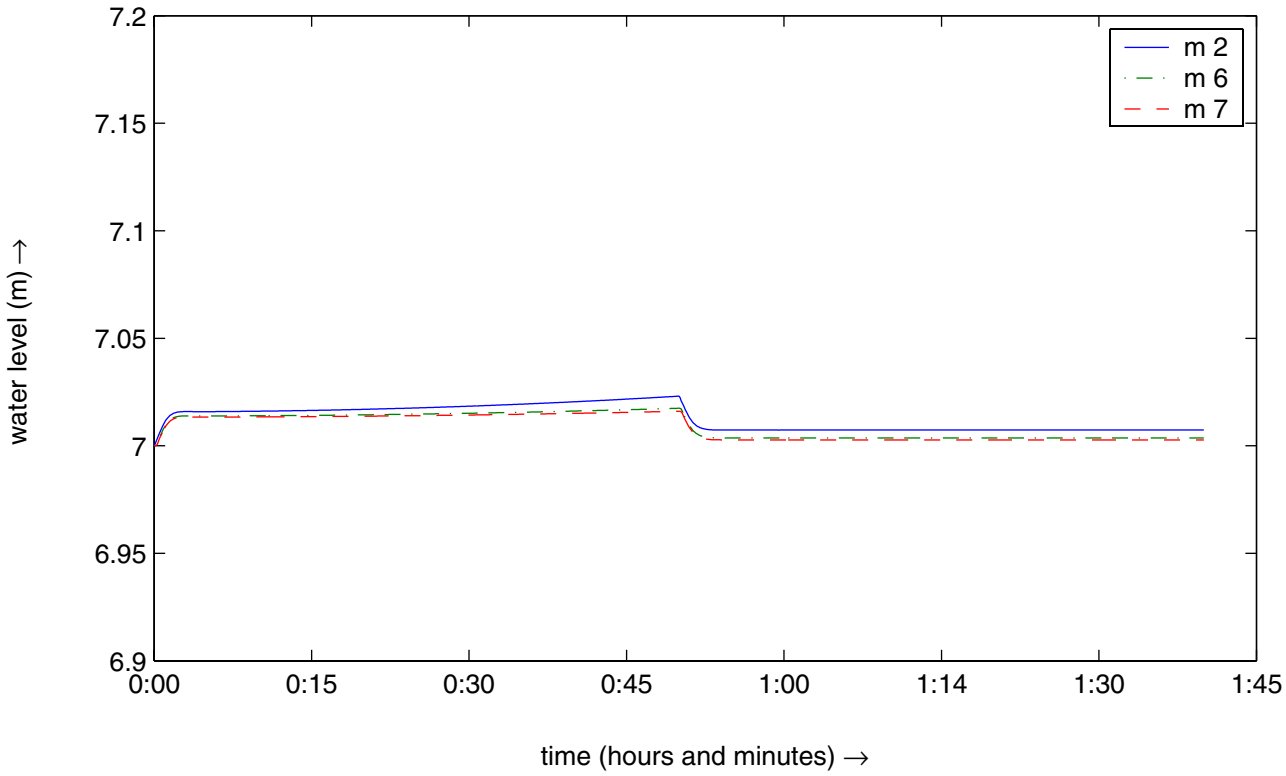

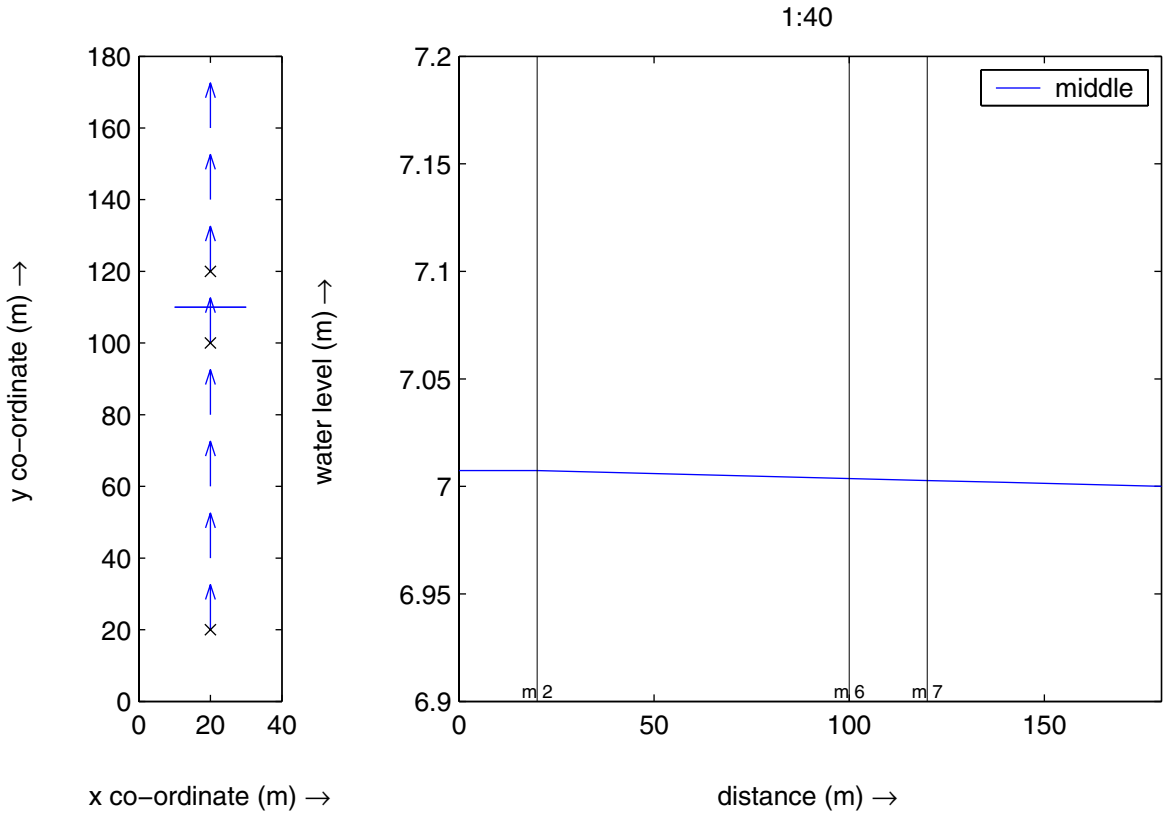

Simulation for a vane height of −1.0 m and a vane angle of 0 degrees relative to the pos. x−axis.	s2v	
WL | DELFT HYDRAULICS	Q2681	D−3

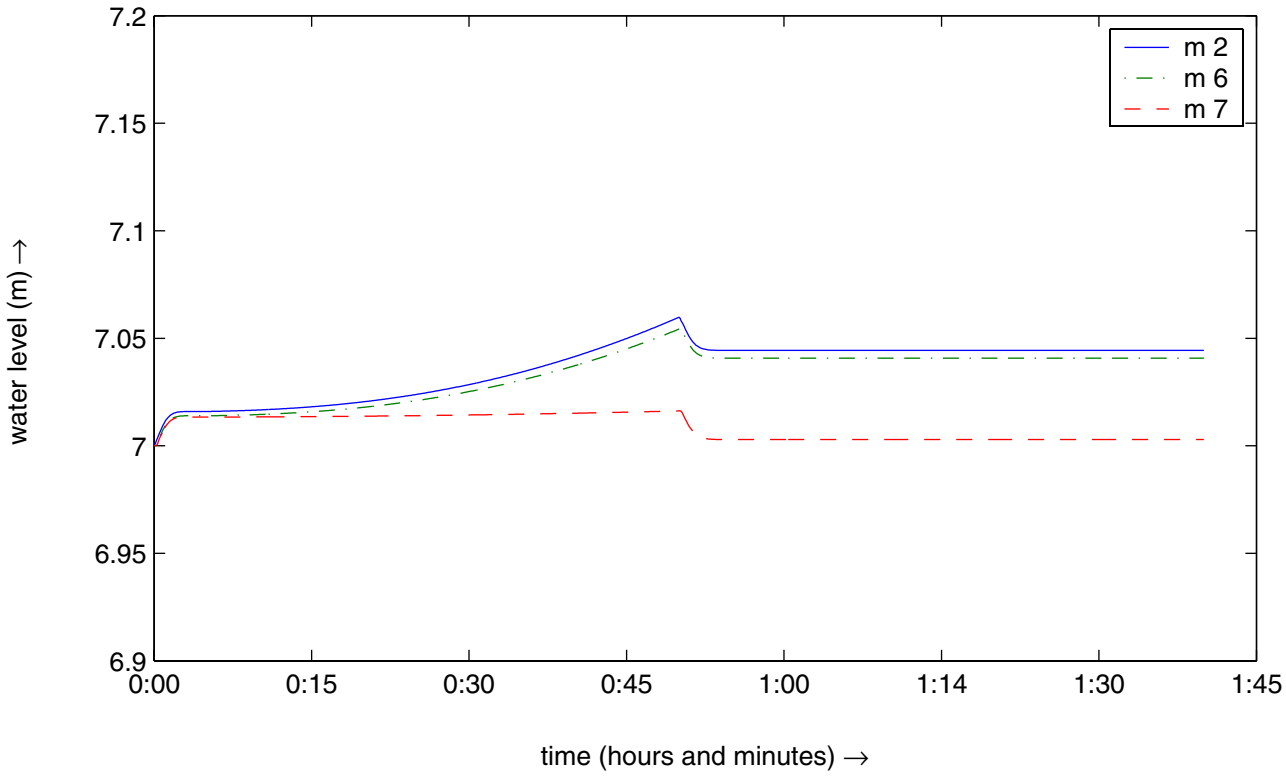

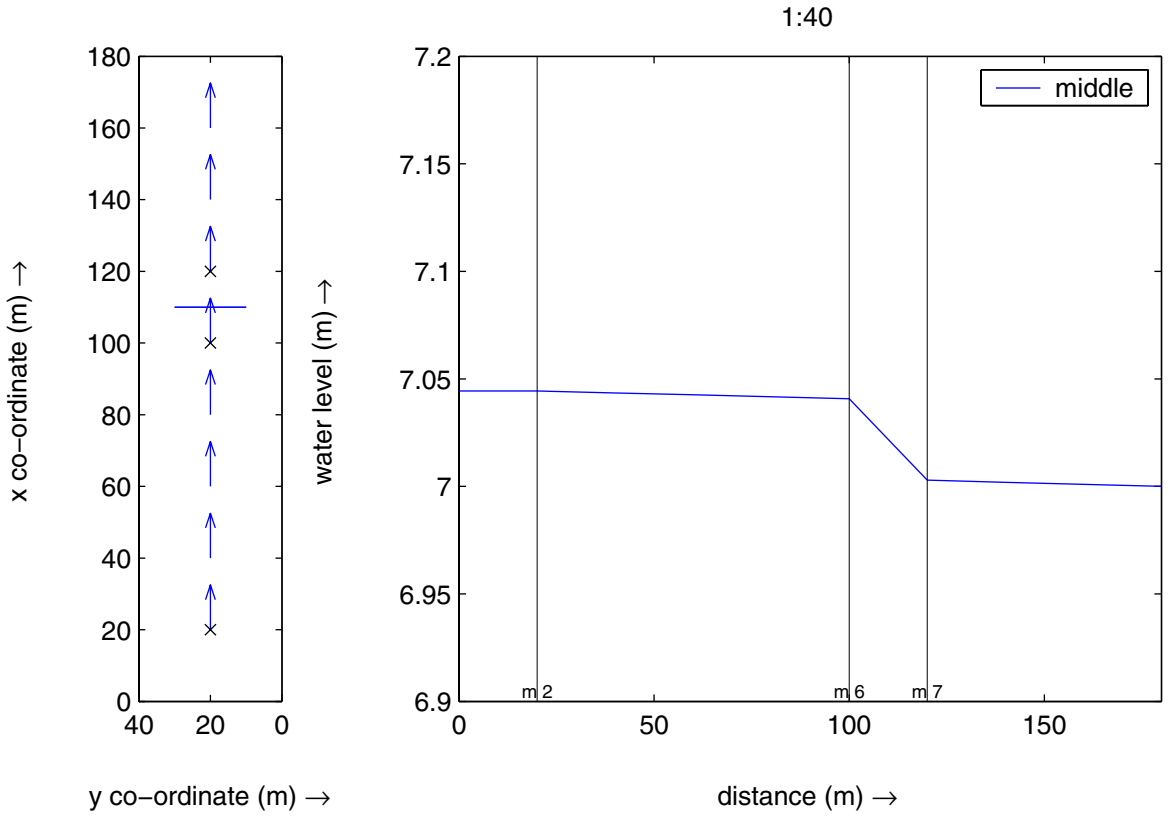

Simulation for a vane height of 0.0 m and a vane angle of 90 degrees relative to the pos. x−axis.	s3u	
WL | DELFT HYDRAULICS	Q2681	D−4

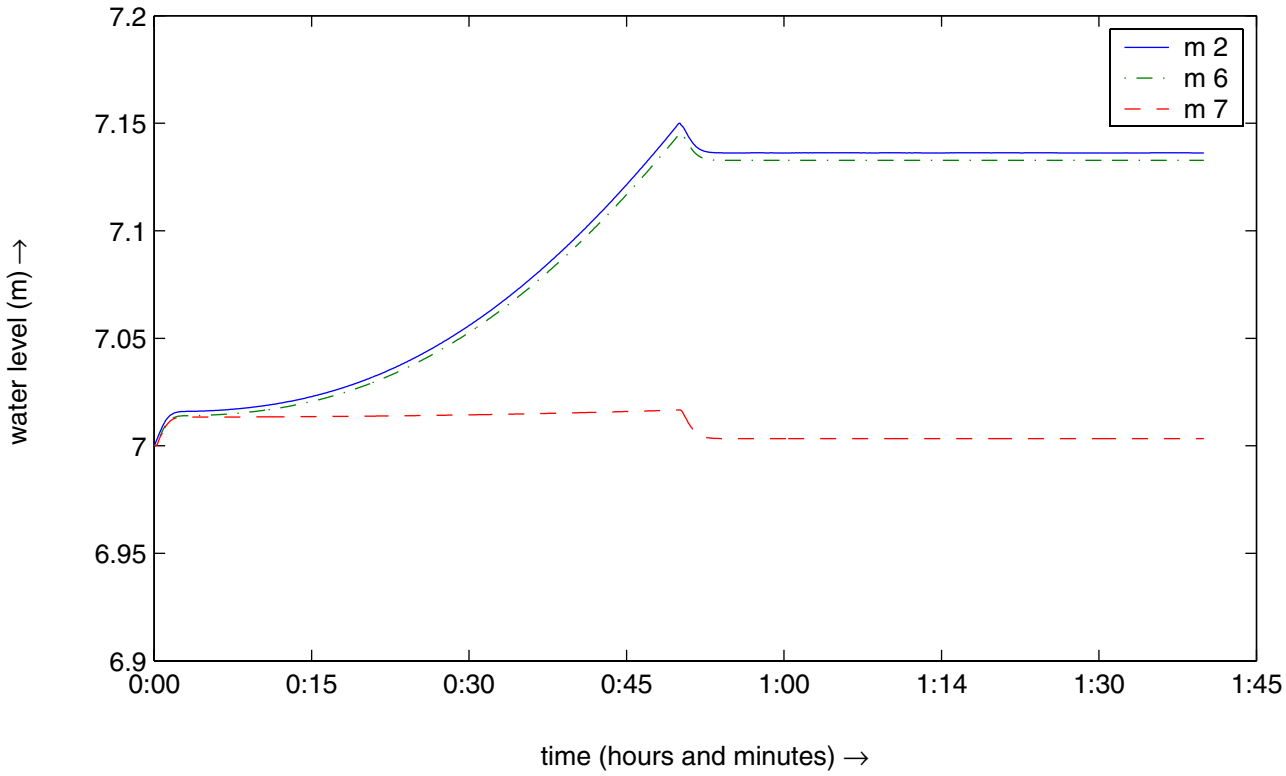

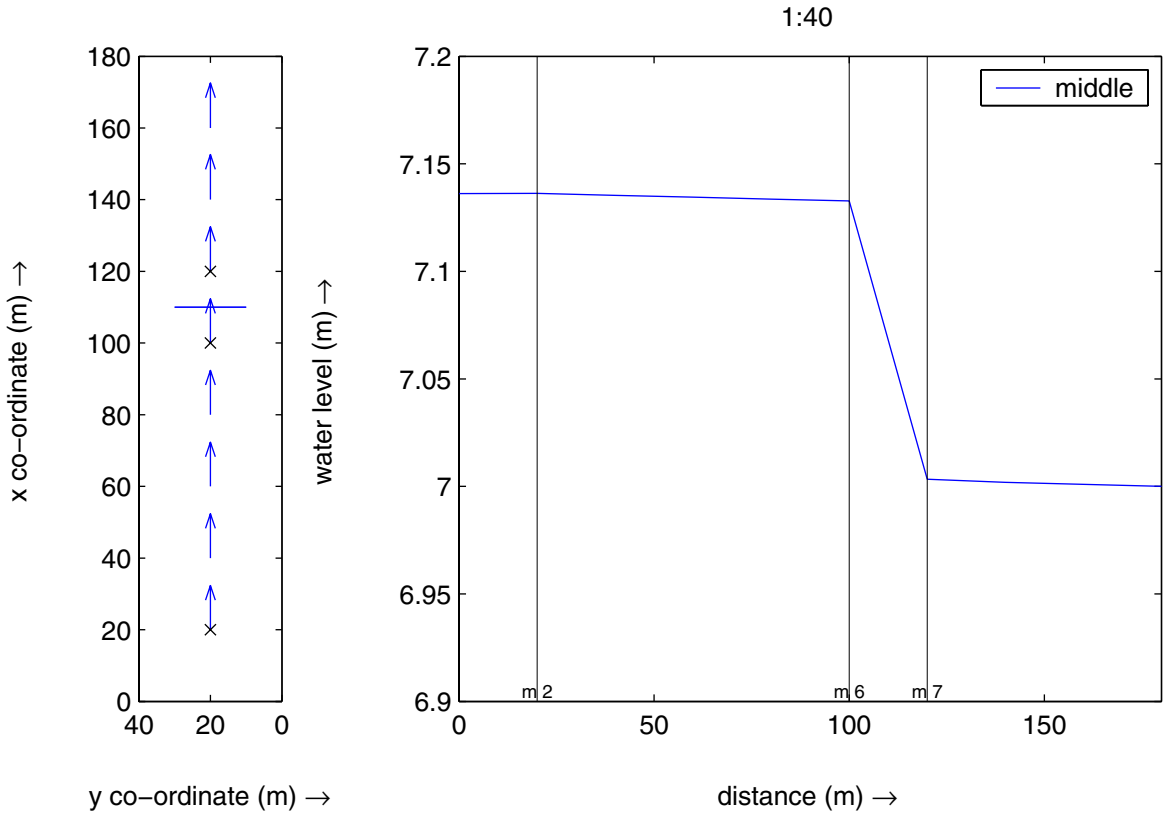

Simulation for a vane height of 3.0 m and a vane angle of 90 degrees relative to the pos. x−axis.	s4u	
WL | DELFT HYDRAULICS	Q2681	D−5

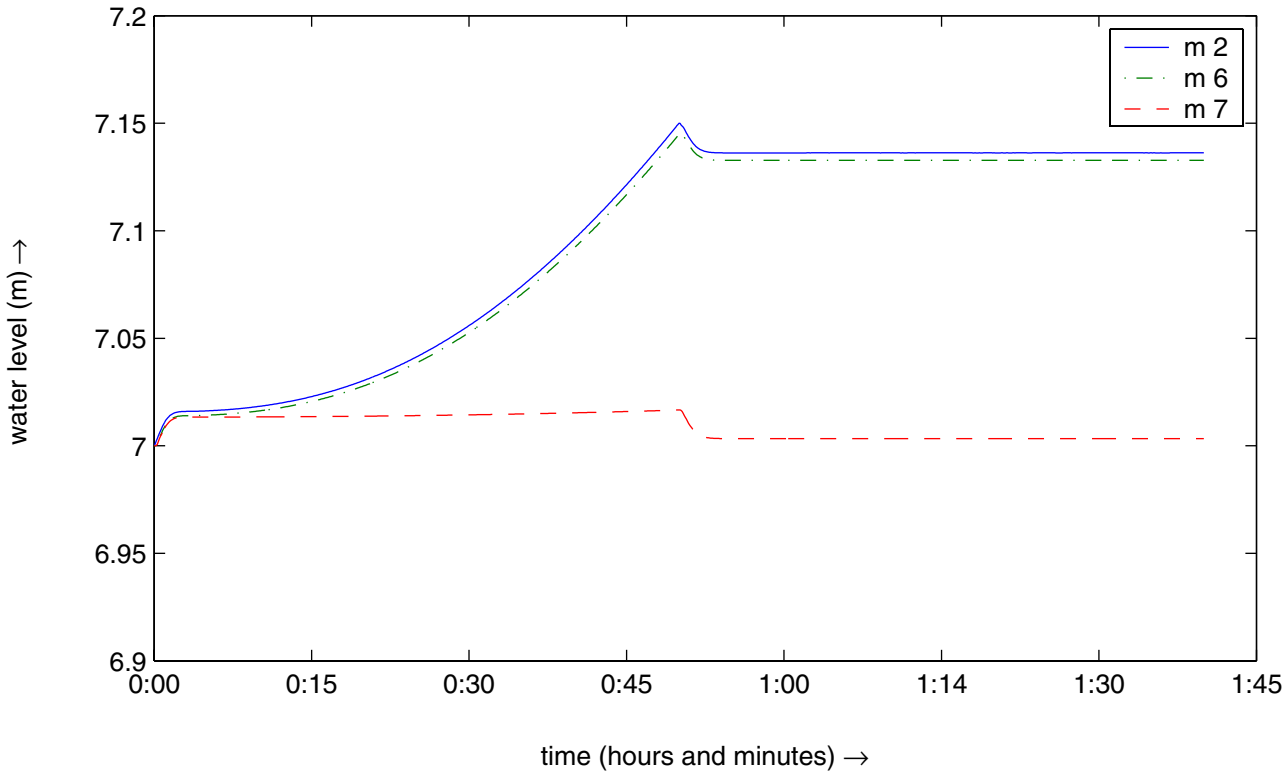

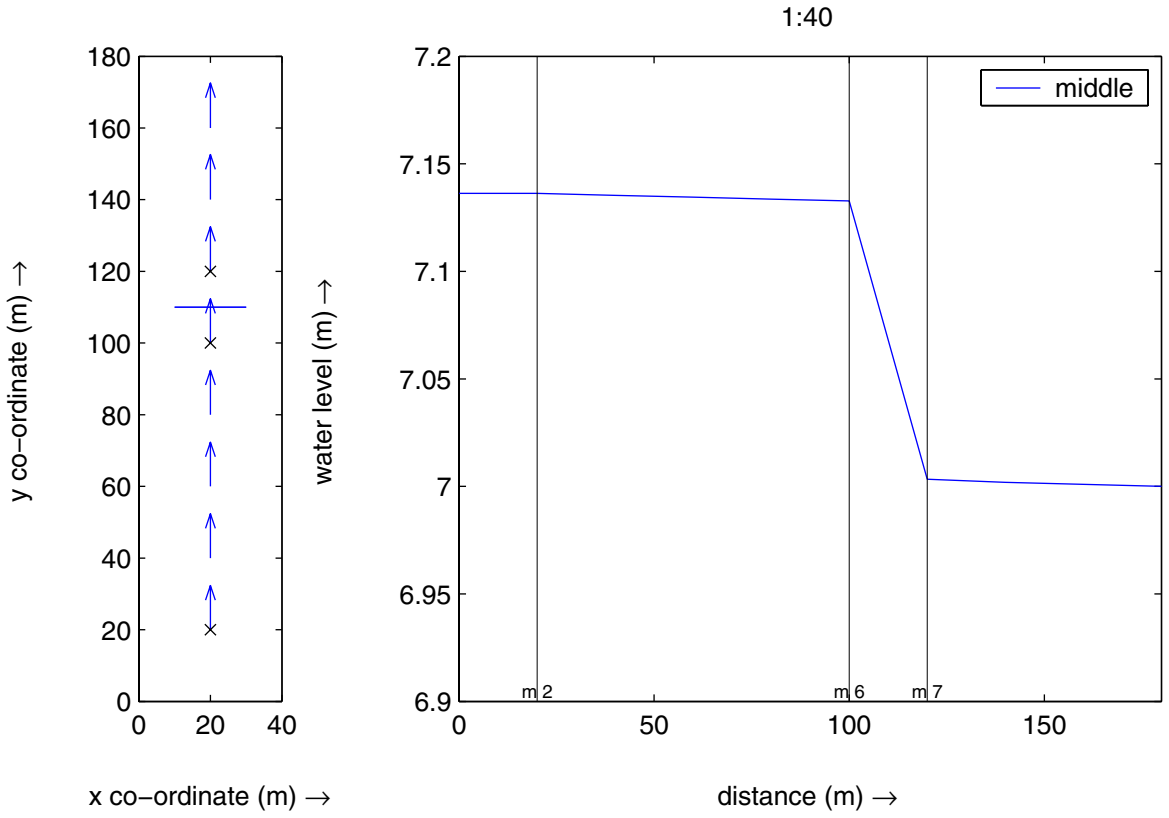

Simulation for a vane height of 3.0 m and a vane angle of 0 degrees relative to the pos. x−axis.	s4v	
WL | DELFT HYDRAULICS	Q2681	D−6

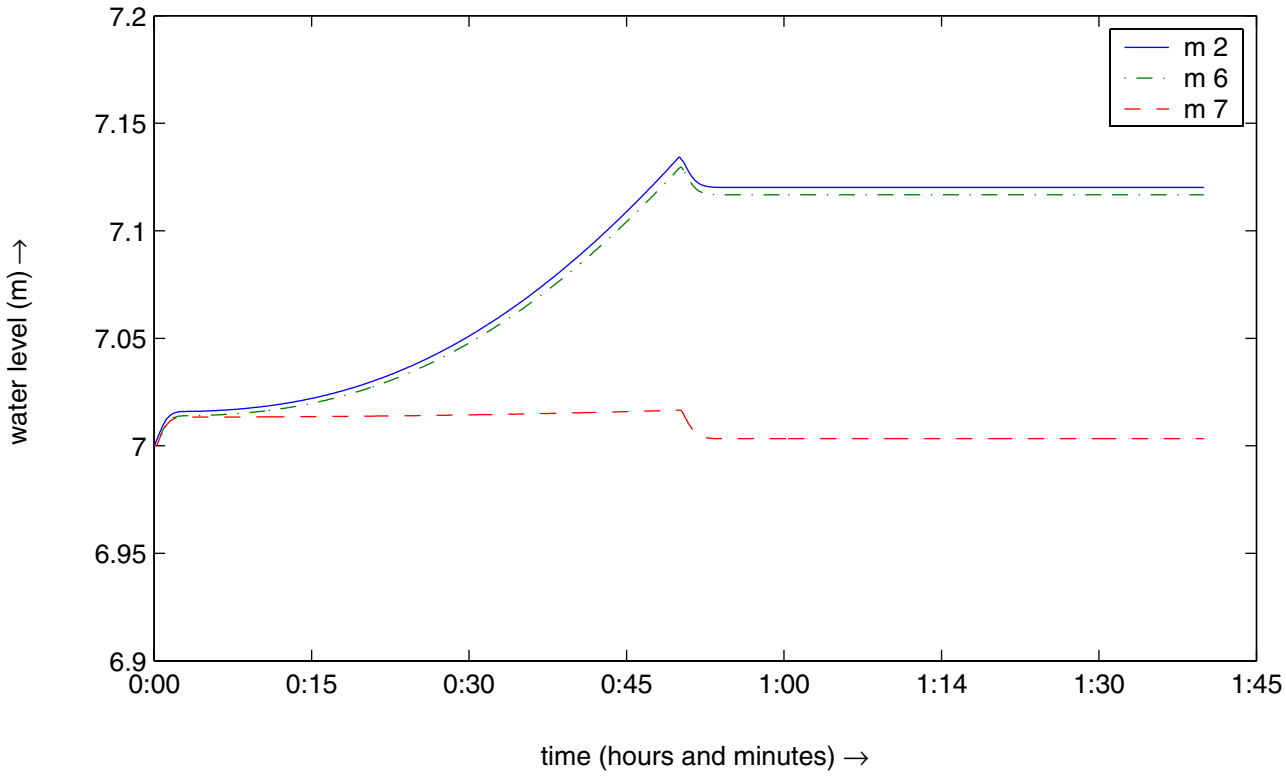

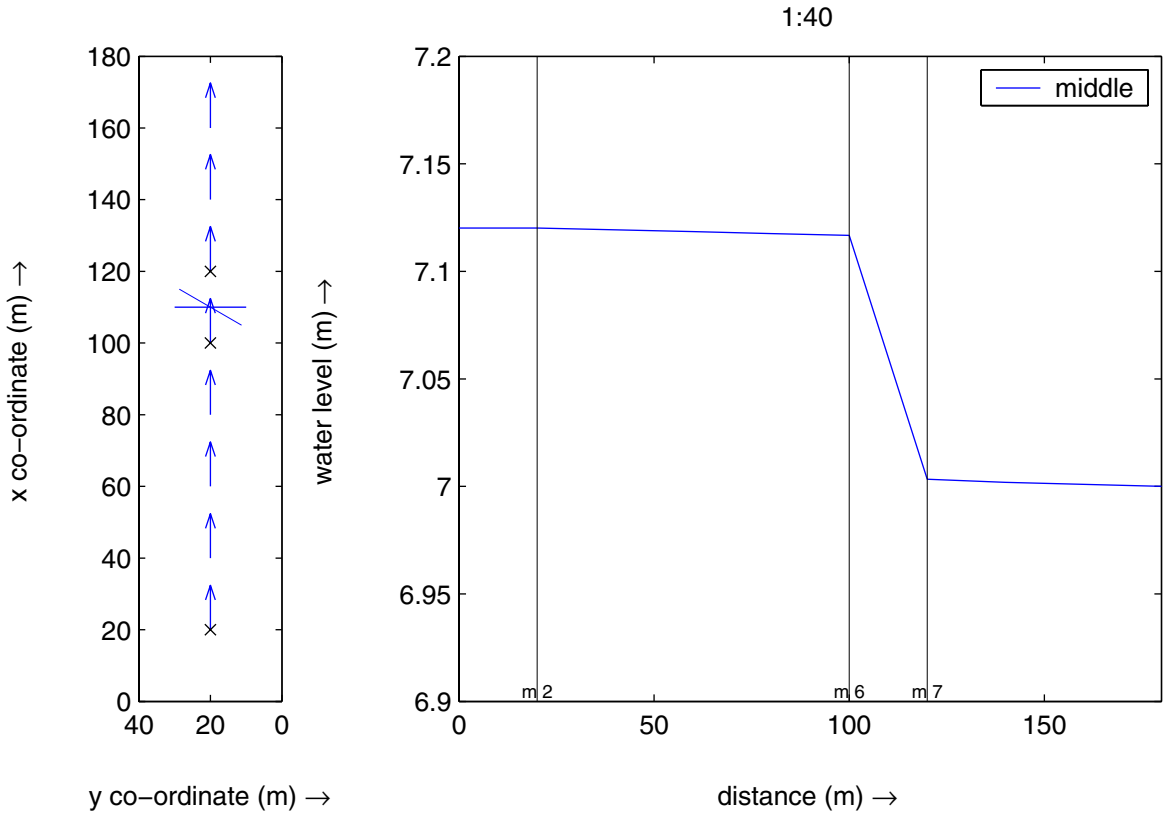

Simulation for a bottom vane height of 3.0 m and a vane angle of 60 degrees relative to the pos. x−axis.	s5u	
WL | DELFT HYDRAULICS	Q2681	D−7

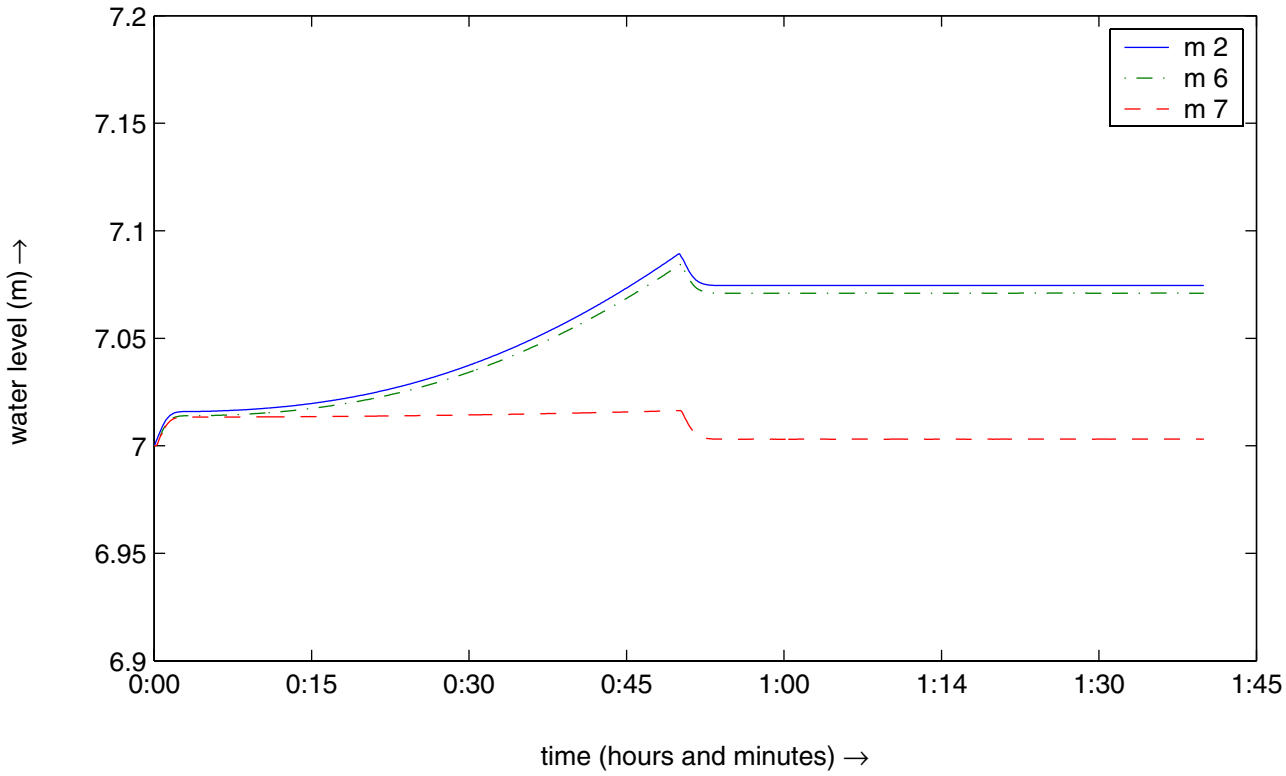

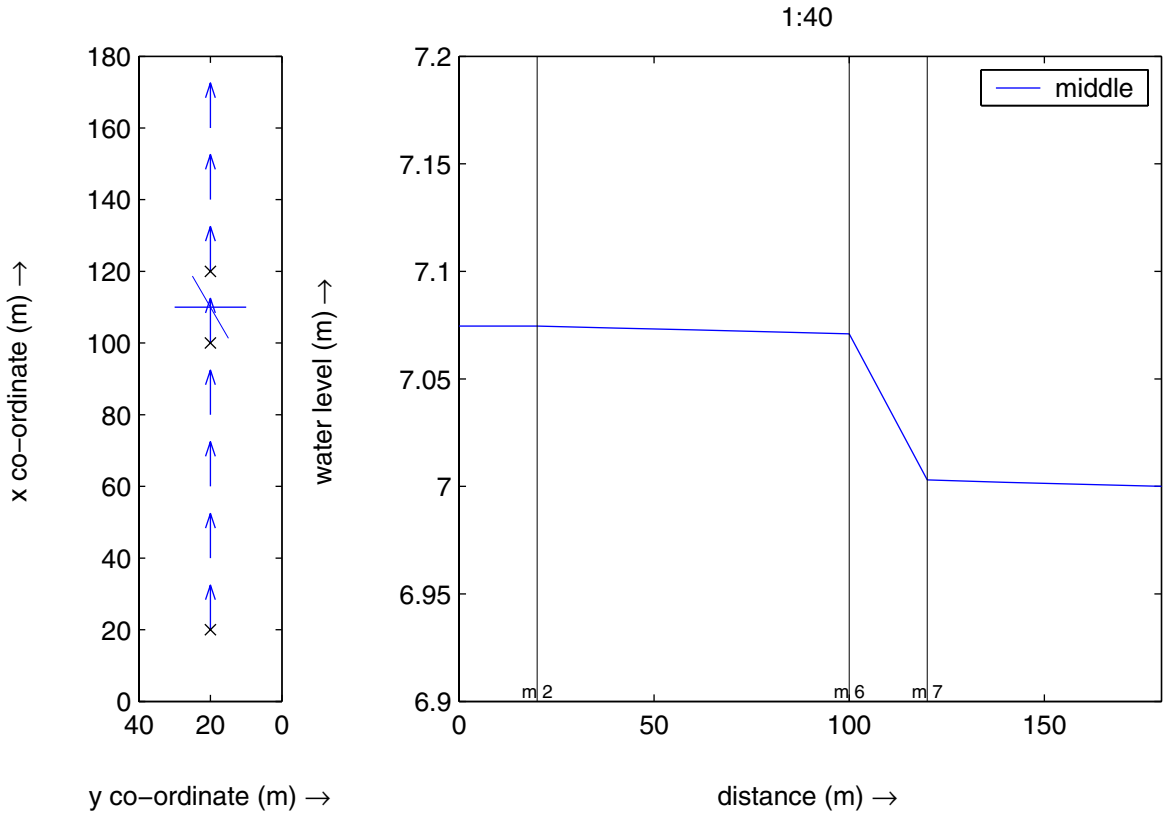

Simulation for a vane height of 3.0 m and a vane angle of 30 degrees relative to the pos. x−axis.	s6u	
WL | DELFT HYDRAULICS	Q2681	D−8

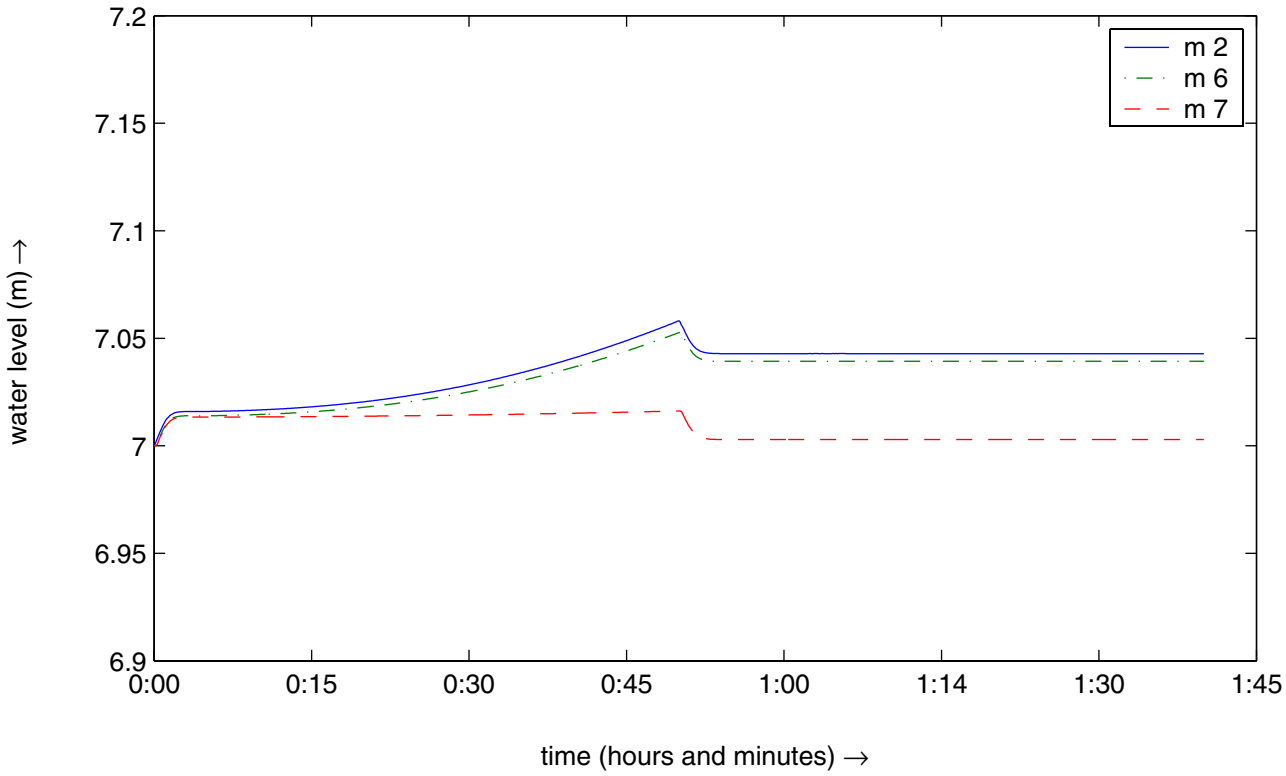

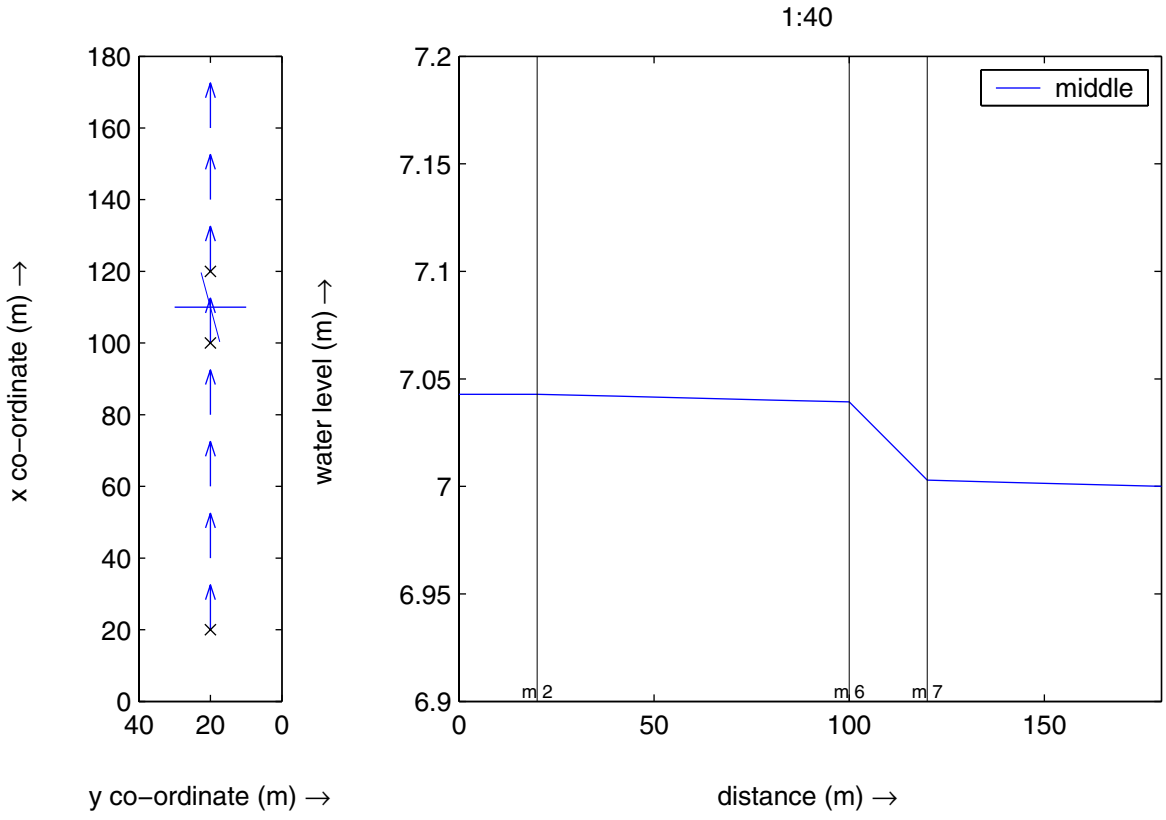

Simulation for a vane height of 3.0 m and a vane angle of 15 degrees relative to the pos. x−axis.	s7u	
WL | DELFT HYDRAULICS	Q2681	D−9

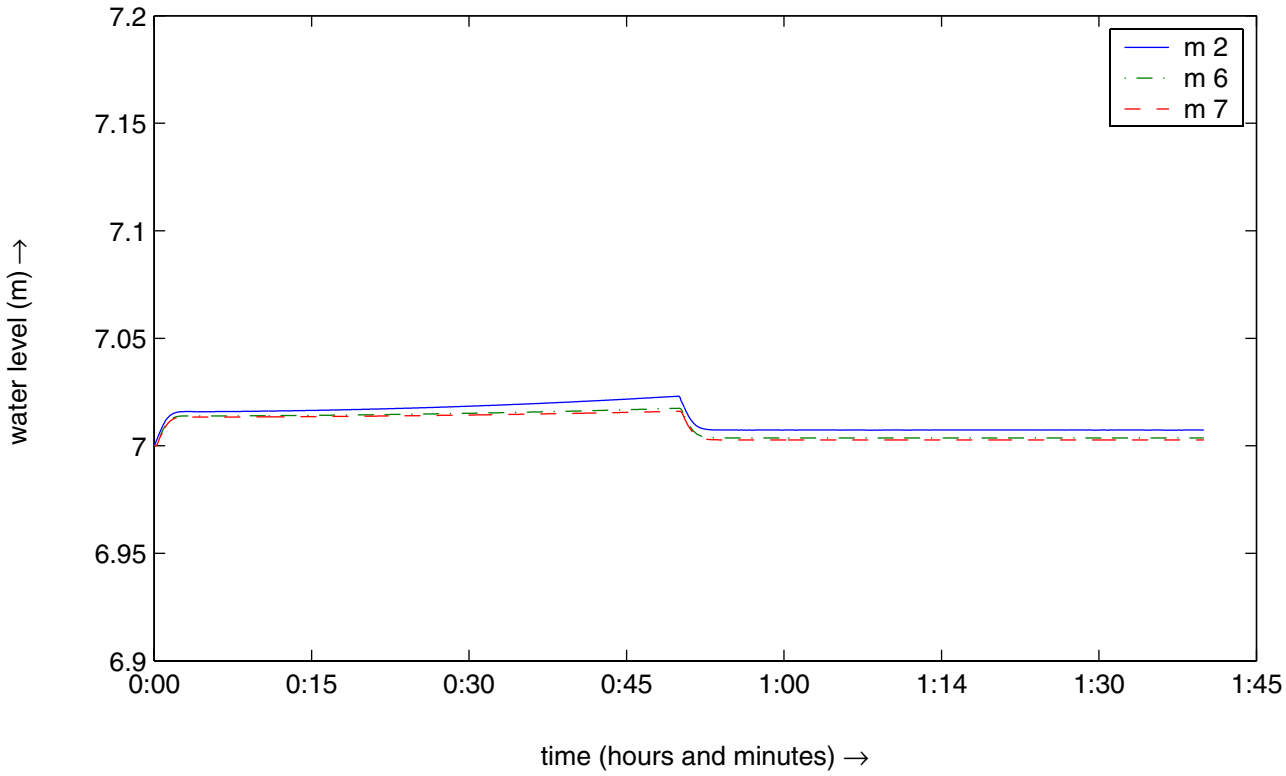

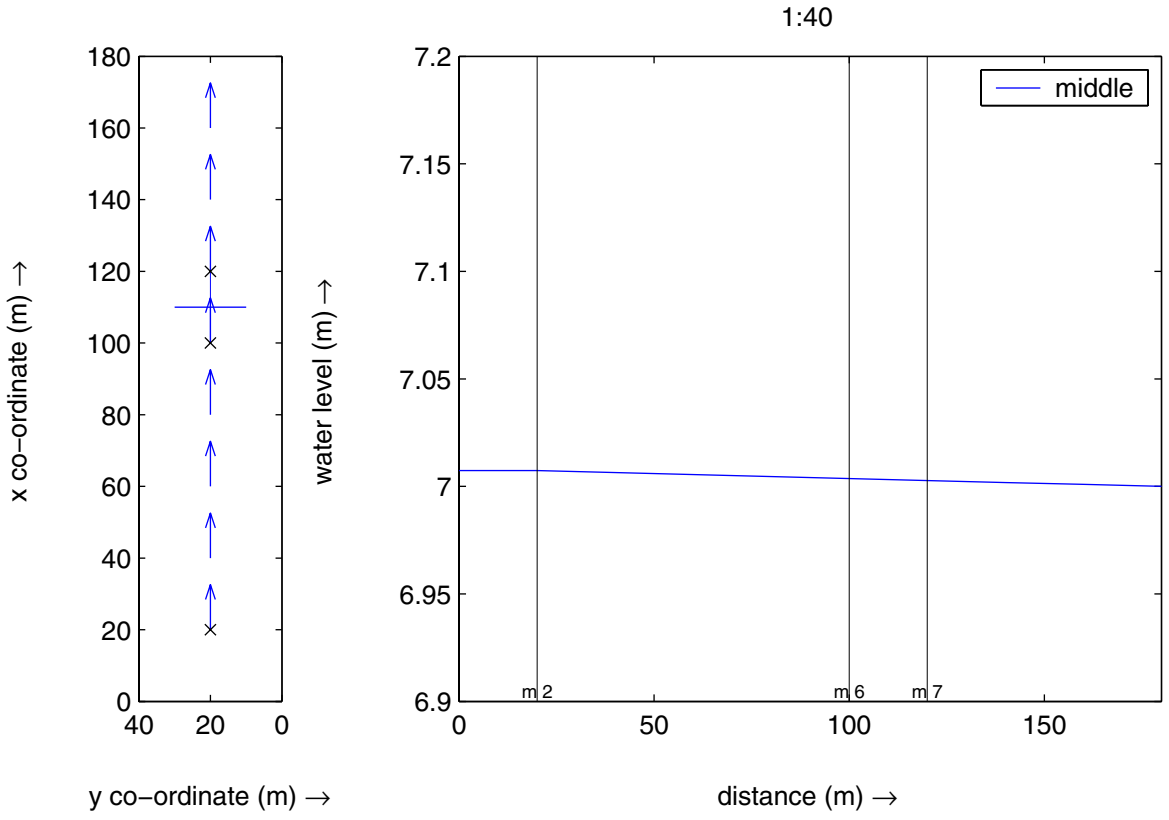

Simulation for a vane height of 3.0 m and a vane angle of 0 degrees relative to the pos. x−axis.	s8u	
WL | DELFT HYDRAULICS	Q2681	D−10

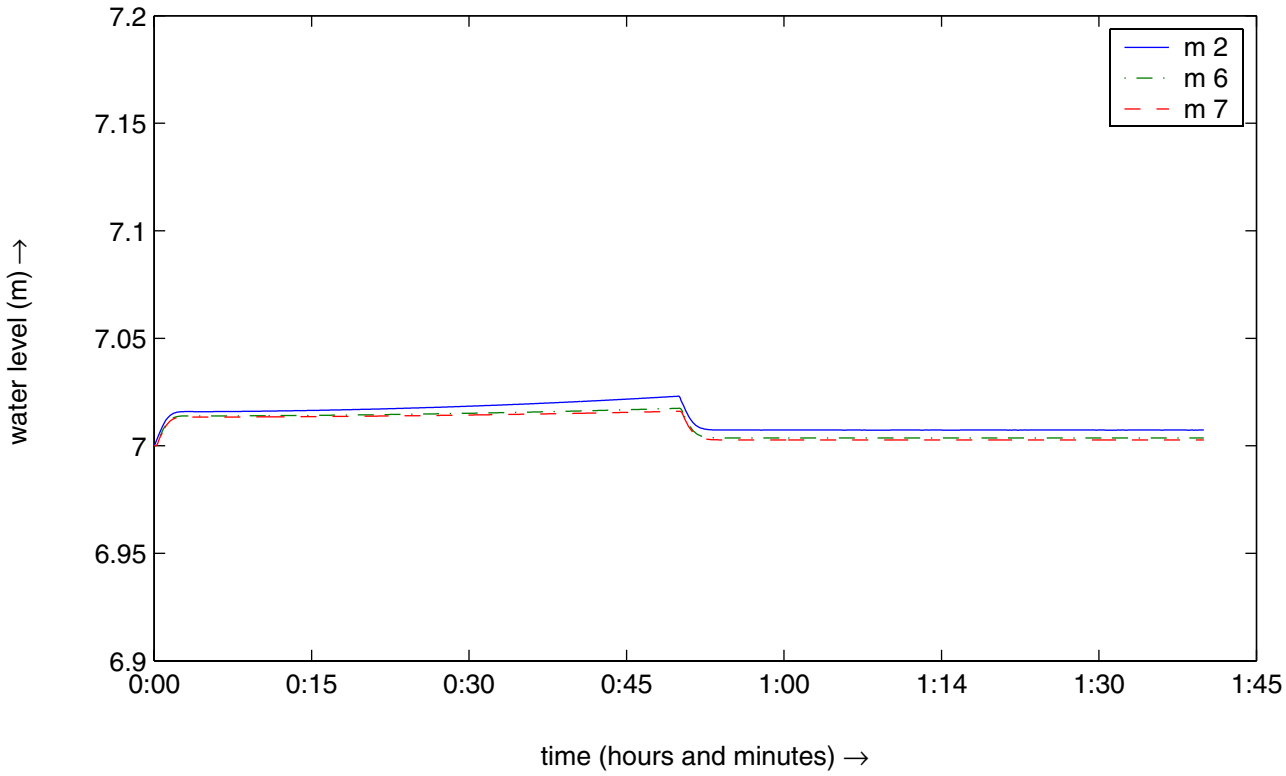

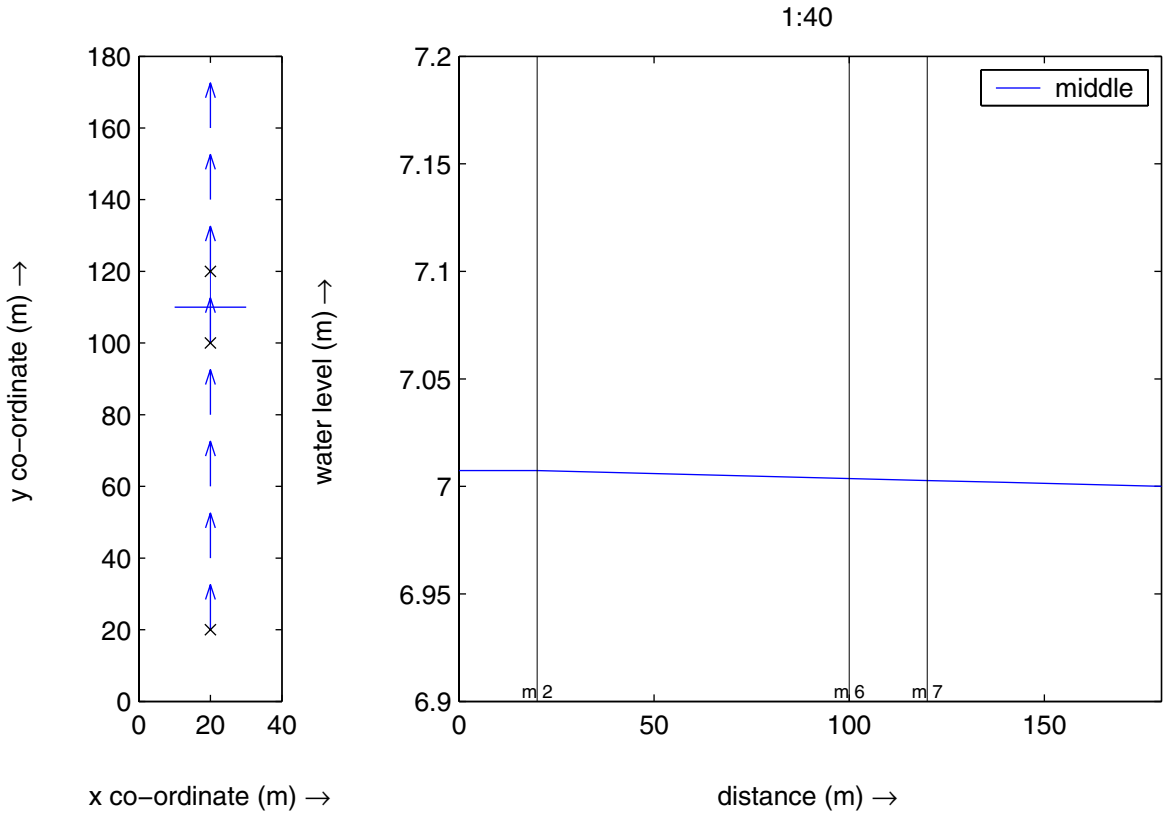

Simulation for a vane height of 3.0 m and a vane angle of 90 degrees relative to the pos. x−axis.	s8v	
WL | DELFT HYDRAULICS	Q2681	D−11

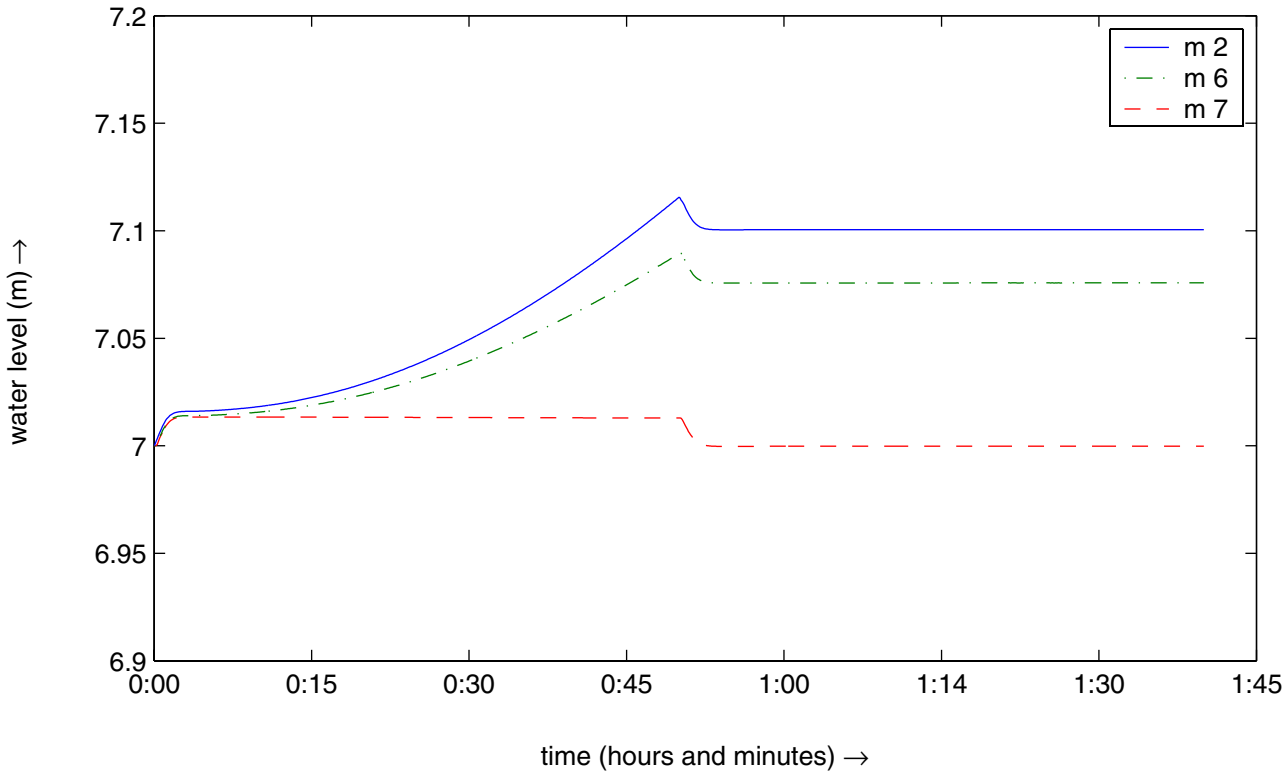

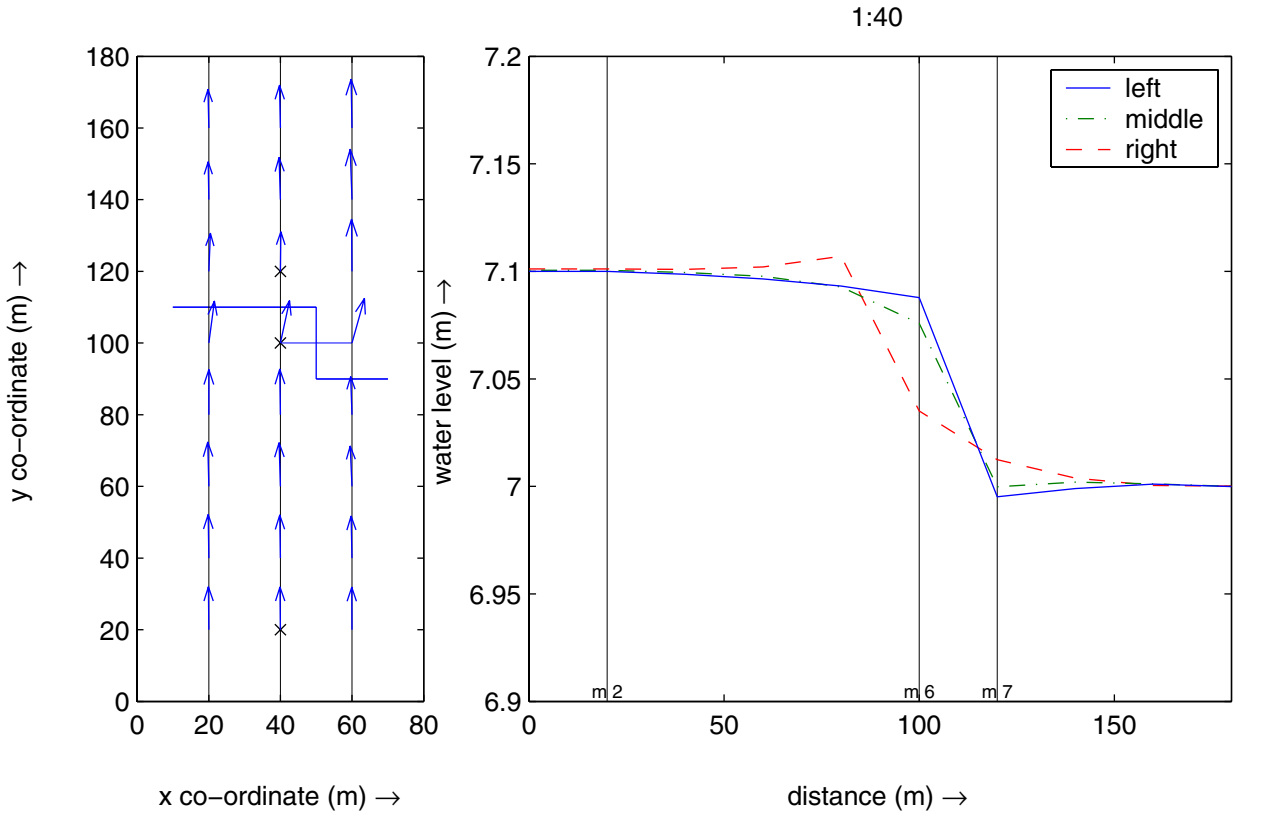

Simulation for a vane height of 3.0 m and a vane angle of 0 degrees relative to the pos. x−axis.	s1m	
WL | DELFT HYDRAULICS	Q2681	D−12

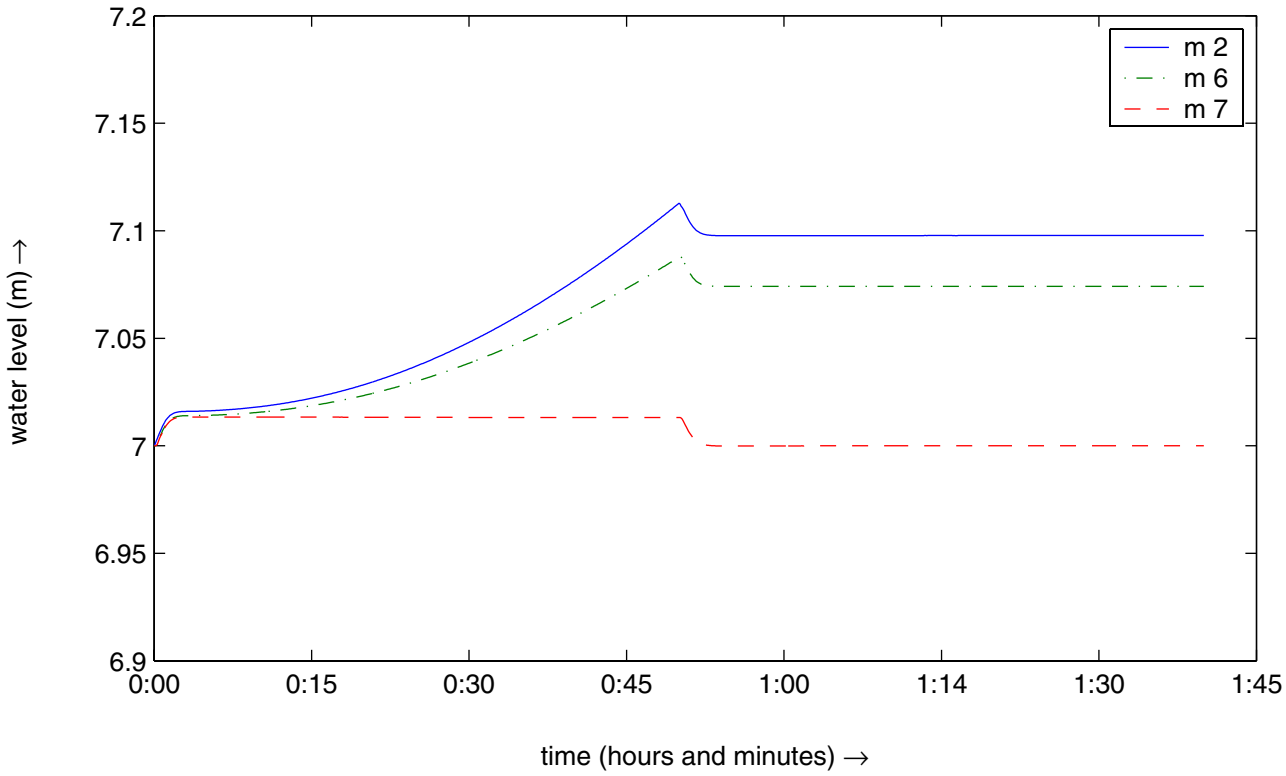

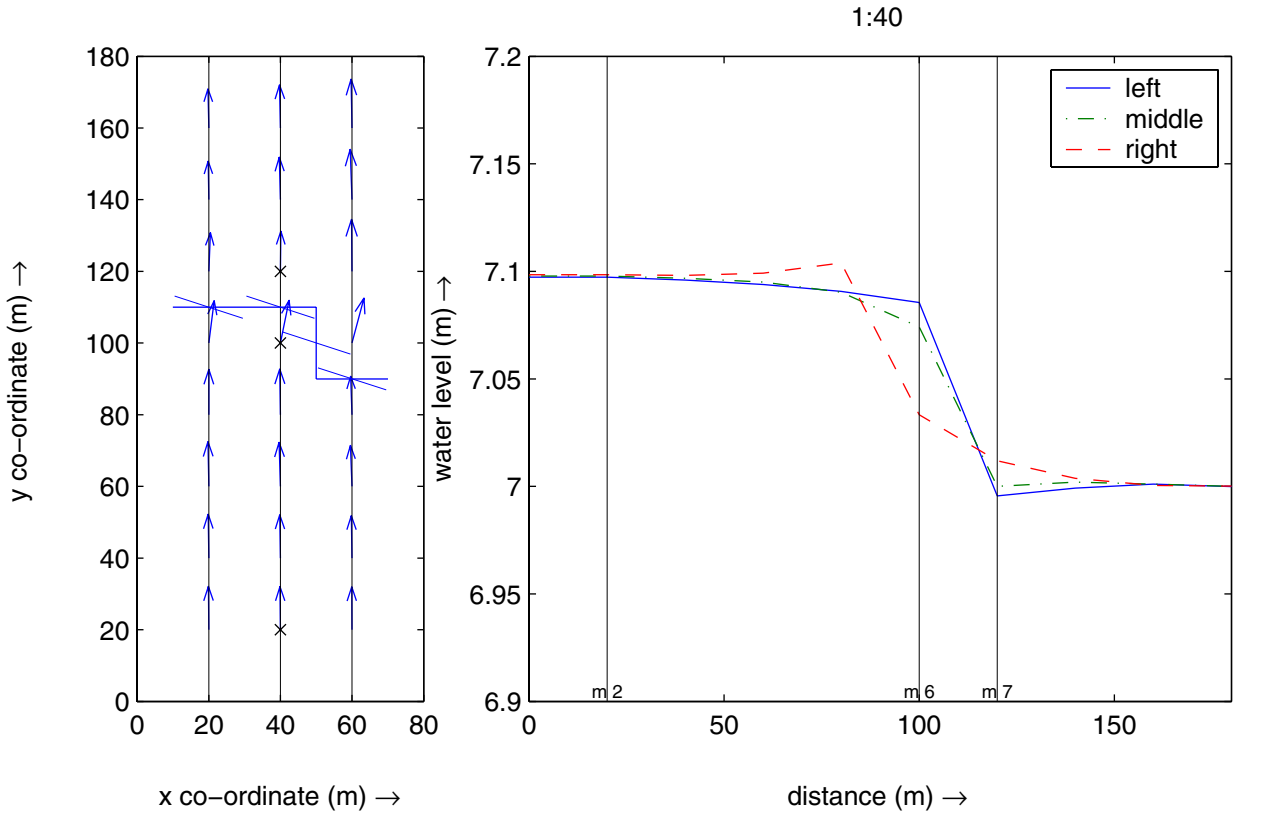

Simulation for a vane height of 3.0 m and a vane angle of 162 degrees relative to the pos. x−axis.	s3m	
WL | DELFT HYDRAULICS	Q2681	D−13

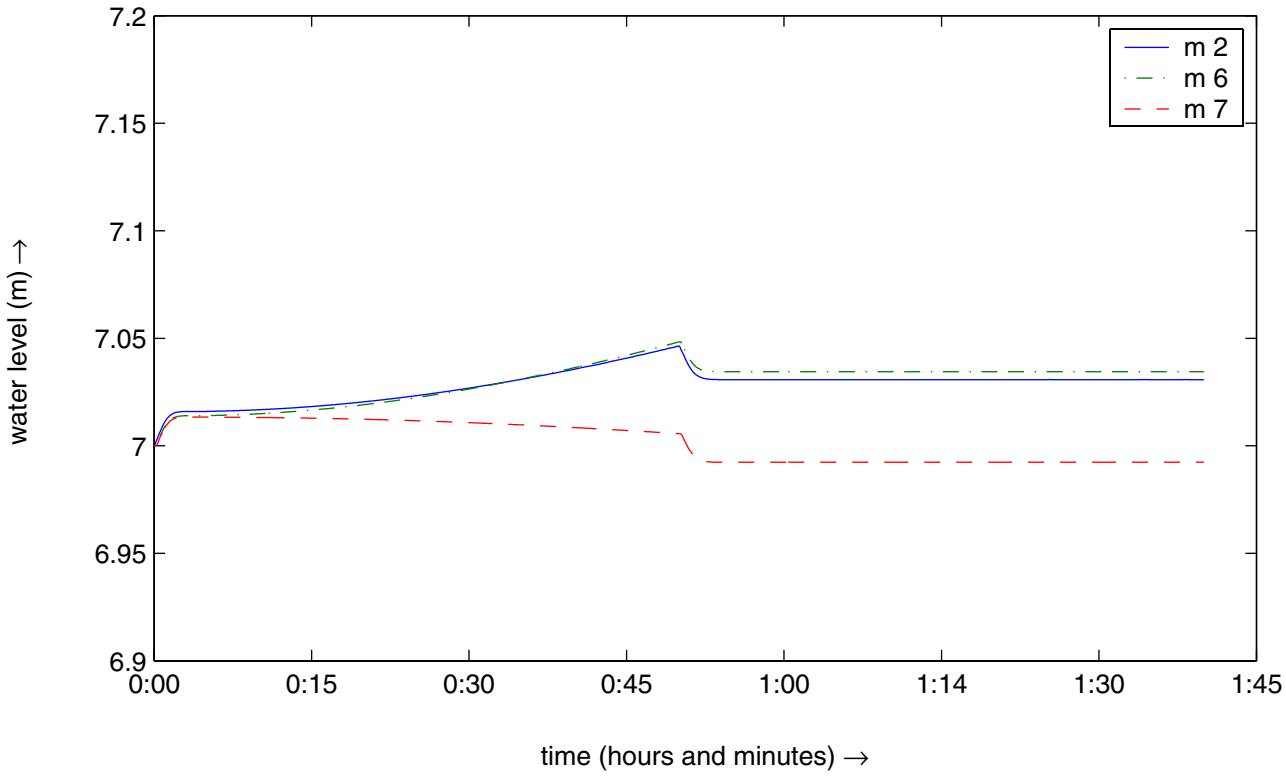

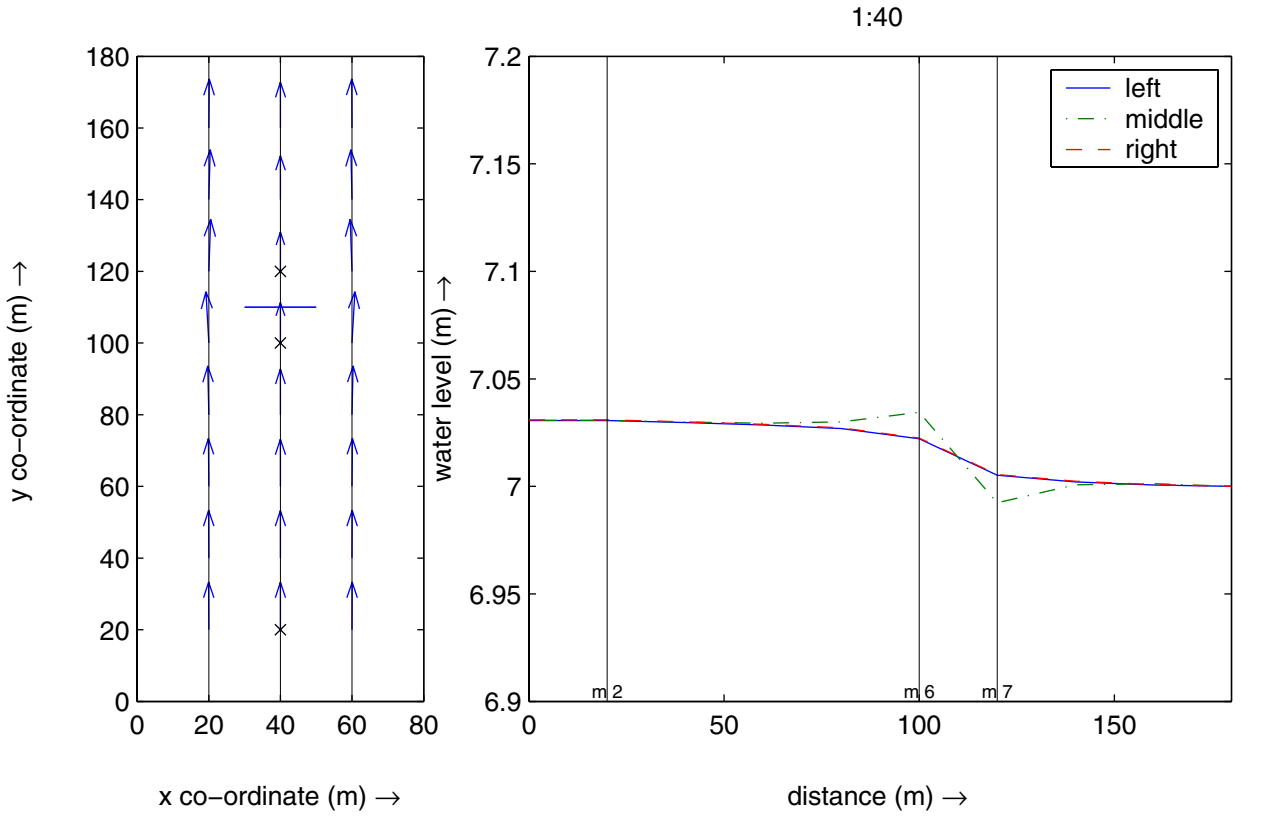

Simulation for a vane height of 3.0 m and a vane angle of 0 degrees relative to the pos. x−axis.	s1c	
WL | DELFT HYDRAULICS	Q2681	D−14

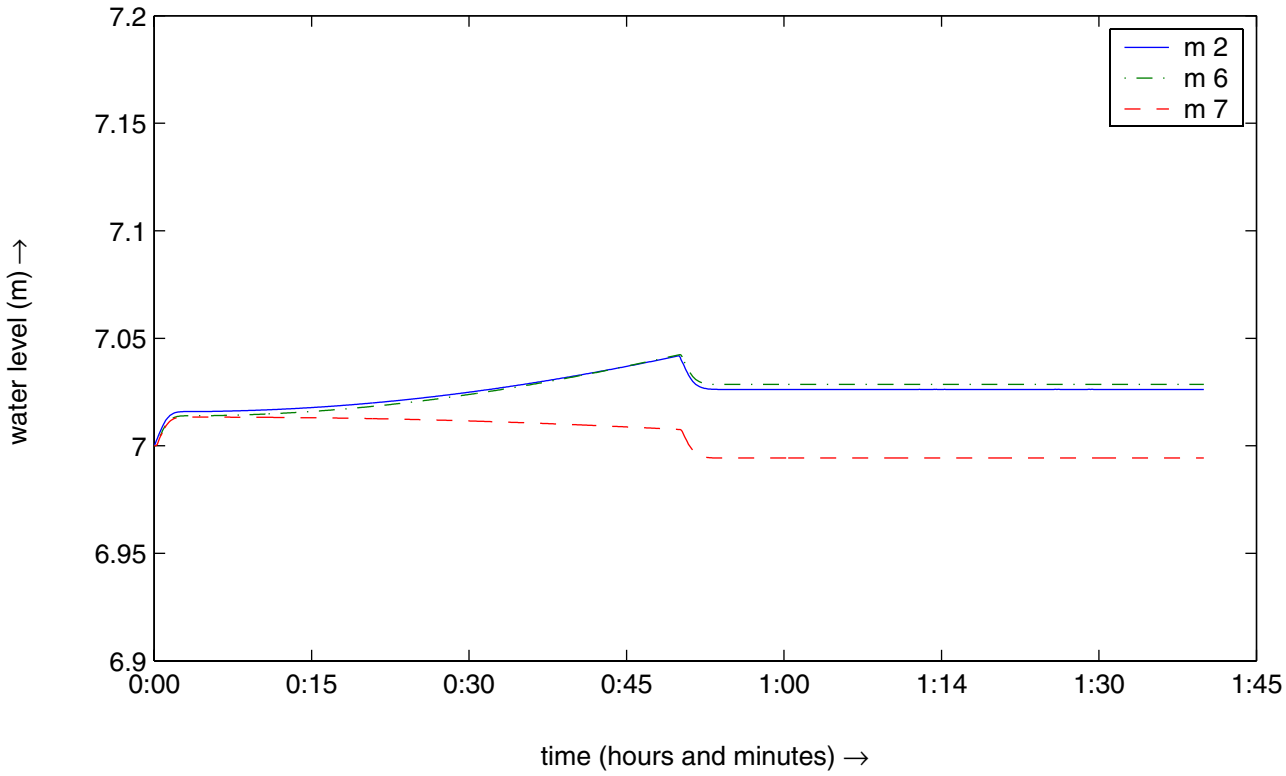

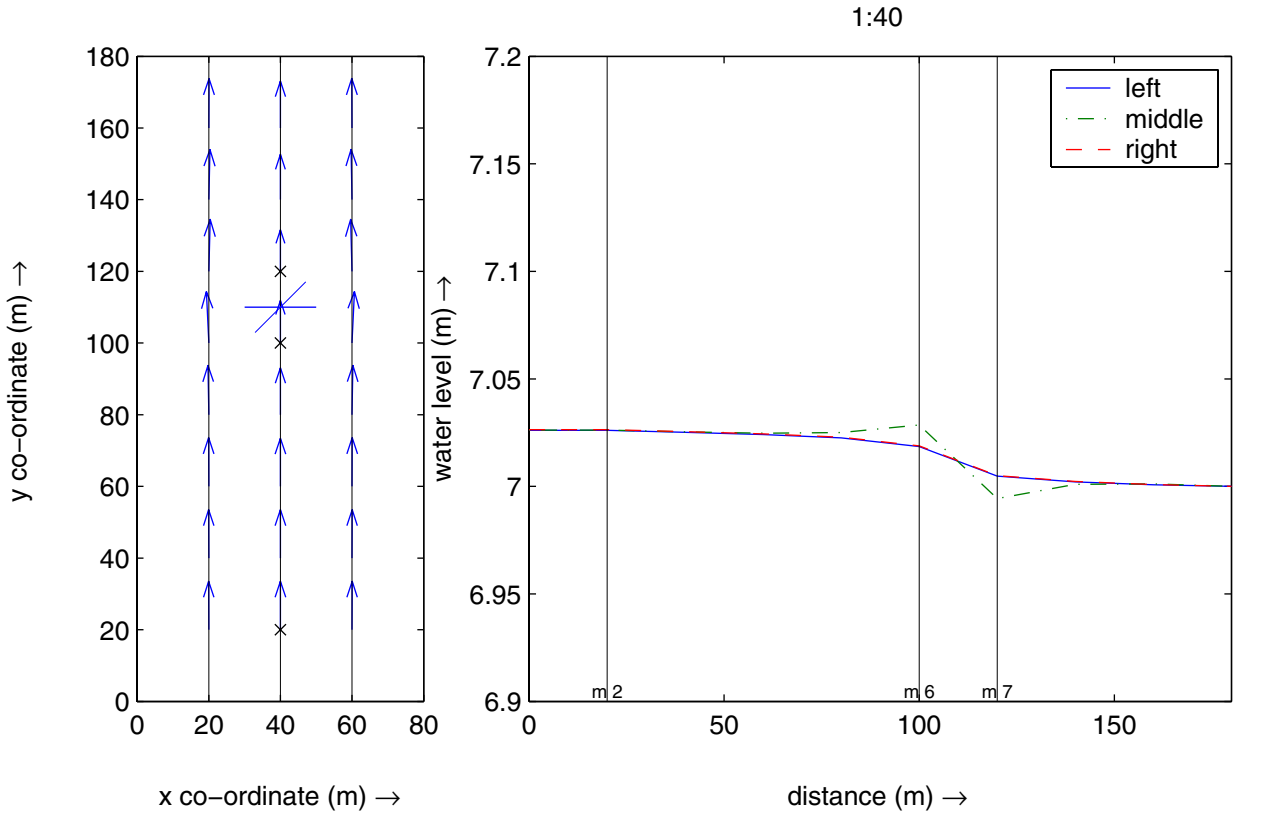

Simulation for a vane height of 3.0 m and a vane angle of 45 degrees relative to the pos. x−axis.	s2c	
WL | DELFT HYDRAULICS	Q2681	D−15

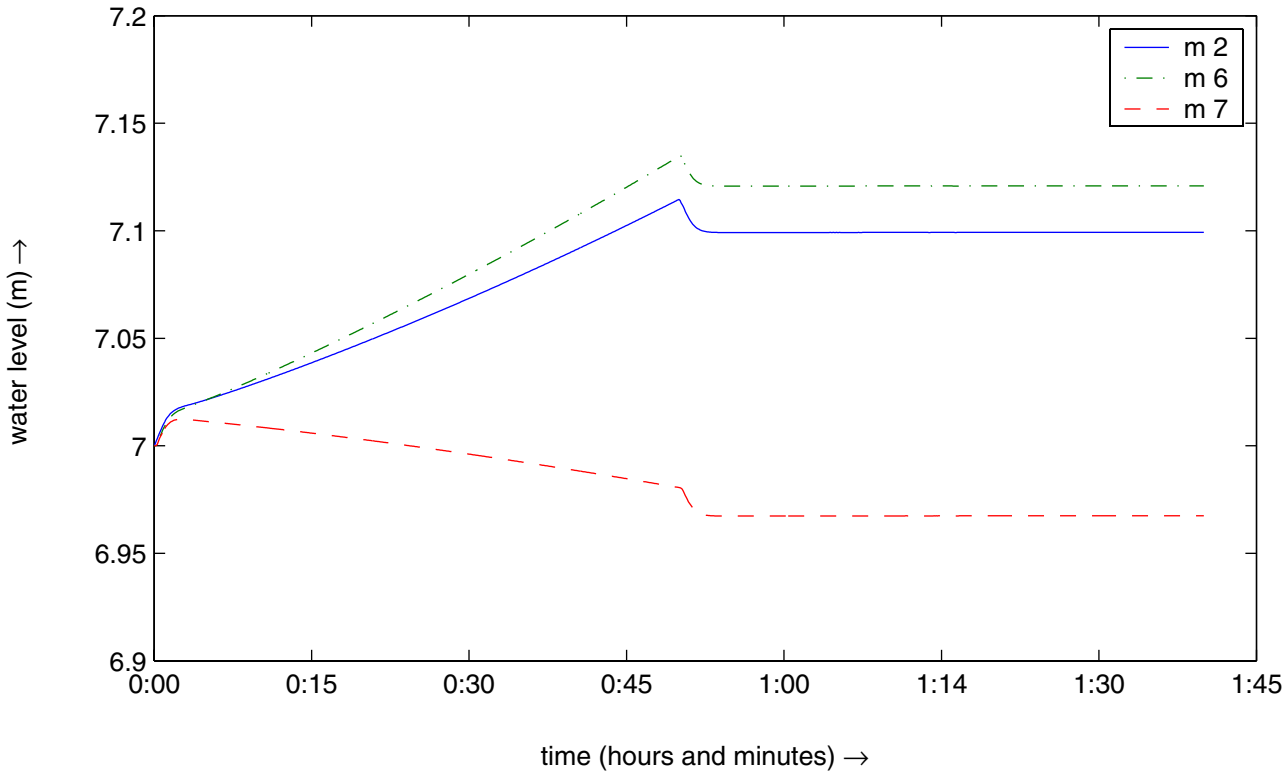

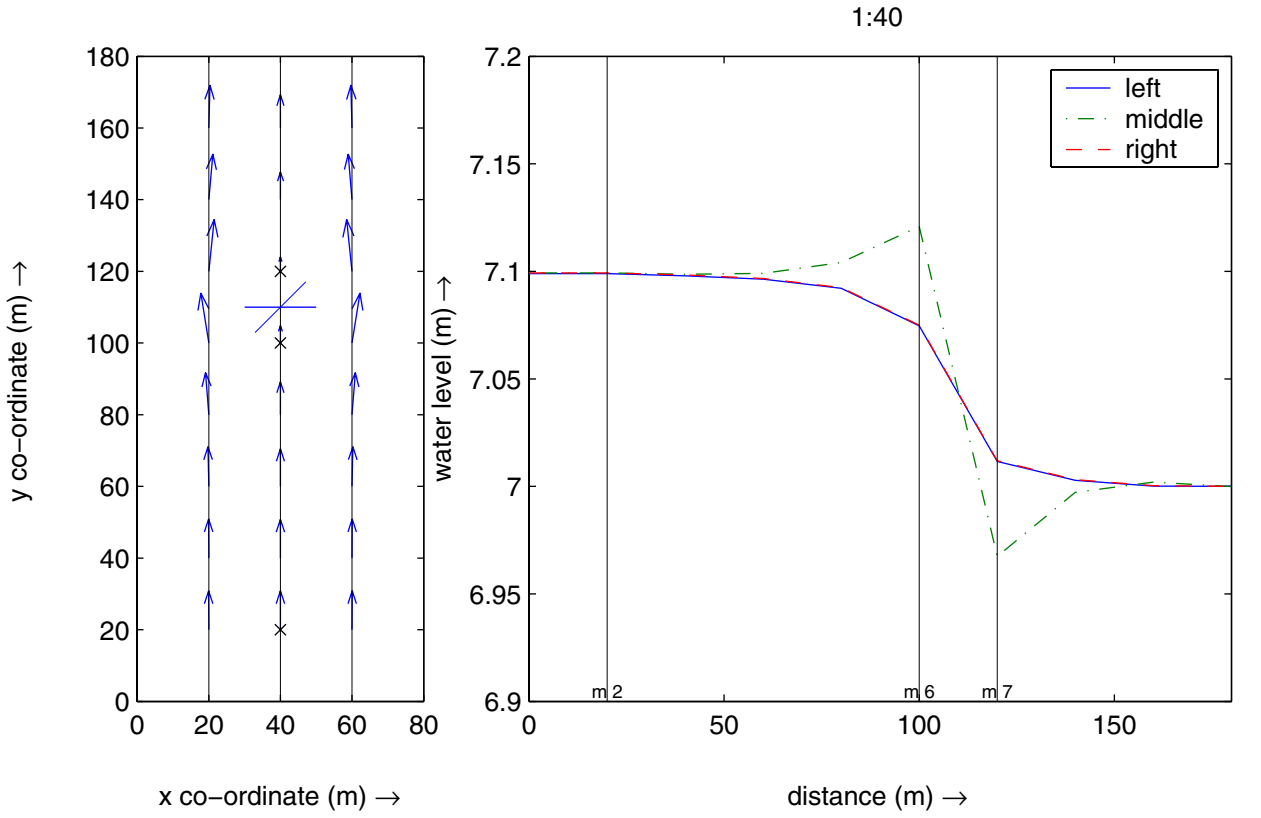

Simulation for a vane height of 6.5 m and a vane angle of 45 degrees relative to the pos. x−axis.	s3c	
WL | DELFT HYDRAULICS	Q2681	D−16

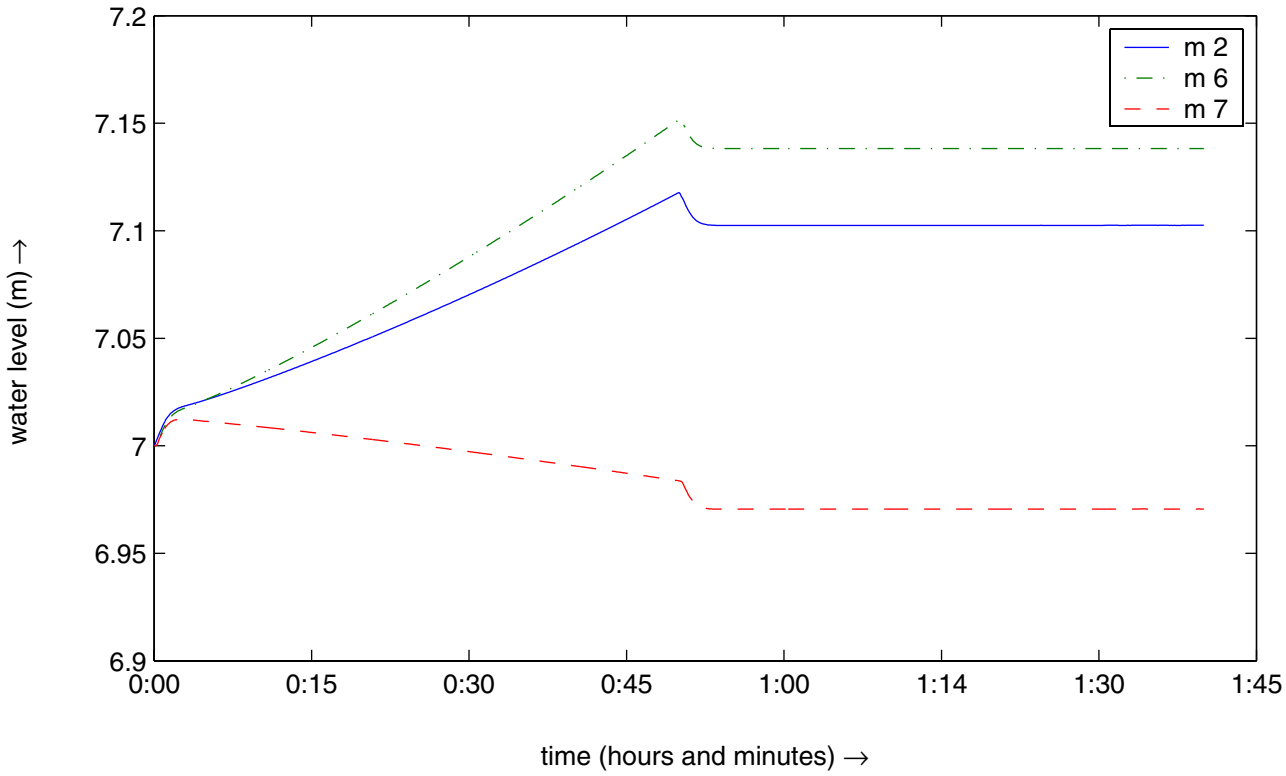

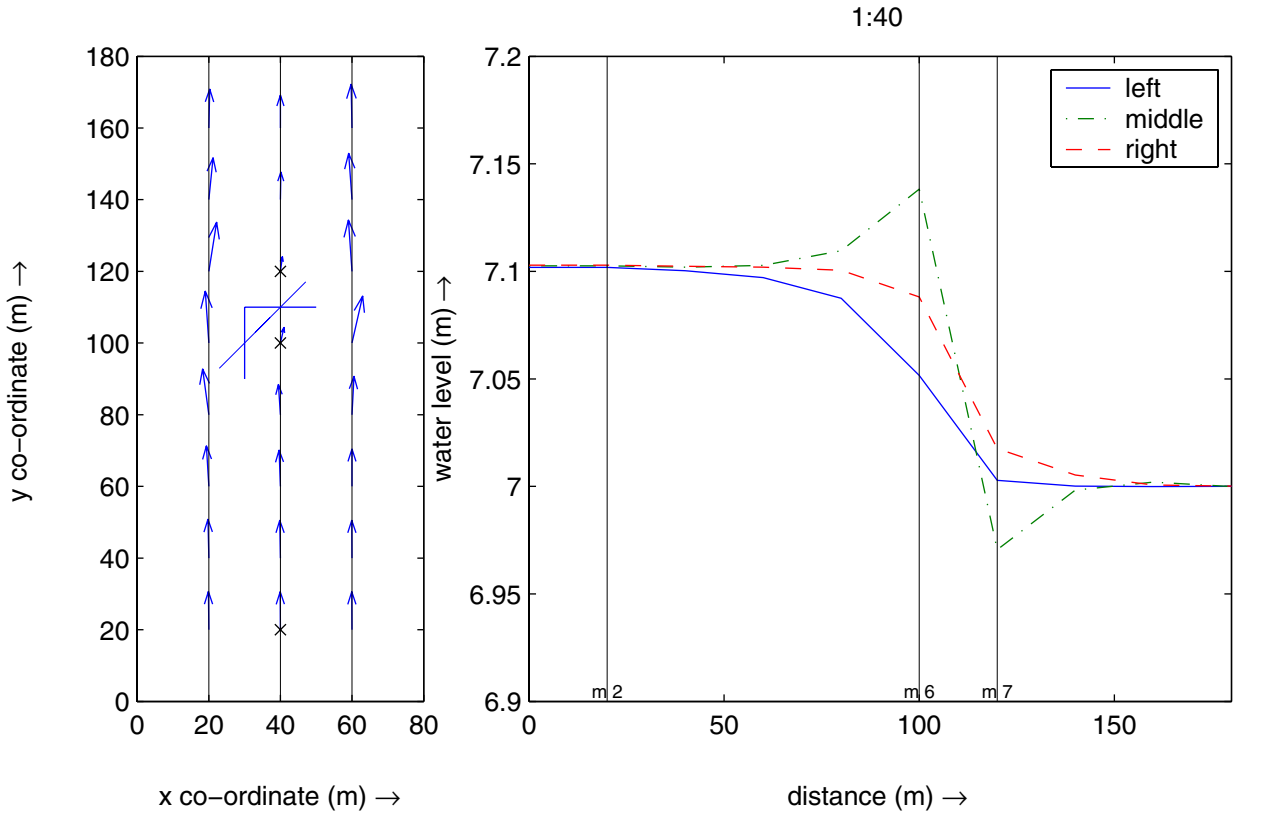

Simulation for a vane height of 6.5 m and a vane angle of 45 degrees relative to the pos. x−axis.	s4c	
WL | DELFT HYDRAULICS	Q2681	D−17

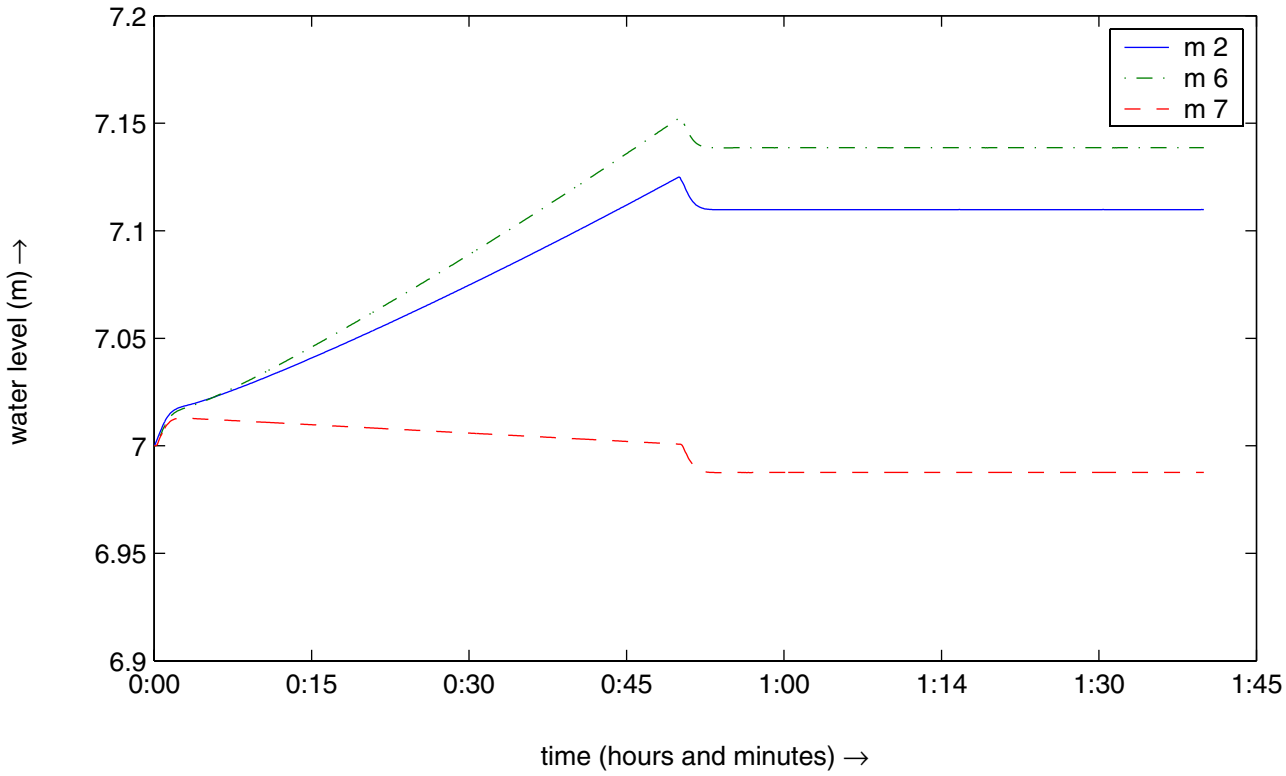

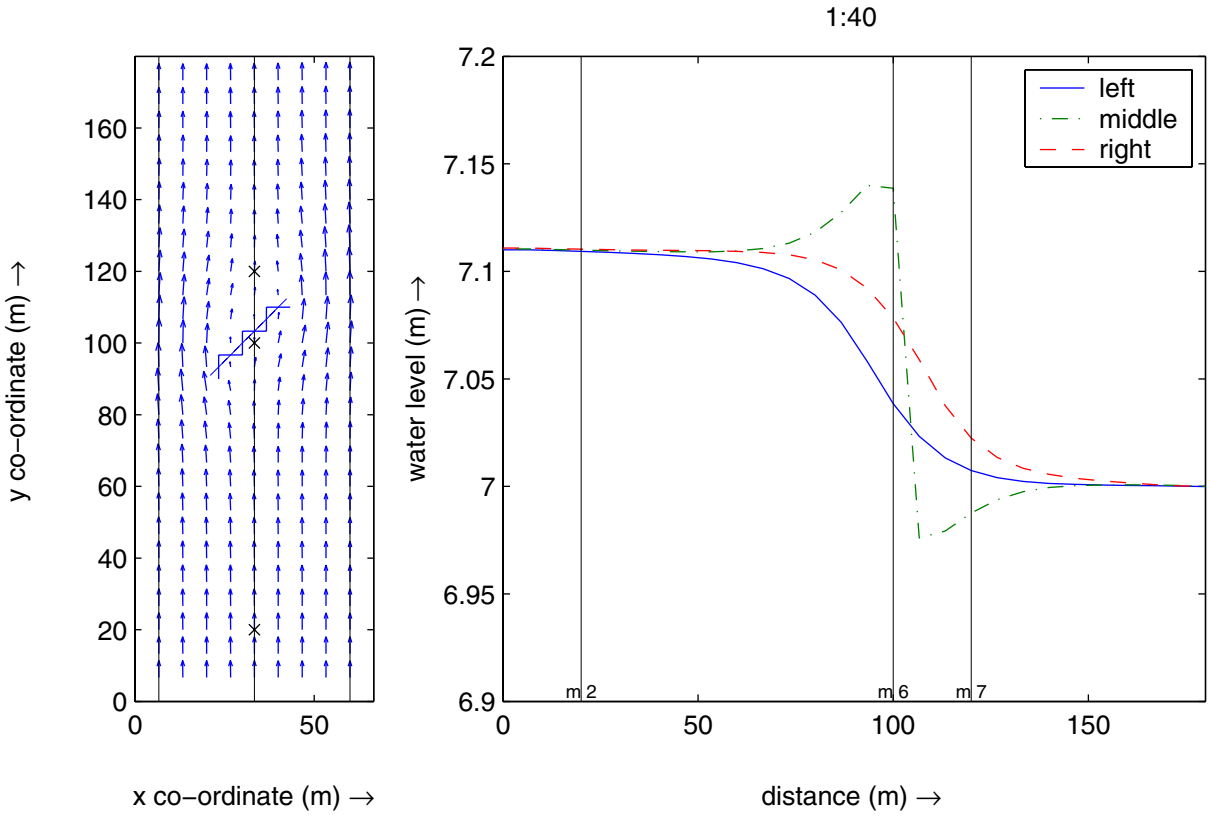

Simulation for a vane height of 6.5 m and a vane angle of 45 degrees relative to the pos. x−axis.	s5c	
WL | DELFT HYDRAULICS	Q2681	D−18

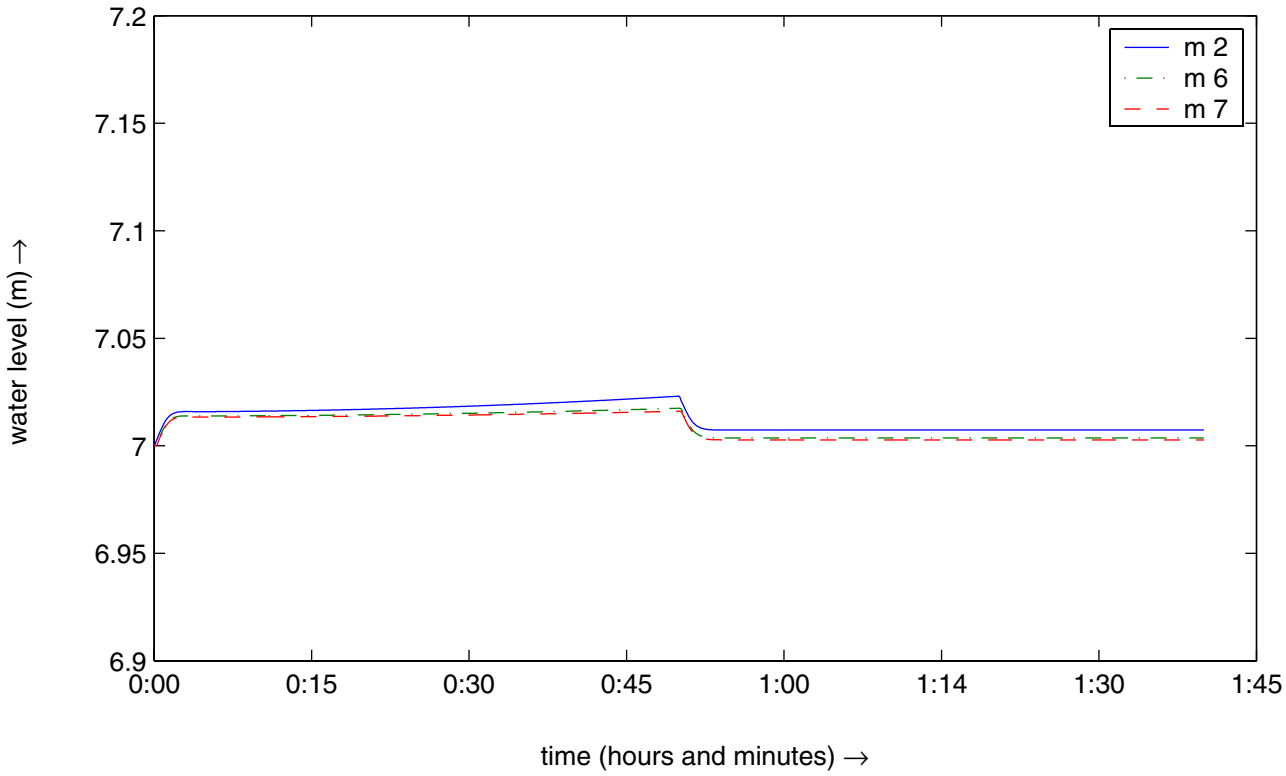

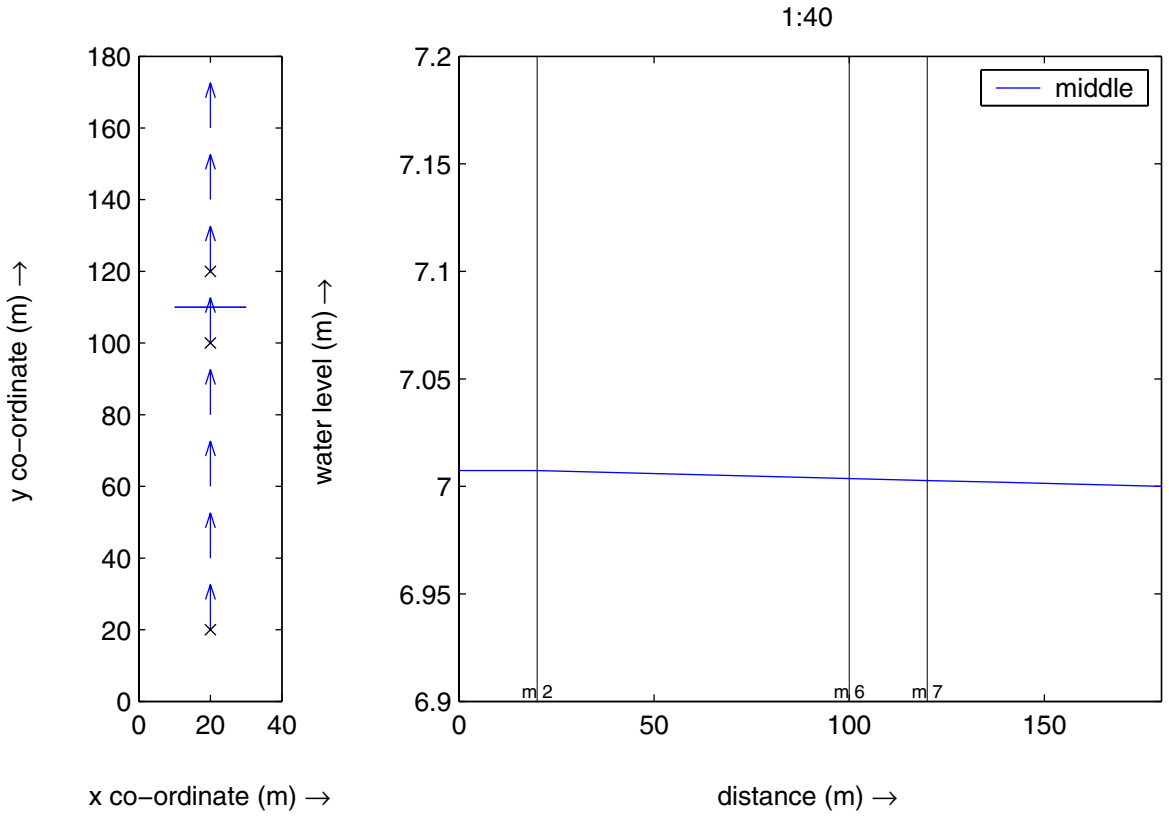

Simulation for a surface vane above the water (lower level at +9 m and a vane angle of 0 degrees relative to the pos. x−axis.)	s1o	
WL | DELFT HYDRAULICS	Q2681	D−19

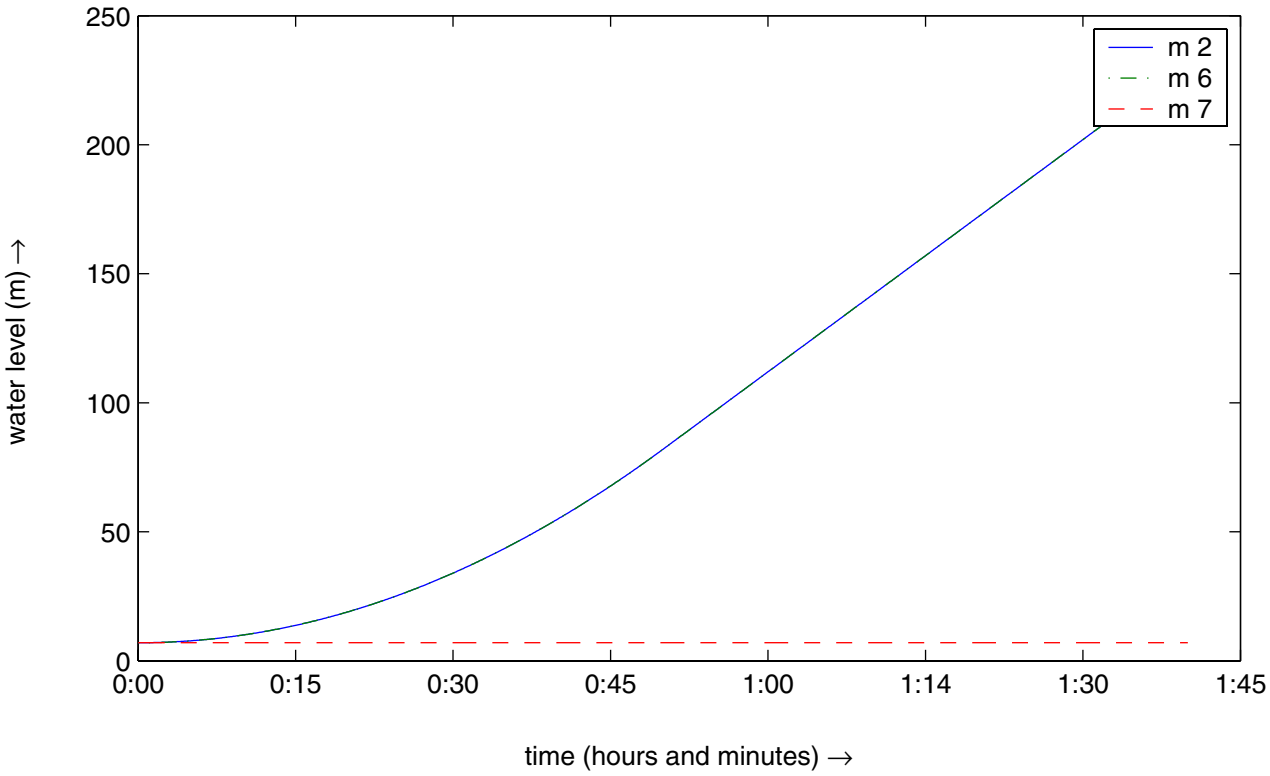

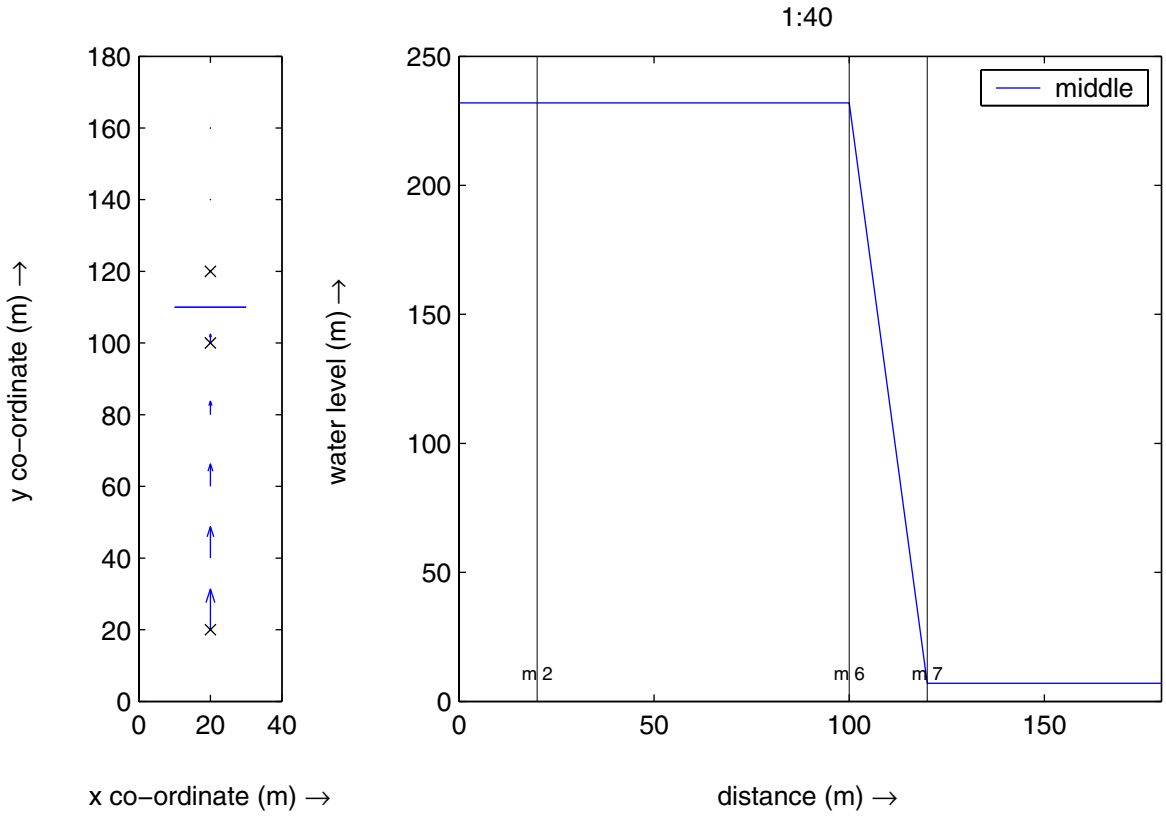

Simulation for a surface vane blocking the flow (lower level at −1.0 m and a vane angle of 0 degrees relative to the pos. x−axis.)	s2o	
WL | DELFT HYDRAULICS	Q2681	D−20

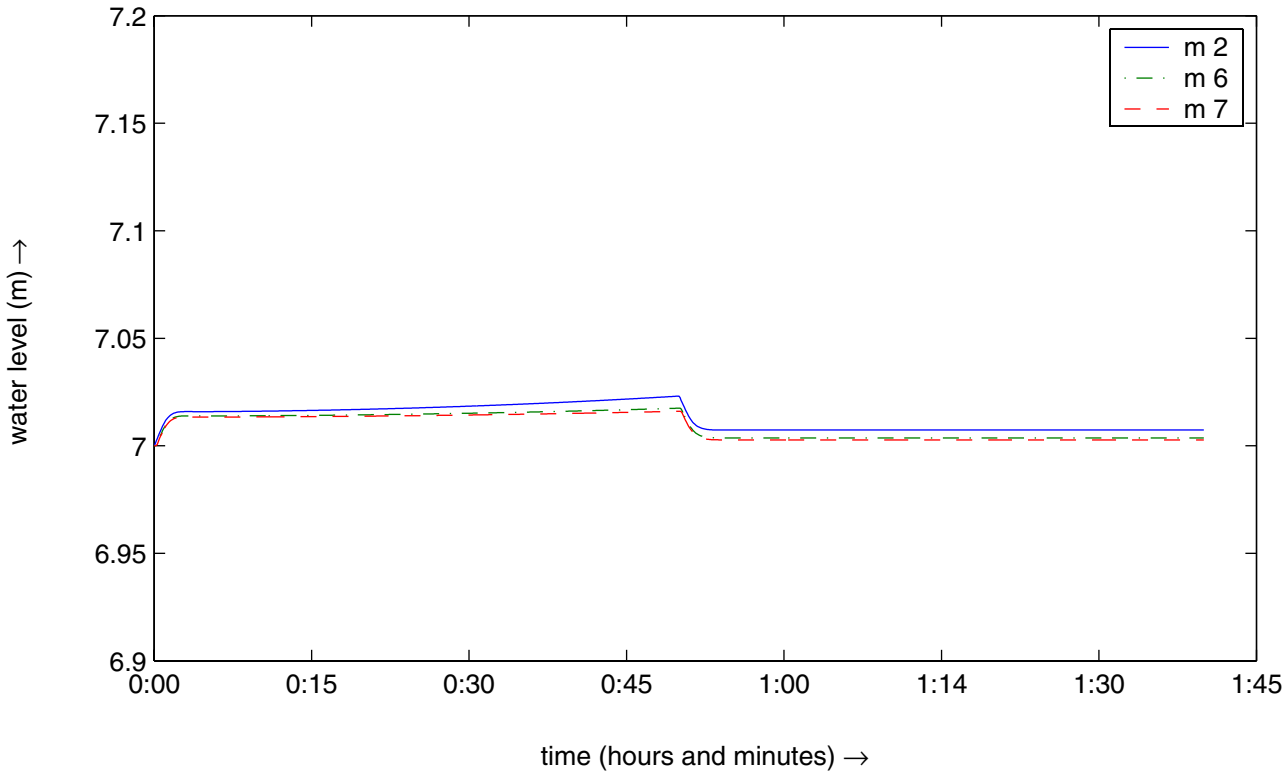

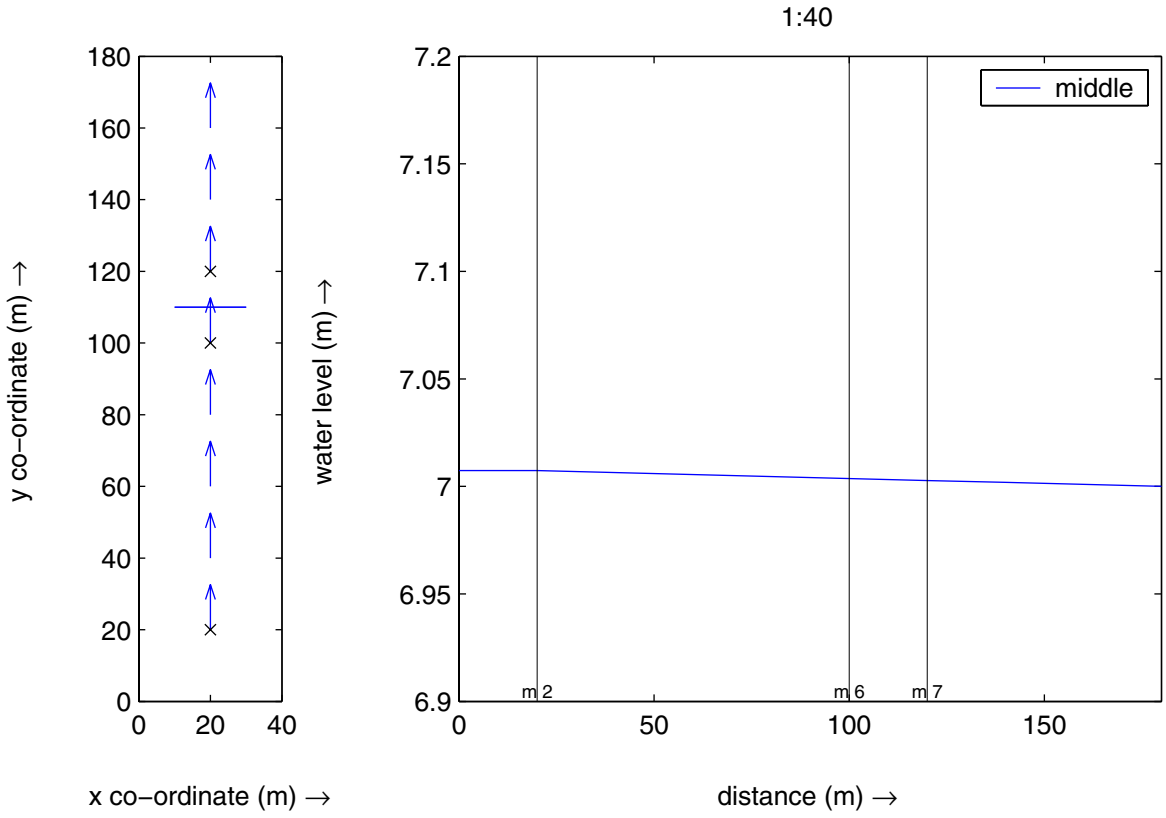

Simulation for a surface vane with its lower level at 7.0 m and a vane angle of 0 degrees relative to the pos. x−axis.	s3o	
WL | DELFT HYDRAULICS	Q2681	D−21

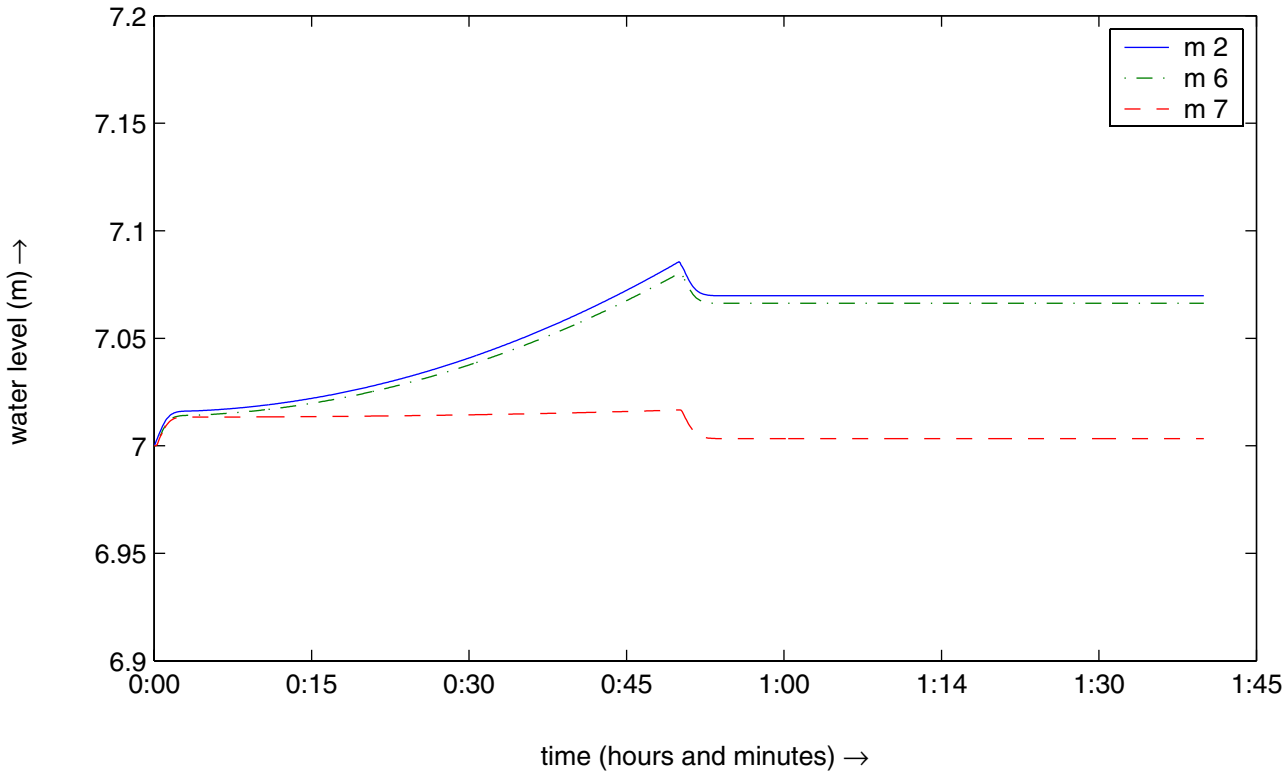

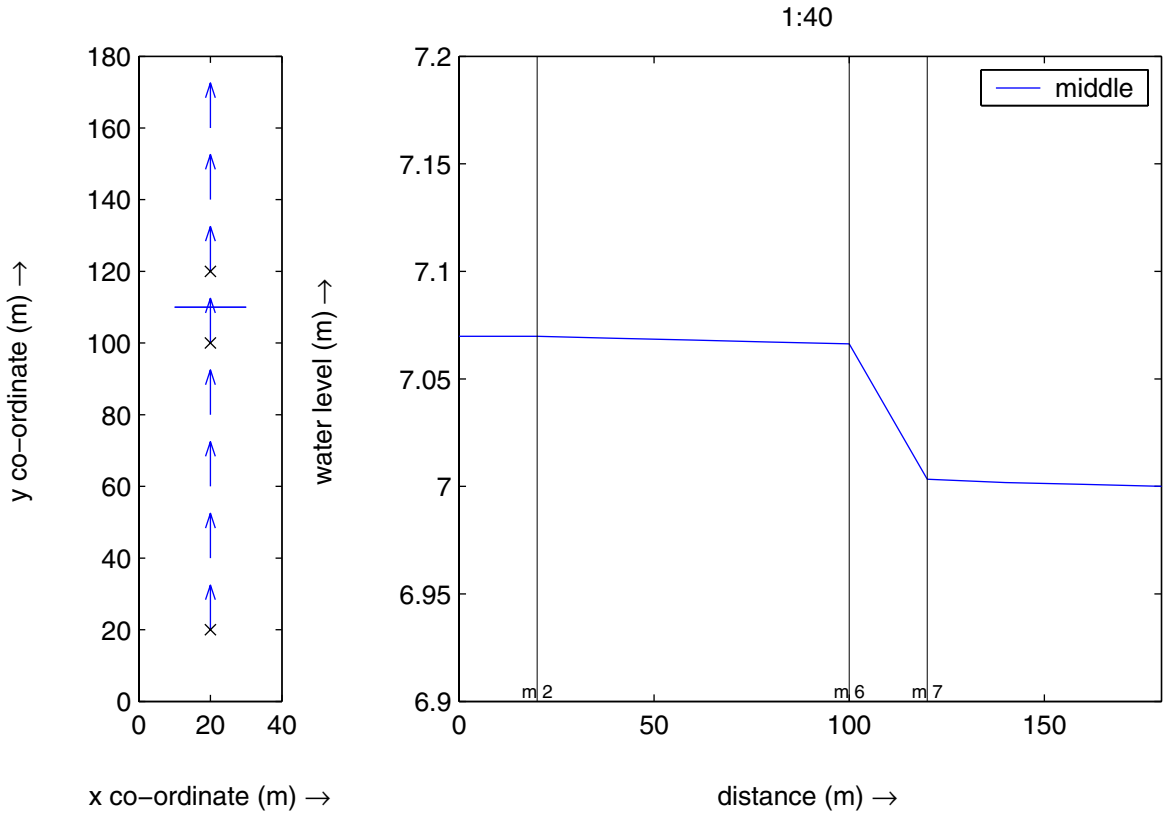

Simulation for a surface vane with its lower level at 4.0 m and a vane angle of 0 degrees relative to the pos. x−axis.	s4o	
WL | DELFT HYDRAULICS	Q2681	D−22

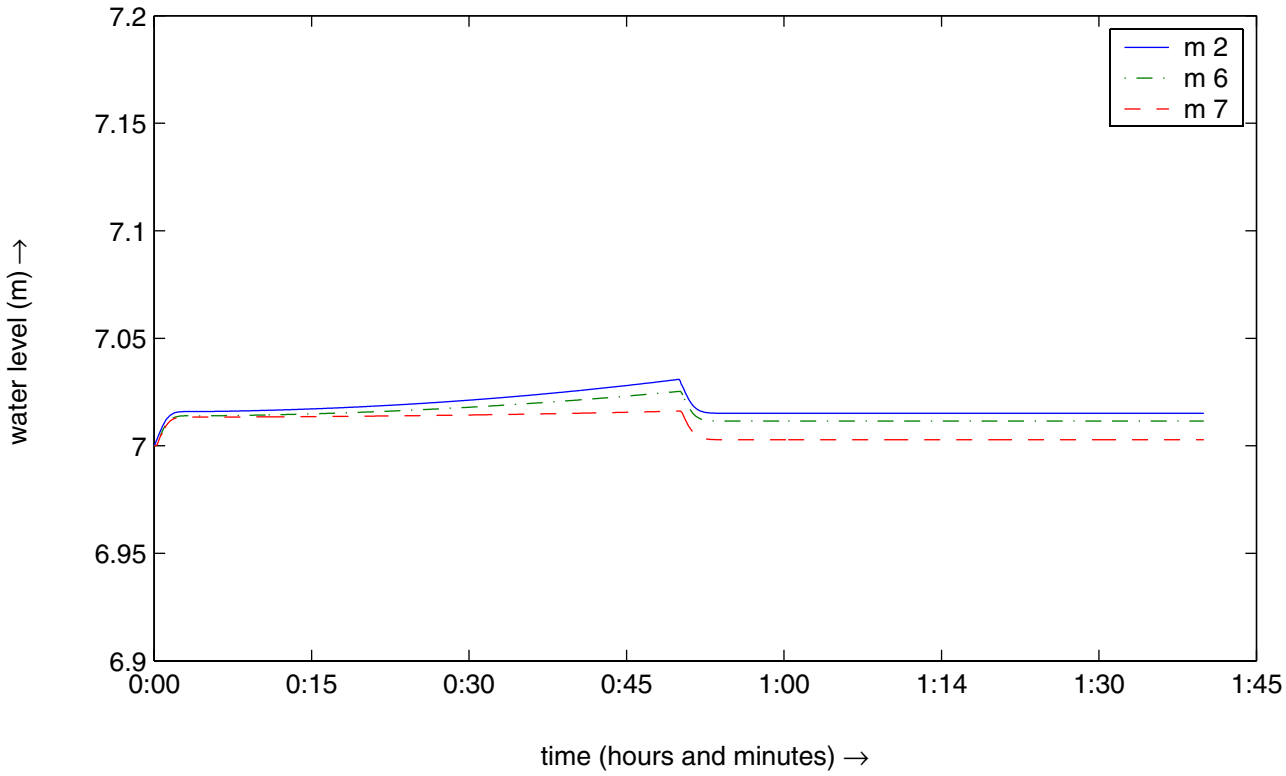

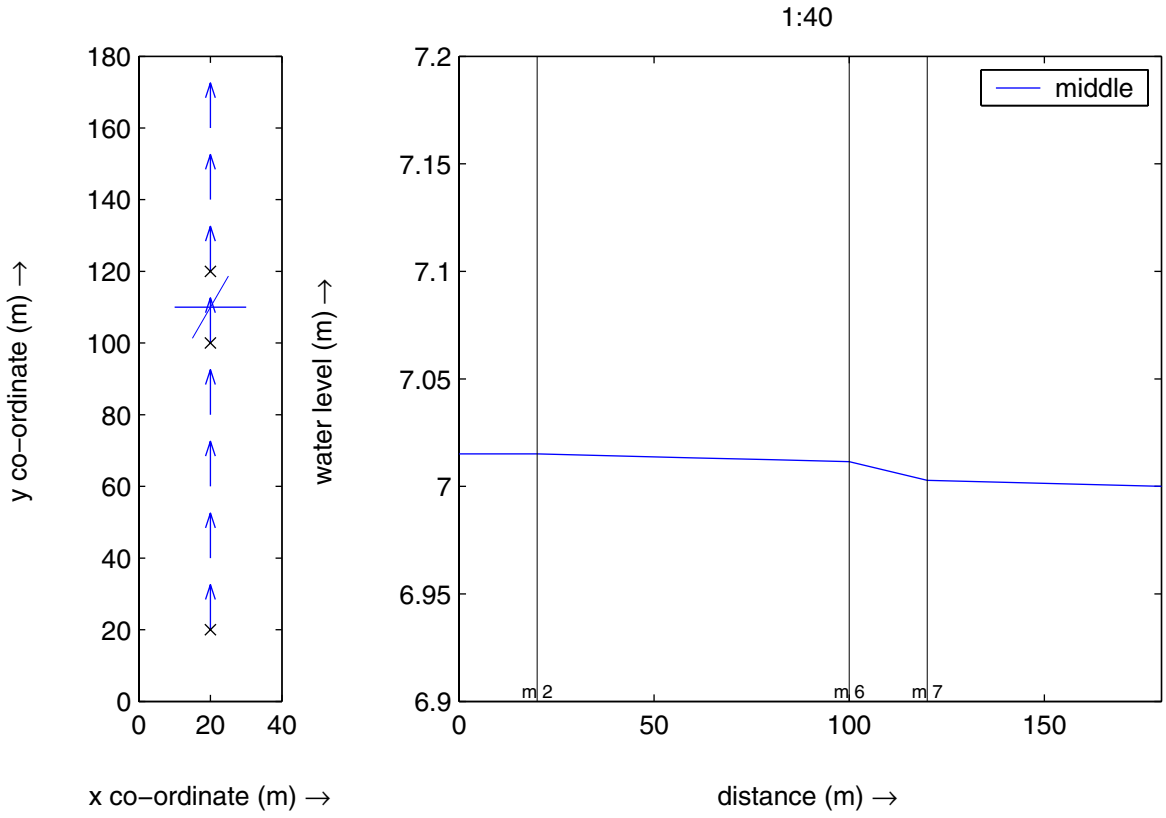

Simulation for a surface vane with its lower level at 4.0 m and a vane angle of 60 degrees relative to the pos. x–axis.	s5o	
WL | DELFT HYDRAULICS	Q2681	D–23

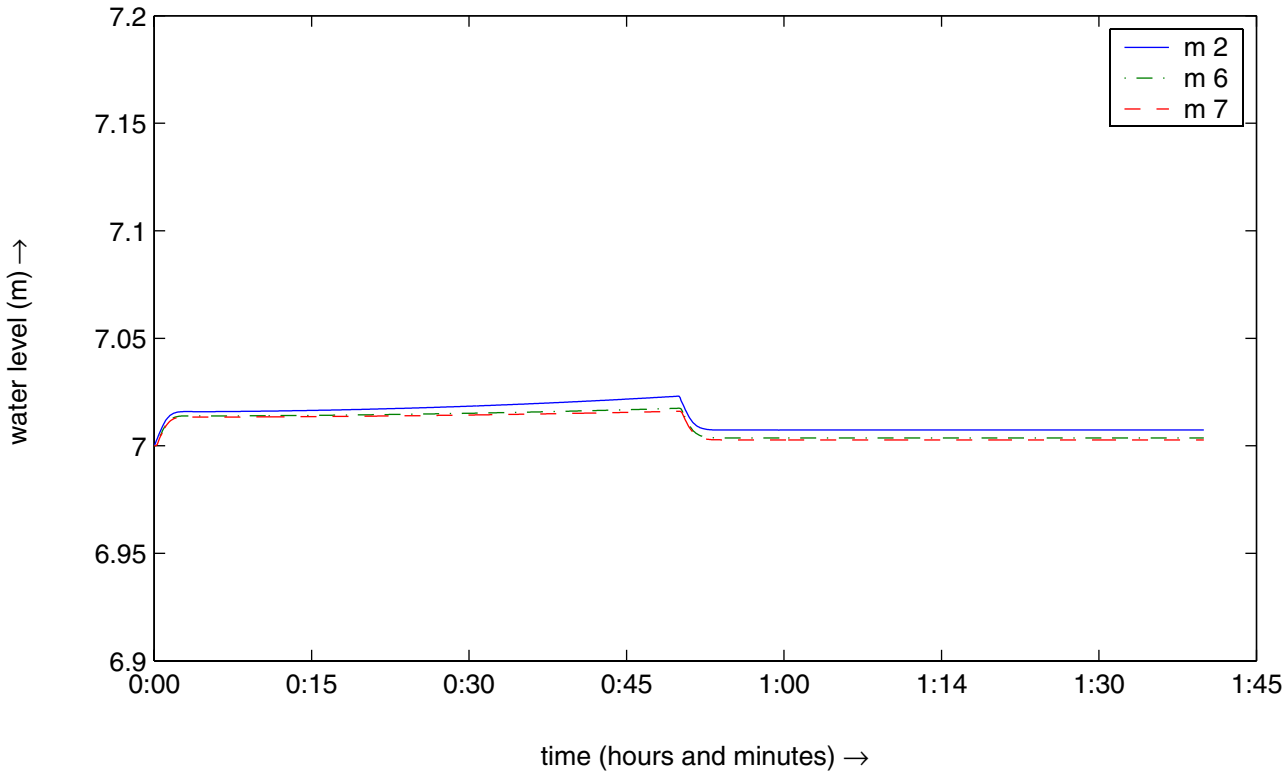

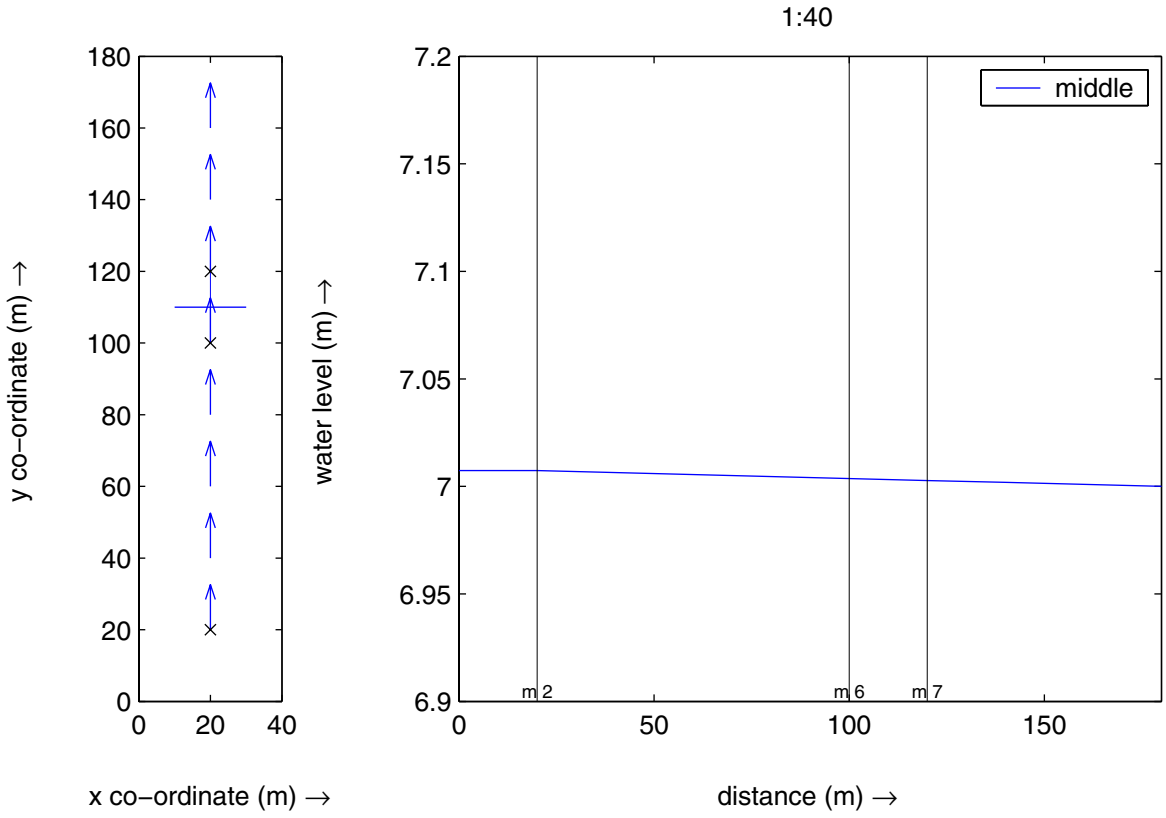

Simulation for a surface vane with its lower level at 4.0 m and a vane angle of 90 degrees relative to the pos. x–axis.	s6o	
WL | DELFT HYDRAULICS	Q2681	D–24

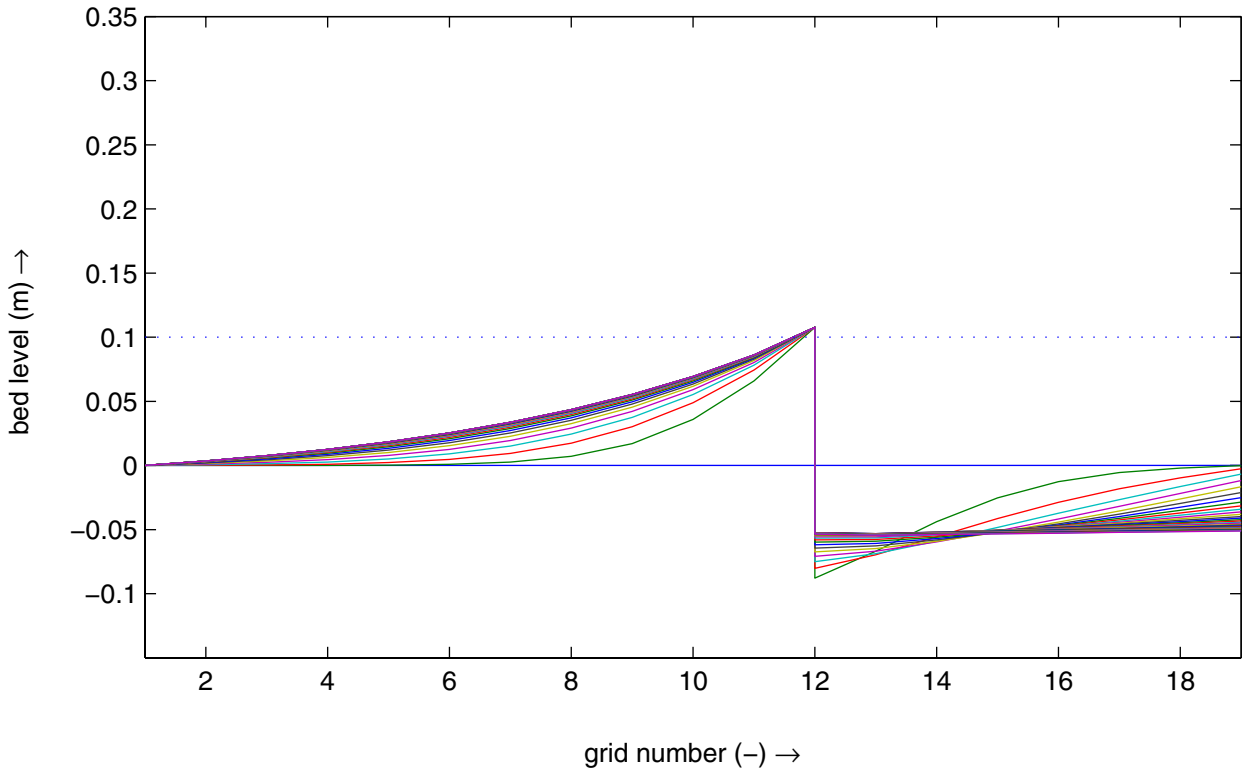

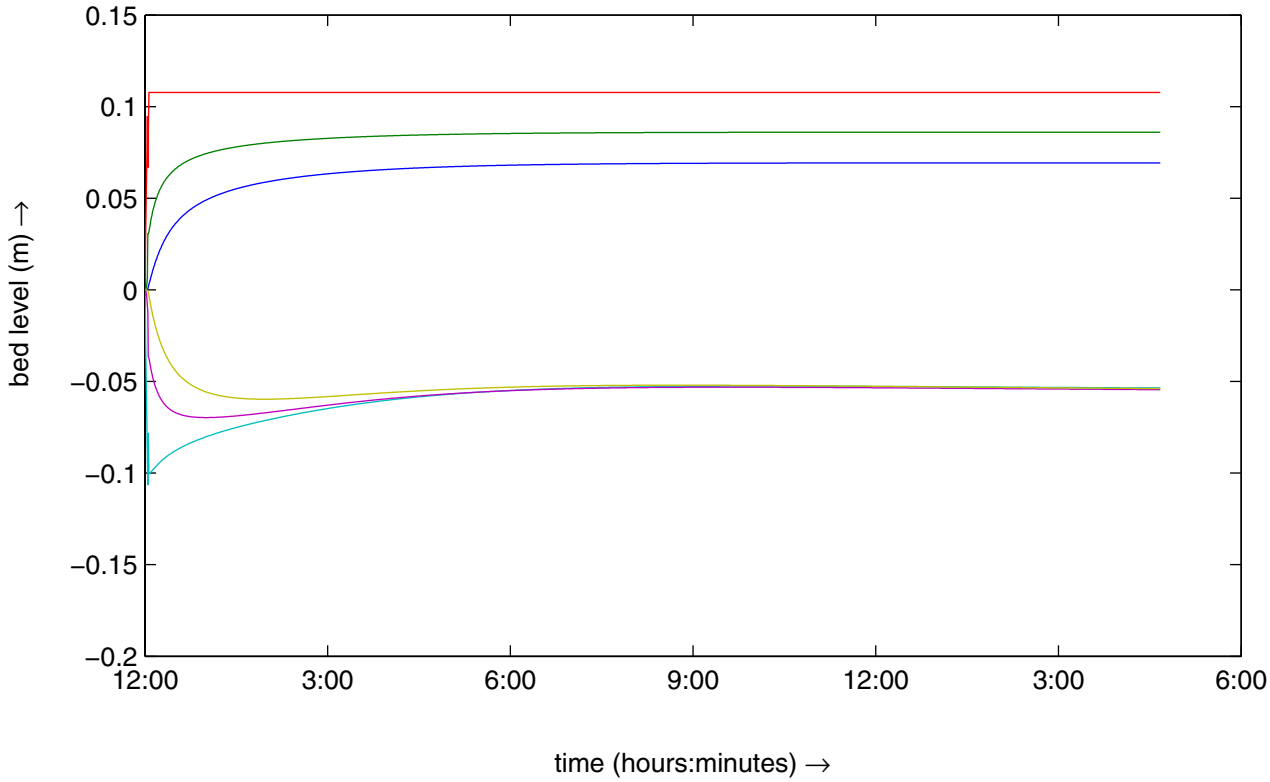

Upper plot: evolution of bed levels (50 computational steps between lines).
Lower plot: bed level development at the location of the vane
and in 2 points just upstream and downstream of the vane

WL | DELFT HYDRAULICS	Q2681	D–25

grid 1

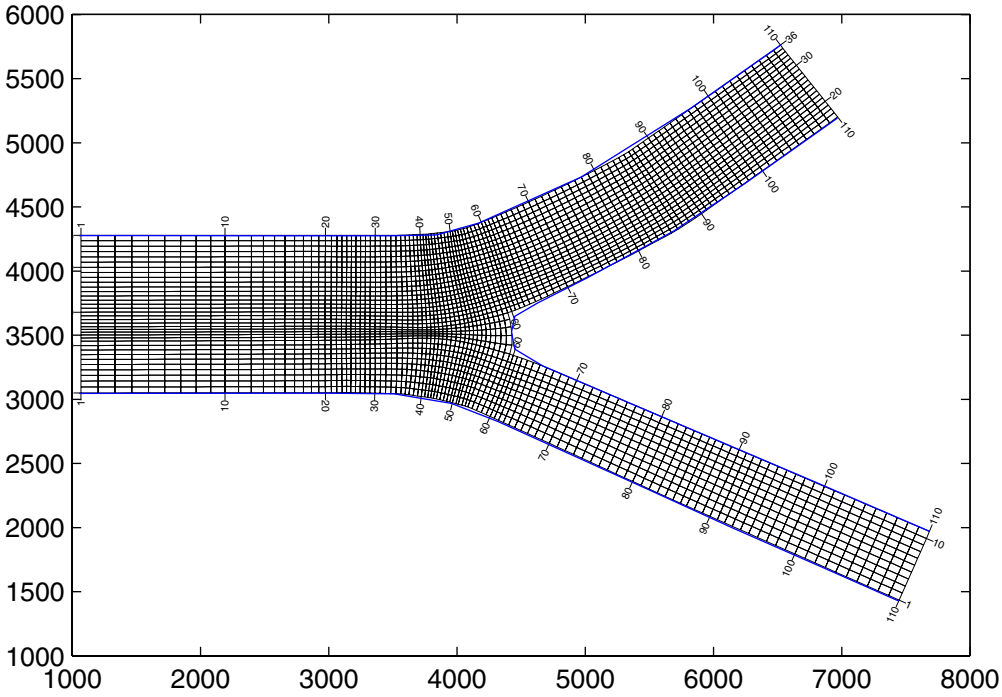

grid 2

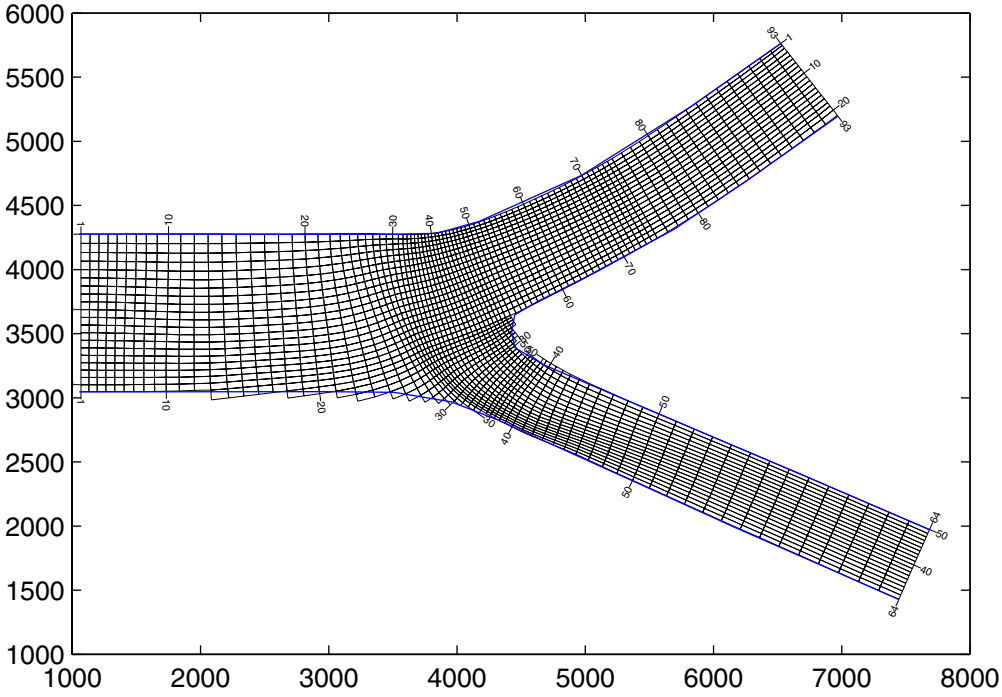

Two different computational grids for the same bifurcation.
Flow from left to right. Distances in metres.

WL | DELFT HYDRAULICS	Q2681 D–26

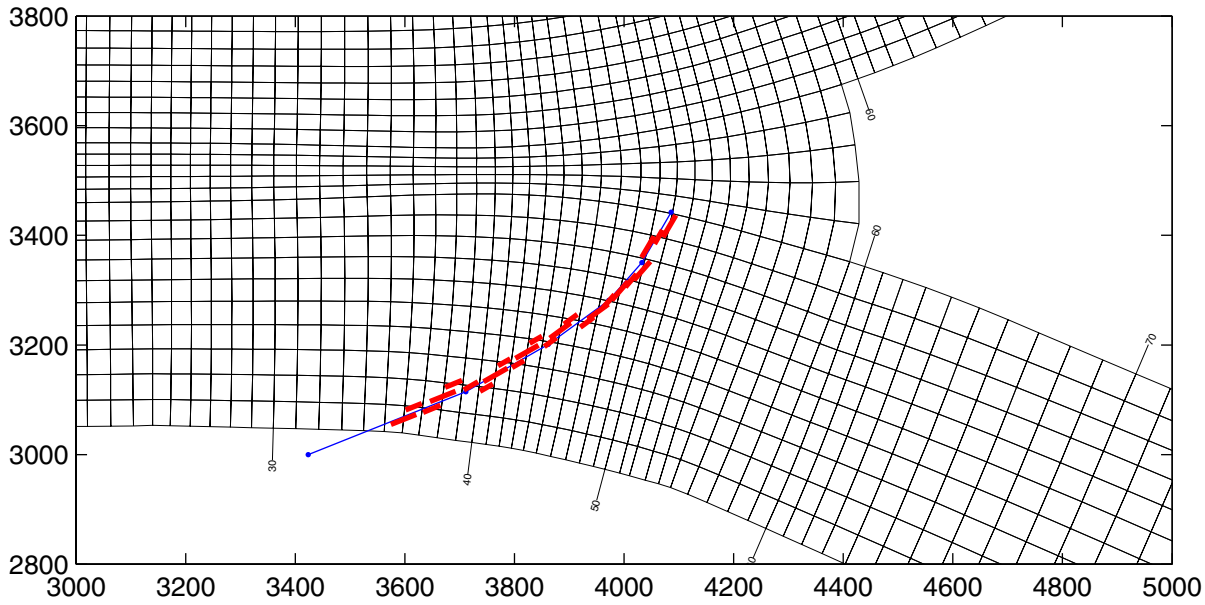

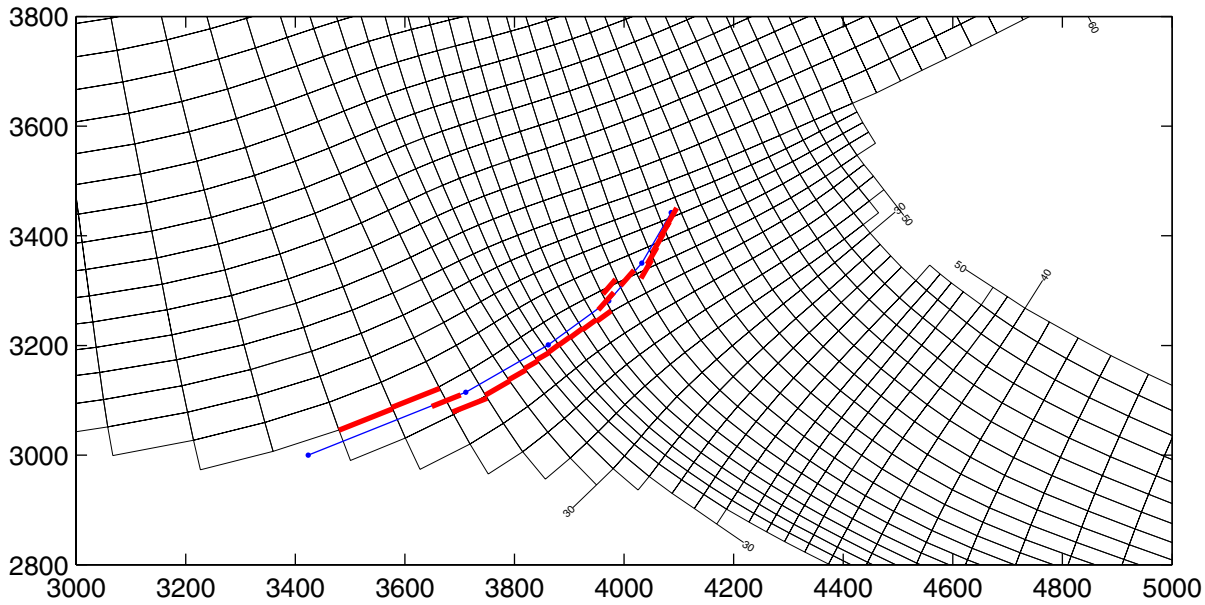

Representation of the type 2 vane on the two variants of the grid.
Flow from left to right. Distances in metres.

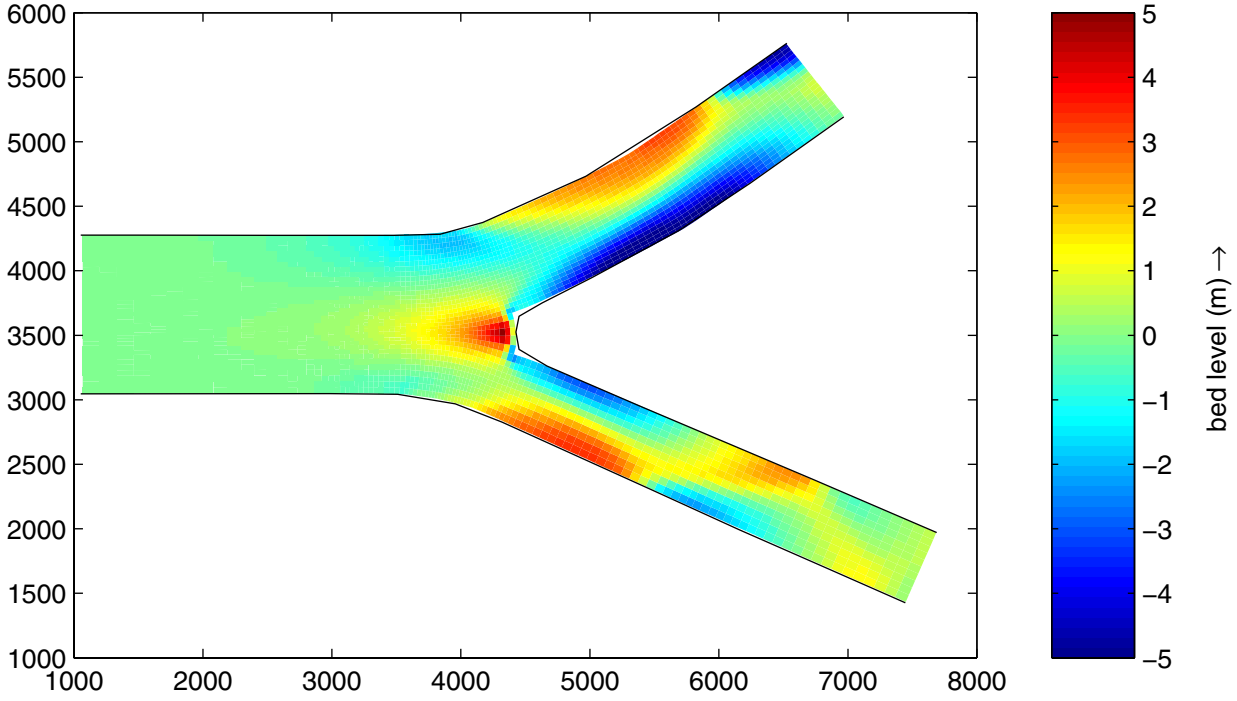

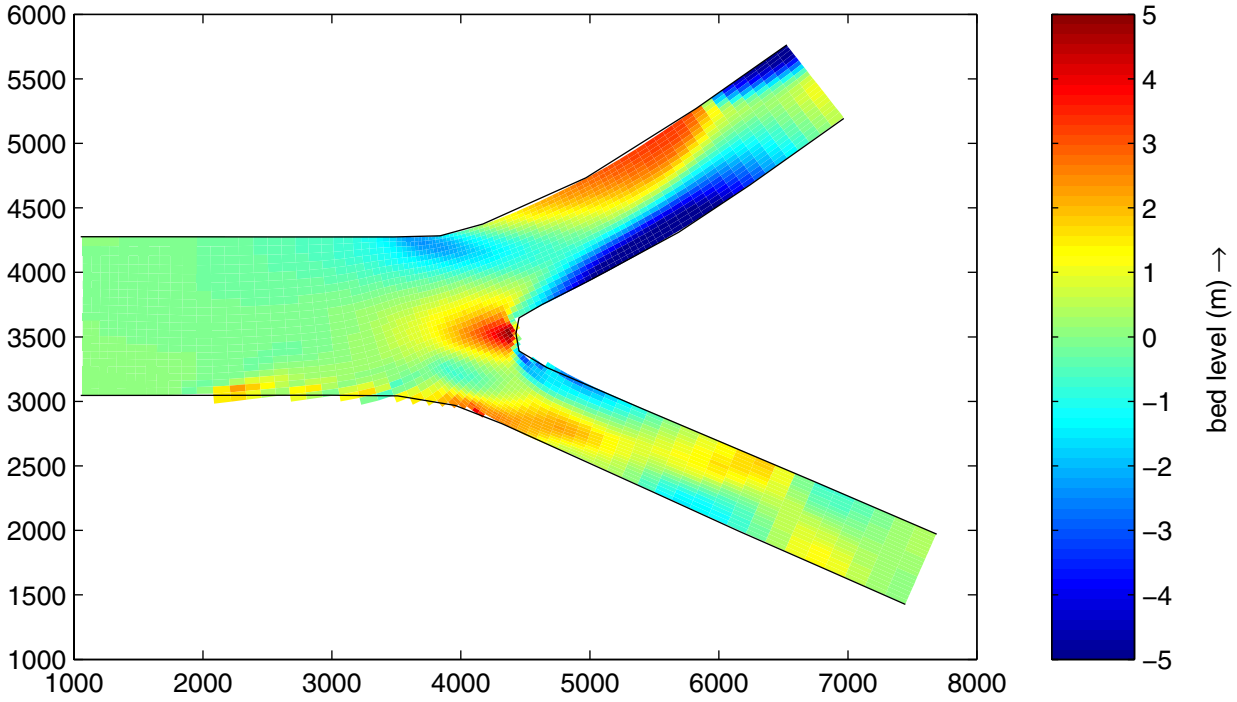

Equilibrium bed levels without vanes.
Determined for the 2 schematisation variants.

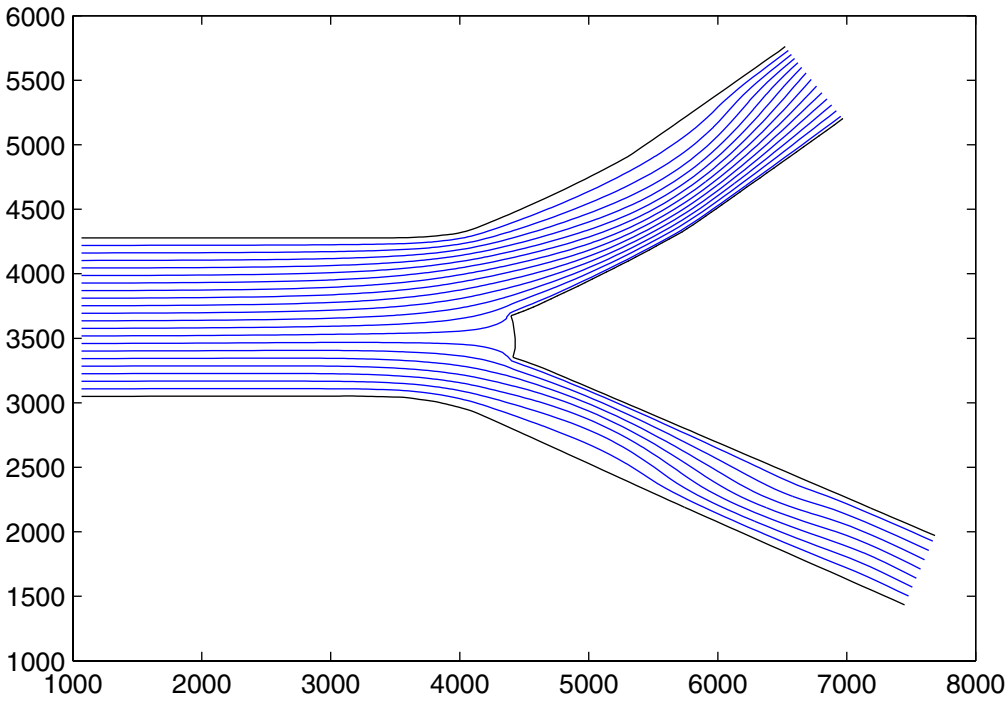

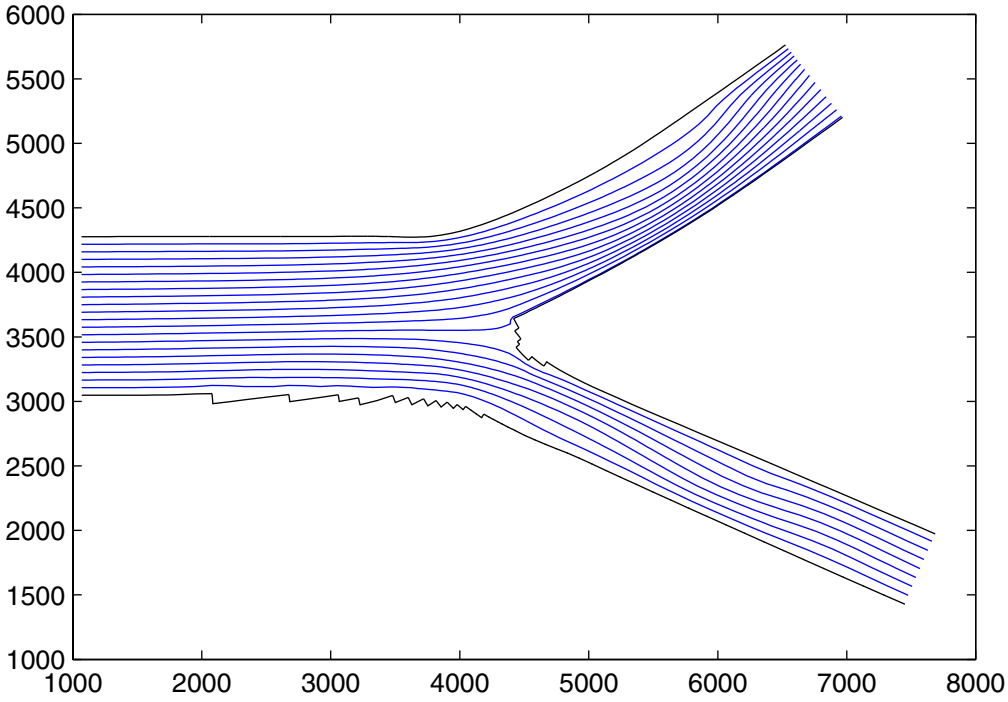

Flow pattern for the equilibrium bed levels without vanes.
Determined for the 2 schematisation variants.

WL | DELFT HYDRAULICS	Q2681	D–29

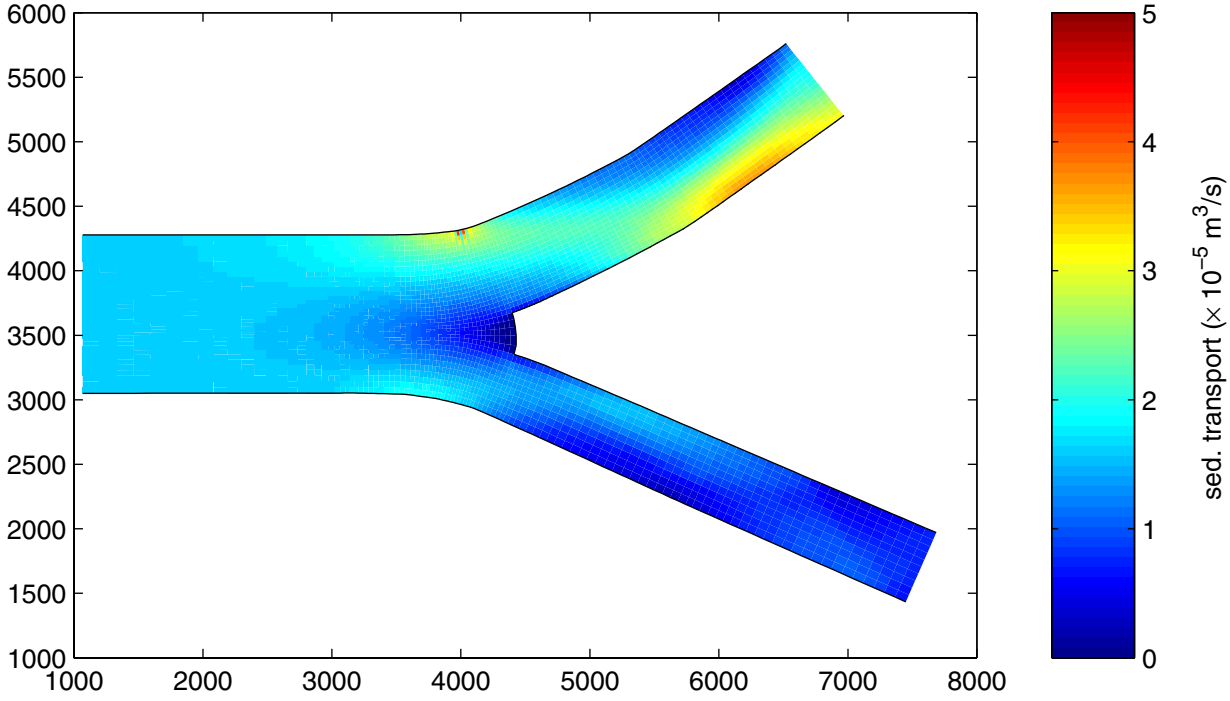

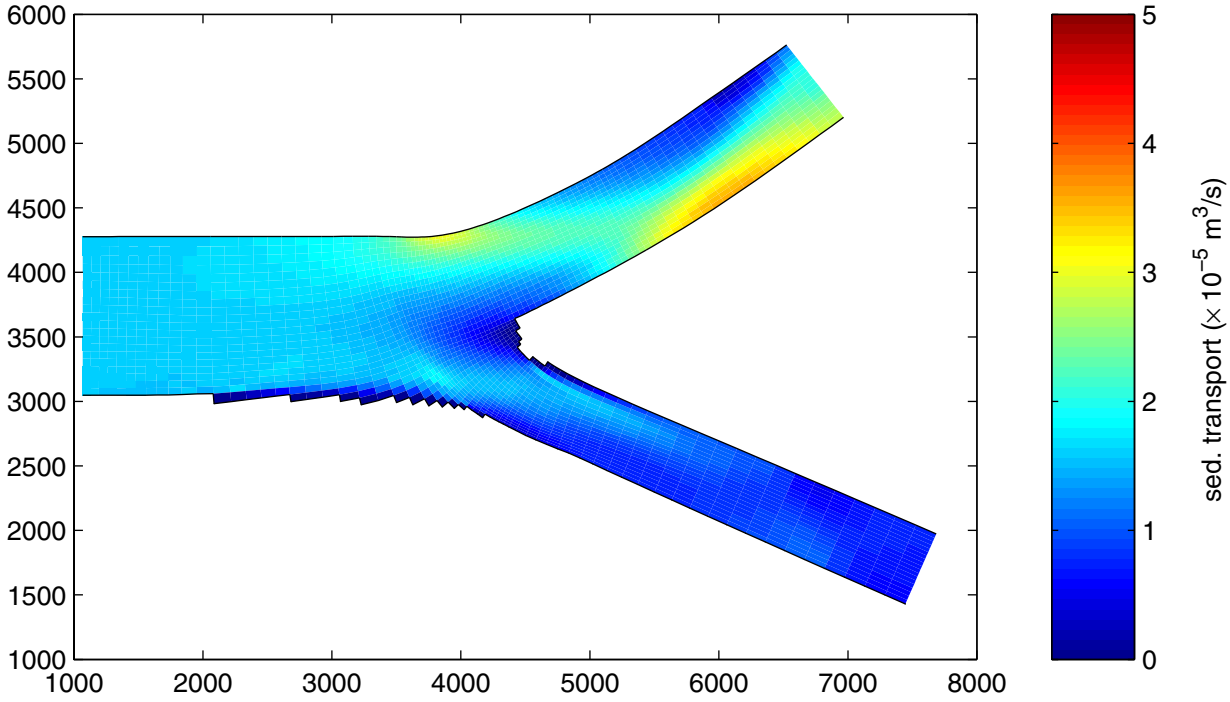

Sediment transport rate associated with the equilibrium conditions.
Determined for the 2 schematisation variants.

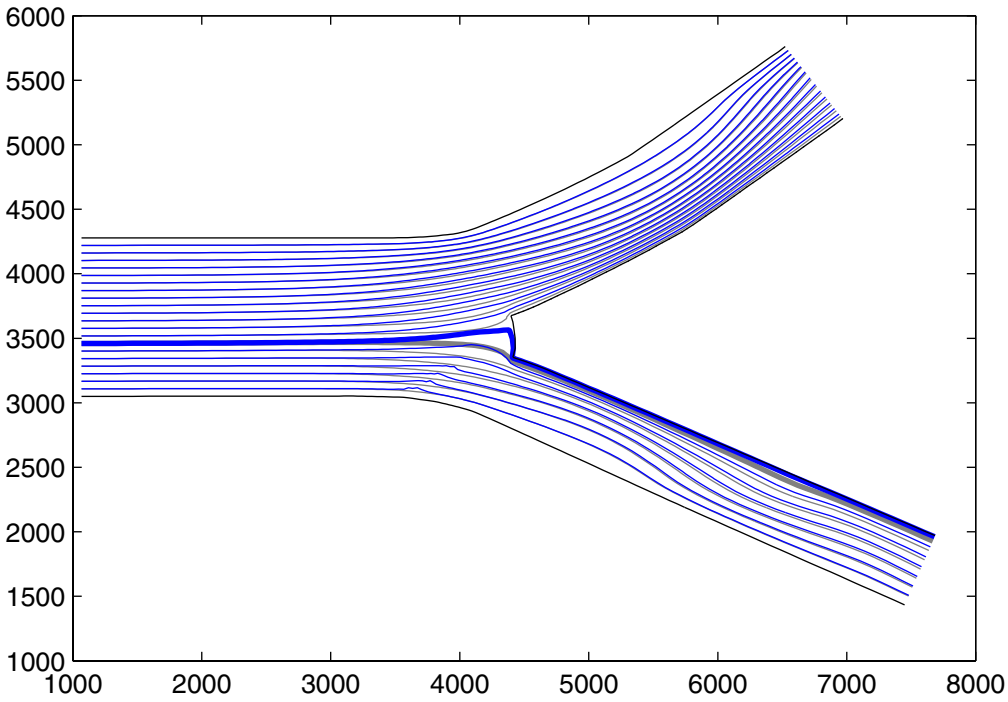

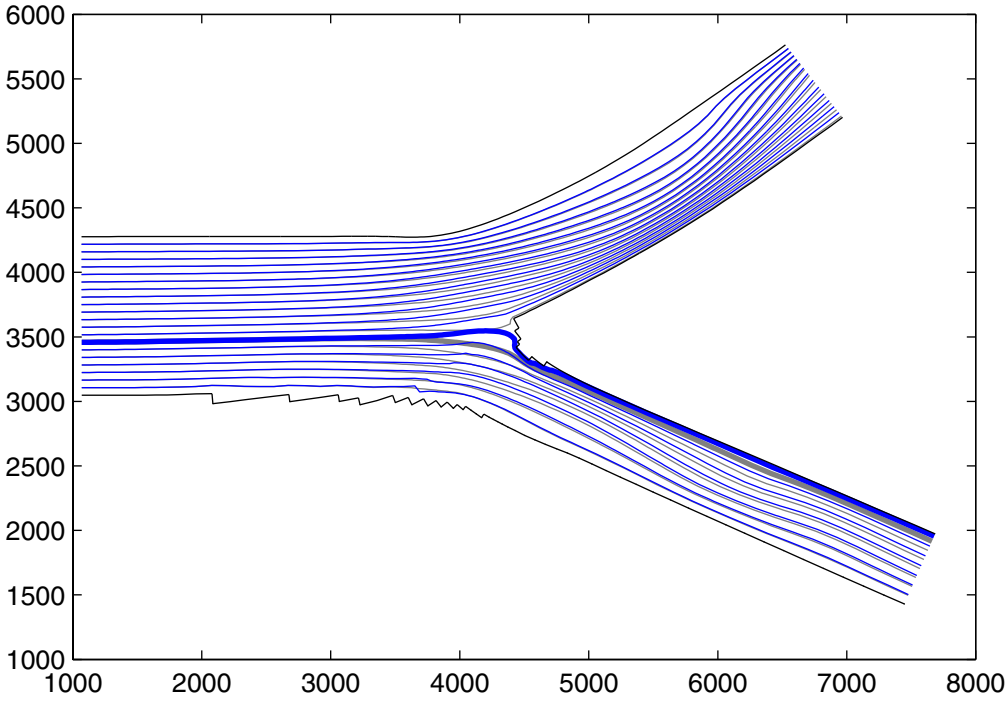

Depth–averaged flow pattern before (gray) and after (blue) construction of the bottom vane.
Determined for the 2 schematisation variants.

WL | DELFT HYDRAULICS	Q2681	D–31

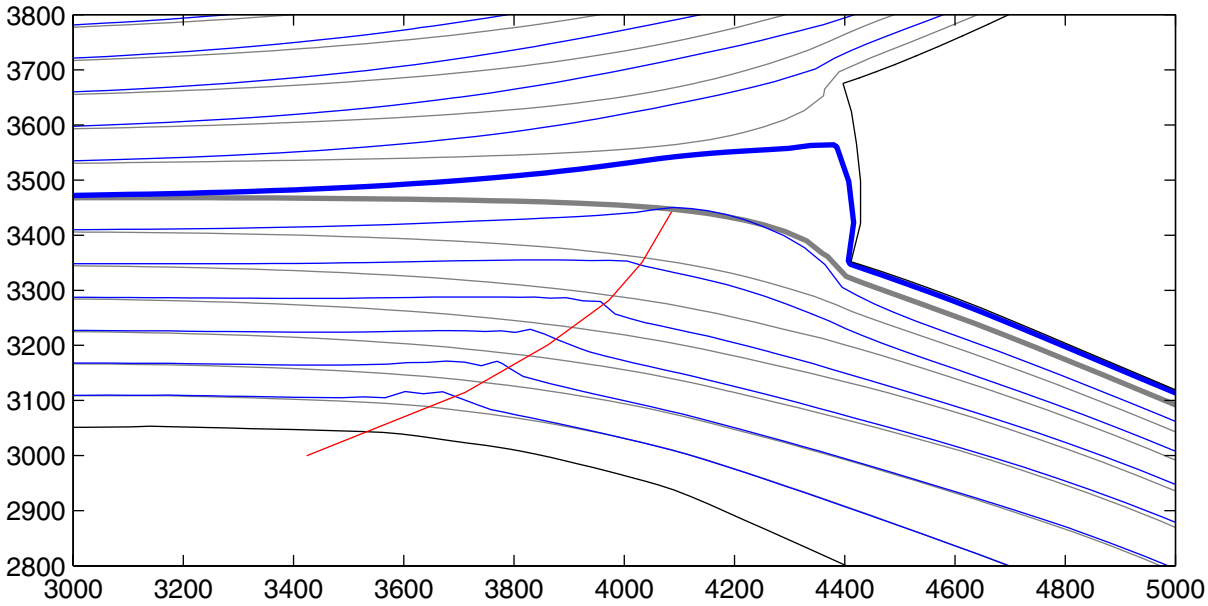

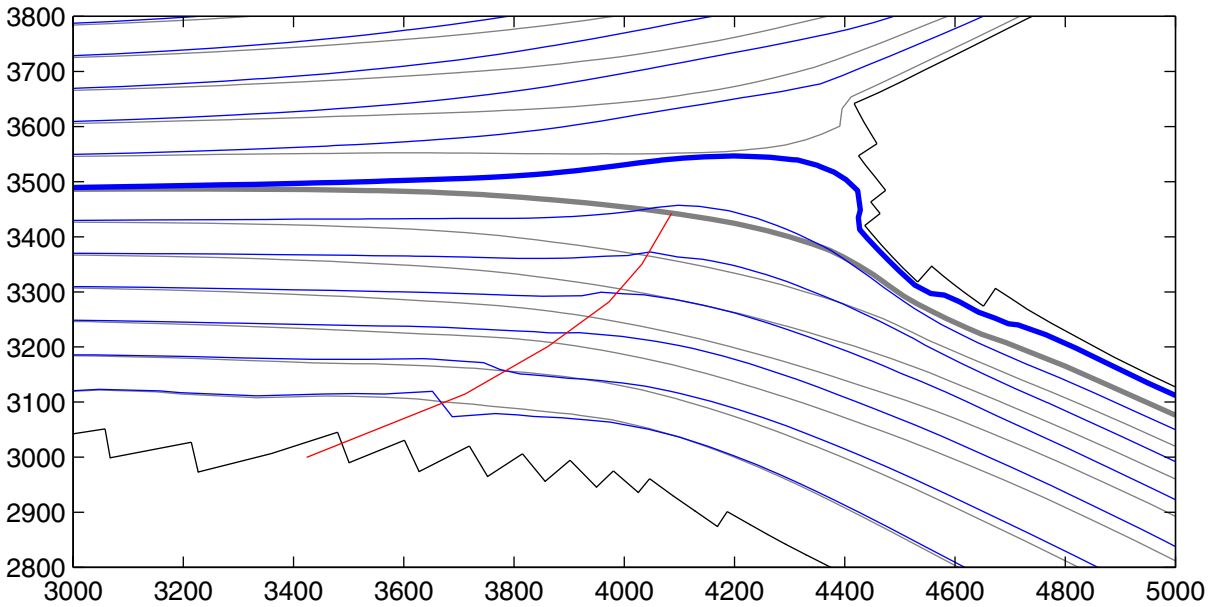

Depth–averaged flow pattern before (gray) and after (blue) construction of the bottom vane.
Determined for the 2 schematisation variants.

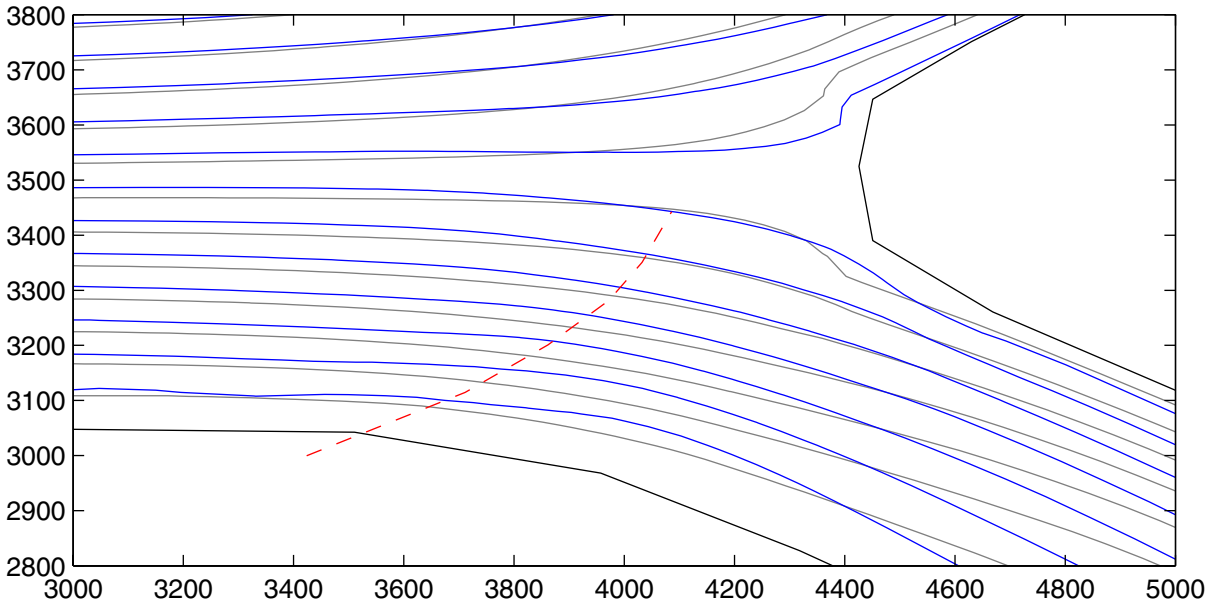

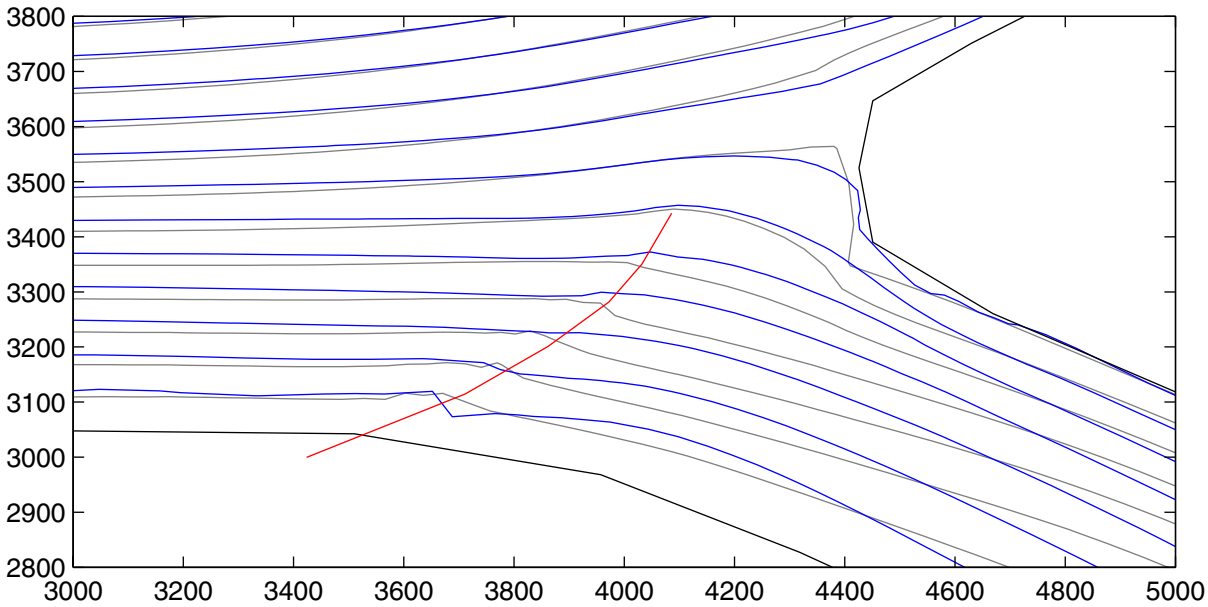

Depth–averaged flow pattern before (top) and after (bottom) construction of the bottom vane.
Determined for the 2 schematisation variants (gray and blue).

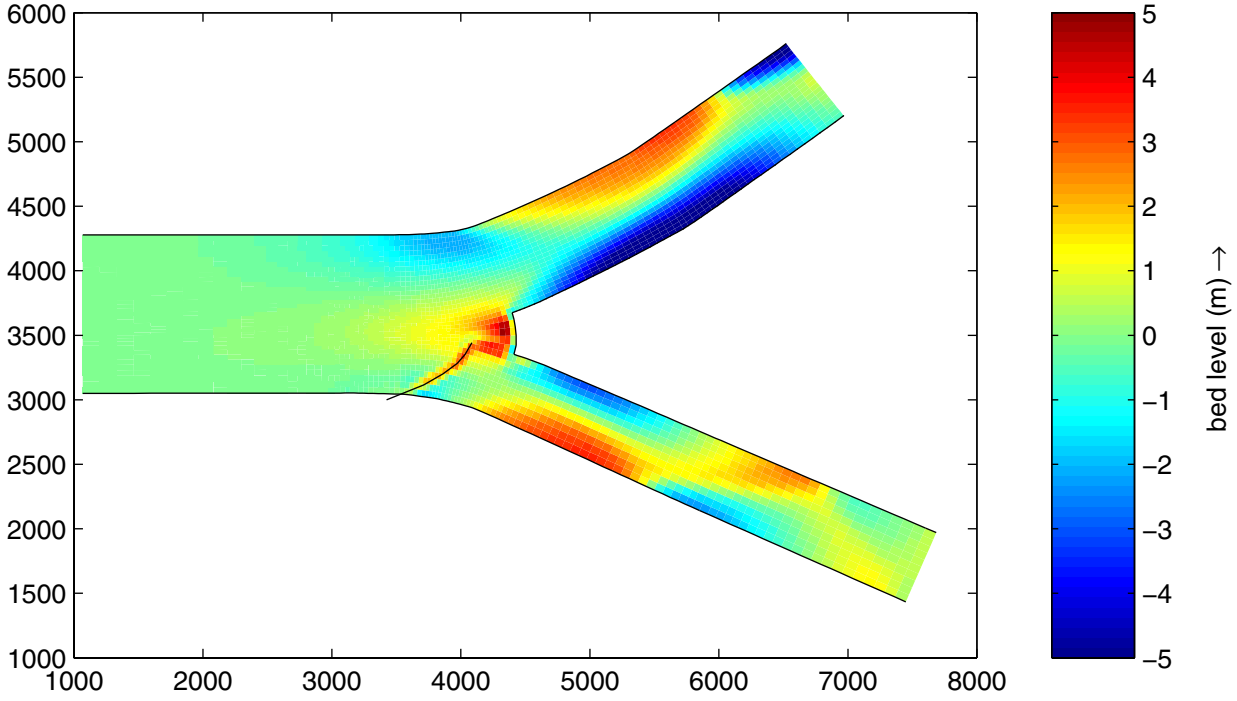

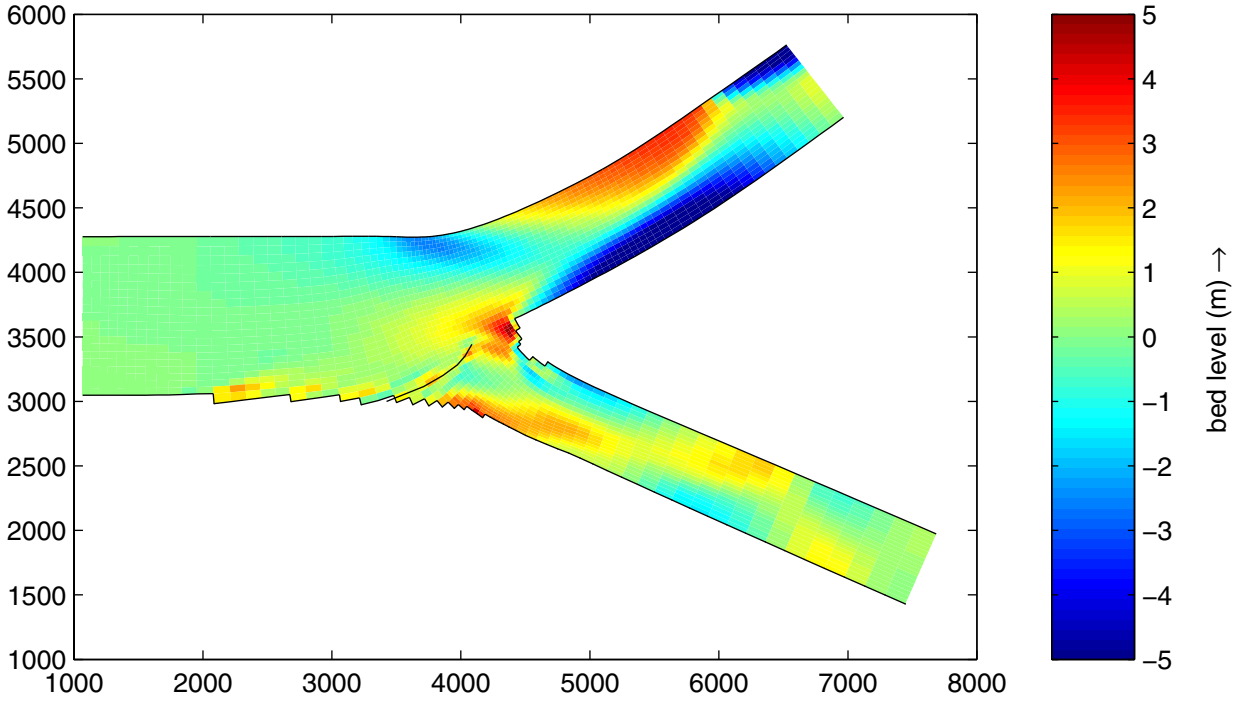

Bed levels 7.5 months after the construction of the bottom vane.
Determined for the 2 schematisation variants.

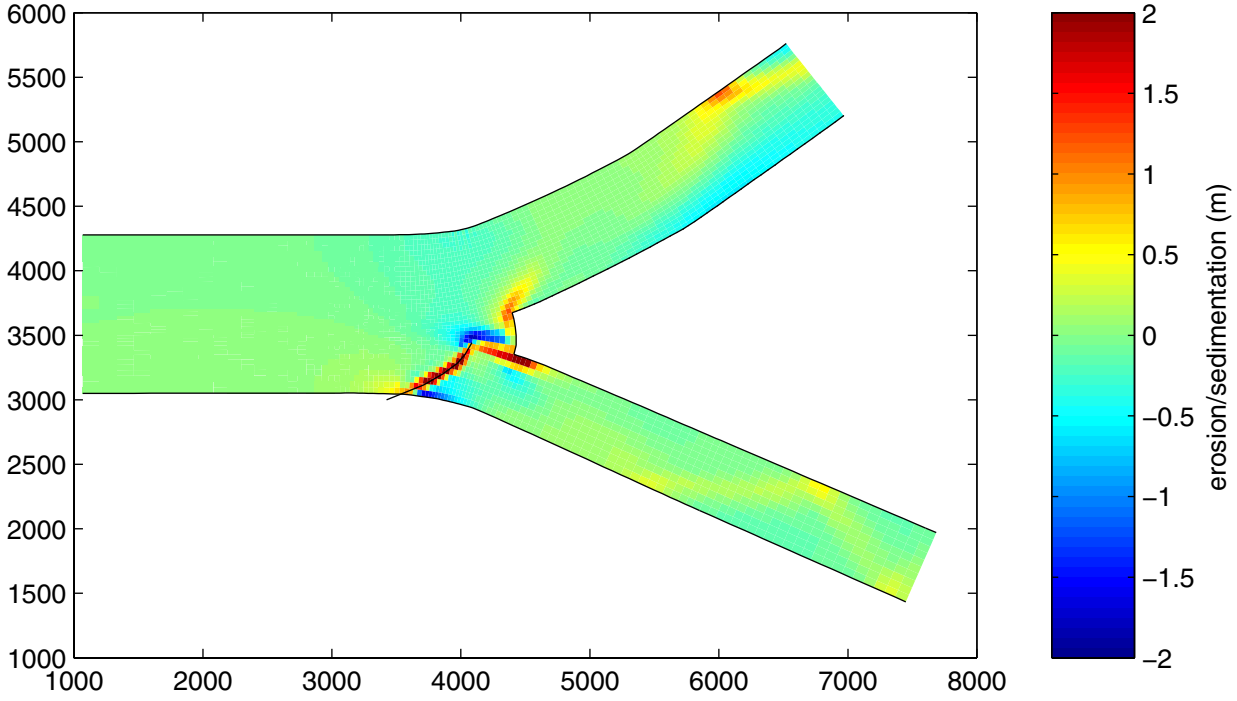

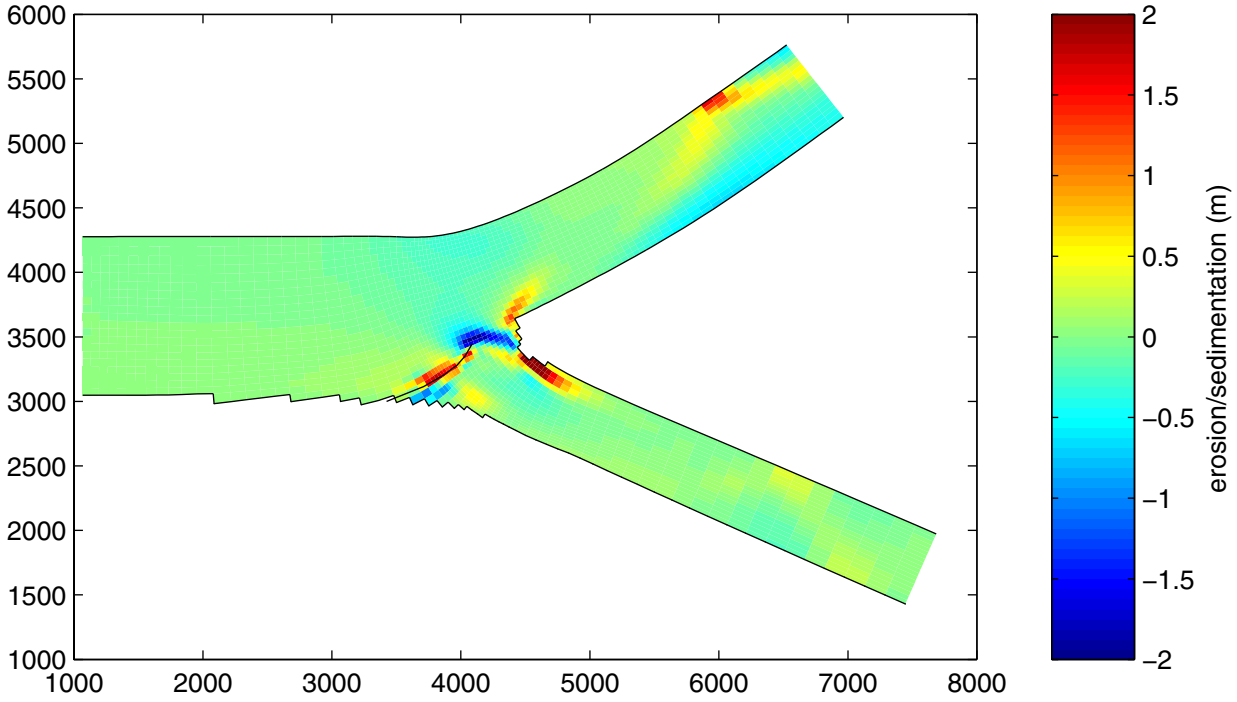

Bed level changes during the first 7.5 months
after the construction of the bottom vane.
Determined for the 2 schematisation variants.

WL | DELFT HYDRAULICS	Q2681	D–35

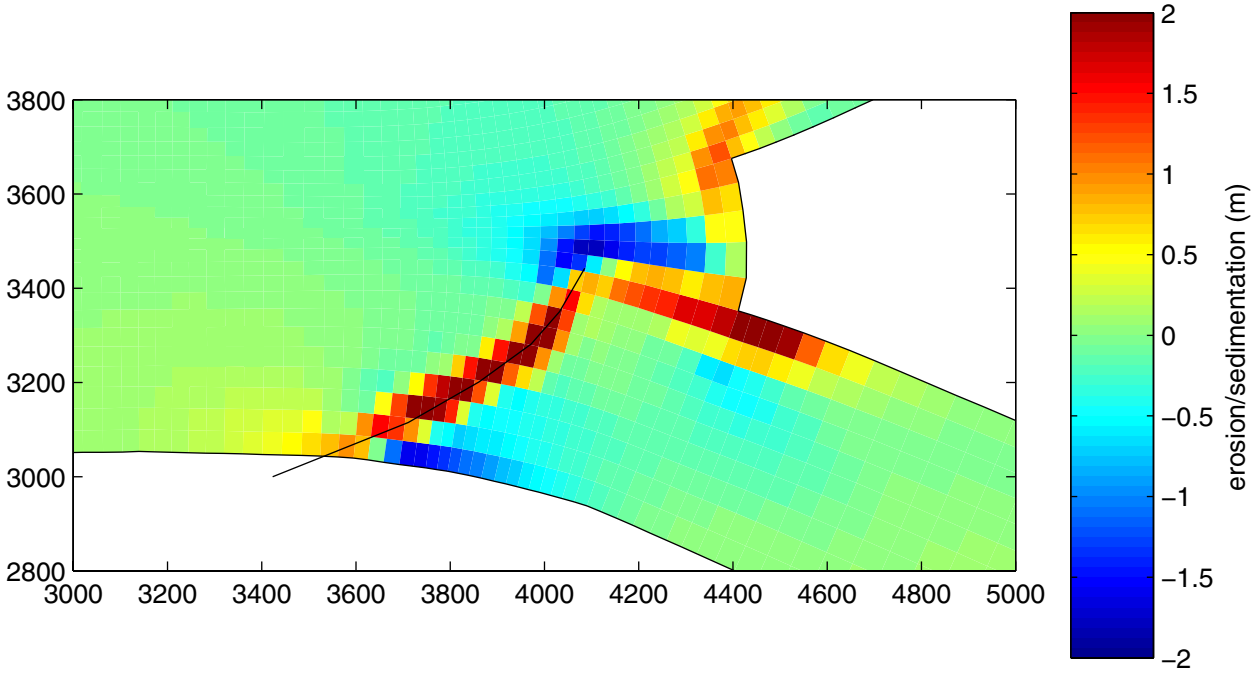

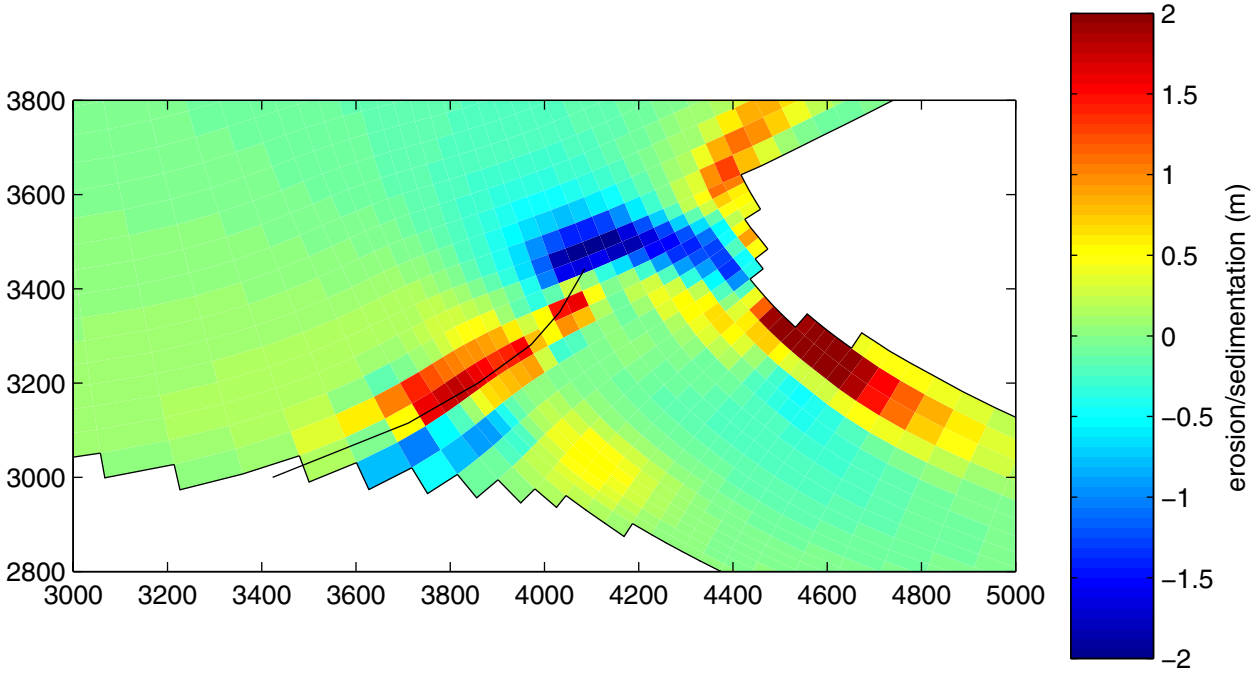

Bed level changes during the first 7.5 months
after the construction of the bottom vane.
Differences determined for 2 schematisation variants.

WL | DELFT HYDRAULICS	Q2681	D–36

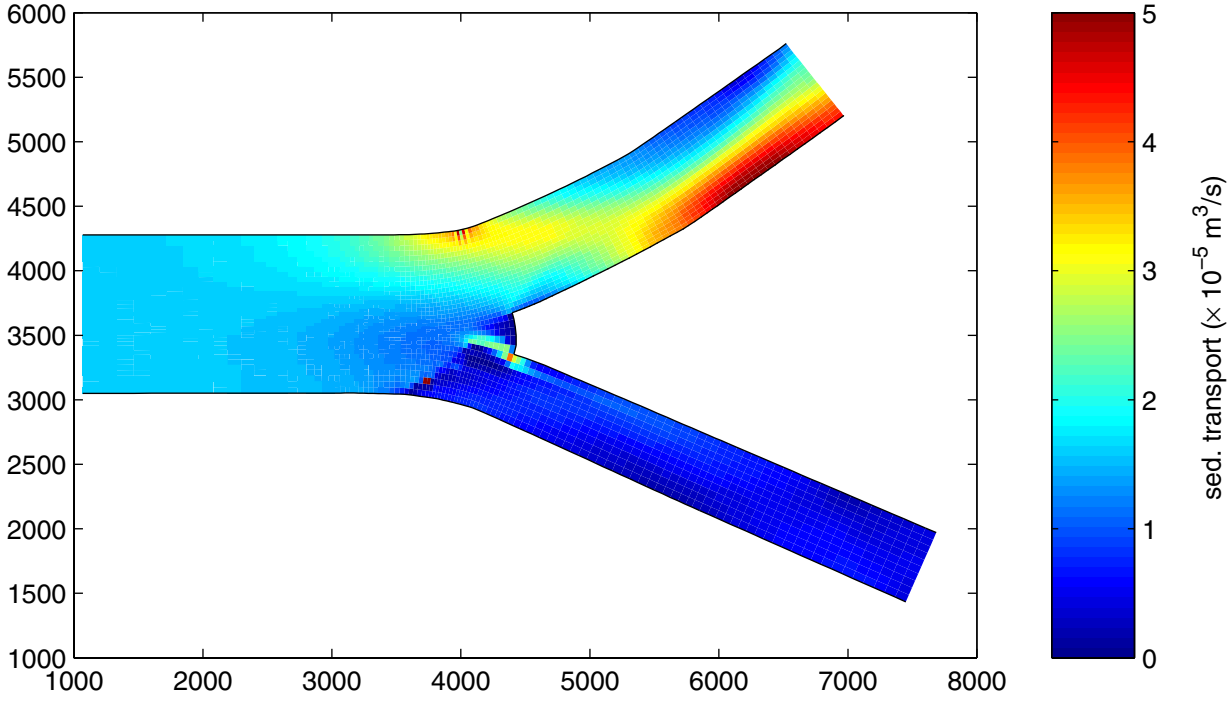

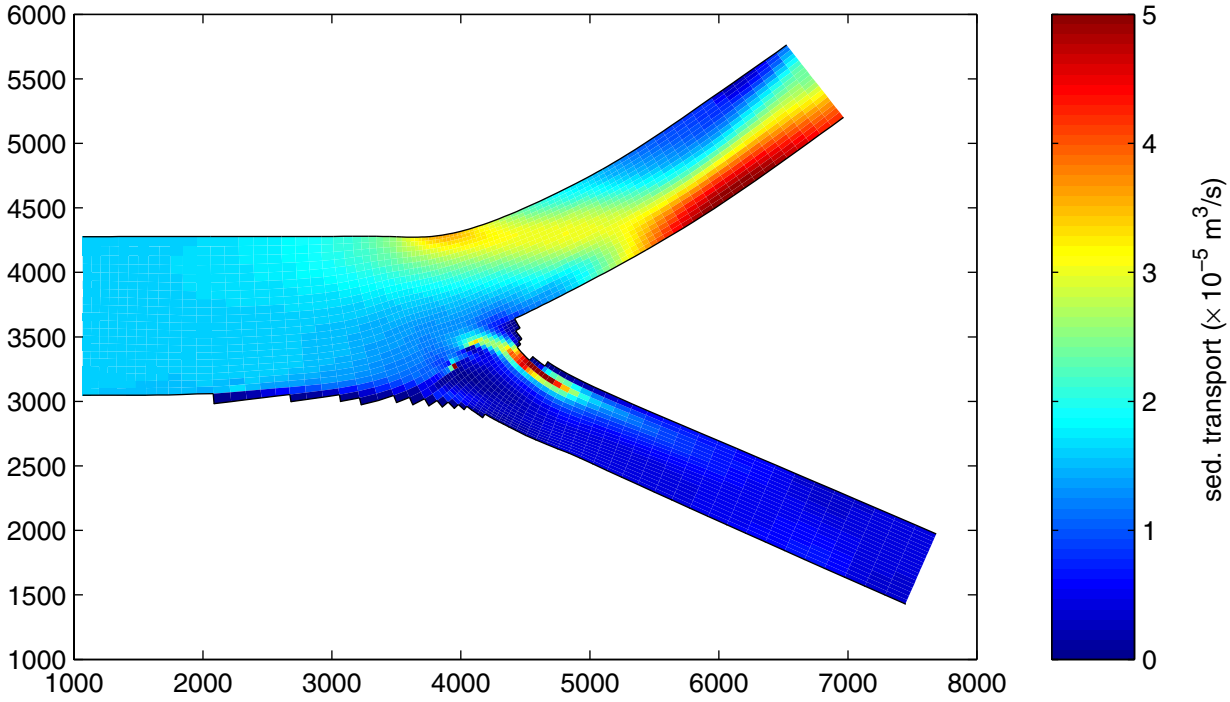

Sediment transport rate after 7.5 months.
Determined for 2 schematisation variants.

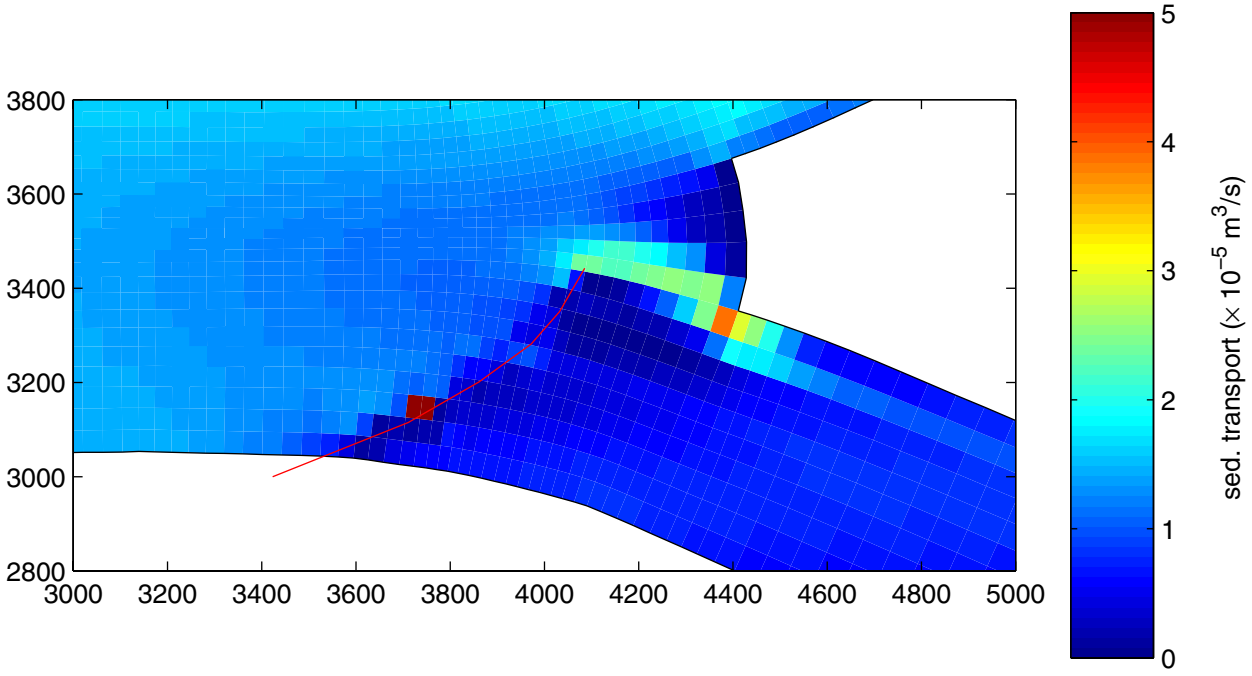

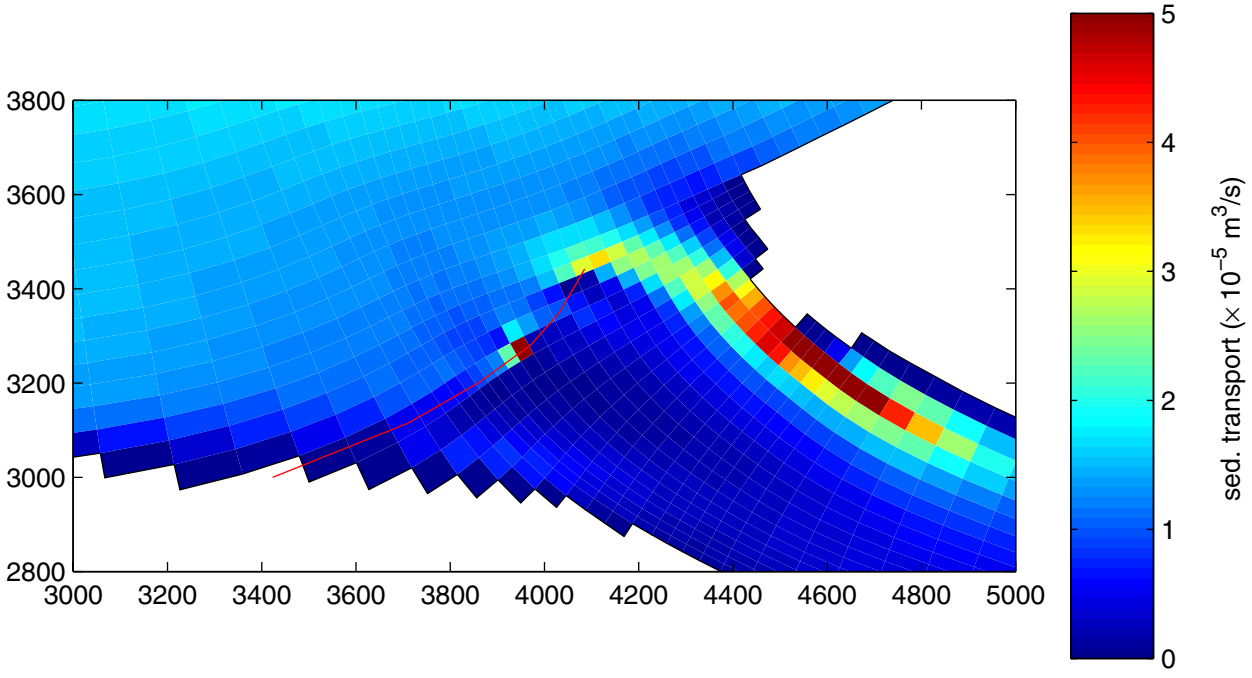

Sediment transport rate after 7.5 months.
Determined for 2 schematisation variants.

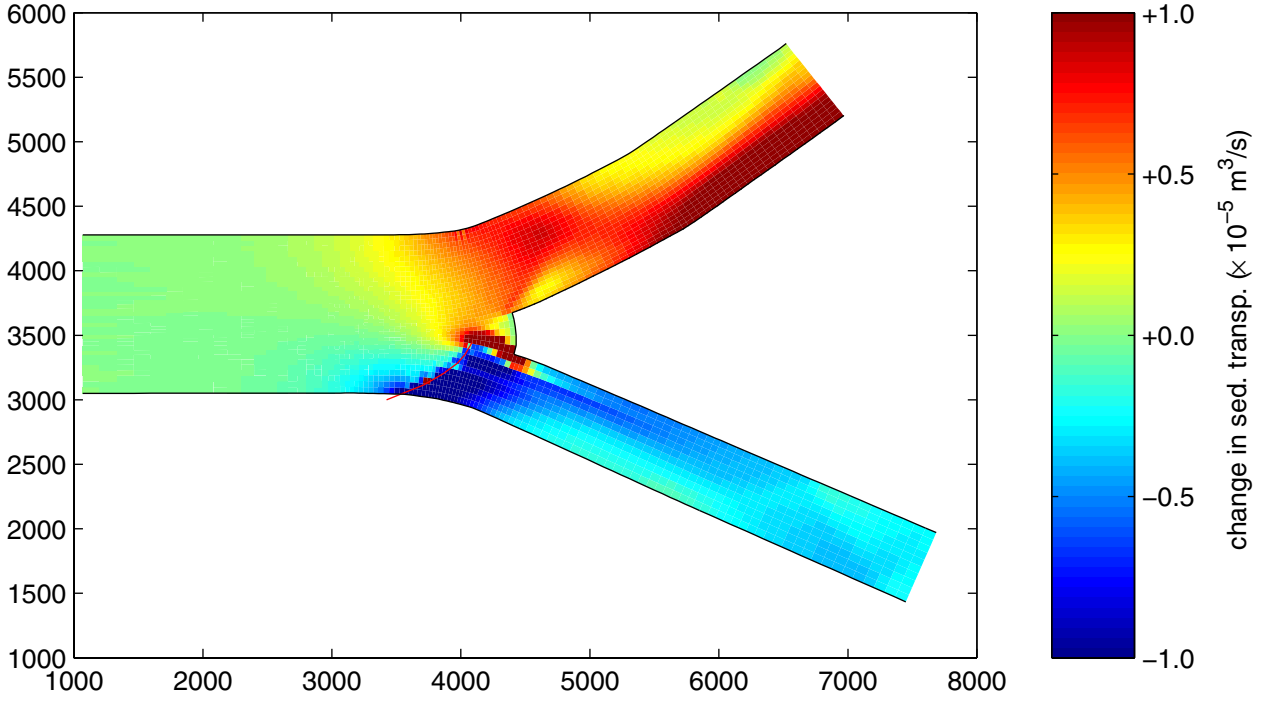

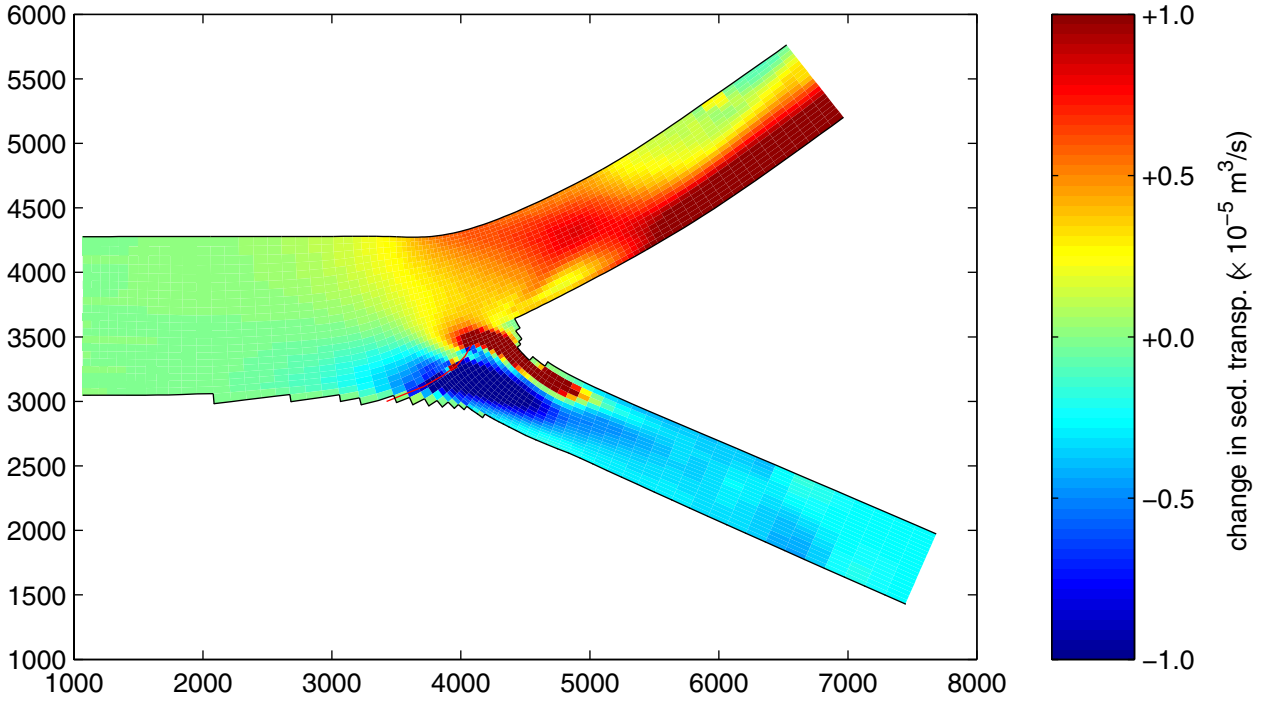

Changes in sediment transport rate after 7.5 months.
Differences determined for 2 schematisation variants.

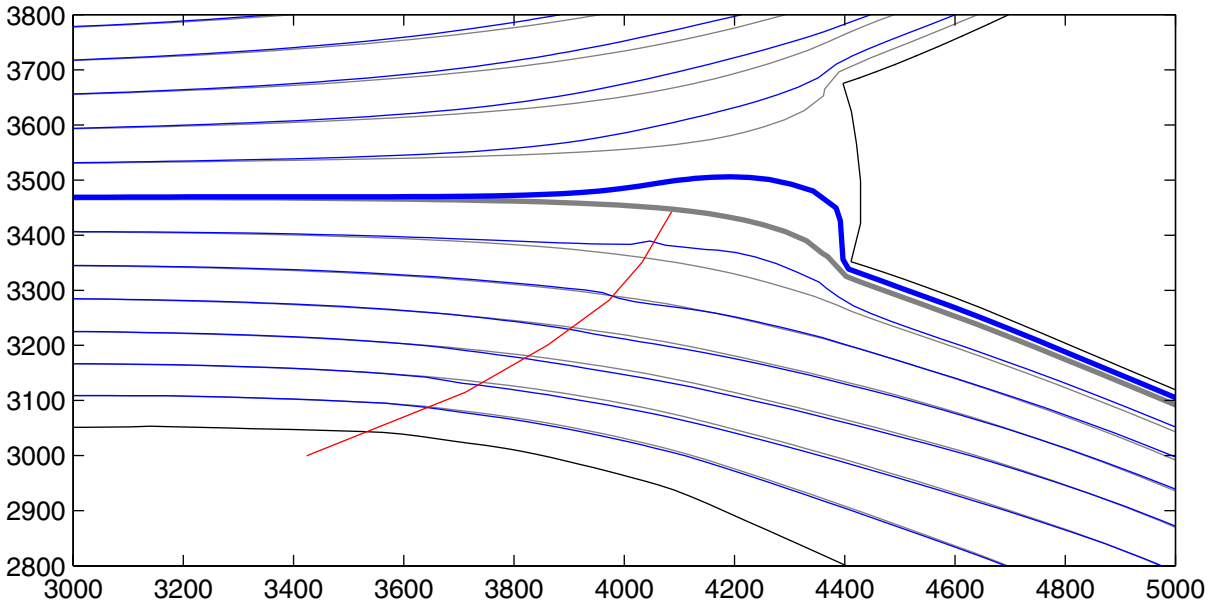

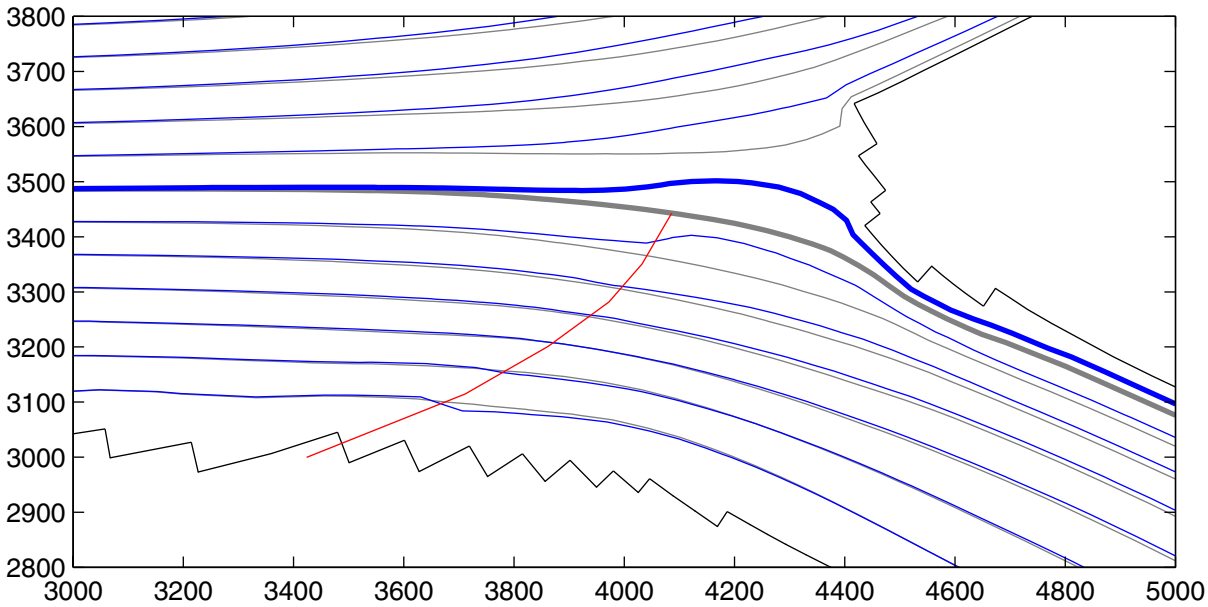

Depth–averaged flow pattern before (gray) and after (blue)
the construction of the surface vane.
Determined for 2 schematisation variants.

WL | DELFT HYDRAULICS	Q2681	D–40

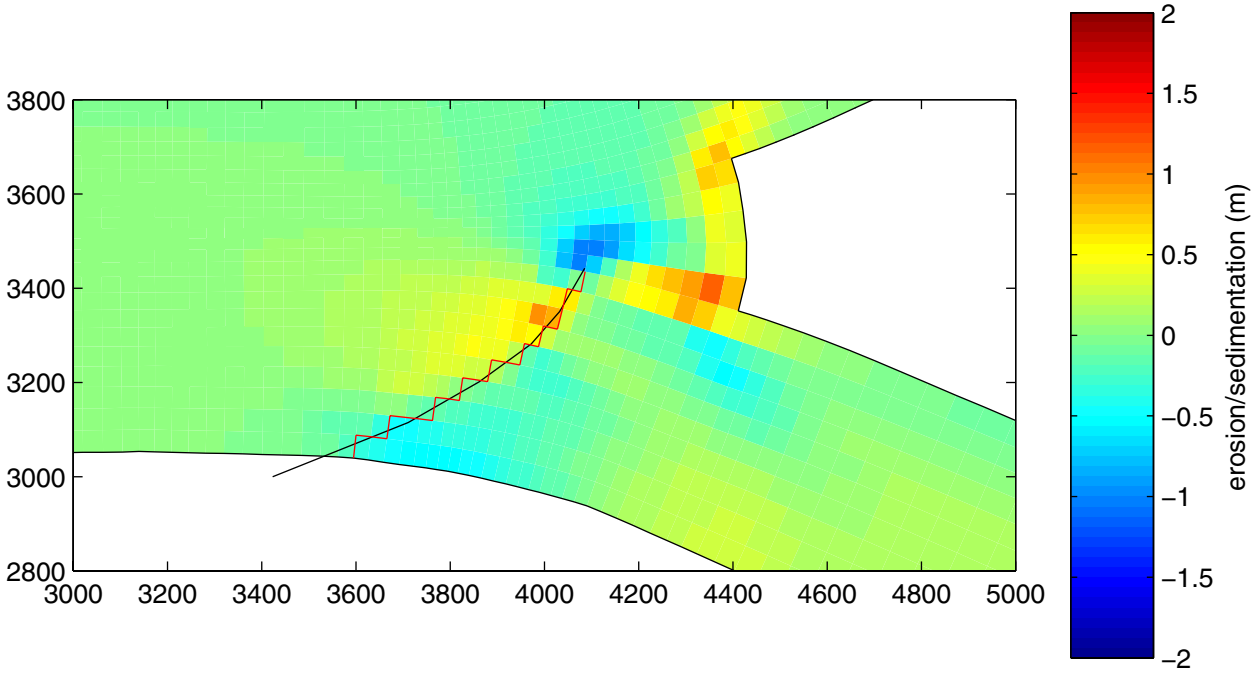

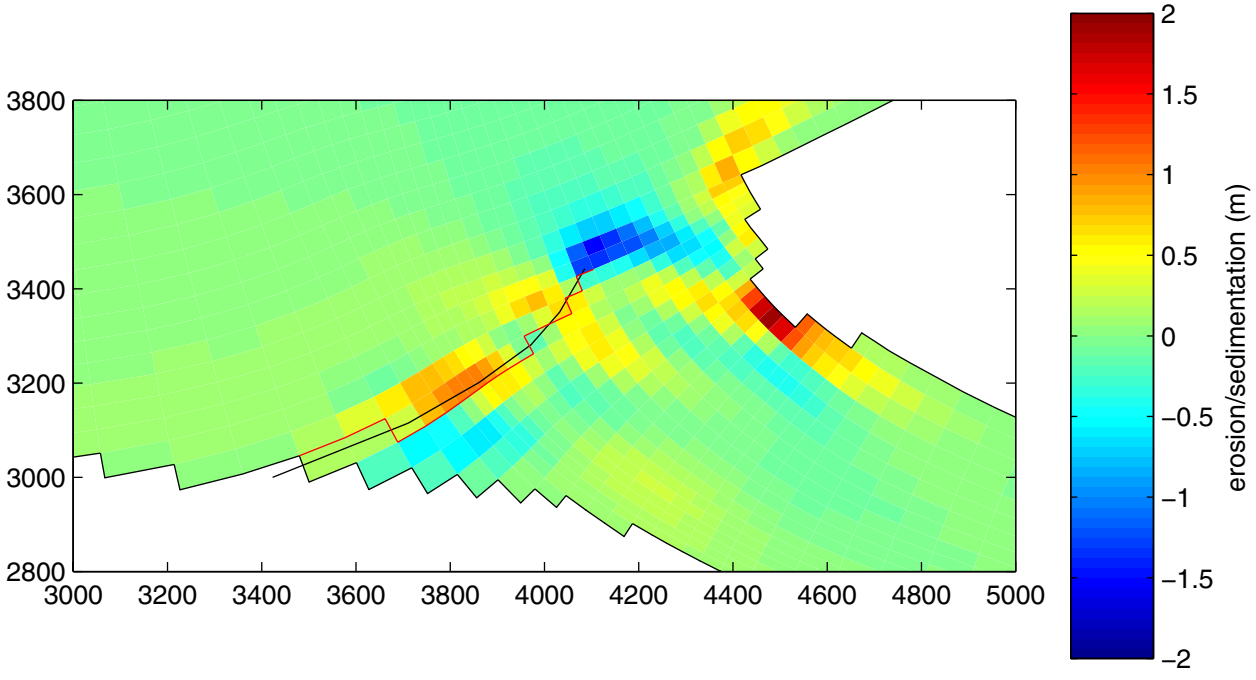

Bed level changes during the first 7.5 months
after the construction of the surface vane.
Determined for 2 schematisation variants.

WL | DELFT HYDRAULICS	Q2681	D–41

Appendix E Gorai river restoration project

GORAI RIVER RESTORATION PROJECT

MORPHOLOGICAL MODELLING OF BOTTOM VANES

(Annex J in report of DHV-Haskoning Consortium for Gorai River Restoration Project, November 2001)

TABLE OF CONTENTS

APPENDICES 37

1. INTRODUCTION

1.1 Gorai River Restoration Project

Submerged vanes have been proposed as a means to control the sediment influx in the Gorai at the offtake near Talbaria. However, the efficiency of vanes (and subsequently, the amount of vanes needed) at this particular location remains to be assessed. For this purpose a model study for the bottom vanes has been defined as part of the Gorai River Restoration Project.

The present report Annex J is the result of this study and it is part of the framework of the Main Report of the Gorai River Restoration Project.

1.2 Bottom Vanes in Delft3D Morphological Model

Although, the functioning of a bottom vane is well understood and reasonably well quantifiable, assessing the morphological impact of a field of submerged vanes requires complex models. This is complicated further as result of the complex and dynamic morphology of the Ganges and the Gorai offtake.

For this purpose use was made of the Delft3D morphological model. Specifically for this project a bottom vanes module was added to the numerical modelling system, developed by WL Delft Hydraulics as part of the Delft Cluster program for Bottom Vanes.
The 3D effect of bottom vanes was introduced in the Delft3D model by a numerical description of the secondary currents cause by each vane. A description of the Delft3D morphological modelling system that resulted is included in Appendices E and F of this report.

The model allowed for a detailed description of the hydraulic and morphological phenomena occurring in the area surrounding the Gorai offtake. Subsequently, it was possible to assess the effect of a field of bottom vanes on the influx of sediment and water into the Gorai offtake. By comparing this situation with the situation without vanes, conclusions can be drawn with respect to the effect of the vanes.

1.3 Guide to the Report

Chapter 2 presents an overview of the design for a field of submerged vanes in the upstream area of the Gorai offtake. This design was described in more detail in Annex G - River Training Works Design of the main report of the Gorai River Restoration Project.

Chapter 3 provides an overview of the modelling approach followed in this study, including the proposed layout of the numerical model for the Gorai offtake area.

Chapter 4 describes the procedure that was followed to calibrate this numerical model, both hydraulically and morphologically. This calibration was based on the available data for the present situation of the offtake area.

Chapter 5 presents the results from a large number of model runs that were carried out to quantify the effect of a field of submerged vanes under various circumstances. Specifically, the influence of a field of submerged vanes on the amount of sediment entering the Gorai offtake under a range of circumstances.

Finally, conclusions are drawn in **Chapter 6**.

2. OVERVIEW DESIGN BOTTOM VANES IN GORAI OFFTAKE

2.1 Works in the Gorai offtake

The following interventions are proposed as initial works in the Gorai offtake area:

- flow divider, to be constructed at the left bank of the Gorai, and protruding into the (main channel of the) Ganges;
- offtake guide bund, narrowing the width of the offtake, reducing the sedimentation.

Although not forming part of these initial works to be implemented as part of option A1, significant attention was paid to the design of a field of bottom vanes. These vanes may be necessary to further reduce the ingress of sediment into the Gorai system, if this would prove to continue to be too large for a restoration of the Gorai River.
Limiting the quantity of sediment that enters the Gorai will considerably contribute to achieving the ultimate goals of the project. A structure considered most suited for the diversion of sediment towards the Ganges is a field of bottom vanes.

2.2 Function of Bottom Vanes

Bottom vanes can be used to reduce the amount of sediment that enters the Gorai. A submerged vane generates a trailing vortex with a limited diameter. Series of parallel vanes create a larger scale circulation, as indicated in Figure 2.1. Also the vane height, length, drag- and lift forces are indicated in this Figure.
Bottom vanes generate a transverse component in the sediment transport: sediment-rich water near the bed is diverted towards the Ganges, while water with less sediment will flow into the offtake near the surface. Thus, water with a reduced sediment concentration enters the Gorai.

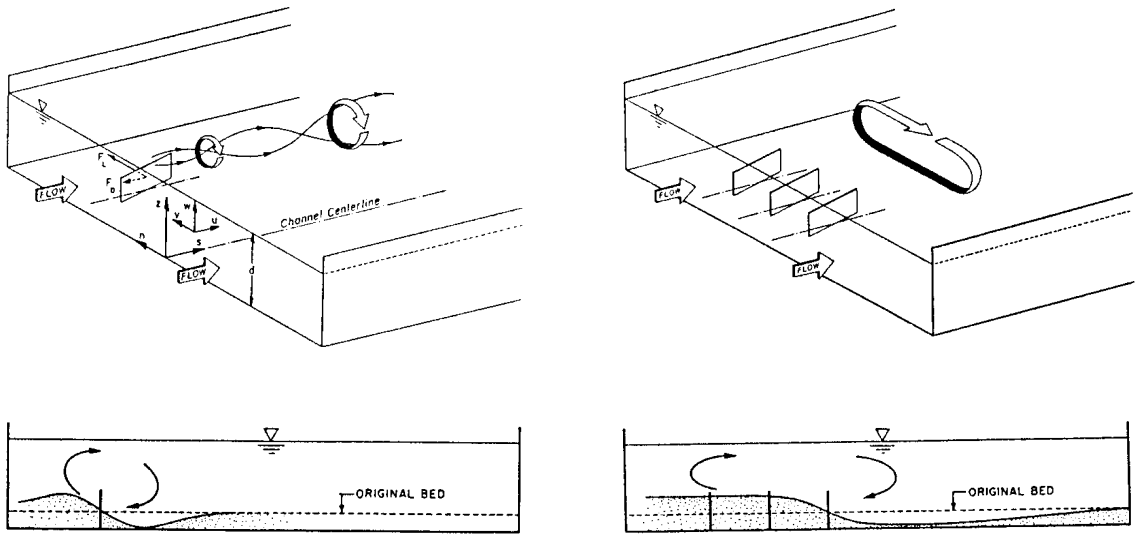

Figure 2.1: Schematic of flow situation showing vane-induced circulation and subsequent change in bed profile, single vane and transverse row of vanes [Odgaard, 1991]

A key factor in the functioning of vanes is the angle of approach: the angle between the depth averaged velocity vector upstream (over the height of the vane) and the longitudinal axis of the vane. For a proper functioning of the vanes the approach angle of the upstream flow should be within close range of the design conditions.

Sediment approaching from upstream along the right river bank of the Ganges will have to be transported sideways beyond the inflow opening of the Gorai, so a substantial number of vanes will be required –a field of approximately 1500 m long and 200m wide.

2.3 Summary of Design of Field of Bottom Vanes

A preliminary design for a field of bottom vanes was proposed in the main Feasibility Report. Vane dimensions and spacings are proposed with produce the maximum effect. Furthermore, it is important that the vanes work together in a field to generate a single circulation. Based on these criteria a vane field with the following characteristics was designed:

- vane height H_v = 5.3 m;
- vane length L_v =16 m;
- nominal angle of attack[1] $\alpha = 16^o$;
- transverse distance vanes in a row Δ_v = 10 m;
- distance between successive rows Δ_u = 130 m is proposed;
- design bed level PWD+0 m, bed dredged and partly filled, bed protection (rock).

An estimate was made for the division flow line upstream of the flow divider. Based on this flow line, the existing water depth and position of structures, the dimensions of the vane field was designed. A schematic impression of the dimensions of the vane field is given in Figure 2.1, Figure 3.1 and Table 2.1. Reference is made to drawing 1410 in the main Feasibility Report drawing: Vanes General Plan and Setting out Details.

Note, that the physical orientation of the vanes was assessed in a later stage (paragraph 5.2) based on the flow pattern and the nominal angle of attack mentioned above.

2.4 Critical Design Parameters

In the design process a number of critical parameters for the functioning of the vanes were identified for the specific situation at the Gorai offtake:

- variations in discharge and water level over monsoon and dry season: a range of discharges of 24,000 m3/s - 62,000 m3/s was adopted, with corresponding water levels at Talbaria PWD +11.6 m to 13.8 m;
- vertical sediment concentration profile: as a result of suspended sediment transport the morphological effect of the vanes is reduced.;
- stability of the large-scale flow pattern in the Ganges: changes in the plan form of the main channel in the Ganges, as well as other river training structures will influence the angle of attack of the vanes. At small angles of attack the vane efficiency increases with and increasing angle of attack, however, at an angle of attack of roughly 22^o the efficiency decreases abruptly as a result of flow separation. Risk that the vane field will be buried with large-scale changes in Ganges plan form.

[1] The angle of attack for submerged vanes is defined as the angle between the approaching flow on the upstream side and the centreline of the vane.

The present study addresses a number of these questions on how effective the vanes would be and how sensitive this performance might be to the factors mentioned above.

Row #	Chainage m from Talbaria	width flowpath m	start row m N of division line	end row m S of division line	length of row m	number of vanes
Talbaria	0	220				
1	360	200	80	160	90	9
2	490	225	60	160	100	11
3	620	251	30	170	140	15
4	750	276	0	180	180	19
5	880	302	-30	170	200	21
6	1010	327	-30	150	180	19
7	1140	353	-40	140	180	19
8	1270	378	-50	130	180	19
9	1400	403	-60	120	180	19
10	1530	429	-80	120	200	21
11	1660	454	-100	120	220	23
12	1790	550	-120	120	240	25
Tip flow div.	2200	700		Total number of vanes		220

Table 2.1: Details of vane field

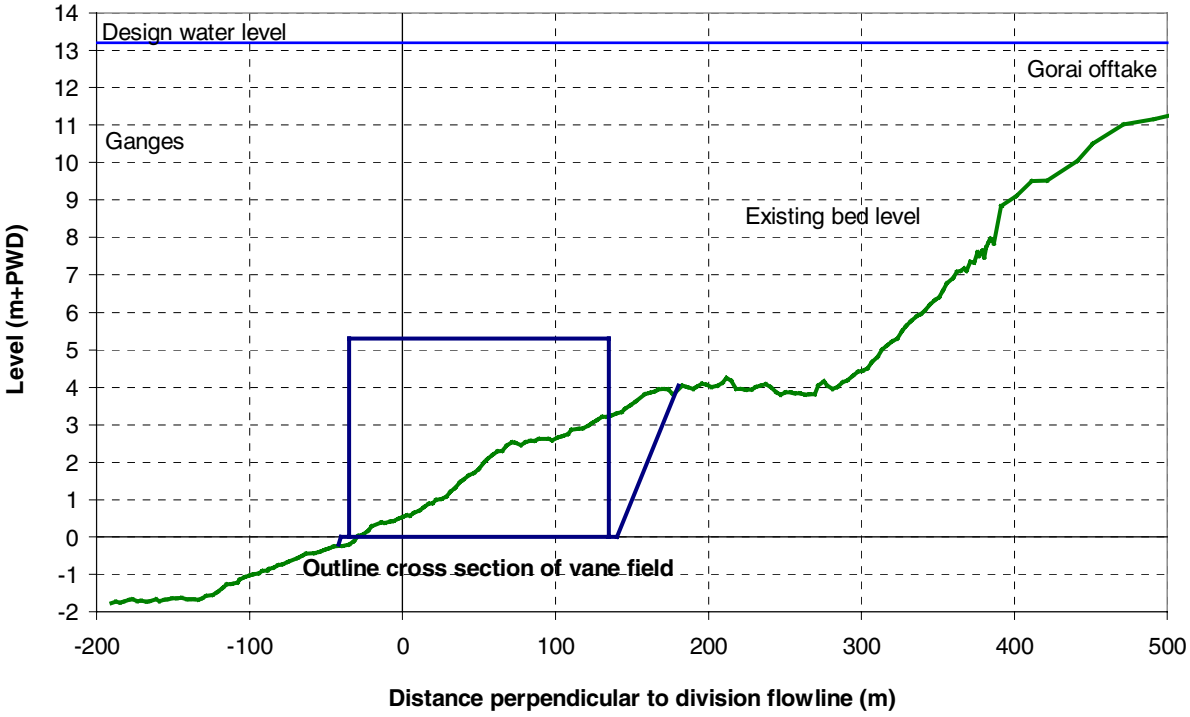

Figure 2.1: Typical cross section 1200 m downstream of Talbaria (cross section indicated in **Figure 3.1**)

3. OVERVIEW OF MODELLING APPROACH

3.1 Objectives of study

The present model study was initiated to substantiate the design of bottom vanes in the Gorai offtake. The following main objectives were adopted for the present study:

1. To assess the effect of vanes on the sediment distribution over both branches, Ganges and Gorai;
2. To assess the influence of the upstream orientation of the main channel on the efficiency of the vanes in preventing sediment from entering the offtake;
3. To assess the local morphological impact of the vanes at the offtake, including the risk of erosion or the vanes being buried.

For this purpose use is made of the Delft3D morphological model, developed by WL | Delft Hydraulics, including a special bottom vanes module. Using this numerical model the Gorai offtake area is modelled and the effect of the bottom vanes assessed.

3.2 Outline of model

In the present study a conceptual approach is proposed in which the emphasis will be on the conceptual functioning of the vanes in the offtake and the sensitivities in this respect, and not so much on a detailed modelling of the (variable) present-day situation at the Gorai offtake.

This approach is also preferred given the inherent uncertainties in sediment transport modelling, the flow pattern in the offtake in a future situation with river training structures and possibly a changing orientation of the upstream flow. Also there is a lack of measured data on the sediment distribution over the offtake. Thus, it is considered more useful to get a feeling for the consequences of these uncertainties, rather than to try and achieve a detailed description of the particular present-day situation.
Nonetheless, the pre-monsoon 2000 bed topography is proposed as a starting point. The model should describe a situation in line with the actual distribution of discharge and sediment (whatever limited data is available), and the large scale morphology at the offtake.

The model will be focused on the effect in the offtake itself. Possible large scale morphological effects on the river system of both Gorai and Ganges are not part of the present study.

3.3 Hydraulic And Morphological Aspects

3.3.1 Discharge and sediment transport regime

Discharges in the Ganges and Gorai rivers vary greatly over the year. Using a frequency distribution of discharge and overall sediment rating curve it is found that the discharge below which 50% of the yearly sediment transport ($S_{50\%}$) occurs) is estimated at 41,000 m^3/s. Given the objectives of the present study it is proposed to use this fixed “dominant” discharge that is considered bed forming in the model.
Based on this discharge the influence of the vanes on sediment transport en morphology will be assessed.

As the Ganges/Gorai river bed is mobile it is an important question to what the degree the dominant discharge can be considered a bed-forming discharge. However, following the conceptual approach of the present study, the effect of vanes at the dominant discharge is assumed to provide a good indication of their overall performance.

3.3.2 Offtake Layout

The offtake guide bund and flow divider have significant influence on the flow pattern in the offtake area. In the Feasibility Report the bottom vanes are proposed as a possible future enhancement of the Gorai River Restoration works in case more sediment needs to be excluded from the Gorai in the future. Moreover, the offtake guide bund and flow divider would be essential to the functioning of submerged vanes, as these control and stabilise the flow pattern in the offtake area.
Therefore, in the present study these structures are assumed to be present and the resulting flow pattern is used as an initial condition for determining the effectiveness of the vanes.

3.3.3 Sediment transport

Sediment transport in the Ganges tends to be in suspension predominantly (>90%). Rouse number is estimated to vary over the range of u^*/w_s = 2.5 to 6.0 . Two components of the sediment transport will be modelled: suspended sediment load and bed load.
For this purpose the Van Rijn formula is used, which describes both types of sediment transport explicitely. Furthermore, this sediment transport relation was found to give results in line with sediment transport measurements in Bangladeshi Rivers during the FAP24 study.

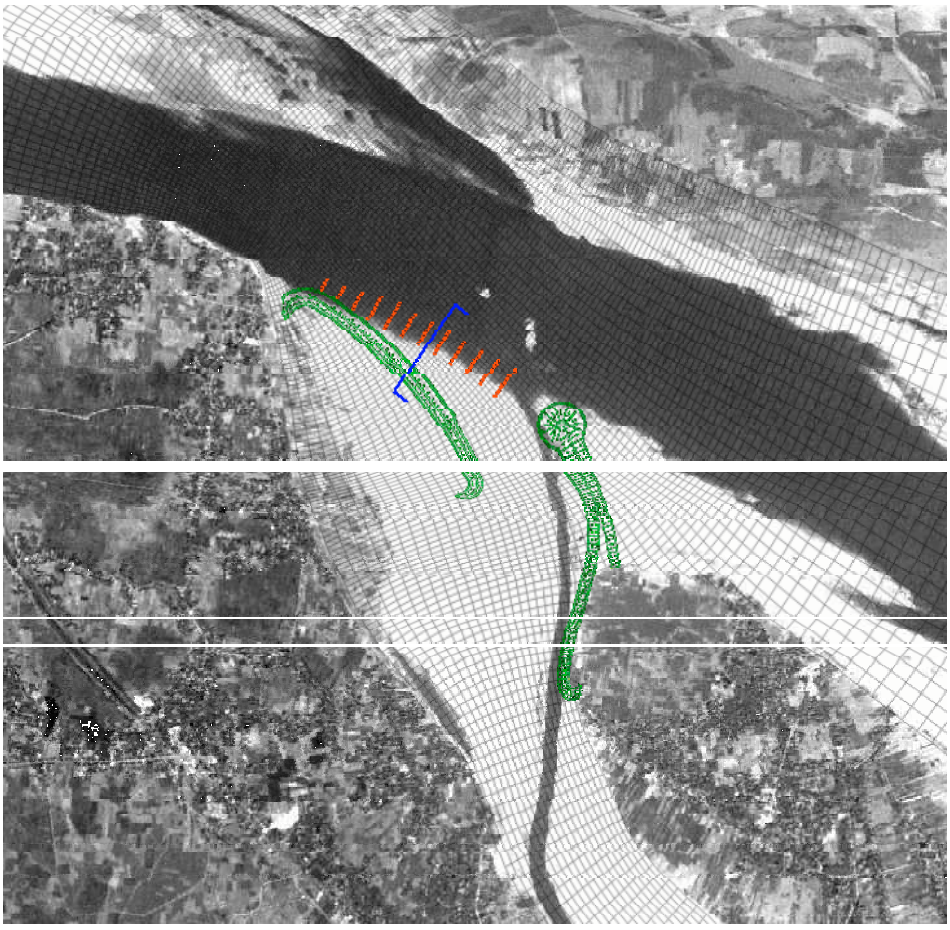

Figure 3.1 Layout of offtake with flow divider and guide bund (in green), field of bottom vanes (in red), cross section from Figure 2.1 (in blue) (Delft3D grid in background)

3.3.4 Upstream flow orientation

For calibrating the model the monsoon 2000 situation is used. It is proposed to assess the effect of the vanes as a function of the orientation of the upstream main channel. For this purpose a more northerly orientation of the main upstream channel will be tested. In the initial bed topography the main channel cross section will be shifted in line with the plan form of the main channel in the Ganges observed in satellite images from previous years:

- 1997 - 2000: main channel along outer bend of Ganges, approaching Talbaria from an easterly direction (Case A);
- 1985 - 1987: main channel approaching Talbaria from north-easterly direction (Case B);
- 1973 - 1980: main channel approaching Talbaria from north-north-easterly (Case C).

These planforms are illustrated in Figure 4.1 in the following chapter.

River bed morphology
For calibrating the model it is proposed to use the surveyed bed topography from the pre-monsoon 2000 situation. The large scale bed topography in the offtake area has been somewhat stable over the years 1997-2000. Based on this fact the assumption is made that there is an equilibrium bed topography in the Ganges at the dominant discharge, which is in line with this observed bed topography.

3.3.5 Roughness modelling

In FAP24 it is concluded that very low roughnesses occur in Bangladesh rivers, an average value of C=80 $m^{1/2}/s$ has been mentioned for the Ganges. In the present conceptual model a simple constant value for C is proposed over the modelled area. In reality distinct differences in bed roughness should be expected between deep an shallow areas, or Ganges versus Gorai.
During the initial hydraulic calibration phase the roughness modelling will be adjusted so that a flow pattern results in line with measurements.

3.4 Setup Numerical Model

3.4.1 Modelled area

A limited extend of the model area is proposed, adequate to represent the morphological situation at the offtake. The adaptation lengths for flow and suspended sediment transport are of importance in this respect. For the main channel these values are of the order of 500 to 4000 m.
Thus, an upstream model boundary is proposed 4000 m upstream from the offtake. Downstream boundary in the Ganges is proposed at a similar distance downstream from the flow divider. At this point a mostly undisturbed flow pattern is expected. In the Gorai a boundary is proposed at km 5.3 near Khustia were water levels are measured.
The wide shallow area in the Ganges inner bend across from the offtake is included in the model to a limited extend only. Based on previous model results from SWMC it was estimated that 95% of the Ganges discharge flows through the modelled area.

3.4.2 Grid

Grid dimensions are determined by the submerged vanes. The grid is to have a maximum density in the offtake area (over the vane field in particular). On the other hand a wide area surrounding the vanes is to be included in the model to reduce the influence of boundary conditions.
Given the practical limits of computational power a grid with dimensions 55 by 165 is proposed with a minimum cell size of approximately 30 m by 30 m in the area surrounding the vanes. Maximum cell dimensions are roughly 100m by 130 m. The modelled area and the grid is indicated on the Figure 3.1

3.4.3 Boundary conditions

Upstream boundary conditions will be based on discharge distribution over the cross section measured in ADCP measurements and on large scale discharge pattern observed in the Mike21 model.
Downstream water level boundaries will be based on measurements at Khustia, water levels occurring in the Mike21C model and on the discharge distribution over both branches.

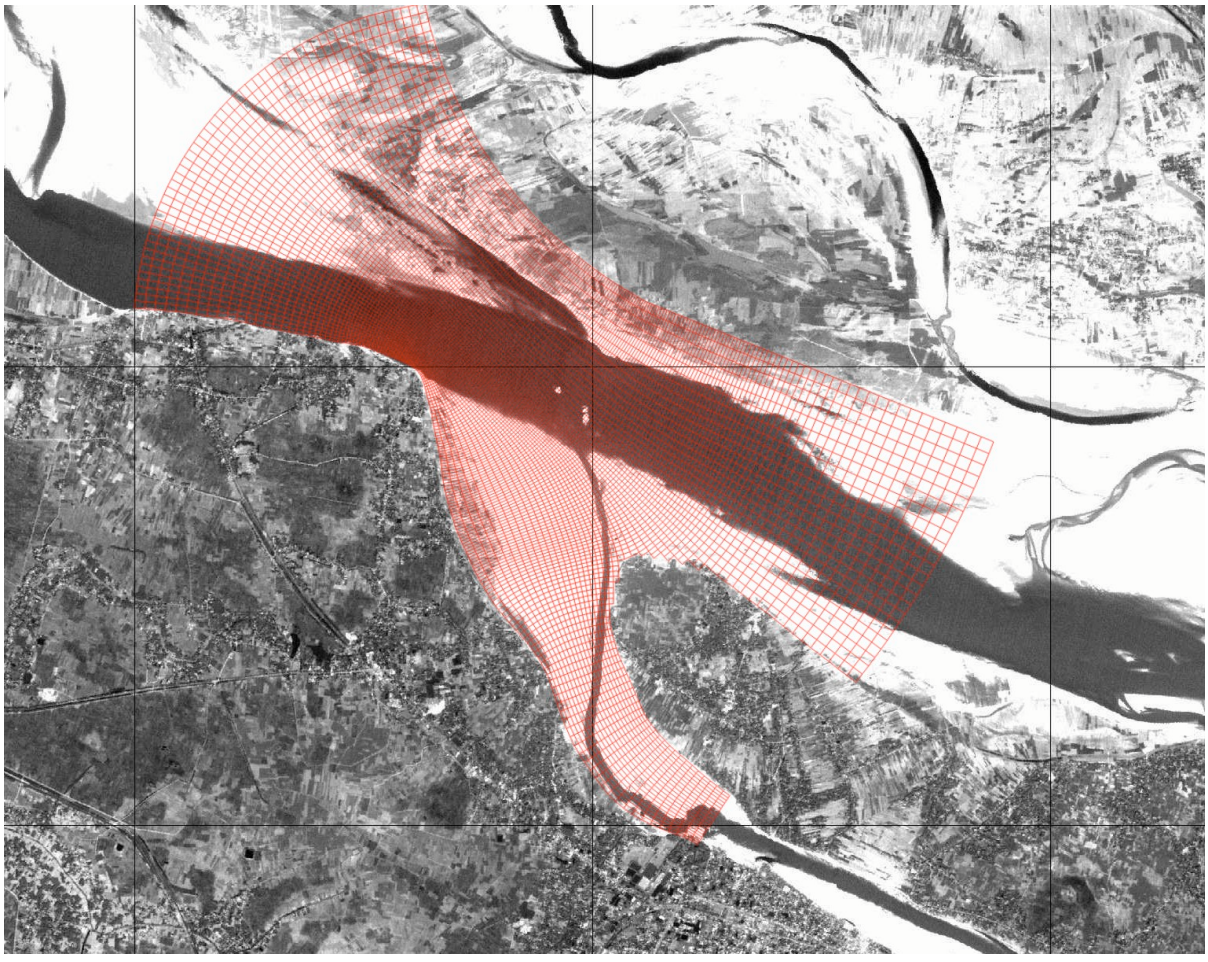

Figure 3.1 Modelled area and grid for Delft3D model (scale: black grid = 5 km)

4. MODEL CALIBRATION

4.1 Procedure Model Calibration And Runs

Initially, model calibration was carried out in 2 phases for the planform of October 2000 (Case A), with an upstream channel in the Ganges approaching from an easterly direction along the right bank at Talbaria:

- For the initial **hydraulic calibration** a fixed bed level is used (based on October 2000), while the roughness, upstream discharge distribution and downstream water levels can be varied. The objective is to have the model represent a flow pattern at the offtake in line with the actual 2000 situation at the dominant discharge 41,000 m^3/s;
- For the **morphological calibration** the objective is to have an equilibrium bed level in the Ganges in line with the actual situation, based on the dominant discharge: parameters to be varied are distribution of sediment transport over the upstream model boundary, calibration factor for the sediment transport formula.

The resulting equilibrium bed level for the Ganges for the existing situation will be used as the **Base Case A**.
After this calibration the flow divider, Ganges-Gorai revetment and new Kushtia groynes will be introduced in the model. The equilibrium bed level in the Ganges resulting from this situation will be considered the **reference situation with structures for Case A**.

Subsequently, this procedure was repeated for a North-Easterly (Case B) and a North-North-Easterly (Case C) orientation of the main channel upstream in the Ganges.

Next, the runs for the various cases are based on an initial situation with an equilibrium planform in the Ganges (from the morphological calibration runs) and a newly dredged channel in the Gorai. From this initial situation a time span of 4 months covering one monsoon season is simulated: starting 1 July to 1 November.

4.2 Hydraulic Calibration

4.2.1 Data Used For Hydraulic Calibration

For the hydraulic calibration the water level and discharge data from SWMC for Gorai and Ganges was studied for the monsoon 2000. Stations at Hardinge Bridge, Talbaria, Shelaidah, Kushtia and Gorai Railway Bridge were used.
Based on this data relations were estimated by interpolation for various water levels, water level slopes and the discharge distribution between both branches. Additionally, based on the scatter in this data, a range of uncertainty was defined. A summary of the resulting data is presented in the Table 4.1.

Firstly, the water level for Talbaria at the discharge of 41,000 m^3/s was used as a central value. All other water levels were derived from the water level at Talbaria to ensure consistent water level slopes.
As indicated earlier (paragraph 3.4.1) it is estimated that 95% of the total Ganges discharge flows through the modelled area: 38,950 m^3/s.

Secondly, the discharge distribution over the offtake was used as a calibration criterion. Note, that the changing bathymetry of the offtake area over the course of the monsoon (in particular due to siltation of the initial deep dredged channel), there is quite some additional uncertainty in this discharge distribution. To account for this effect, the high estimate for the Gorai discharge 3,835 m^3/s (Table 4.1) will be used in the initial situation with a deep dredged channel present.

As a third and dominant calibration criterion the objective was to recreate a Base Case with a flow pattern that is in line with the actual situation. For this purpose the flow field (velocity magnitudes and velocity direction) surrounding the offtake will be compared from 2 ADCP velocity profile measurements that are available for the offtake:

- 17 to 21 August 1999 at an estimated discharge of 41,000 m^3/s;
- 8 and 9 September 1999 at an estimated discharge of 47,500 m^3/s.

It is noted that the discharge distribution over the upstream model boundary is an uncertain factor. These are closely related to the (variable) bed levels at this boundary. Use was made of model results from SWMC at a fixed discharge. However, this provided a first indication only, as became clear from the morphological calibration later.

	low estimate	**average**	**high** estimate
Discharges (m^3/s)			
Ganges upstream discharge		41,000	
Gorai discharge	3,435	3,635	3,835
Water level slopes (-)			
Water level slope Hardinge Bridge - Talbaria	3.6E-05	8.5E-05	9.4E-05
Water level slope Talbaria - Shelaidah	3.6E-05	3.9E-05	9.4E-05
Water level slope Talbaria - Kushtia	6.5E-05	7.2E-05	7.9E-05
Water level difference (m)			
Water level diff. upstream boundary - Talbaria	0.20	0.30	0.33
Water level diff. Talbaria - downstr. bound. Ganges	0.22	0.23	0.41
Water level diff. Talbaria - downstr. bound. Gorai	0.44	0.49	0.54
Water level (m+PWD)			
Talbaria water level	12.5	12.62	12.7
Water level upstream model boundary Ganges	12.82	12.92	13.05
Water level downstream model boundary Ganges	12.21	12.39	12.40
Water level downstream model boundary Gorai	12.08	12.13	12.18

Table 4.1: Summary of hydraulic data for Ganges discharge 41,000 m^3/s

4.2.2 Bathymetry Used For Hydraulic Calibration

For the initial hydraulic calibration the October 2000 bathymetry was used for the Ganges river. This bathymetry is expected to be in line with representative nominal flow conditions that occurred over the monsoon 2000. However, to study the siltation of the Gorai, this was combined with the June 2000 bathymetry for the Gorai and the offtake, which includes the dredged channel.
Secondly, given the uncertainties in the discharge distribution over the upstream model boundary, the inner bend of the Ganges was smoothed, as well as the shallow part of the offtake. The resulting bathymetry is presented in Figure 4.1.

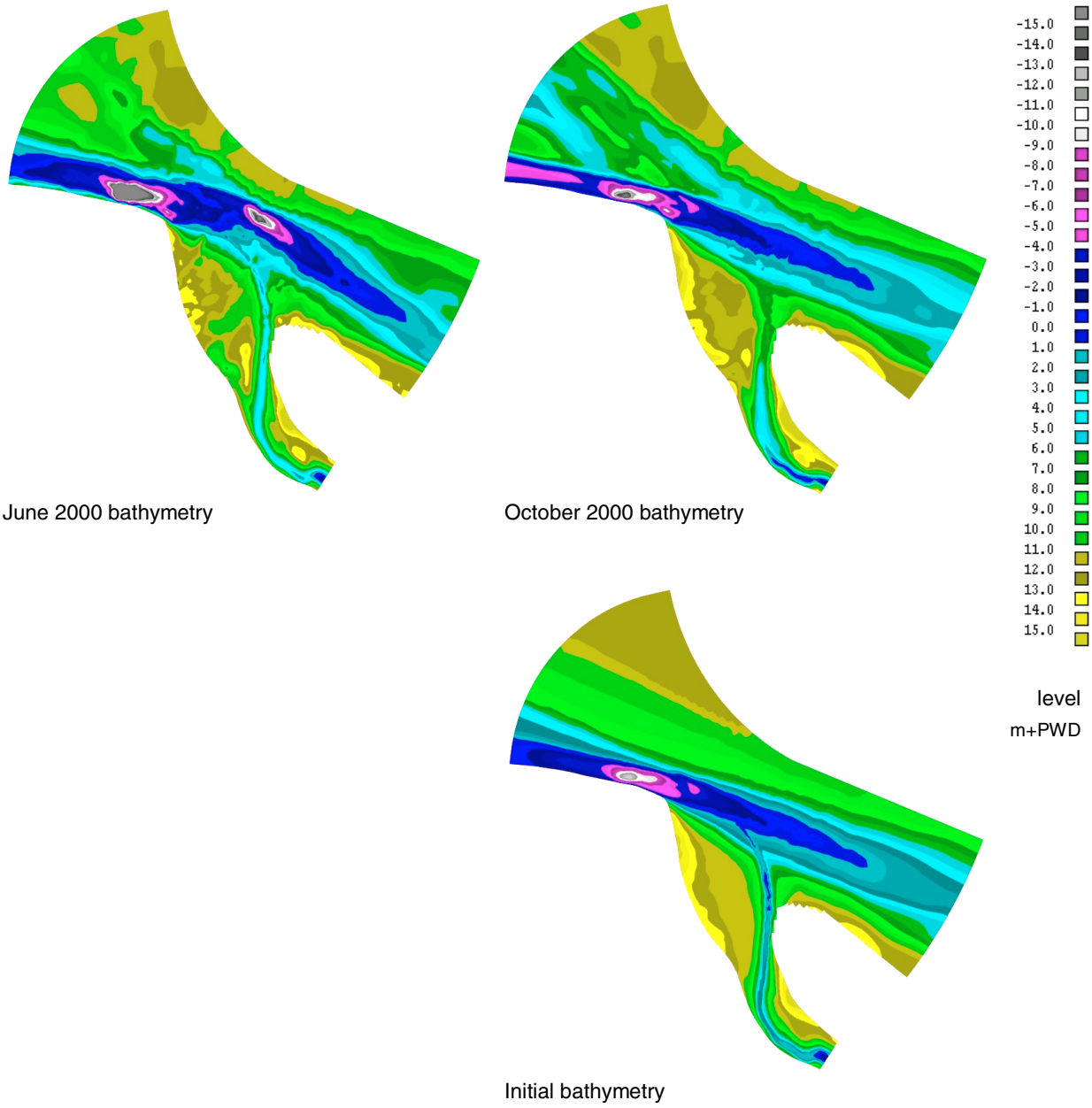

Figure 4.1 Initial model bathymetry versus monsoon 2000 bathymetry

4.2.3 Hydraulic Calibration Results for Ganges Channel Case A

In the hydraulic calibration process it was noted that the water level slopes were sensitive the discharge distribution over the upstream model boundary. As little information was available in this respect, this resulted in some additional uncertainty in the water level slopes in the model versus the prototype.
Additionally, the range in the water level slopes indicated in Table 4.1 was tested. Based on these inaccuracies/uncertainties in the data a margin of error results in the bed roughness. Thus, assuming a constant Chezy roughness, a value for C in the range of 80 to 100 $m^{0.5}/s$ can be justified, with C = 90 $m^{0.5}/s$ as a best estimate.

Secondly, the discharge distribution over both river branches was calibrated by adjusting the downstream water level boundary at Kushtia. It proved to be necessary to raise this water level by as much as 0.15 m above the best estimate based on measurements. This is presumed to be the result of the very high global Chezy roughness coefficient (based on Ganges water level slopes), which could underestimate the roughness over the shallower Gorai. However, given the conceptual approach of the present study this was accepted.

For the next steps, the morphological calibration and the cases, a morphological equilibrium situation for the Ganges is used. However, this modelled river bed will differ to some degree from the measured bed level in October 2000. This results in (minor) differences in the flow field and the water levels.
This was compensated by an updated hydraulic calibration of the model, after a morphological equilibrium situation in the Ganges was achieved for the Base Case. In this case, the downstream water level boundary in the Ganges and Gorai were adjusted only, to optimise the water level at Talbaria and the discharge distribution over both rivers.

The results from the hydraulic calibration for the Base Case A with a upstream flow along the right bank of the Ganges are presented in the following Table 4.1.

Discharges (m^3/s)	
Ganges nominal discharge	41,000
Ganges discharge in model (95%)	38,950
Initial Gorai discharge in model	3,886
Water level (m+PWD)	
Talbaria water level	12.59
Water level upstream model boundary Ganges	12.92
Water level downstream model boundary Ganges	12.29
Water level downstream model boundary Gorai	12.18
Various coefficients	
Chezy roughness ($m^{1/2}/s$)	90
Hydrodynamic viscosity (m^2/s)	10
Hydrodynamic diffusivity (m^2/s)	10
Drying criterion water depth (m)	0.6

Table 4.1: Summary of results hydraulic calibration for Base Case A

The flow field for the end monsoon 2000 situation for the Base Case can be compared with the ADCP measurements mentioned in paragraph 4.3.1 from the offtake area: Figure 4.1 and Figure 4.2.

From these figures the following conclusions are drawn:

- the general flow pattern compares reasonably well with the ADCP measurements;
- as a result of the dredged channel through the offtake area velocities are too high in this region, while flow velocities outside of the main channel of the Gorai are slightly too low, possibly as a result of the constant roughness value used;
- in the offtake a circulating flow pattern develops in the model, which is not observed in the measurements. This leads to low flow in a part of the offtake that will result in exaggerated siltation. This flow pattern is an indication for the importance of the flow momentum factor in the 2D flow, relative to the small bed friction factor;
- flow velocities in the Ganges immediately North of the offtake proper compare well with the measurements.

Given the conceptual approach of the present study, this hydraulic calibration is considered adequate. The morphology in the Gorai offtake will be addressed in the following paragraphs.

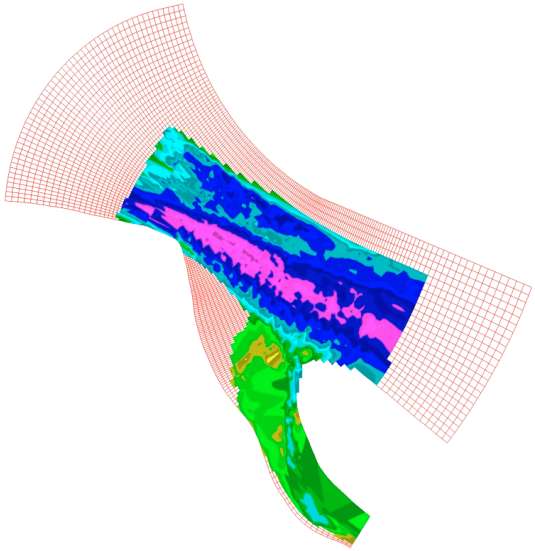

ADCP velocities measured 17 to 21 August 1999 discharge 41,000 m^3/s

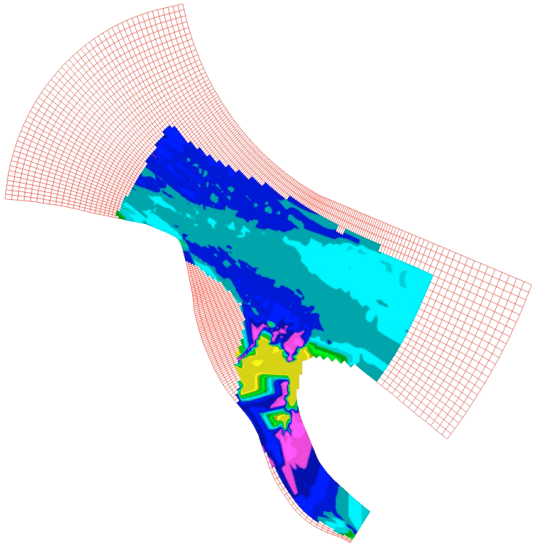

ADCP flow direction measured 17 to 21 August 1999 discharge 41,000 m^3/s

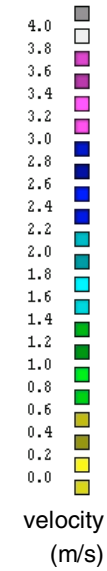

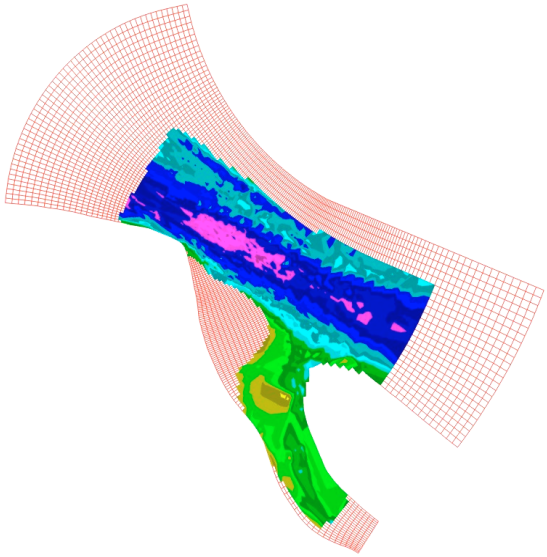

ADCP velocities measured 8 and 9 September 1999 discharge 47,500 m3/s

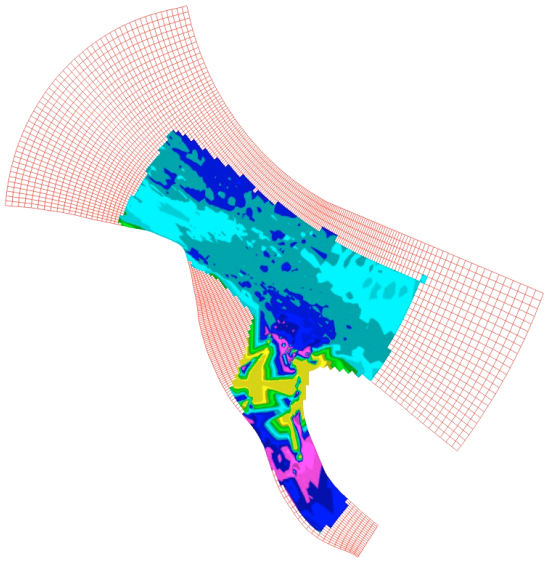

ADCP flow direction measured 8 and 9 September 1999 discharge 47,500 m3/s

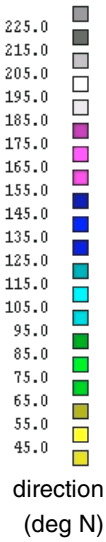

Figure 4.1 Flow velocities and directions in offtake area from ADCP measurements, for a situation in 1999, in line with Case A

Model velocities for Base Case A

Model flow direction for Base Case A

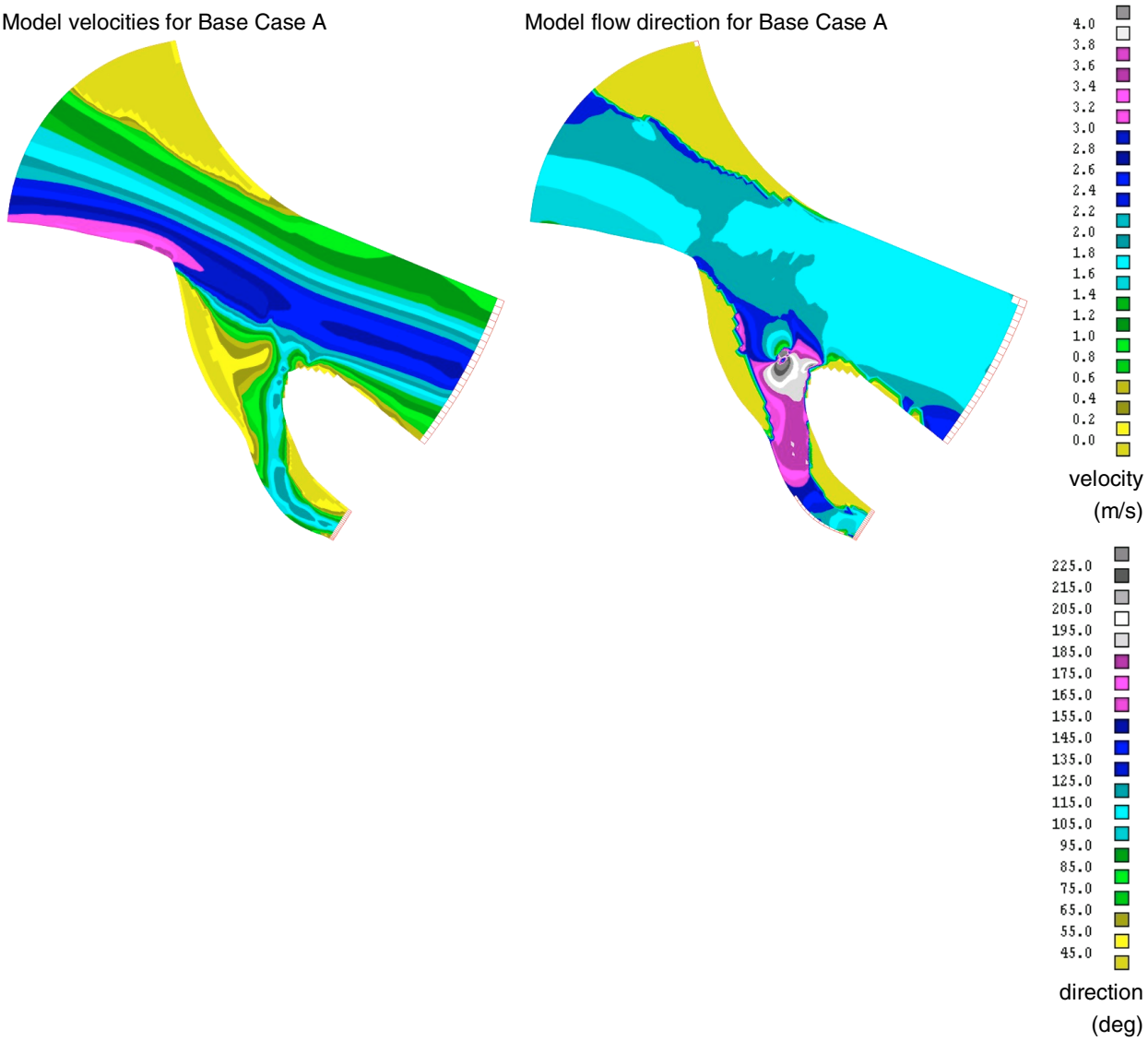

Figure 4.2 Flow velocities and directions in offtake area from end monsoon 2000 situation for Base Case A

4.2.4 Hydraulic Calibration Results for Ganges Channel Case B and C

Based on the Hydraulic Calibration for Case A with the upstream Ganges main channel along its right bank, the hydraulic calibration was carried out for the situation with the main channel oriented further to the Ganges left bank (Case B and Case C respectively).
The central criteria in this hydraulic calibration were:

- flow velocity distribution over the upstream model boundary comparable to Case A (specifically, the flow velocity relative to the water depth);
- a water level at Talbaria identical to Case A and an unchanged water level for the downstream model boundary for the Gorai, resulting in an identical water level gradient over the Gorai offtake.

Given the fact that no measured velocity data is available for this situation it is difficult to check the resulting flow pattern. However, in comparing the resulting flow patterns in Figure 4.1 for Case B and C versus Case A, it is felt that a realistic flow pattern was modelled for these situations.
Resulting values for the calibration are presented in Table 4.1 and Table 4.2. Note, that in these Tables values are presented for the initial bathymetry for the morphological runs, which can differ slightly from the values in the actual hydraulic calibration, where the bed at the end of the morphological calibration was used, including a Gorai offtake that included some siltation.

Discharges (m^3/s)	
Ganges nominal discharge	41,000
Ganges discharge in model (95%)	38,950
Initial Gorai discharge in model	3,993
Water level (m+PWD)	
Talbaria water level	12.67
Water level upstream model boundary Ganges	12.98
Water level downstream model boundary Ganges	12.29
Water level downstream model boundary Gorai	12.18

Table 4.1: Summary of results hydraulic calibration for Base Case for Case B

Discharges (m^3/s)	
Ganges nominal discharge	41,000
Ganges discharge in model (95%)	38,950
Initial Gorai discharge in model	3,862
Water level (m+PWD)	
Talbaria water level	12.70
Water level upstream model boundary Ganges	12.95
Water level downstream model boundary Ganges	12.05
Water level downstream model boundary Gorai	12.18

Table 4.2: Summary of results hydraulic calibration for Base Case for Case C

Model velocities for Base Case A

Model flow direction for Base Case A

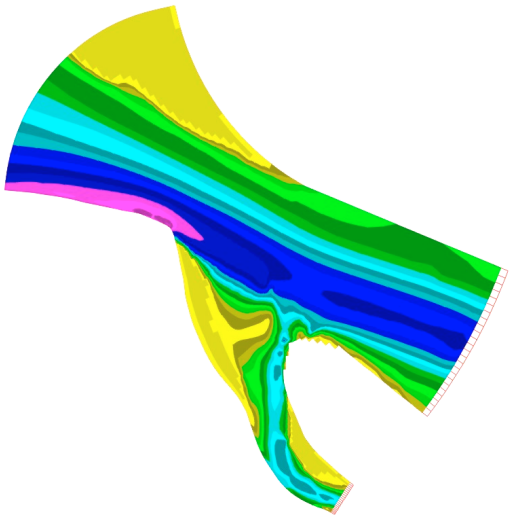

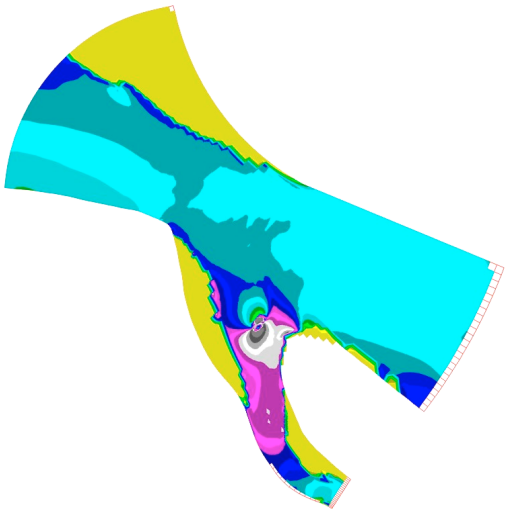

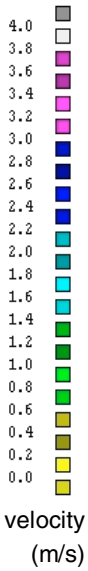

Model velocities for Base Case B

Model flow direction for Base Case B

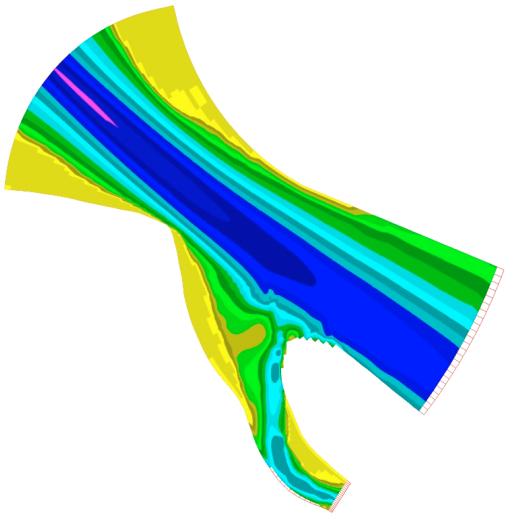

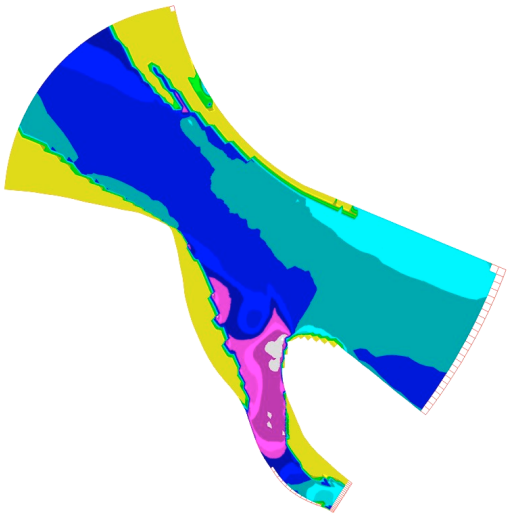

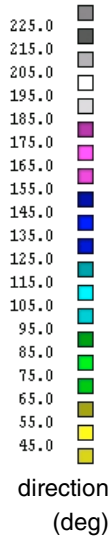

Model velocities for Base Case C

Model flow direction for Base Case C

)

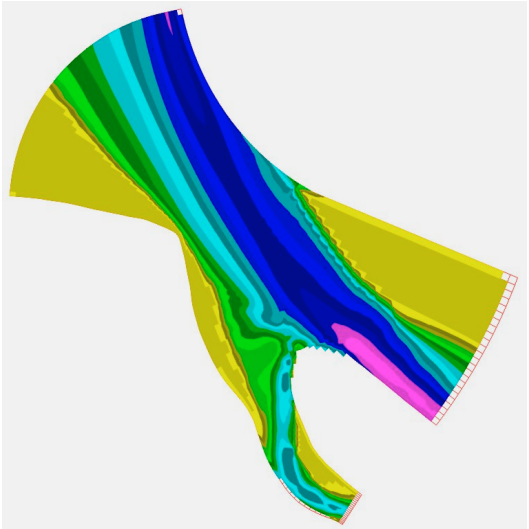

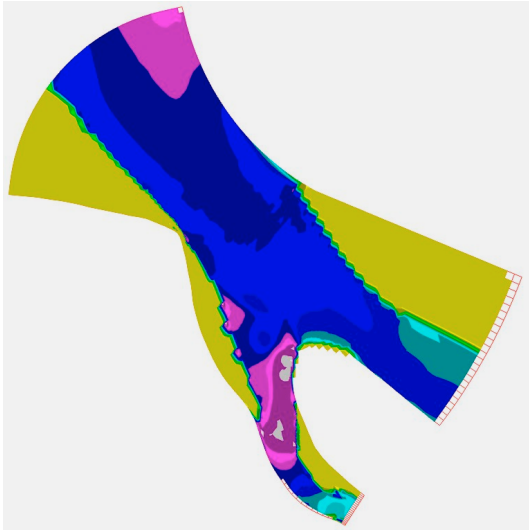

Figure 4.1 Flow velocities and directions in offtake area from end monsoon 2000 situation for the Cases A, B and C

4.3 Morphological Calibration

4.3.1 Data Used for Morphological Calibration

Average sediment transport in the rivers at the Ganges discharge were based on Annex Morphological Studies of this Feasibility Report. Based on the range of values from various existing sediment transport relations for Ganges and Gorai Rivers Table 4.1 was composed. Grain sizes were used from sediment samples, described in Annex C in the Feasibility Report. From this data with significant scatter the summary of sediment characteristics was composed in Table 4.2. Based on this Table and the morphological calibration process a grain size of 190 μm was used in the model for the Ganges and a grainsize of 160 μm for the Gorai and the offtake, indicated in Figure 4.1.

	low estimate	**average**	**high** estimate
Sediment Transport (kg/s)			
Ganges	1.2E+4	2.3E+4	3.5E+4
Gorai (at 3,635 m^3/s discharge)	1.2E+3	2.4E+3	3.7E+4

Table 4.1: Summary of sediment transport data for Ganges discharge 41,000 m^3/s

	D10 mm	**D16** mm	**D35** mm	**D50** mm	**D65** mm	**D84** mm	**D90** mm
Ganges	0.10	0.11	0.15	0.19	0.23	0.28	0.36
Gorai Offtake	0.10	0.11	0.14	0.16	0.19	0.26	0.29
Upper Gorai	0.10	0.11	0.14	0.16	0.19	0.25	0.28

Table 4.2: Summary of sediment samples

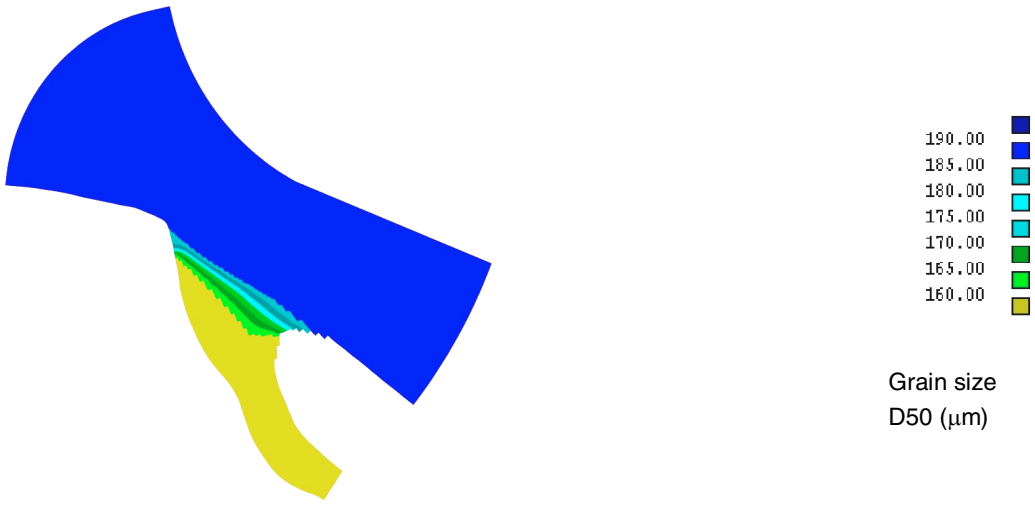

Figure 4.1 Grain size 190 μm (Ganges) to 160 μm (Gorai) applied in model grid

4.3.2 Morphological Calibration Results for Case A

Crucial in the morphological calibration process was the resulting planform in the Ganges and the Gorai offtake. As indicated before the October 2000 bathymetry was used as a reference.
Reproducing the observed bathymetry required precise fine-tuning. In particular, the planform proved to be sensitive to the following parameters:

- discharge distribution over the upstream model boundary;
- bed levels along the upstream model boundary;
- grain size in Ganges;
- grain size in offtake and Gorai, relative to grain size in Ganges;
- dispersion coefficient for suspended sediment transport.

Based on the elaborate calibration the following observations were made:

1. The discharge distribution over the upstream model boundary strongly determines the flow contraction at Talbaria and thus the depth and the streamwise extend of the scour hole at this point. For this critical parameter very little data was available.
2. Flow velocities occurring on the upstream model boundary directly influence the amount of sediment entering the model and thus the scour pattern surrounding the offtake. Flow velocity, and discharge distribution used over the upstream boundary is indicated in Figure 4.1.
3. Siltation in the Gorai offtake is exaggerated consistently. Using a uniform sediment grain size over the Ganges and the Gorai offtake results in even higher rates and morphological development at the offtake. Thus the use of a varying grain size in line with sediment samples found in the prototype is essential.
4. Siltation in the shallow parts along the right bank of the Gorai offtake is exaggerated consistently.

4.3.3 Results For Sediment Transport Relation

Van Rijn formula gives sediment transport rates in line with the estimated values based on observations, provided that the height at which the sediment concentration near the bed is evaluated for the suspended transport profile is set at a level of a few mm (here 4 mm was used). This appears to be larger than expected based on the D_{90} and the very low bed roughness.

Furthermore, it is important to realise that the Van Rijn sediment relation is used here in a situation with an extremely smooth river bed (extremely high Chezy value). However, the relation was developed for situations with more common (much higher) bed shear stresses, relative to the flow velocity. As this roughness is related to the roughness height and the shear stress on the grains, it is conceiveable that in this case the value for n in $s \sim u^n$ is not adequately represented by the Van Rijn relation over the entire range of water depths (0 to 30 m) and flow velocities (0 to 3.5 m/s)
This is a possible explanation for the exaggerated siltation in the shallow areas of the Gorai offtake in the model.

Sediment transport (kg/s) for Case A	
Ganges sediment transport in model	2.1E+4
Gorai sediment transport chainage 1 km	1.2E+3
Various coefficients Van Rijn formula	
Multiplication factor α (-)	1.00
D_{90} (μm)	360
Height for evaluation near bed sediment concentration (m)	0.004
Fall velocity for Ganges D_{50} = 190 μm (m/s)	0.024
Fall velocity for Gorai D_{50} = 160 μm (m/s)	0.018
Other coefficients	
Upstream suspended sediment concentration	equilibrium
Dispersion in suspended transport (m^2/s)	10

Table 4.1: Summary of results morphological calibration for initial situation Base Case A

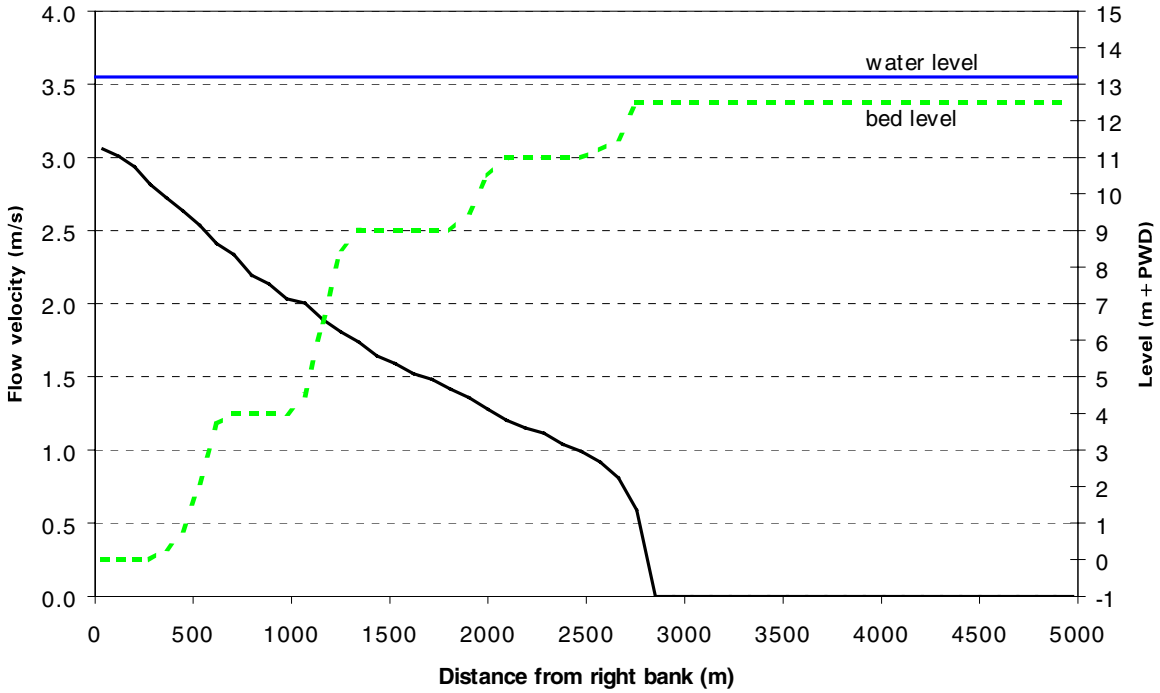

Figure 4.1 Inflow velocity distribution over upstream model boundary resulting from morphological calibration of the Base Case A

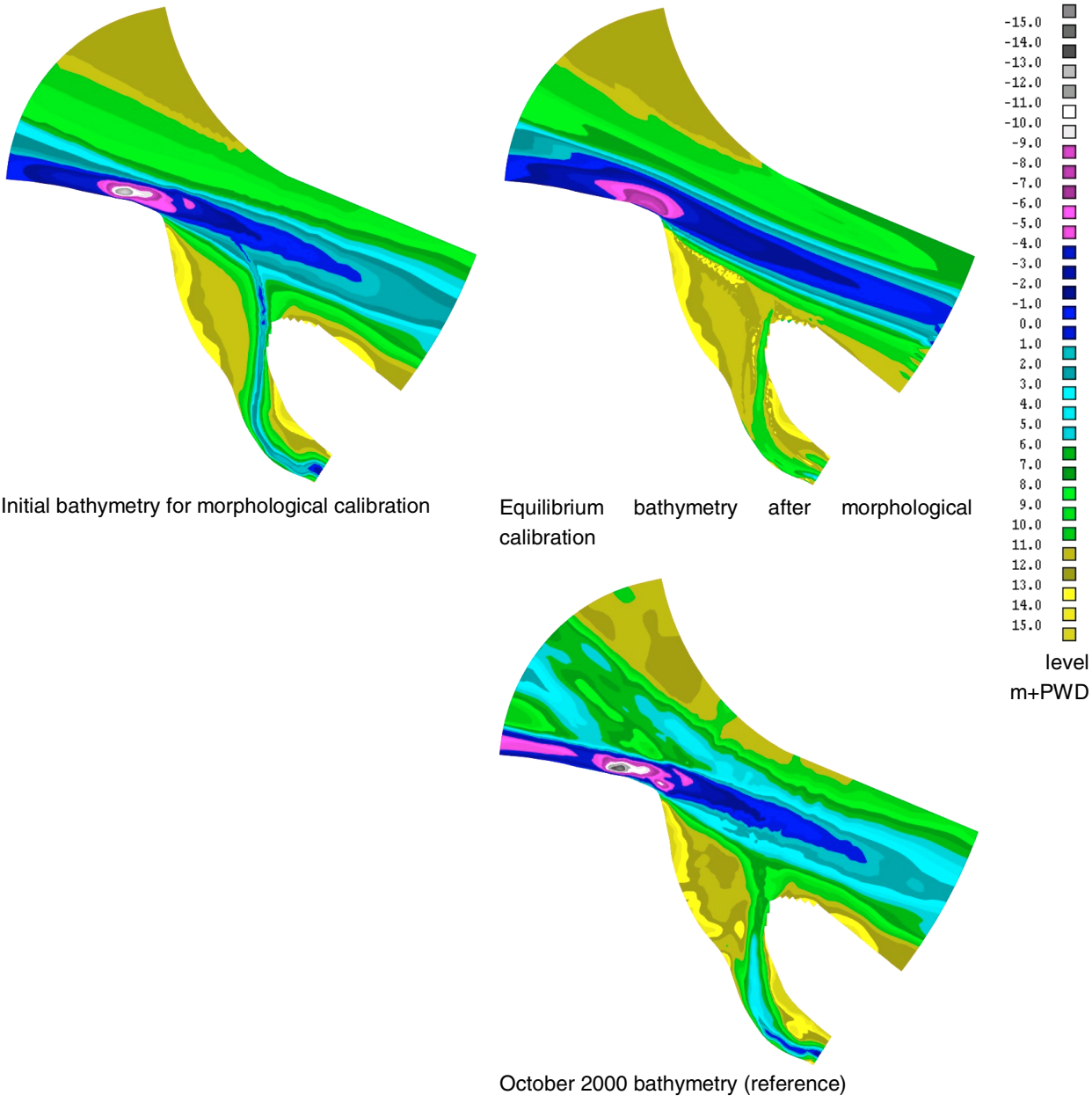

Initial bathymetry for morphological calibration

Equilibrium bathymetry after morphological calibration

October 2000 bathymetry (reference)

Figure 4.2 Equilibrium bathymetry after morphological calibration versus initial model bathymetry for Case A

4.3.4 Morphological Calibration Results for Ganges Main Channel Case B and C

After the morphological calibration for Base Case A the situations with other planforms in the Ganges would be used, as described in paragraph 3.3.4:

- Base Case A: 1997 - 2000: main channel along outer bend of Ganges, approaching Talbaria from an easterly direction;
- Case B: 1985 - 1989: main channel approaching Talbaria from north-easterly direction;
- Case C: 1973 - 1980: main channel approaching Talbaria from north-north-easterly.

The upstream model boundary was modified according to this planform and the initial bed level modelled accordingly. The inflow velocities were adjusted so that these were in line with the morphological calibration situation. The resulting velocity distribution and bed level along the upstream model boundary is plotted in Appendix D.
Subsequently, the morphological calibration was carried out for the situation with the upstream Ganges main channel further to the north. As no bathymetry data was available this procedure was restricted to minor adjustments of the velocity distribution and bed level along the upstream model boundary. Other parameters were kept constant and identical to the values resulting from the morphological calibration for Case A.

Resulting bed levels were compared to the bed levels observed in Case A and satellite images capturing the layout of the Ganges under these kind of circumstances in previous years. Resulting bed levels are plotted in Figure 4.1. These are considered reasonable approximations of the situation that have occurred in reality.

Resulting sediment transport rates are presented in Table 4.1. All values are well within the range of values that is expected, based on the data presented in Table 4.1. It is noted that Gorai sediment transport is somewhat low. Thus, an exaggerated siltation is expected in the model in the Gorai offtake.

Sediment transport (kg/s) for Case A	
Ganges sediment transport in model	2.1E+4
Gorai sediment transport chainage 1 km	1.2E+3
Sediment transport (kg/s) for Case B	
Ganges sediment transport in model	1.9E+4
Gorai sediment transport chainage 1 km	1.8E+3
Sediment transport (kg/s) for Case C	
Ganges sediment transport in model	2.0E+4
Gorai sediment transport chainage 1 km	1.9E+3

Table 4.1: Summary of results morphological calibration for initial situation Cases B and C.

4.3.5 Resulting Bed Topography From Morphological Calibration

Subsequently, for each of these cases the model was run until an equilibrium bed had developed in the Ganges, which required approximately 360 days of real time, corresponding to 3 monsoon seasons. This “equilibrium” bed for the Ganges was combined with the June 2000 bed for the Gorai and the offtake area, including a newly dredged channel.
The resulting “equilibrium” beds are plotted in Figure 4.1, with observed planforms of the offtake area as reference. Note, that the resulting bed level in the Ganges is but an approximation of an equilibrium situation, as the discharge of water and sediment through the Gorai will have an input on the Ganges planform. However, as the Gorai is small relative to the Ganges, this is a reasonable approximation. Importantly, it ensures that no significant morphological developments will occur upstream of the offtake, resulting in an initial access load of sediment entering the Gorai offtake.

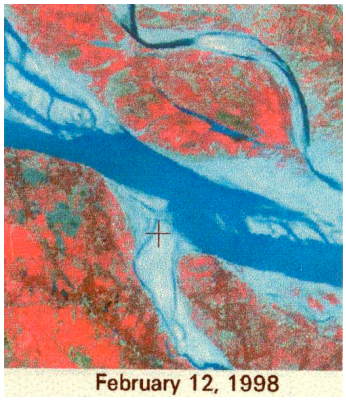

versus Base Case A

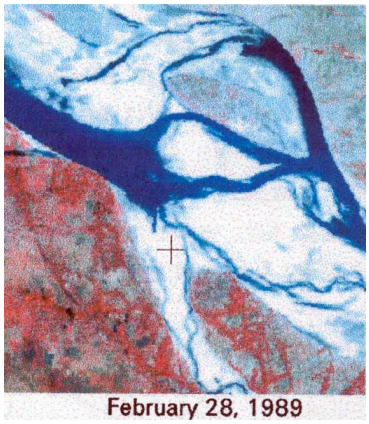

versus Case B

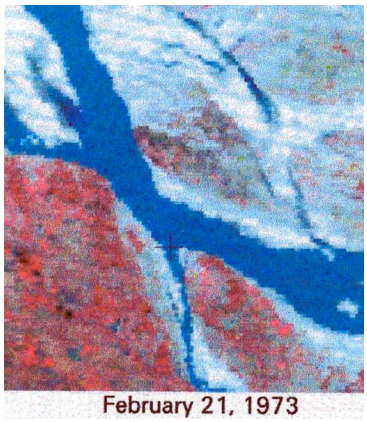

versus Case C

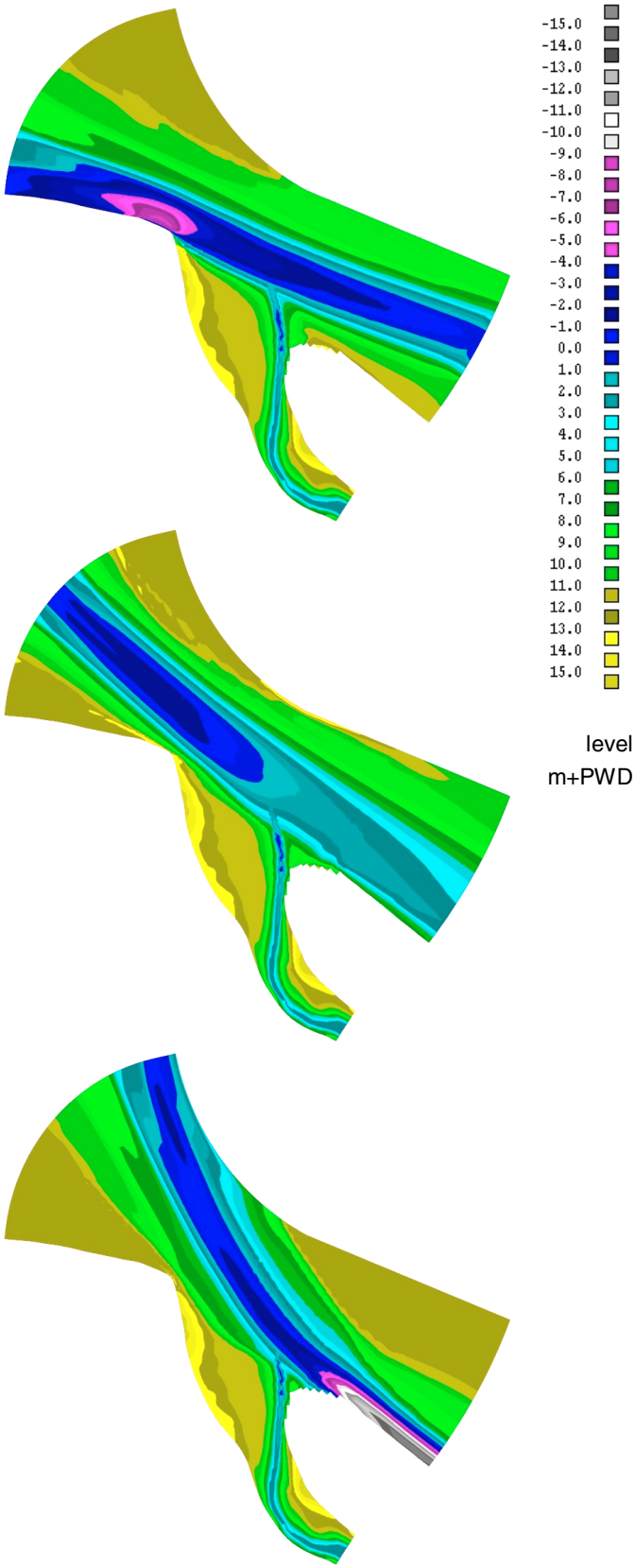

Figure 4.1 Equilibrium bathymetry in Ganges, intial bed level for Base Case A, Case B and Case C, compared with observed planform in previous years

5. MODEL RESULTS

5.1 Approach Model Runs

Subsequently, this bed was used as the initial condition for the runs. For each of the Situtations A, B and C, 3 runs were made:

1. Case without works;
2. Case with training works only: offtake guide bund and offtake flow divider;
3. Case with training works and bottom vanes.

Subsequently, conclusions are drawn on the effect of the structures by comparing the resulting planforms and by comparing the influence on the sediment transport and discharge distribution over the Ganges and Gorai.

5.2 River Training Works and Submerged Vanes in Model

The river training works proposed in the main report of the Gorai River Restoration Project are introduced in the model for the basic situation for each Case. These works comprise:

- offtake guide bund;
- offtake flow divider.

These works were modelled as closed boundaries in the model and were plotted with the model results.

Next, submerged vanes were introduced in the model. As the vane orientation (and thus the angle of attack) are critical in the efficiency of submerged vanes, this angle was selected based on the flow pattern observed in the initial situation for the Case A (Bottom Vane Orientation 1). Resulting flow velocities and directions are plotted in Figure 5.1. As the actual heading of the flow will vary and flow separation (at an angle of attack greater that 22^o) is not desirable, a moderate and safe angle of attack of 13^o was chosen.
Additionally, a second Vane Orientation 2 for the bottom vanes was tested for Case A, based on the flow pattern at the end of the monsoon and the same nominal angel of attack of 13^o.

Note, that the resulting angle of attack for the vanes and thus the effect resulting from the field of submerged vanes is expected to vary as a result as a result of the morphological development. In particular, this is the case for Case B and C with a different angle of the upstream main channel of the Ganges.

Model velocities for Case A with vanes

Model flow direction for Case A with vanes

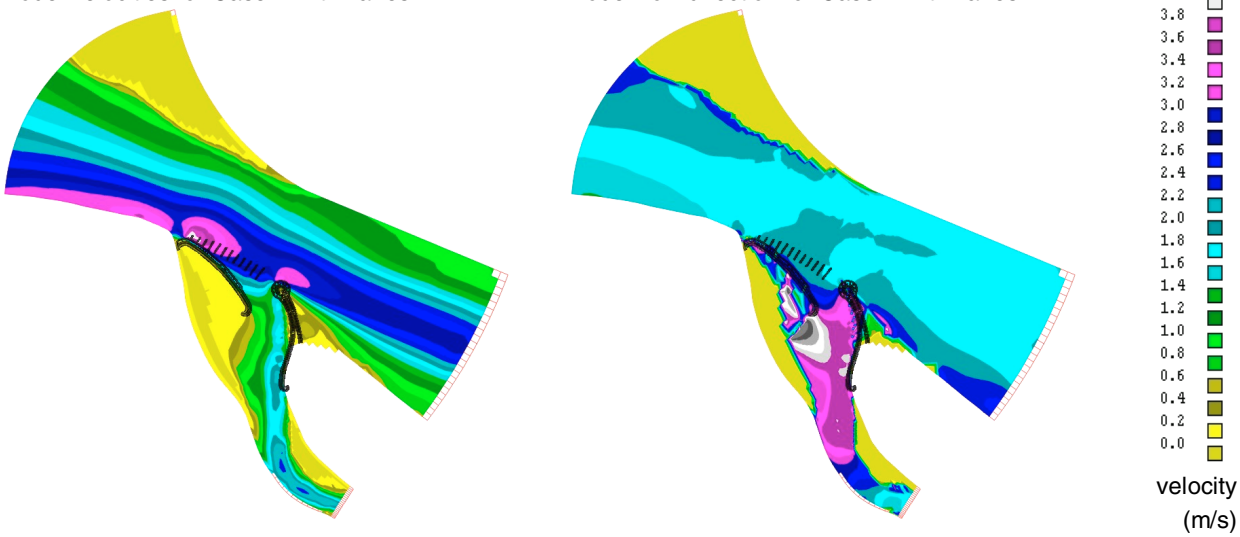

Model velocities for Case B with vanes

Model flow direction for Case B with vanes

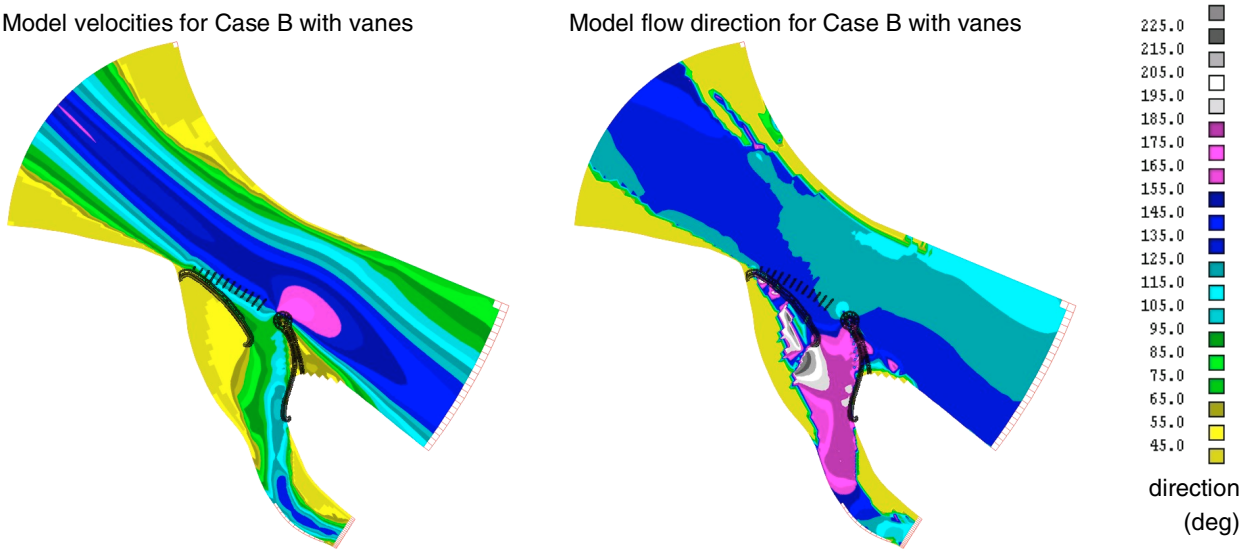

Model velocities for Case C with vanes

Model flow direction for Case C with vanes

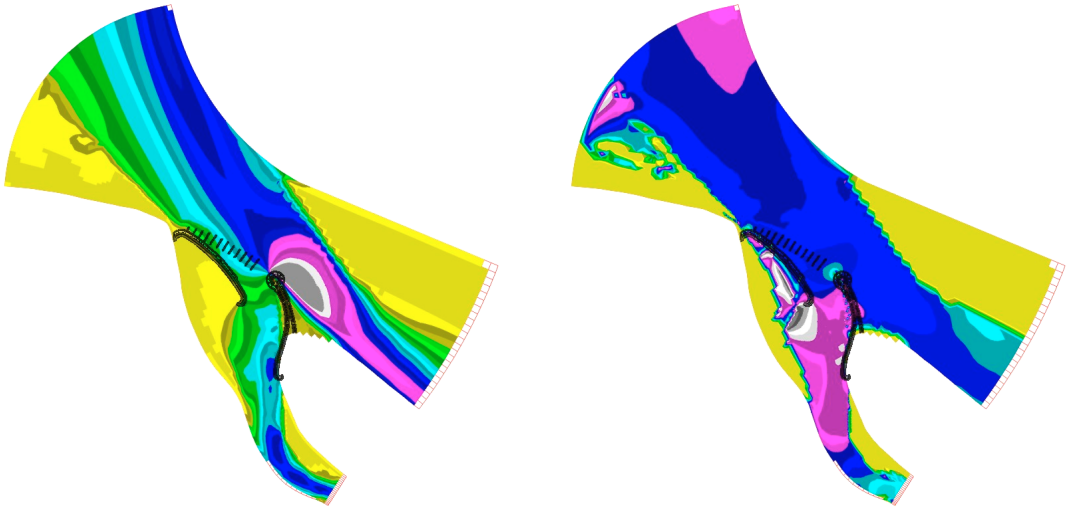

Figure 5.1 Flow velocities and directions in offtake area for Cases A, B and C with structures and vanes for initial situation

5.3 Overview Model Results

Model results are studied in the following paragraphs based on the planform development observed in the model over 1 monsoon season (4 months, 1 July to 1 November). The resulting planform development for all of the runs is plotted in Appendices A1 through C3.

Secondly, over this period the discharge and the sediment transport is monitored entering the Gorai, relative to the values in the upstream Ganges. The sediment transport and discharge distributions are plotted in Figure 5.1, Figure 5.1 and Figure 5.1. In these plots the development in time is indicated as 3 points:

- after 1 month after the start of the monsoon season (1 July);
- after 2 months of monsoon season (1 September);
- after 4 months of monsoon season (1 November).

5.4 Results for Base Case A (2000 Planform)

In the planform plots in Appendix A1 it is clearly seen that the model exaggerates the siltation occurring in the upstream part of the Gorai. In reality, the siltation occurring over 1 monsoon period is known to be significantly less. Nonetheless, based on the development of sediment transport and discharge conclusions can be drawn regarding the effect of proposed works and the bottom vanes.

In the following plot, it is clearly seen that the proposed river training works in the Gorai offtake result in a substantial reduction (roughly 40% after 2 months) the amount of sediment entering the Gorai, while increasing the discharge slightly. Additionally, the proposed field of submerged vanes results in a reduction of roughly 10% to 20% of the amount of sediment entering the Gorai. This limited efficiency is believed to be the result of the nature of the sediment transport, where a significant quantity of the sediment is transported in suspension, higher in the water vertical. Vanes have little effect on this part of the sediment transport.

Also, it is noted that there is little difference in the effect of Vane Orientation 1 versus Vane Orientation 2, except that the latter has a slightly better effect at the end of the monsoon season. It might be possible to increase the effect of the vane field, however this will have negative consequences in case of a more northerly orientation of the upstream main channel in the Ganges (such as in Case B and C).

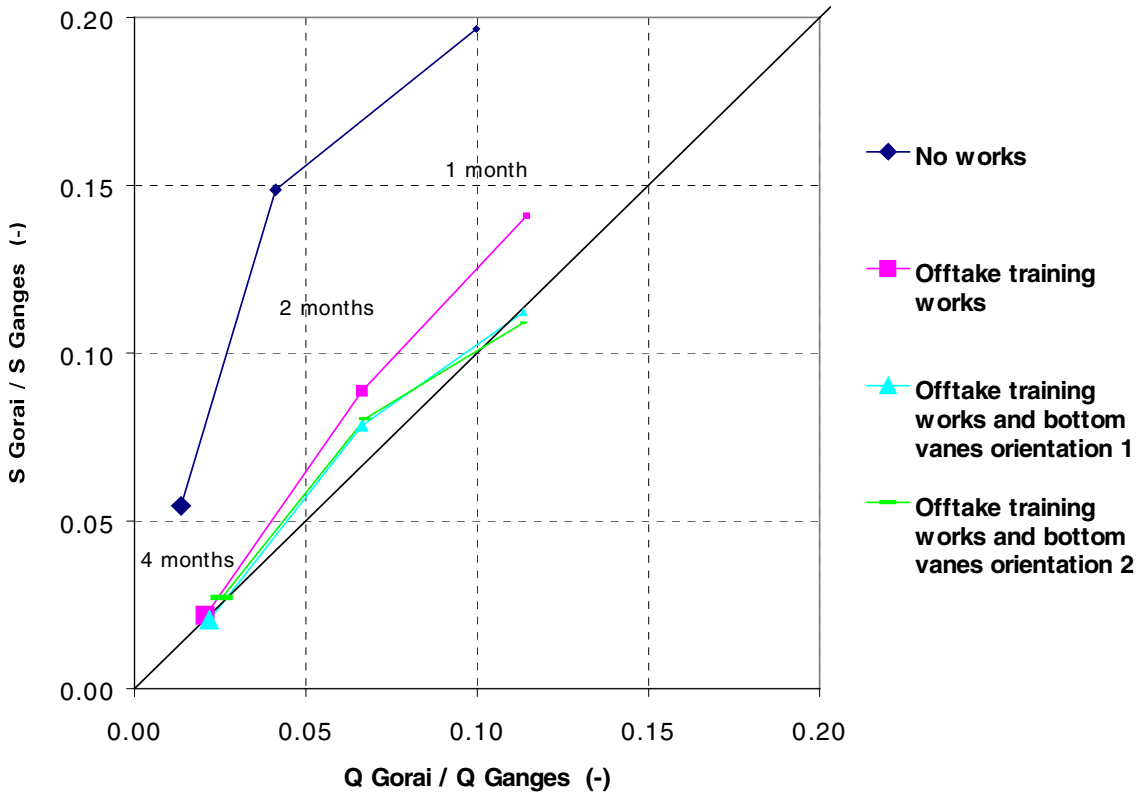

Figure 5.1 Sediment distribution over Ganges (upstream) and Gorai (chainage 1 km) in runs for Base Case A. Plotted points for situation after 1 month, 2 months and 4 months (end) during monsoon season. Development in time indicated. [for bottom vanes first point plotted only, additional points to be added]

5.5 Results for Case B (1989 Planform)

With a more northerly orientation of the Ganges main channel the amount of sediment entering the Gorai is reduced substantially. As a result the siltation in the offtake area is strongly reduced compared to Case A (2000 Planform).This is clearly seen in comparing Figure 5.1 with Figure 5.1. This can also be seen in the planform plots in Appendix B1, where a deeper channel is maintained in the Gorai over the monsoon season.

Furthermore, it is noted that the river training works initially have little effect, but an increase of the amount of water entering the Gorai. Subsequently, this configuration leads to a significant reduction of the amount of sediment entering the Gorai (some 50% after 4 months).

The Bottom Vanes initially result in a 10% - 20% reduction of the sediment entering the Gorai, and in a later stage this configuration results in a substantial increase of the monsoon discharge entering the Gorai.

Detailed analysis revealed that with this orientation of the upstream Ganges main channel, the angle of attack of the bottom vanes is increased by some 7^{o} to 10^{o} compared to Case A. Given the design of the vane field, most vanes have a high angle of attack (18^{o} - 24^{o}). As a result a greater effect of the vane field is found compared to Case A.

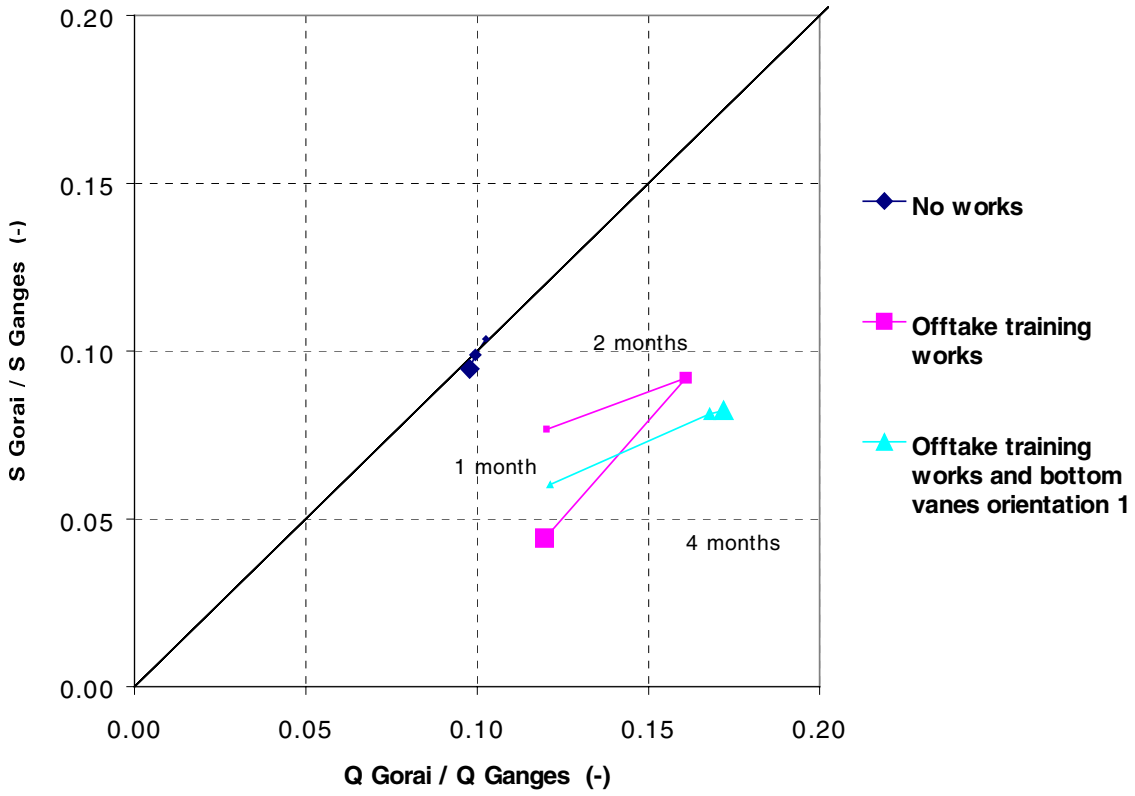

Figure 5.1 Sediment distribution over Ganges (upstream) and Gorai (chainage 1 km) in runs for Case B. Plotted points for situation after 1 month, 2 months and 4 months (end) during monsoon season. Development in time is indicated

5.6 Results for Case C (1973 Planform)

In this third Case C, again the situation of the Gorai offtake in an outer bend of the Ganges main channel results in reduced amount of sediment entering the Gorai and little siltation occurring in the situation without works. Over the course of the monsoons season, the Gorai discharge is fairly constant.

Again, the proposed river training works result in a substantial reduction of the amount of sediment entering the Gorai offtake. Over the course of the modelled monsoon season, this results in a significant increase of the Gorai discharge. Note, that the increase of a Gorai discharge up to 30% of the Ganges discharge is exaggerated. This can be explained along the same lines as the exaggerated siltation occurring in the offtake in Case A.

The field of submerged vanes has little effect in this case. Detailed analysis revealed that this is a result of the excessive angles of attack occurring in the vane field (20^o - 32^o), resulting in flow separation occurring at the bigger part of the vanes. Thus, hardly any positive effect remains. At the end of the monsoon period, the vane field has an increasing effect, as a result of an decreasing angle of attack.

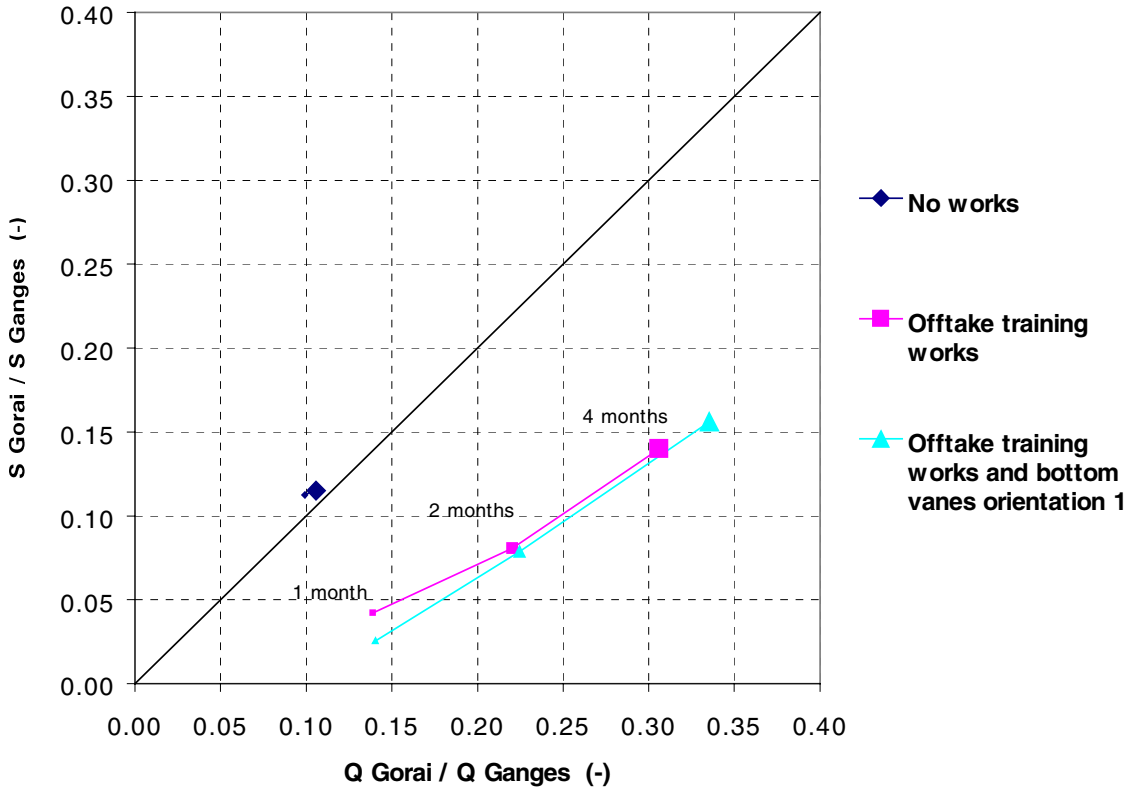

Figure 5.1 Sediment distribution over Ganges (upstream) and Gorai (chainage 1 km) in runs for Case C. Plotted points for situation after 1 month, 2 months and 4 months (end) during monsoon season. Development in time is indicated

6. CONCLUSIONS

6.1 Conclusions Related to Bottom Vanes

Based on the results of the modelling effort a number of conclusions can be drawn with respect to the functioning of bottom vanes:

1. For the present situation of the main channel in the Ganges the field of 212 bottom vanes would result in an reduction of 10% to 20% of the amount of sediment entering the Gorai offtake. This is additional to the reduction as a result of the proposed river training works.
2. The angle of approach of the main channel in the Ganges upstream influences the angle of attack of the bottom vanes. With the main channel in the Ganges according to the October 2000 situation, the angle of attack of the vanes changes within a range of roughly 12^{o}.
3. If the main channel in the Ganges were to shift to a north-easterly orientation the angle of attack in the field of bottom vanes is expected to increases by roughly 7 - 13^{o}, approaching the critical angle of attack (roughly 22^{o}). This results in an increase efficiency of the vanes, but at some vanes flow separation is expected. This strongly increases if the main channel in the Ganges would shift in a north-north-easterly direction, eliminating the effective working of the submerged vanes. In reality this would result in increased turbulence levels.
4. In the resulting morphological development in the model of the Gorai offtake, the impact of the vanes is limited. However, this image is believed to be influenced by the exaggerated siltation that occurs in the offtake in all cases in the model.

6.2 Other Morphological Conclusions

Secondly, conclusions can be drawn that are not specific for the situation with bottom vanes:

5. The orientation of the upstream main channel in the Ganges is an important factor in the morphological development of the Gorai. A northerly orientation tends to lead to a rise of the water level at Talbaria and to reduce the influx of sediment.
6. Irrespective of the orientation of the upstream channel, the proposed river training works (flow divider and offtake guide bund) result in a significant improvement of the ratio of discharge and sediment entering the Gorai offtake.
7. The location, width and depth of the main channel in the Ganges is very sensitive to variations in the discharge distribution over the upstream model boundary. This also holds for the dimensions of the scour hole at Talbaria.

6.3 Conclusions Related to Model Representation

Finally, some conclusions are mentioned that relate to the model representation of the prototype situation:

8. The model consistently exaggerates siltation in the offtake area. Although Van Rijn formula for sediment transport predicts average sediment transport rates that are in line with observations, it is concluded that power n in $s \sim u^n$ is overestimated for this condition with a very smooth river bed.
9. Circulation flow patterns over shallow parts of the offtake were observed in the model that are not seen in reality. This suggests that a constant Chezy value underestimates the bed friction over shallow areas.

6.4 Overall Conclusions and Recommendations

On a conceptual level it is believed that the numerical model that was developed for the Gorai offtake provides an reasonable representation of the hydraulic and morphological patterns in the offtake area.
The functioning of the field of submerged vanes is strongly influenced by the orientation of the main channel in the Ganges. For the vanes to function properly, this requires a limited nominal angle of attack in the design situation, so that flow separation does not occur as soon as there is a shift in the channel. Nonetheless, flow separation could occur if there would be a drastic shift of the Ganges main channel to the north.

Additionally, the effect of vanes is reduced by the relatively high sediment concentration in the upper part of the vertical. In all, this results in a limited effect of the vane field on the influx of sediment in the Gorai: a reduction of roughly 10% at times of a favourable orientation of the main channel in the Ganges.
Possibly, further optimisation of the position and angle of the bottom vanes, relative to the orientation of the main channel in the Ganges may lead to a higher efficiency in reducing the amount of sediment entering the Gorai.

APPENDICES

APPENDIX A1 Bed Development For Base Case A - No Works

Initial bathymetry (1 July)

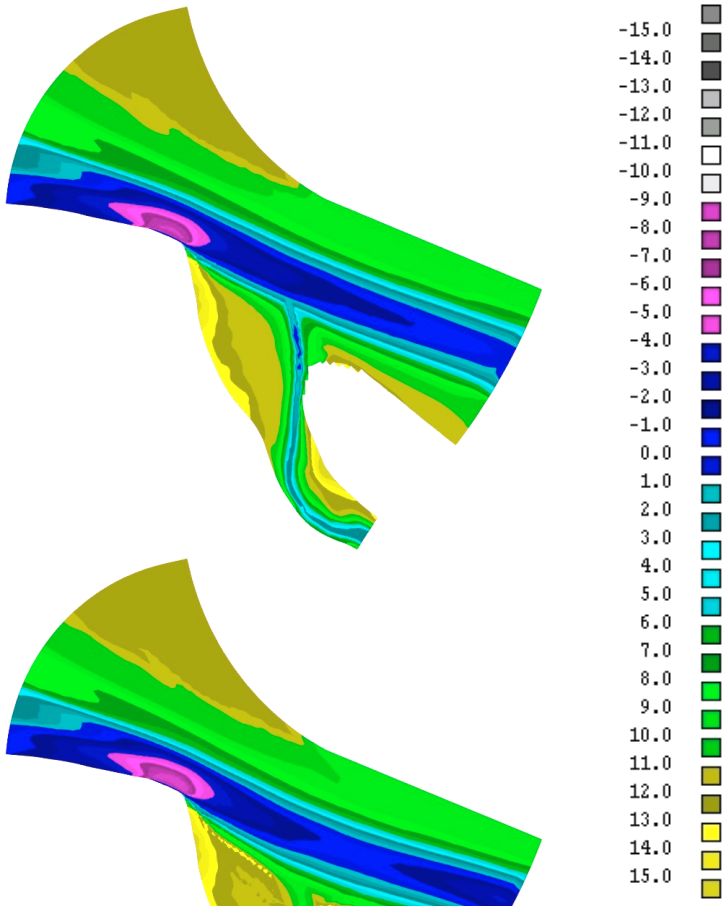

(1 September)

(1 November)

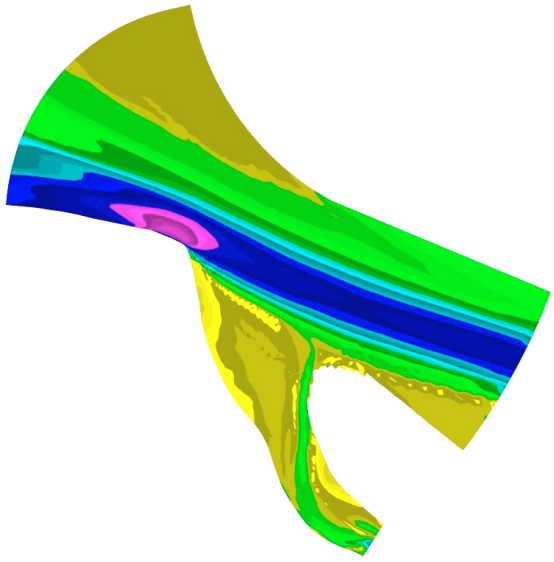

APPENDIX A2 Bed Development For Base Case A - Offtake Training Works

Initial bathymetry (1 July)

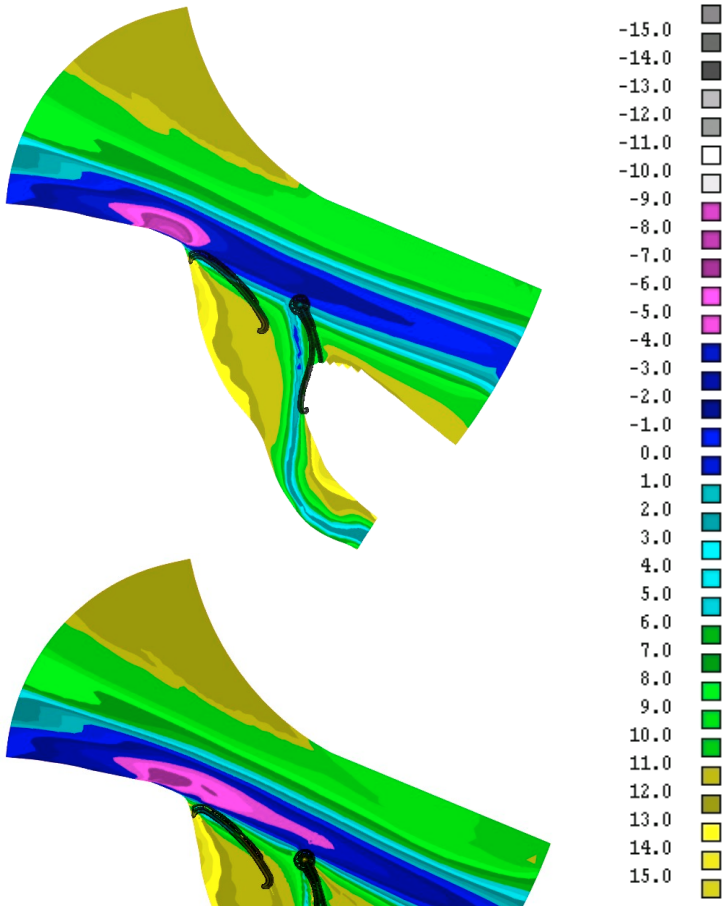

(1 September)

(1 November)

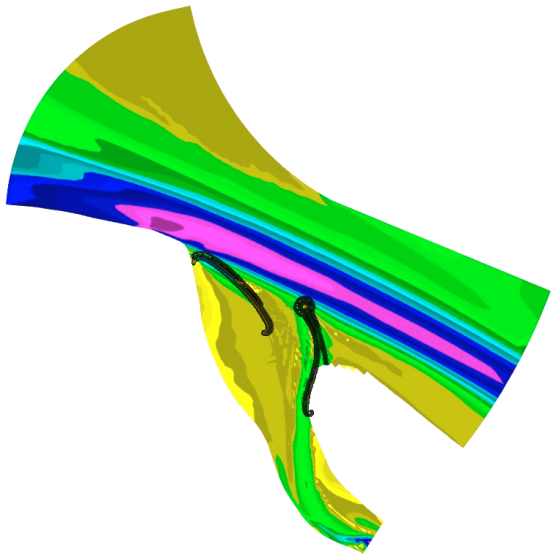

APPENDIX A3 Bed Development For Base Case A - Offtake Training Works And Bottom Vanes Orientation 1

Initial bathymetry (1 July)

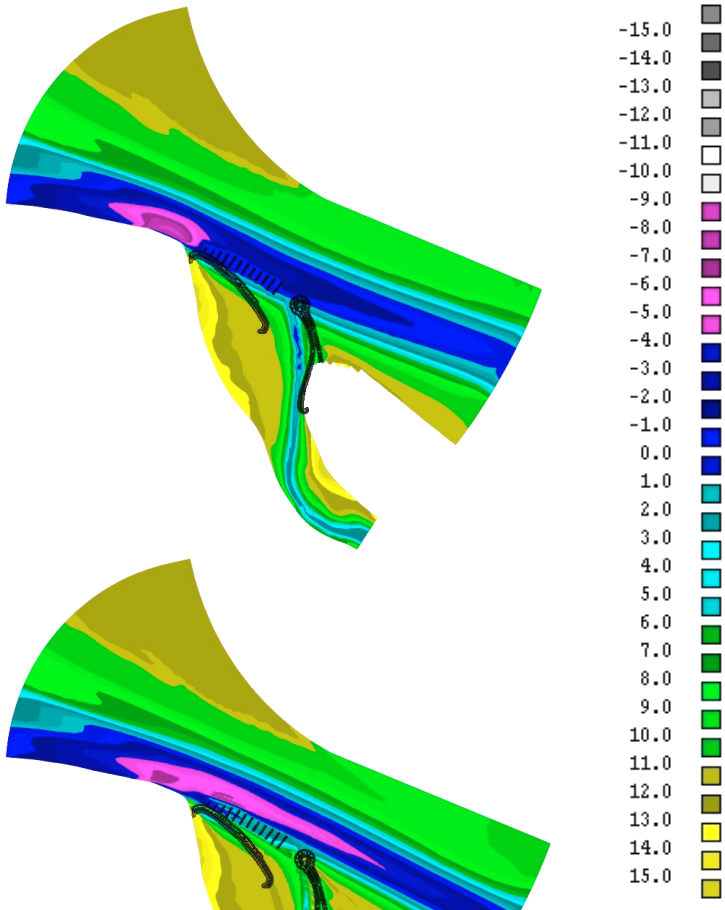

(1 September)

(1 November)

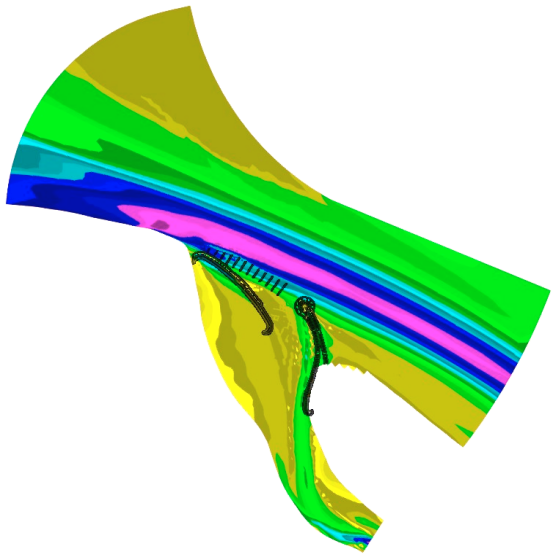

APPENDIX A3 Bed Development For Base Case A - Offtake Training Works And Bottom Vanes Orientation 2

Initial bathymetry (1 July)

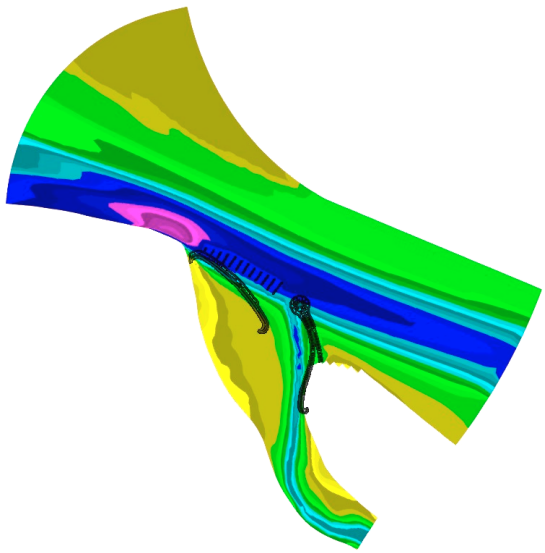

(1 September)

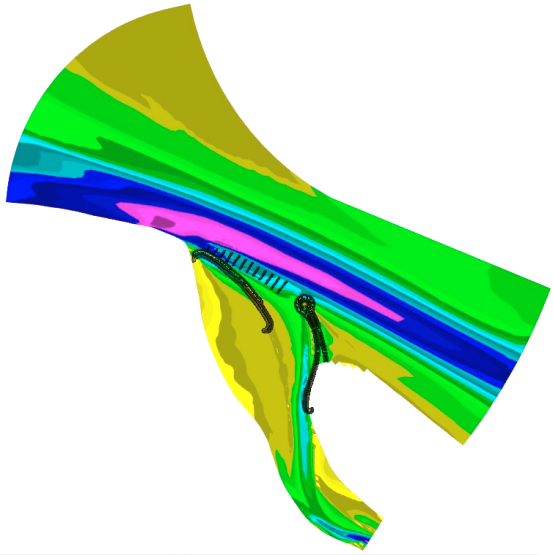

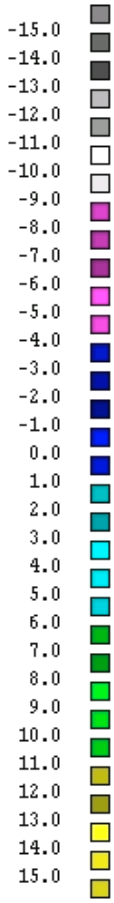

(1 November)

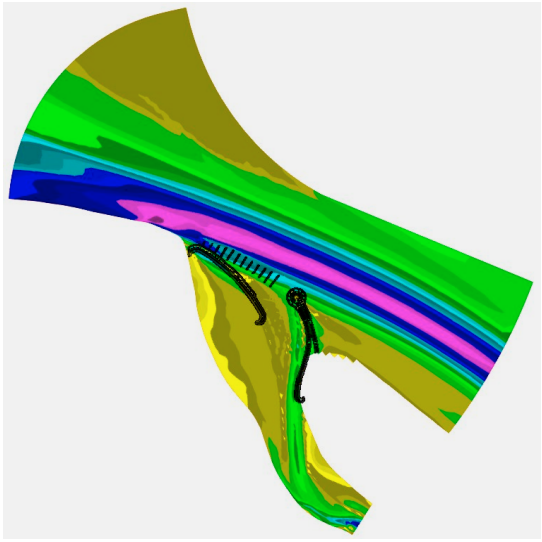

APPENDIX B1 Bed Development For Case B - No Works

Initial bathymetry (1 July)

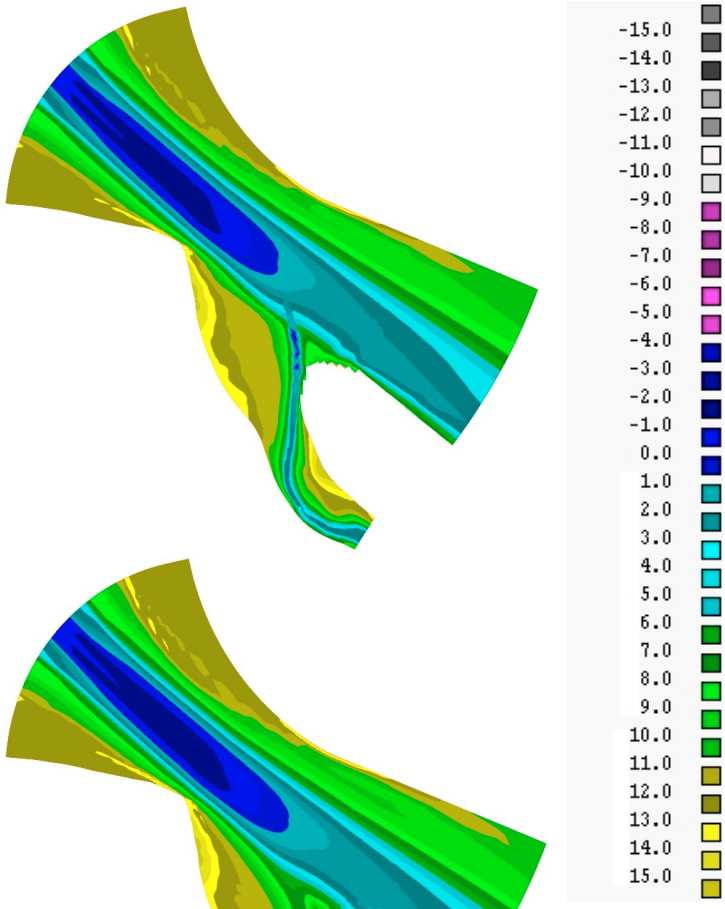

(1 September)

(1 November)

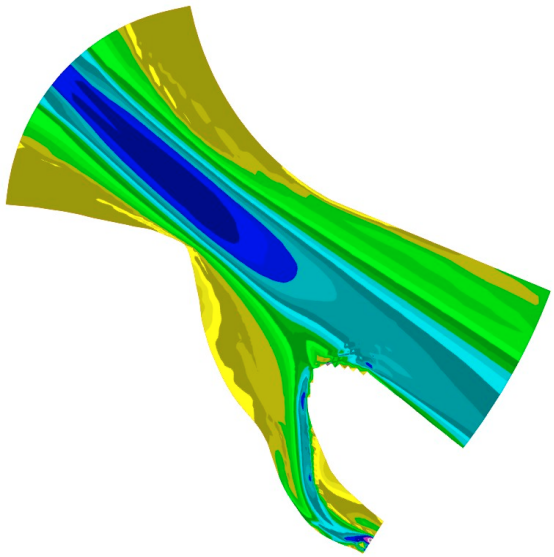

APPENDIX B2 Bed Development For Case B - Offtake Training Works

Initial bathymetry (1 July)

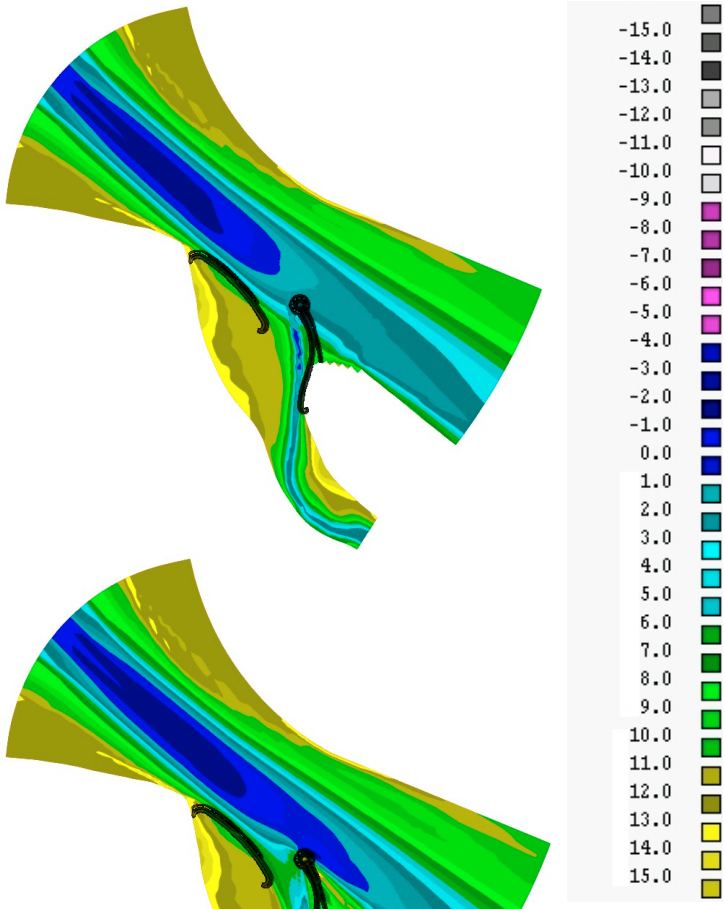

(1 September)

(1 November)

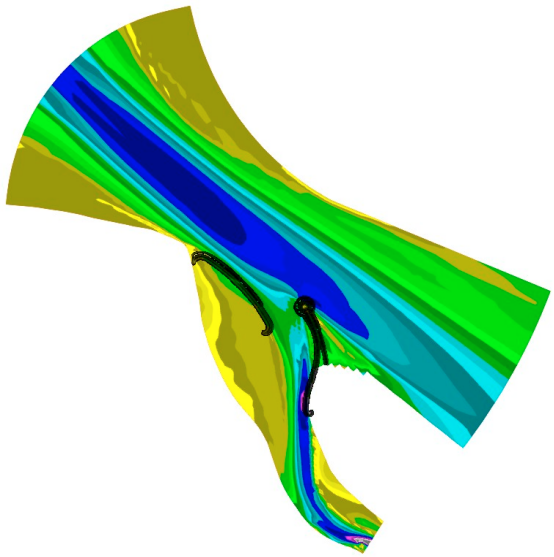

APPENDIX B3 Bed Development For Case B - Offtake Training Works And Bottom Vanes Orientation 1

Initial bathymetry (1 July)

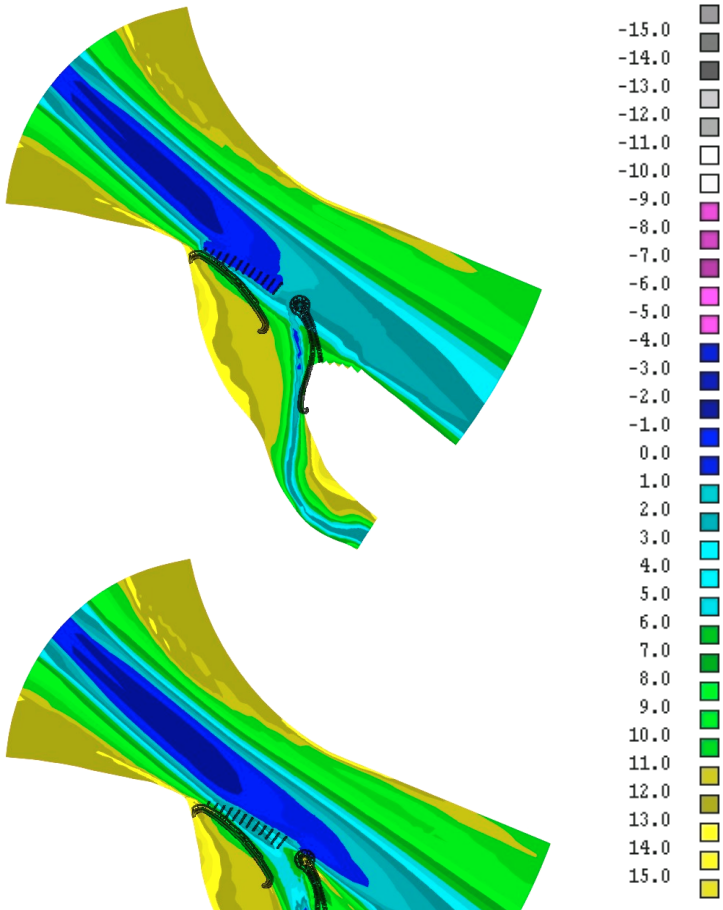

(1 September)

(1 November)

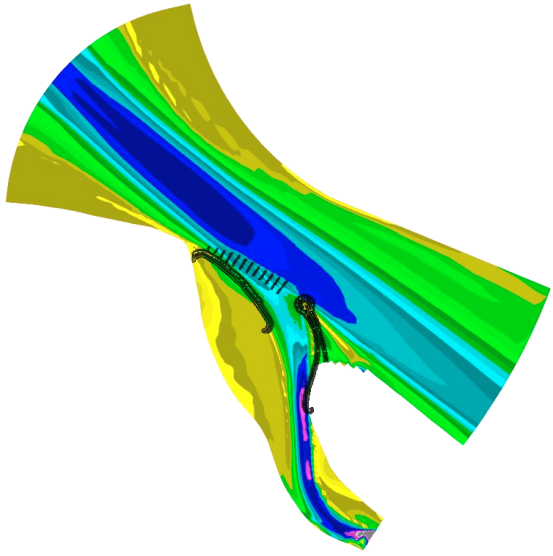

APPENDIX C1 Bed Development For Case C - No Works

Initial bathymetry (1 July)

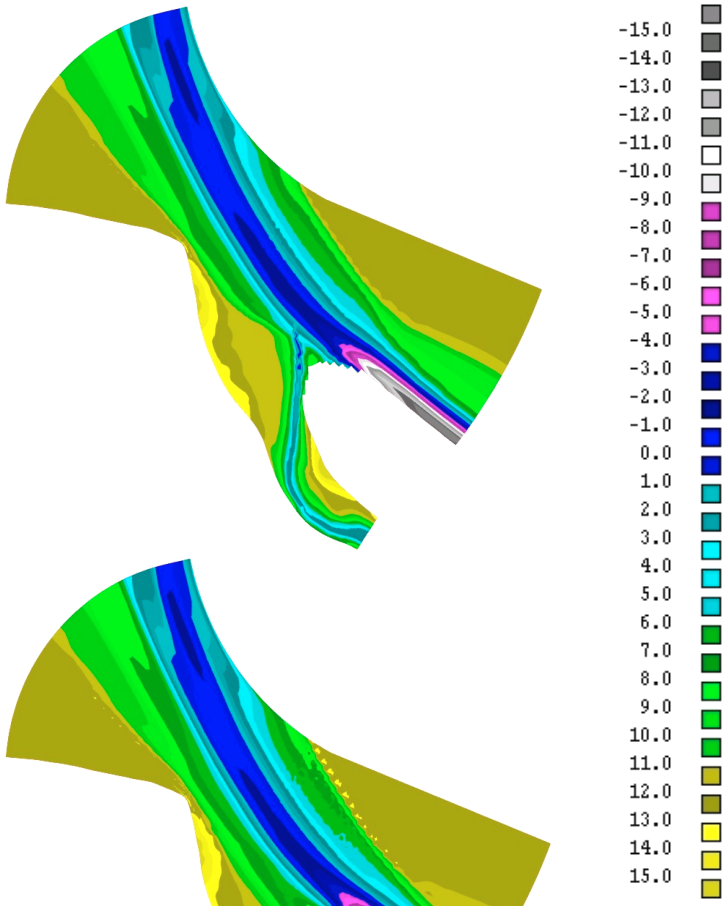

(1 September)

(1 November)

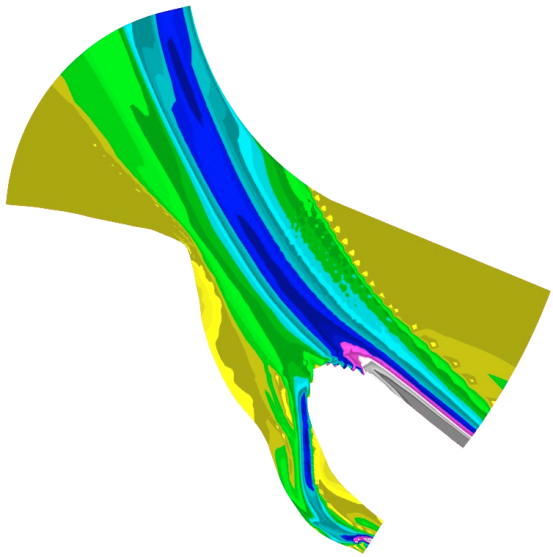

APPENDIX C2 Bed Development For Case C - Offtake Training Works

Initial bathymetry (1 July)

(1 September)

(1 November)

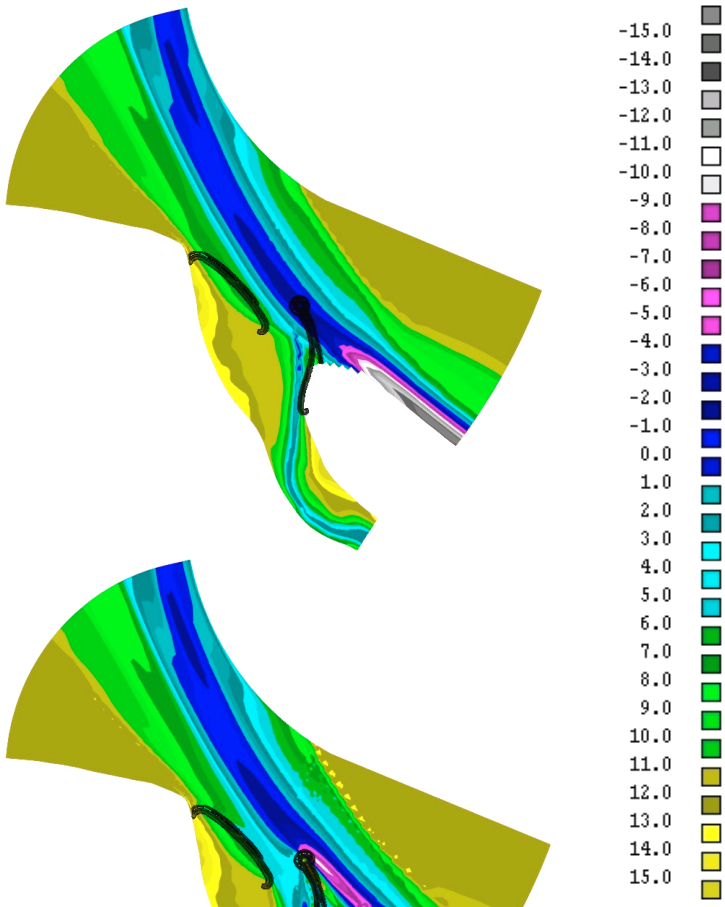

APPENDIX C3 Bed Development For Case C - Offtake Training Works And Bottom Vanes Orientation 1

Initial bathymetry (1 July)

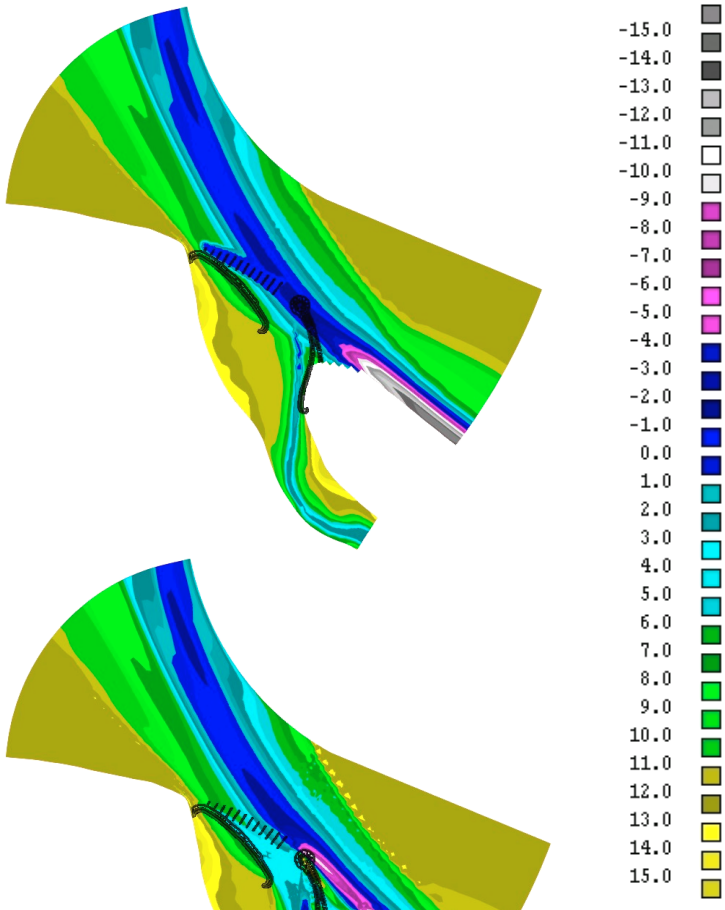

(1 September)

(1 November)

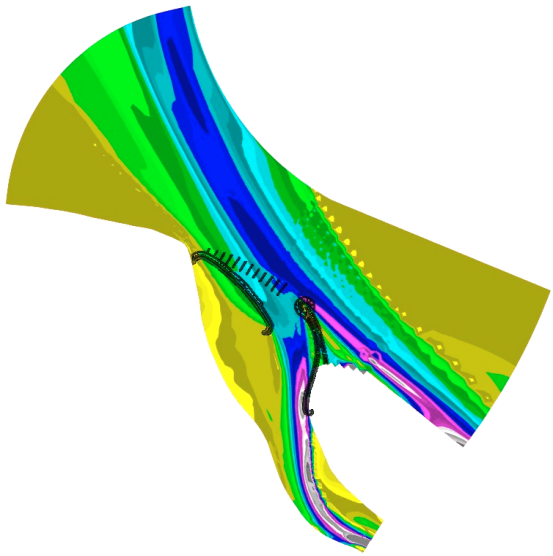

APPENDIX D Velocity Disribution Over Upstream Model Boundary

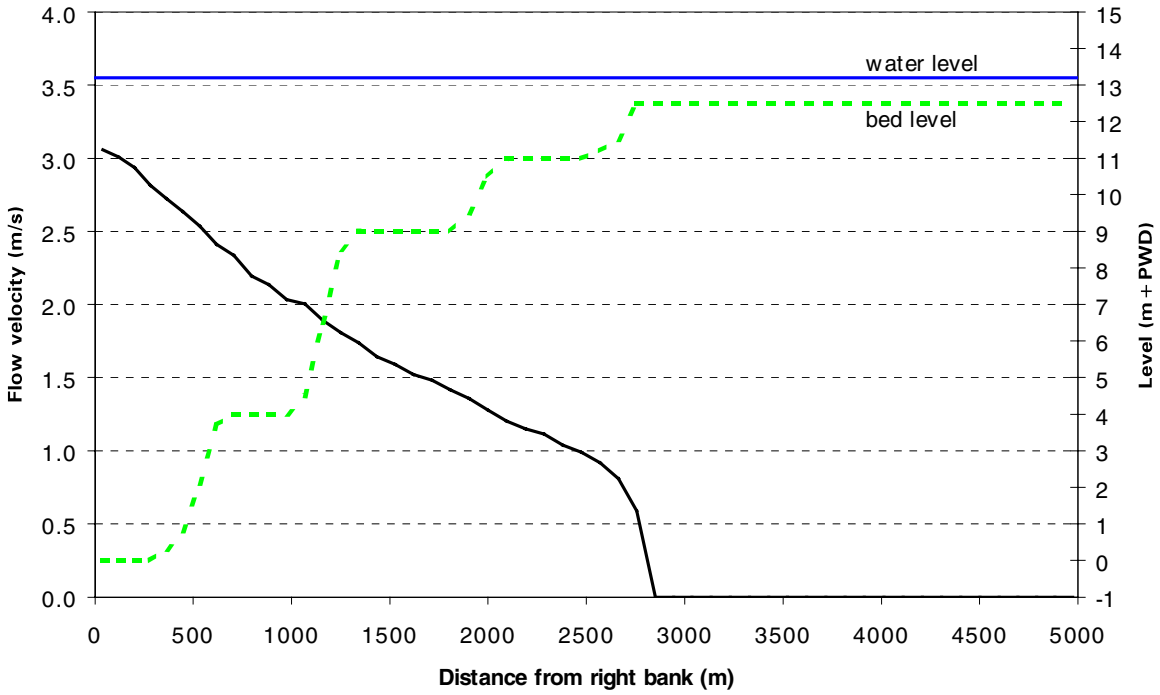

Inflow velocity distribution over upstream model boundary resulting from morphological calibration of Base Case A

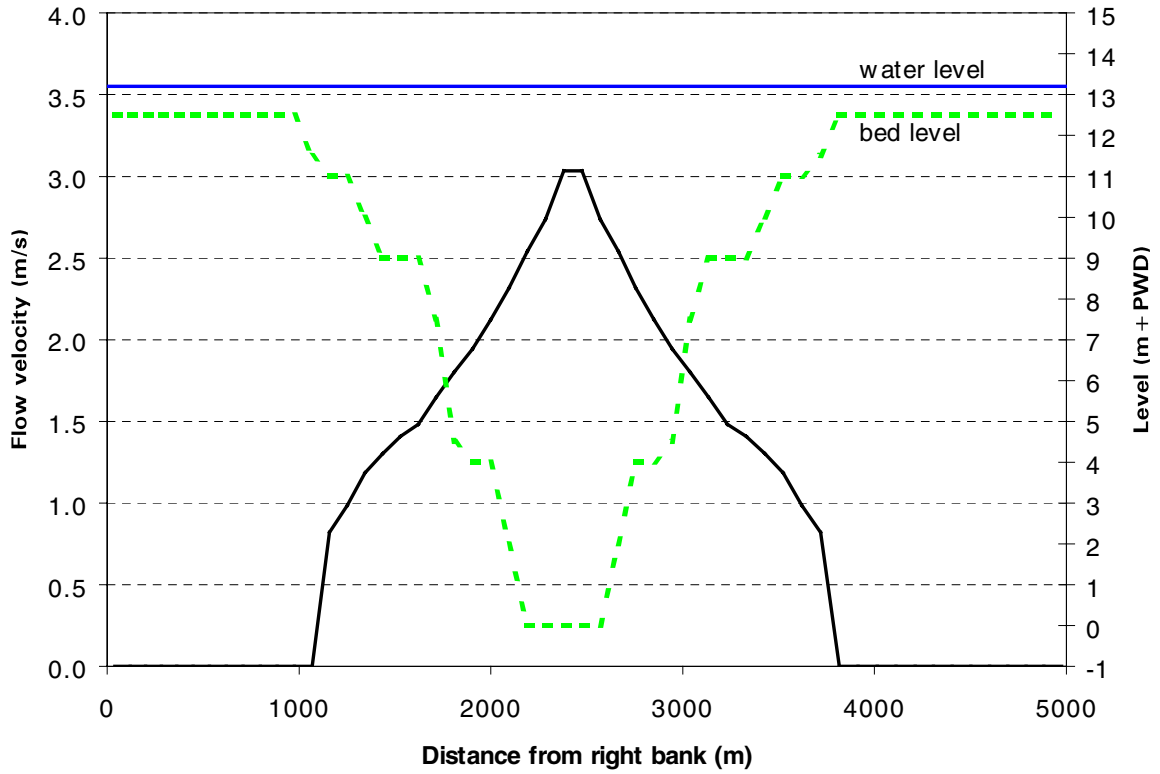

Inflow velocity distribution over upstream model boundary for Case B

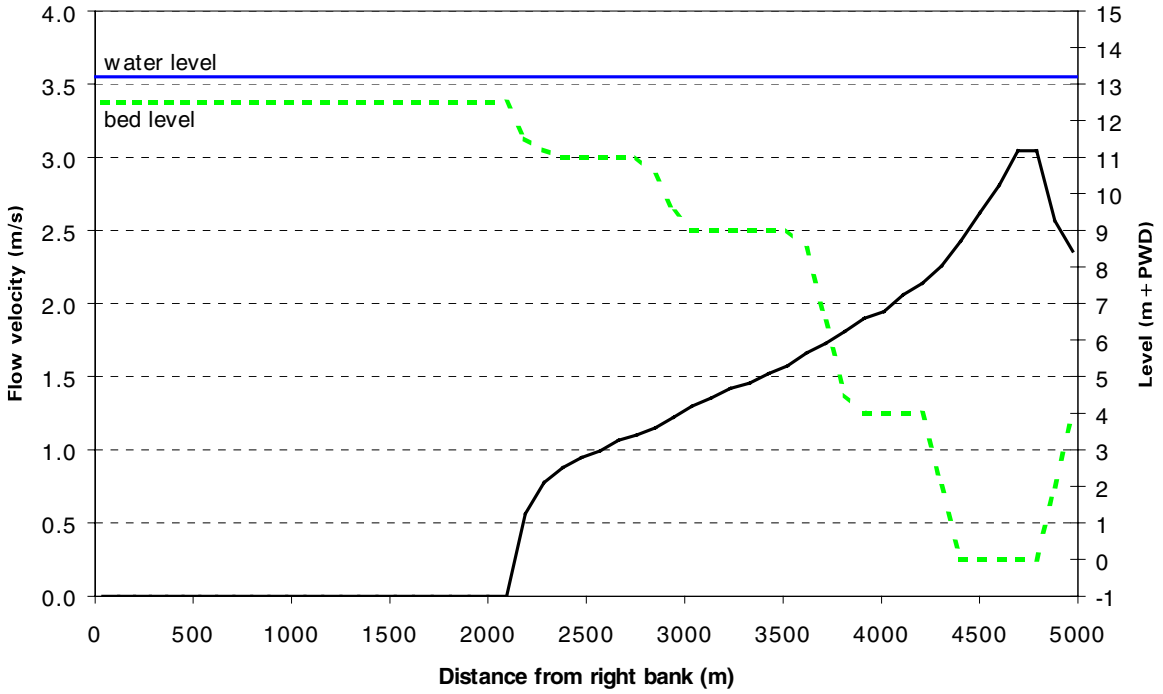

Inflow velocity distribution over upstream model boundary for Case C

APPENDIX E Delft3D Model Description

INTRODUCTION

WL | Delft Hydraulics has developed a unique, fully integrated modelling framework for a multi-disciplinary approach and 3D computations for coastal, river, lake and estuarine areas. It can carry out simulations of flows, sediment transports, waves, water quality, morphological developments and ecology. It has been designed for experts and non-experts alike. The Delft3D framework is composed of several modules, grouped around a mutual interface, while being capable to interact with one another.

Delft3D can switch between the 2D vertically averaged and 3D mode simply by changing the number of layers. This feature enables to set up and investigate the model behaviour in 2D mode before going into full 3D simulations.
Areas of application
Delft3D can be applied, but is not limited, to the following areas of applications:

- flows due to tide, wind, density gradients and wave induced currents;
- propagation of directionally spreaded short waves over uneven bathymetries, including wave-current interaction;
- advection and dispersion of effluents;
- on-line morphodynamic computations (local scour, short time and length scales);
- sediment transport of cohesive and non-cohesive sediment;
- water quality phenomena including ecological modelling, the prediction of heavy metal concentrations, interaction with organic and in-organic suspended sediment, interaction between the water and bottom phase (such as sediment oxygen demand), algae blooms;
- particle tracking, including oil spill and dredging plume modelling;
- initial and/or dynamic (time varying) 2D-morphological changes, including the effects of waves on sediment stirring and bed-load transport.

Delft3D framework overview
Delft3D is composed of a number of modules, each addressing a specific domain of interest, such as flow, near-field and far-field water quality, wave generation and propagation, morphology and sediment transport, together with pre-processing and post-processing modules. All modules are dynamically interfaced to exchange data and results where process formulations require. In the following chapters these modules are described in more detail.

All features are embedded in a state-of-the-art Graphical User Interface based on the OSF/MOTIF and X-Windows (Unix workstations) or the MS Windows (Wintel-platforms) standards. An application (model) can be completely defined, inspected and analysed through this menu-driven, user-friendly, graphical interface.

System architecture of Delft3D

The basic processes covered by each of the modules is:

- Delft3D-FLOW 2- and 3-D hydrodynamic, salinity, temperature, transport and on-line sediment transport and morphology
- Delft3D-WAVE short wave propagation (HISWA and SWAN)
- Delft3D-WAQ general field water quality
- Delft3D-PART particle tracking, oil spill modelling
- Delft3D-ECO complex eutrophication and ecological modelling
- Delft3D-SED cohesive and non-cohesive sediment transport
- Delft3D-CHEM chemical components and interactions
- Delft3D-MOR morphodynamic simulations

HYDRODYNAMIC MODULE

The hydrodynamic module, Delft3D-FLOW, is a multi-dimensional hydrodynamic simulation program that calculates non-steady flow and transport phenomena resulting from tidal and meteorological forcing on a curvilinear, boundary-fitted grid. In 3D simulations, the hydrodynamic module applies the so-called sigma co-ordinate transformation in the vertical, which results in a smooth representation of the bottom topography. It also results in a high computing efficiency because of the constant number of vertical layers over the whole computational domain.

Module description

The hydrodynamic module is based on the full Navier-Stokes equations with the shallow water approximation applied. The equations are solved with a highly accurate unconditionally stable solution procedure. The supported features are:

- three co-ordinate systems, i.e. rectilinear, curvilinear and spherical in the horizontal directions and a sigma co-ordinate transformation in the vertical;
- tide generating forces (only in combination with spherical grids);
- simulation of drying and flooding of inter-tidal flats (moving boundaries);
- density gradients due to a non-uniform temperature and salinity concentration distribution (density driven flows);
- for 2D horizontal large eddy simulations the horizontal exchange coefficients due to circulation's on a sub-grid scale (Smagorinsky concept);
- turbulence model to account for the vertical turbulent viscosity and diffusivity based on the eddy viscosity concept;
- selection from four turbulence closure models: k- , k-L, algebraic and constant coefficient;
- shear stresses exerted by the turbulent flow on the bottom based on a Chézy, Manning or White-Colebrook formulation;
- enhancement of the bottom stresses due to waves;
- automatic conversion of the 2D bottom-stress coefficient into a 3D coefficient;
- wind stresses on the water surface modelled by a quadratic friction law;
- space varying wind and barometric pressure (specified on the flow grid or on a coarser meteo grid), including the hydrostatic pressure correction at open boundaries (optional);
- simulation of the thermal discharge, effluent discharge and the intake of cooling water at any location and any depth in the computational field (advection-diffusion module);
- the effect of the heat flux through the free surface;
- on-line analysis of model parameters in terms of Fourier amplitudes and phases enabling the generation of co-tidal maps;
- drogue tracks;
- advection - diffusion of substances with a first order decay rate;
- online simulation of the transport of sediment (silt or sand) including formulations for erosion and deposition and feedback to the flow by the baroclinic pressure term, the turbulence closure model and the bed changes;
- the influence of spiralling motion in the flow (i.e. in river bends). This phenomenon is especially important when sedimentation and erosion studies are performed;
- modelling of obstacles like 2D spillways, weirs, 3D gates, porous plates and floating structures;
- wave - current interaction, taking into account the distribution over the vertical;
- many options for boundary conditions, such as water level, velocity, discharge and weakly reflective conditions;
- several options to define boundary conditions, such as time series, harmonic and astronomical constituents;
- on-line visualisation of model parameters enabling the production of animations.

Applications areas

Delft3D-FLOW can be applied to the following application areas:

- salt intrusion in estuaries;
- fresh water river discharges in bays;
- thermal stratification in lakes and seas;
- cooling water intakes and waste water outlets;
- short-term sediment transport including feedback on the flow;
- transport of dissolved material and pollutants;
- storm surges and typhoon modelling;
- river flows, meandering and braided rivers;
- floodplains, with or without vegetation;
- reservoir siltation and degradation below dams;
- bottom vanes, spurs, groynes, bridges, weirs and levees.

Coupling with other modules
The results of the hydrodynamic module are used in all other modules of Delft3D. The results are dynamically exchanged between the modules through the use of a so-called communication file. Basic (conservative) water quality parameters like concentrations of dissolved material and pollutants, can be included in the computations. But, for more dedicated water quality simulations, the hydrodynamic module is coupled with the far-field water quality module (Delft3D-WAQ) , the nutrient phytoplankton module (Delft3D-ECO) and the near-field particle tracking module (Delft3D-PART). A coupling with the sediment transport module (Delft3D-SED) is available to simulate cohesive and non-cohesive sediment transport processes, e.g. in the case of erosion and sedimentation studies. For wave-current interaction a dynamic coupling is provided with the wave module (Delft3D-WAVE) and for morphodynamic simulations the hydrodynamic module is integrated with the wave module and a sedimentation and erosion module into a morphodynamic module (Delft3D-MOR).

To simulate a model defined on a curvilinear grid system, an orthogonal grid must be provided. To generate such a grid the program Delft-RGFGRID is provided, though the grid can be generated by any grid generator program as long as the grid is delivered in the prescribed (ASCII) file format. The generation of a curvilinear grid is an important and somewhat complex task. Along with the main model parameters, the grid will ultimately determine the accuracy of the final model results.

To prepare the bottom topography or other grid-related data, such as a non-constant initial condition file, the program Delft-QUICKIN is provided. This program interpolates the scattered, digitised chart data to depth-values at the grid points in the model. Many powerful interactive processing options to further adjust the topography are supported, e.g. manual adjustment of the values at individual points, selection of the domain of influence, group adjustments, and smoothing. The output of this program (ASCII-file) can be imported into other Delft3D modules.

Analysis and interpretation of a hydrodynamic simulation in terms of tidal quantities can be performed by the program Delft-TRIANA. Delft-TRIANA performs off-line tidal analyses of time-series of either water levels and/or velocities. The results from these analyses can be subsequently compared with observation data supplied by the user.
In case the open boundaries of a (detailed) Delft3D-FLOW model are located within the model domain of a coarser Delft3D-FLOW model, the coarse model can generate the boundary conditions of the detailed, nested model. The offline generation of boundary conditions is done by Delft3D-NESTHD.

MORPHODYNAMIC MODULE

The morphological module, Delft3D-MOR, integrates the effects of waves, currents, sediment transport on morphological development, related to sediment sizes ranging from silt to gravel. It is designed to simulate the morphodynamic behaviour of rivers, estuaries and coasts on time-scales of days to years.

The typical problems to be studied using this system involve complex interactions between waves, currents, sediment transport and bathymetry. To allow such interactions, the individual modules within Delft3D all interact through a well-defined common interface; a flexible steering module controls the calling sequence of the individual modules.

The computational modules within Delft3D are identical to their stand-alone counterparts and each offer the full range of physical processes. In this way, WL | Delft Hydraulics combined experience of over thirty years in computer modelling is built into this system.

A morphological simulation in Delft3D is defined as a tree structure of processes and sub-processes down to elementary processes which contain calls to the computational modules. The user is free to build up processes of increasing complexity, from a single call to the flow model to morphodynamic simulations spanning years, with varying boundary conditions.
This module simulates the processes on a curvilinear grid system used in the hydrodynamic module, which allows a very efficient and accurate representation of complex areas.

Module description
Delft3D-MOR contains or is able to utilise the following components:

Steering module
Allows the user to link model inputs for the module components. The morphological process can be specified as a hierarchical tree structure of processes. Time intervals for the elementary processes are defined. Processes may be executed a fixed number of times, for a given time span or as long as a certain condition is not satisfied. A variety of options are available to specify the time progress.

Waves
The wave module (Delft3D-WAVE) is built around the stationary short-crested wave model HISWA (Holthuijsen et al., 1989). This model computes the effects of refraction, shoaling, wave dissipation by bottom friction and breaking and wave blocking for a discrete directional wave spectrum, over a two-dimensional bathymetry. Within the module the user can specify several HISWA computations in one run, with varying boundary conditions, and for each boundary condition various nested runs can be executed. Flow and water level information can be used from a flow run, and the results can be passed on to the flow module.

At present also the SWAN model is available in the wave module of Delft3D. The SWAN model is fully spectral (in all directions and frequencies) and computes the evolution of random, short-crested waves in coastal regions with shallow water and ambient currents. The SWAN model accounts for (refractive) propagation - as the HISWA model - and represents the processes of wave generation by wind, dissipation due to white-capping, bottom friction and depth-induced wave breaking and non-linear wave-wave interactions (both quadruplets and triads) explicitly with state-of-the-art formulations. It is noted that the SWAN model (as the HISWA model) does not account for diffraction effects.

Hydrodynamics
The hydrodynamic module (Delft3D-FLOW) used by Delft3D-MOR is based on the shallow water equations, including effects of tides, wind, density currents, waves, and turbulence models up to k- . The module includes a transport solver for salinity, temperature and conservative substances. The effects of salinity and temperature on the density and on the momentum balance are taken into account automatically.

The module uses a curvilinear grid in the horizontal plane. The vertical grid sizes are proportional to the local water depth.

For efficient morphological computations a one-layer, depth-averaged approach is used. The effects of spiral flow, i.e. in river bends, are computed by a secondary flow module which takes into account the advection of spiral flow intensity and the effect of the secondary flow on the primary current.

Wave effects in the model include radiation stress gradients associated with wave dissipation, wave-induced mass flux and enhanced bed shear stress, computed by a choice of formulations.

Sediment transport
The sediment transport module computes the bed-load and suspended-load sediment transport field over the curvilinear model grid, for a given period of time.

The bed-load transport is computed as a local function of wave and flow properties and the bed characteristics. The equilibrium suspended load is also computed as a local function of these parameters. The module then recognises two modes of transport: total transport (equilibrium) mode, or suspended load mode. In the first, the total transport is simply the addition of bed-load and equilibrium suspended-load transport. In the second mode, the entrainment, deposition, advection and diffusion of the suspended sediment is computed by a transport solver. Here, a quasi-3D approach is followed, where the vertical profiles of sediment concentration and velocity are given by shape functions.

The bed-load and equilibrium suspended-load transport can be modelled by a range of formulations, among which are Engelund-Hansen, Meyer-Peter-Muller, Bijker, Bailard and Van Rijn for sand, and a separate formulation for silt transport.

Effects of the bed slope on magnitude and direction of transport, and effects of non-erodible layers can be taken into account for all formulations.

Bottom change
The bottom update module contains several explicit schemes of Lax-Wendroff type for updating the bathymetry based on the sediment transport field. Options are available for fixed or automatic time-stepping, fixed (non-erodible) layers, various boundary conditions, and dredging.

Numerical aspects
All modules except the wave module operate on the same rectangular or curvilinear, orthogonal grid. Fully implicit ADI or AOI schemes are applied in the hydrodynamic module for the momentum and continuity equations. The solver has robust drying and flooding procedures for both 2D and 3D cases. In the transport solver a Forrester filter can be applied which guarantees positive concentrations throughout.

The same transport solver is applied for suspended sediment computations.

The wave model HISWA operates on rectangular grids, and uses an implicit scheme in propagation direction, combined with a forward marching technique. The wave module takes care of all transformations and interpolations between these rectangular grids and the curvilinear flow and transport grid. The wave model SWAN can perform computations directly on a curvilinear grid.

The bottom update model uses an explicit scheme of Lax-Wendroff type. This leads to a Courant type stability criterion. However, cheap intermediate "continuity correction" steps keep the computational effort at a reasonable level.

Application areas
Delft3D-MOR is designed to simulate wave propagation, currents, sediment transport and morphological developments in coastal, river and estuarine areas.

Coastal areas including beaches, channels, sand bars, harbour moles, offshore breakwaters, groynes and other structures. The coastal areas may be intersected by tidal inlets or rivers; parts of it may be drying and flooding.

Rivers including bars, river bends (spiral flow effect), bifurcations, non-erodible layers, dredging operations and having arbitrary cross-sections (with overbank flow). Various structures may be represented. Special features for 2D river applications are presently being developed and validated, such as a bottom-vanes and graded-sediment.

Estuarine areas including estuaries, tidal inlets and river deltas influenced by tidal currents, river discharges and density currents. Sediment can be sandy or silty. The areas may include tidal flats, channels and man-made structures, e.g. docks, jetties and land reclamations.

APPENDIX F Delft3D Submerged Vanes Module

Two types of bottom vanes are included in the program. The first type of bottom vane is relatively small (subgrid scale) and placed in a direction slighlty deviating from the flow direction. The goal of this type of bottom vane is to counteract the spiral motion present in curved flow and thereby to reduce, for example, the transverse bed level slope in a river bend. The physics of the bottom vane is too complicated to be incorporated straightforwardly in DELFT3D because a 3D description is essential for the vortex-generation by the vane which requires a very small grid step and a large computational effort. Therefore far-reaching simplifications are applied, which is based on the observation that the bottom vane a vortex line generates at the topside of the vane running downstream. This vortex line generates at the bed a transverse velocity, which interacts with the spiral motion and affects the sediment transport direction. The original theory for this type of vane has been derived by Odgaard and co-workers. The Delft3D-MOR code contains some extensions of this theory. Furthermore an empirical approach of the bottom vanes based on model measurements of vane induced flows is included.

The second type of bottom vane is relative large (multiple grid cells in length) and it is intended to be placed at a higher angle to the main flow. The goal of this type of bottom vane, which blocks the lower part of the water column, is to impose a flow direction near the bed and, thereby, to steer the main direction of sediment transport. The relatively clear water near the surface should continue over the bottom vane. An alternative to this second type of bottom vane is the surface vane. The surface vane, which blocks the upper part of the water column, intends to change the flow direction near the water surface. Sediment rich water near the bed should continue under the surface vane.

General Appendix: Delft Cluster Research Programme Information

This publication is a result of the Delft Cluster research-program 1999-2002 (ICES-KIS-II),
that consists of seven research themes:
(1) Soil and structures, (2) Risks due to flooding, (3) Coast and river, (4) Urban infrastructure,
(5) Subsurface management, (6) Integrated water resources management, (7) Knowledge management.

This publication is part of: Coast and river.

Research Theme	:	Coast and River		
Base project name	:	Rivers		
Project name	:	Vanes and Screens		
Project leader / Institute		Ir. T.H.G. Jongeling		WL | Delft Hydraulics
Project number	:	03.03.01		
Project duration	:	01-03-2000	-	30-06-2003
Financial sponsor(s)	:	Delft Cluster		
		WL | Delft Hydraulics		
		Technical University Delft, Faculty of Civil Engineering and Geo Sciences		
		Royal Haskoning		
Project participants		Delft Cluster		
		WL | Delft Hydraulics		
		Technical University Delft, Faculty of Civil Engineering and Geo Sciences		
	:	Royal Haskoning		
Total Project budget		€ 397.000		

Theme Management team: Coast and river

Name	**Organisation**
Prof. Dr. Ir. M.J.F. Stive	Technical University Delft – Faculty of Civil Engineering and Geo Sciences
Dr. C. Laban	TNO-NITG

Project group

During the execution of the project the research team included:

Name	**Organisation**
1 Ir. C. Flokstra	WL | Delft Hydraulics
2 Ir. H.R.A. Jagers	WL | Delft Hydraulics
3 Ir. T.H.G. Jongeling	WL | Delft Hydraulics
4 Dr. Ir. E. Mosselman	Technical University Delft, Faculty of Civil Engineering and Geo Sciences
4 Ir. F.E. Wiersma	Royal Haskoning